VOLUME 49, NUMBER 9

September, 1961

published monthly by The Institute of Radio Engineers, Inc.

Proceedings of the IRE®

contents

COVER

That the IRE is an international organization is illustrated by the fact that it has 8 Regions in the United States and Canada and 11 Sections on 4 other continents. An important report on its activities outside of North America appears on page 1376.

published monthly by The Institute of Radio Engineers, Inc.

Proceedings of the IRE®

continued

PROCEEDINGS OF THE IRE, published monthly by The Institute of Radio Engineers, Inc., at 1 East 79 Street, New York 21, N. Y. Manuscripts should be submitted in triplicate to the Editorial Department. Correspondence column items should not exceed four double-spaced pages (illustrations count as one-half page each). Responsibility for contents of papers published rests upon the authors, and not the IRE or its members. All republication rights, including translations, are reserved by the IRE and granted only on request. Abstracting is permitted with mention of source.

Thirty days advance notice is required for change of address. Price per copy: members of the Institute of Radio Engineers, one additional copy $1.25; non-members $2.25. Yearly subscription price: to members $9.00, one additional subscription $13.50; to non-members in United States, Canada, and U. S. Possessions $18.00; to non-members in foreign countries $19.00. Second-class postage paid at Menasha, Wisconsin, under the act of March 3, 1879. Acceptance for mailing at a special rate of postage is provided for in the act of February 28, 1925, embodied in Paragraph 4, Section 412, P. L. and R., authorized October 26, 1927. Printed in U.S.A.

September, 1961
Vol. 49 No. 9

Proceedings of the IRE

Poles and Zeros

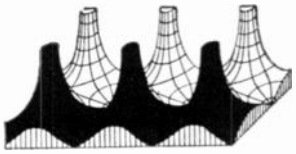

Radio. According to Webster, the word "radio" as a noun means "radiotelegraphy, radiotelephony, or other system employing radio waves. A radio message." As an adjective, Webster states, "Of or pertaining to, employing, or operated by, radiant energy, specifically that of electric waves; . . ." How did the word "radio" come into being? The Editor's curiosity was aroused, concerning the origin of the word, by copies of correspondence that crossed his desk in which the origin of the word "radio" was discussed by Managing Editor Gannett and Secretary Pratt.

A cursory investigation made clear that the origin is obscure and a more thorough exploration yielded some interesting bits of information, some directly relevant to the word as we use it today, others perhaps irrelevant, but nevertheless interesting. The earliest use of "radio," in the communications art, was as a prefix. Though not directly related to our usual understanding of the term, E. Mercadier, in 1880, proposed the term "radiophone" as a general term signifying an apparatus for the production of sound by any form of radiant energy.

The earliest disclosure of the prefixial use of the term, in a context pertinent to the communications art and leading directly to later usage, appears to have occurred in 1898. The magazine "Tit-Bits," in May 1898, made reference to "M. Branly, whose 'radioconductor' or 'coherer' is used by Marconi in his wireless telegraph." The word "radiotelegraphic" appeared in *Nature* in September 1902; "radiotelegram" was used in the *Scientific American Supplement* of November 15, 1902; and "radiotelegraph" appeared in *Nature* on April 23, 1903.

It is quite clear that during the period from approximately 1895 to 1908, the terms most commonly used were "wireless" or "electric wave" telegraphy. The Germans, in 1903, called an international conference which is recorded historically as the "International Conference on Wireless Telegraphy." This was an unsuccessful conference, but its successor conference was named the "International Radiotelegraphic Conference of Berlin of 1906." It was at this latter conference that the term "radio" was suggested as the mark of wireless telegrams. Evidence is also available to show the increasing use of the prefix "radio" from the year 1906 on.

As an example of the trend away from "wireless" towards the use of "radio," a perusal of J. A. Fleming's text is instructive. The first edition of "The Principles of Electric Wave Telegraphy" was published in the year 1906. The index of this edition does not contain a single item using the term "radio." A new impression of this text, with additions, appeared in 1908. The author's note to the new impression calls attention to extending and bringing up to date the section of the last chapter dealing with Directive Radiotelegraphy; in the original edition this chapter was called Directed Electric Wave Telegraphy. The new impression also contained in the index the words "radiogoniometer" and "radiotelegraphy." The second edition of Fleming's book, which appeared in 1910, contained twelve index items using "radio" as a prefix.

Another illustration of 1906 as the beginning of the trend toward "radio" is afforded by the formation or establishment, on September 15, 1906, of the Amalgamated Radio-Telegraph Co. This appears to have been the first company to have used "radio" in its name.

The origin of the independent use of the word "radio" is also difficult to identify. Perhaps the fact that the 1906 Berlin Conference suggested "radio" as the mark of wireless telegrams was its true origin. A Dictionary of Americanisms notes that "radio" was adopted in 1912 by the U. S. Congress in accord with the Berlin Conference suggestion. Another source cites the year 1915 as marking its first independent use. It is evident, however, that the use of the word "radio" by IRE's founders in 1912 may have been one of the earliest applications of its use as a word in its own right.

That the transition from "wireless" to "radio" was not a readily accepted one is emphasized by the many years that "wireless" remained the accepted term in England, and is further emphasized in the annals of IRE. The Preliminary Report of the Committee on Standardization of the IRE, dated September 10, 1913, contains the following definition:

> *Radio Telegraphy and Radio Telephony.* Further divisions of radio communication. It is proposed that the term "wireless" shall be entirely eliminated, as inaccurate and inappropriate.

The Editor makes no pretense that this Poles and Zeros item constitutes as thorough a study of the neological problem as might be desirable. Comments and suggestions on the subject will be appreciated.

Musical Chairs. In April 1960, Poles and Zeros announced IRE acquisition of the building at 984 Fifth Avenue. Renovation and restoration have been completed, and by September 1, 1961, 75 members of IRE headquarters' staff will be housed at 984. For those who visit headquarters, herewith instructions as to how to find your favorite people. Professional Groups Secretary L. G. Cumming has moved from the fourth to the fifth floor of 5 E. 79th Street; Managing Editor E. K. Gannett has moved from 5 E. to the third floor of 1 E. 79th. Executive Secretary George W. Bailey and Office Manager Emily Sirjane will be found holding forth at their usual locations in 1 E., and Chief Accountant John B. Buckley still handles the finances from the third floor of 5 E. Hope no one gets lost during his next visit.—F. H., Jr.

A. B. Bereskin

Director, 1961–1962

Alexander B. Bereskin (A'41–M'44–SM'46–F'58) was born in San Francisco, Calif., on November 15, 1912. He received the E.E. degree in 1935 and the M.S. degree in engineering in 1941, both from the University of Cincinnati, Cincinnati, Ohio, where he is presently Professor of Electrical Engineering. He is also active in consulting engineering and is a Registered Professional Engineer in the State of Ohio.

In the interval between 1935 and 1939 he was employed by the Champion Paper and Fibre Company, the Commonwealth Manufacturing Corporation, and the Cincinnati Gas and Electric Company. In 1944–1945 he was employed by the Western Electric Company as Field Engineer.

He has published work on vacuum tube and transistor audio power amplifiers, low-level transistor audio amplifiers, video amplifiers, regulated power supplies, and power factor meters. He has also done work in the fields of special RC oscillators, frequency selective amplifiers, low jitter multivibrators, special stabilized power supplies, and transistor pulse amplifiers.

Professor Bereskin is a member of the Administrative Committee of the PGA. He has been National Chairman of the PGA, Editor of IRE TRANSACTIONS ON AUDIO, and a member of the Education Committee, the Professional Groups Committee, and the Sections Committee. He has also been Institute Representative at the University of Cincinnati, and Chairman, Vice Chairman, and Treasurer of the Cincinnati Section. He is a member of AIEE, Sigma Xi, Etta Kappa Nu, and Tau Beta Pi.

Scanning the Issue

The IRE International Activities Committee (McFarlan, p. 1376)—The IRE is one of the few technical societies in the world that does not have the name of a country in its title. The omission was deliberate. The founders intended that this society should be international rather than national in scope. The IRE has been privileged to have members from abroad for nearly half a century, Sections outside the U. S. for 35 years, and distinguished engineers from other countries on its Board of Directors for 30 years. Today there are some 7000 members and two dozen Sections located outside the U. S. Half of these are in Canada and enjoy full representation and participation in IRE affairs as the Canadian Region of IRE. The remainder are scattered over four continents. Last year they were provided a more direct representation on the Board of Directors with the creation of the office of Vice President residing elsewhere than in North America. This January the Board took a further significant step by establishing an Ad Hoc Committee on IRE International Activities Outside of Existing Regions. Five IRE Fellows from three countries, including three past presidents, were appointed to serve by President Berkner. Early this summer this distinguished group made an unprecedented trip abroad on behalf of the IRE. Their itinerary included the United Kingdom, France, the Netherlands, Denmark, Norway, Sweden, Germany, Switzerland, and Italy. Their mission was to explore with officials of major societies and leading engineers in each country how the IRE might better serve the professional interests of its many members who reside outside North America, by such means as increased Section and Professional Group activity and through cooperative efforts with national engineering societies abroad. A preliminary report has been prepared for the issue by the Chairman of the International Activities Committee which describes in abridged form the objectives of the trip and what was accomplished. Its two pages add an important chapter to the history of IRE's growth as a major international organization.

Reflections of a Communication Engineer (Golay, p. 1378)—The diversity of science is amply demonstrated by the many technical fields of endeavor it has fathered, each field in turn producing its own several and separate branches of specialization. It is well that we be reminded, too, of the unity of science. One such occasion presented itself last March when the following three events took place: A communication engineer addressed a meeting of chemists. A winner of the IRE Harry Diamond Memorial Award received a high award from the American Chemical Society. An engineer spoke of information theory and cosmology in one breath. In reality, the three events took place at one time and involved the same person. His remarks covered a wide range of subjects, culminating in an absorbing discussion of whether man possesses the intelligence to surmount a staggering challenge, namely, to prevent the eventual total decay to which our universe is apparently doomed. The talk was first published in the ACS journal *Analytical Chemistry*. Although it is not the general policy of the PROCEEDINGS to reprint articles, we believe every reader will find this article to be a most stimulating and well-justified exception.

An Analysis of the Modes of Operation of a Simple Transistor (Gibbons, p. 1383)—This paper discusses the fact that a simple transistor oscillator can operate in more than one mode, a matter which has been causing some confusion recently. The author deals principally with two modes; with the transistor operating as a three-terminal element in one case, and as a so-called transit-time diode in the other case. The transit-time mode, although first recognized some time ago, escaped attention until recently when it was found that oscillations could be obtained at frequencies considerably higher than the maximum frequency specified for the three-terminal mode. This strange behavior, which has been commented on recently in the literature, is made a good deal less strange by an illuminating analysis that clarifies the distinction and the relation between the two modes. The paper thus ties together a number of scattered and inadequately explained phenomena that have been puzzling people lately. It also provides practical design information and may stimulate further discoveries in the application of transistors in the kilomegacycle region of the frequency spectrum.

Actual Noise Measure of Linear Amplifiers (Kurokawa, p. 1391)—Few subjects have generated more discussion, less agreement and greater interest than the quest for a meaningful, usable, unambiguous, quantitative measure of the noise performance of an amplifier. The advent of tunnel diodes, parametric amplifiers and masers added more fuel to the long-smoldering fire by bringing into the picture circuit conditions which were not adequately covered by earlier definitions and concepts. The situation was perhaps pointed up best by the July letter to the Editor which called attention to the rise of a new sport, which its author called "noisemanship." Despite the confusion, sound progress has been made recently in developing improved methods of expressing noise performance, especially in the introduction of a new quantity called "noise measure" in 1958. This paper proposes a new "noise measure" which differs from the earlier one in that it includes the contribution from the noise originating in, and reflected back to, the load. The difference becomes of practical significance when dealing with devices having negative input or output impedances and, hence, having unmatched input or output circuits, conditions particularly pertinent to tunnel diodes, parametric amplifiers and masers.

IRE Standards on Radio Interference: Methods of Measurement of Conducted Interference Output to the Power Line from FM and Television Broadcast Receivers in the Range of 300 kc to 25 Mc (p. 1398)—If the foregoing title is the longest of any Standard published by the IRE, it is more than justified by the fact that it supercedes and replaces three previous Standards. Moreover, it concerns a subject of considerable practical interest. High-level signals such as arise in the IF or horizontal deflection system of FM or TV receivers are frequently potential sources of interference to other receivers. This Standard specifies how to measure the interference conducted by the power line from these sources.

The Delay-Lock Discriminator: An Optimum Tracking Device (Spilker and Magill, p. 1403)—The delay-lock discriminator described in this paper provides an improved technique for estimating the delay difference between a continuous, random transmitted signal and its reflection from a target, using a system which employs a form of cross-correlation along with feedback. It differs from ordinary FM radars in that it avoids the so-called fixed error, is free of much of the ambiguity common to periodically modulated systems, and can discriminate between multiple targets on the same bearing from the antenna. It appears to be especially suited to tracking rapidly moving targets under poor SNR conditions.

A Sequential Detection System for the Processing of Radar Returns (Galvin, p. 1417)—In dealing with very-high-velocity targets, the problem arises of detecting a narrow-band radar return within a wide-Doppler-band environment. This can be done by monitoring the spectrum with a sufficient number of narrow-band matched filters to cover the Doppler band. However, the number of filters required to do this can reach into the thousands. This paper presents a two-step detection process, coarse and then fine, which greatly reduces the number of filters required for this important task.

The IRE International Activities Committee*

R. L. McFARLAN, *Chairman*, FELLOW, IRE

IN RECOGNITION of the professional interests of its thousands of members outside of North America, the increasing membership and Section activities abroad, and a demand for greater accessibility to IRE services and publications the IRE Board of Directors, at its meeting of January 4, 1961, authorized President Lloyd V. Berkner to appoint a committee to consider ways and means for more effectively serving these members. The Board further outlined the scope of this committee—The 1961 Ad Hoc Committee on IRE International Activities Outside of Existing Regions—to include:

1) The development, establishment and operation of Sections.
2) Affiliation with qualified societies.
3) Extension of Professional Group activities internationally.
4) Potential development of Regions.
5) Visual-Audio aids to Sections.

President Berkner, accordingly, has appointed the following members of this committee:

Dr. R. L. McFarlan, Consultant, *Chairman*
1960 President IRE
Mr. E. Finley Carter, President, Stanford Research Institute
Director-at-large IRE
Dr. John T. Henderson, Principle Research Officer, Canadian Research Council, Ottawa
1957 President IRE
Ir. H. Rinia, Director of Research, Philips Research Laboratories, Eindhoven, Netherlands
1956 Vice-President IRE
Dr. Ernst Weber, President, Polytechnic Institute of Brooklyn
1959 President IRE.

IRE recognizes that its members outside of North America are also members of the appropriate professional societies of the countries in which they live, and that IRE services to these members must not be given at the expense of or in interference with the activities of these national professional societies. Therefore, the resolution of the IRE Board which established this committee emphasized clearly that IRE is not attempting to compete with national societies, nor does it have any desire to replace them. The IRE interest is simply to establish a mechanism whereby those desiring to form a Section in any particular area outside North America, whether it be Europe, South America, the Orient, or elsewhere, would find it convenient to take the necessary steps toward such formation. These steps would be taken with the full knowledge and invited cooperation of the appropriate national society.

* Received by the IRE, July 24, 1961.

IRE membership and publication records show an increasing interest on the part of European national societies in the establishment of IRE activities in their countries. This may be due to the success of existing IRE Sections in Europe—Benelux, Italy, Switzerland—and to the cooperative spirit displayed by these Sections towards national societies. Not only are any possible earlier misgivings about the IRE attitude being dispelled, but also these societies are beginning to realize the benefits which IRE can bring to their countries. These benefits not only include IRE's world-wide technical publications—PROCEEDINGS, TRANSACTIONS, and so forth—but also cooperatively sponsored international symposia and forums. IRE's many Professional Groups can be especially helpful in these areas. In addition, IRE wishes to ensure that qualified scientists and engineers from all over the world are brought to the attention of its committees as candidates for annual awards and Fellow membership.

In order to discuss possible affiliation arrangements with some of the great electronic professional societies in Europe, and through discussions with IRE members in Europe and their representatives, the IRE International Activities Committee as a whole visited, during the early summer of 1961, those countries in Europe where there is an appreciable IRE membership. Extensive discussions were held with IRE members and with electronic and engineering leaders throughout Europe. Since the IRE International Activities Committee is not a negotiating body, any understandings resulting from conversations with representatives of the various national professional societies are subject to subsequent review and modification by the IRE Board of Directors. The countries visited are listed below in the same sequence as they were visited by the IRE International Activities Committee.

UNITED KINGDOM

A meeting with the liaison committee of the Institution of Electrical Engineers resulted in a proposal to establish an IRE Advisory Committee of IRE members resident in the United Kingdom, and an IEE-IRE liaison committee composed equally of a small number of IEE and IRE members. This liaison committee would be given the task of working out the details of IEE-IRE cooperation in the United Kingdom.

FRANCE

Conversations with the officers and directors of the Societe Francaise des Electriciens et des Radioelectriciens confirmed an earlier decision by the SFER to support the formation of an IRE Section in France. The Section organizing committee comprises M. George Gaudet, M. Jean Lebel, and Mr. Joseph R. Pernice.

The Netherlands

The members of the Benelux Section Executive Committee met in Den Haag with the IRE International Activities Committee to discuss problems connected with Section operation, and also future plans. The desirability of establishing a Region 9 in Europe was considered in detail.

Denmark

A luncheon conference with the Director of the Danish Engineering Society, the President of the Electrotechnical Section, and Prof. Rybner, included discussions on the potential IRE role in Denmark. There was some indication that the Society of Danish Engineers would welcome IRE cooperation with and through their Electrotechnical Section.

Norway

Conversations with the officers and other representatives of the Norwegian Society of Engineers and the Norwegian Electrotechnical Society resulted in the proposal to establish a joint liaison committee charged with the development of better ways to serve IRE members in Norway. It is proposed to name three individuals—including two IRE members—to serve on a liaison committee with the Norwegian Society of Engineeers and the Norwegian Electrotechnical Society.

Sweden

Considerable interest was evidenced in IRE activities, and in the possible formation of an IRE Section in Sweden. Dr. Granqvist, 1958 IRE Vice-President, arranged for some very productive discussions with the officers of the Swedish Engineering Society, and contributed considerably to their success.

Germany

A great deal of interest exists in Munich, Germany in forming an IRE Section, and the visit to Munich of the IRE International Activities Committee probably has helped to hasten the formation of such a Section. The officers and other representatives of the German Engineering Society were most cooperative.

Switzerland

A meeting of the Geneva Section was held at which a panel composed of the members of the International Activities Committee undertook to discuss future trends in electronics. Discussions with various officers and members of the Geneva Section considered various problems of Section operation and the desirability of forming a Region 9 in Europe.

Italy

Since the Italy Section has strong groups in both Milan and Rome conferences were held with IRE members in both cities. Unlike the Benelux and Geneva Sections the Italy Section uses the Italian language for its meetings. A formal Section meeting in Rome was well attended.

In general, it can be said that a strong interest in IRE exists in Europe today, and there is every reason to expect this interest to increase in the future. As a result of its visits, discussions, and meetings in Europe, the IRE International Activities Committee has arrived at certain general conclusions regarding the international activities of the IRE.

1) The initiative for forming new Sections or Regions is the prerogative of the membership involved. It is a function of the International Activities Committee to assist and support any such actions.
2) Setting up a new Section requires the maximum transmission of information from existing Sections. As soon as new Sections are formed the new Chairmen and Secretaries should be invited to meet with the Chairmen and Secretaries of existing Sections.
3) All Section Chairmen should be kept as fully informed as possible, especially regarding the reasons behind Executive Committee and Board of Directors decisions.
4) Information sent to the Section Chairmen should also be supplied to IRE delegates and liaison chiefs in countries where liaison committees with national professional societies have been established.
5) In view of the national character of the IRE Sections in Europe, and those being formed, as well as IRE Sections elsewhere outside North America, some modifications in Section and Region organization and procedures may be found to be necessary. Until more experience is gained a certain degree of flexibility may be required.

In conclusion, mention should be made of the very many gracious acts of hospitality and courtesy which were shown the IRE International Activities Committee in all of the countries where it visited. To mention by name all of the individuals who contributed to the work and pleasure of the Committee would unduly extend the length of this brief report. To all of these individuals the IRE Committee on International Activities expresses its deep appreciation. And finally, as *Chairman*, I should like to mention my own personal appreciation of the hard work, keen insight into international problems, and understanding tact of my fellow committee members on this truly international committee.

Reflections of a Communication Engineer*

MARCEL J. E. GOLAY†, FELLOW, IRE

In March, of this year, the American Chemical Society heard an address by the recipient of its Sargent Award in Chemical Instrumentation. The recipient, however, was not a chemist; he was a communication engineer, IRE Fellow, and holder of the Harry Diamond Memorial Award. And he did not speak on chemistry. Indeed, his remarks were so thought provoking and of such broad interest to PROCEEDINGS readers that the text has been reprinted below from the ACS journal *Analytical Chemistry*.
—*The Editor*

I CANNOT TELL A LIE—I am not a chemist. That is why I have decided to change the subject of my talk. Others will tell you, more competently than I could, about the physical chemistry of chromatography. It is as a communication engineer that I will talk to you. And if the things I say increase in strangeness as I go along, I will ask you to remember two things.

The first is this: Many of the recent advances in science are due to the cross-fertilization of, at first view, separate and distinct fields.

And the second is this: Of all the disciplines guilty of such fruitful incests, communication engineering is the guiltiest of them all, with its inroads in physics and chemistry, in biology, in sociology through automation, in philosophy through information theory. Communication engineering—or should I say communication philosophy—appears as an octopus, with its tentacles stirring thought here, there, and everywhere, an octopus intimately linked to the development of social man, and to the reflections of individual man.

I owe the good fortune of being with you today to the accident of having noted that, in a simplified form, the chromatographic partition process could be described by the telegrapher's equation. Nothing more would have happened if my friends at The Perkin-Elmer Corp. had not asked me to stick numbers in the equation—after all, a consultant must earn his keep. This led to the finding that the packed chromatographic column of five years ago had a basic efficiency, as measured by the Performance Index, of around 0.01 per cent. This finding led in turn to the idea of making a column which had the form of the simple model adopted for the theoretical study—namely, an open tube coated with a retentive layer. That is all.

I said I would talk as a communication man about communication philosophy and the strange lands where it may take us. It is not every day that I have the opportunity of addressing a kindly inclined and nearly captive, well guarded audience about my extracurricular thoughts, and I will start with a reminiscence. I will reminisce about a time when I was a little boy, going shopping with my mother, walking alongside, and trying to digest something metaphysical I had read, which I was probably too young to read. Yet all of a sudden, all my thoughts came into a focus, and I started to speculate: Suppose there had been nothing at all, no time, no space, no matter, no people. But there is something and I am part of this something, playing my role in it. There was rain falling on the pavement on that day and I remember that, too.

Surely the simple thought that there is a universe and that we should not be indifferent to our privilege of playing our part in it has been the underlying incentive to the building and the evolution of our philosophy and cosmology.

The beginnings of our cosmology appear naive in retrospect. Some of you may recall learning in your history class about the early mythological world, flat and carried by a large elephant, with his feet on four turtles swimming in a sea of milk. Little by little these notions became purified. We made a notable step forward when we accepted a universe not centered in our little earth. For a long time the concepts associated with the origin of our universe oscillated between an instinctive belief in a beginning, a creation, and a scientific opinion that we lived in a static universe with time stretching indefinitely backwards and forwards. And then, last century, budding physical chemistry led us to a real difficulty.

It was in the early part of the last century that Carnot formulated what became accepted as the second law of thermodynamics. As further developed by Helmholtz, this law stated, in effect, that there is a continuous degeneracy, a continuous decay of energy. You can mix hot and cold water, but you cannot unmix them.

When you extend this principle to our whole universe—and it is the virtue of any principle that you can do

* Reprinted with permission of the American Chemical Society from *Analytical Chemistry*, vol. 33, pp. 23A–31A; June, 1961.

† Consultant, The Perkin-Elmer Corp., and the Philco Corp., 116 Ridge Road, Rumson, N. J.

so with it—you come to the metaphysical conclusion that this irreversibility of nature's processes demands that there be a definite beginning, a creation. But the semireligious concept of a creation, with the corollary concept of a Creator, was scientifically inadmissible, so it was thought, and matters stayed in that impasse through three generations of scientists. In order to get out of this difficulty, as able a philosopher as Poincaré made intellectual somersaults worthy of a devil caught in the holy fonts. He surmised, for instance, that if time marched forward in one part of the universe, this was made up by time going backward in some other regions, which is, of course, inadmissible. The clock cannot run backward.

Static Universe Concept Is Untenable

Things were in this impasse when two additional discoveries, taken together, made the concept of a static, uncreated universe completely untenable. The first was the discovery of radioactivity. Many natural radioactive isotopes such as thorium, uranium, and potassium have a very low rate of decay, and the fraction remaining today establishes a rough epoch for their creation, of the order of several billion years ago.

The second discovery was made by the astronomer Hubble in an entirely different domain. Hubble observed that many large galaxies are receding from us at a high speed. Galaxies are assemblies of from a billion to a quadrillion stars, and as they recede from us their characteristic color is shifted towards the red. Hubble observed that the farther the galaxies, the greater the red shift. But we are not in the center of the universe. The universe has no center in the sense that an orange has a center. Thus every galaxy must be receding from every other. This can only mean that we have a general explosion, and Hubble calculated that galaxies receded from each other as if this general explosion started at roughly the same epoch already determined by a study of the rate of decay of our radioactive minerals.

It was a Belgian cleric, the Abbé Lemaitre, who cut the Gordian knot by saying: "Let us postulate that the whole universe started several billion years ago with a single enormous atom." And it turned out that his daring hypothesis led to fewer difficulties than any other. This is the decisive test of any physical theory. The postulate of Lemaitre is generally accepted today, and you will find in the scientific literature quite serious speculation as to the state of the universe two minutes after its creation, for instance.

You may well ask: But what was there before and why did it all start? And of course, the question remains unanswered.

You may well ask also: Did it start with a pinpoint of matter of no size and infinite density? This is an interesting question to think about, for the following reason. When we permit two masses to come together by gravitational attraction, like a mass of water falling towards the earth center through a hydroelectric plant, we derive useful energy at the expense of the negative gravitational potential energy of these two masses. And when we calculate the total negative gravitational energy for the entire universe, using available astronomical data, we find that it is of the order of magnitude of the total positive energy in the form of masses, radiation, kinetic energy, and so forth. So we are led to ask: Could it be that the total energy of the universe is actually zero, that the positive energy we have in the form of mass and radiation is merely the result of a trade for negative gravitational energy? Then, if this is so, perhaps the Creator did not require the enormous mass of all the stars that we see, but required merely the intelligence to trigger the process, after which it kept going. We shall come back to this, but let us, for the time being, remember that some ten billion years ago a quite extraordinary event took place, beyond which the veil of history is forever closed to us.

First Protozoic Life

Now let us look at another historical puzzle, of a completely different order. Some two billion years ago, when our universe was already several billion years old, another extraordinary event took place on this earth. It was nothing as spectacular and grandiose as the creation of our macrocosm. It was microscopic in nature, but may turn out to be the most significant thing in the history, not of just our little earth, but of our entire universe. I refer, of course, to the appearance of the first protozoic life. After its creation, life evolved, and culminated in the appearance of man. Last century this process of evolution, especially in its last stages, was a subject of debate and controversy. Much ado was made about missing links, but today we think we understand better this evolution process, and why few ancestral forms, not just of man, but of most living creatures, are ever found. What we do not understand is the very beginning of the process: what produced this first molecule? We may be tempted to be superficial and shrug off the question by saying that the first living molecule was produced by chance, but let us give this problem a second look, in the light of information theory.

New Discipline-Information Theory

Information theory is a recent addition to our family of disciplines and it deals with a subject which is closely related to the second law of thermodynamics, the very law which states that the passage of time is marked by a decay of energy, and hence that there must have been a beginning to our universe. In many respects information theory constitutes that chapter of communication theory which has had, and will continue to have, an impact on metaphysics and philosophy.

The beginnings of information theory are curious. Nearly a century ago Maxwell expressed his impatience with the second law of thermodynamics by inventing a little demon, Maxwell's demon, which was to haunt two

generations of scientists. As you know, Maxwell's demon is perched by a trapdoor in a wall separating two identical gas masses, and every time a molecule comes from the first gas mass in the direction of the trapdoor he opens it for an instant and lets that molecule pass through to the second gas mass. After a while you have more molecules and more gas pressure in the second gas mass than in the first, and that extra gas mass can expand into the first and produce useful work, while cooling. This constitutes a violation of the second law because useful work has been obtained from the heat of two gas masses originally in temperature and pressure equilibrium. A good paradox deserves a good answer, and a clever demon deserves a clever exorcism, and it was not until 1929 that this was done by the physicist Szilard, who said that Maxwell's demon cannot operate, because he does not have the information as to when to open his trapdoor.

For some 15 years Szilard's article remained unappreciated by almost everyone, including Szilard himself. His original manuscript had been noticed on his desk by friends, who persuaded him to let them mail it to their scientific journal; otherwise it might have remained unpublished. But shortly after the last war, certain statistical aspects of the theory of communication became of interest simultaneously to several researchers. In 1948 Shannon published his classic article, which became the foundation of information theory. In this article he noted the similarity between the entropy of the thermodynamicist and the negentropy of information. If you will pardon a personal reference, I heaped the last indignity on the poor demon when I showed that even with the most efficient transmission system, the energy required to communicate to the demon the information he needs would at least equal the useful energy he could retrieve by operating his trapdoor. So, even if the information the demon needed were available at no cost, it could not be communicated to him, without destroying his raison d'être.

I am talking at length about information theory because of the dualism between the second law and information theory on the one hand and the dualism between the creation of the universe and the creation of life on the other hand. It is information theory, and the new scientific attitude produced by information theory, which has revealed some interesting aspects of living molecules and living cells.

Information theory has taught us how to deal quantitatively with structure, with pattern, with what the Germans call Gestalt. There is even speculation about the admission of beauty and esthetics to the community of scientific concepts by information theory.

We can place within the scope of information theory the following problem, which was examined by the mathematician Von Neumann. Suppose we wanted to build a machine capable of reaching into bins for all of its parts, and capable of assembling from these parts a second machine, just like itself. What is the minimum amount of structure or information which should be built into the first machine? The answer came out to be of the order of 1500 bits—1500 choices between alternatives which the machine should be able to decide. This answer is very suggestive, because 1500 bits happens to be also the order of magnitude of the amount of structure contained in the simplest large protein molecule which, immersed in a bath of nutrients, can induce the assembly of these nutrients into another large protein molecule like itself, and then separate itself from it. That is what the process called life consists of, and unless and until we discover a new process in which simpler molecules have semilife properties, the inquiry into the birth of life can be reduced to an inquiry into the possibility or probability of the spontaneous assembly of such a molecule, out of a bath of its essential constituents. And this is exactly where we run into an interesting difficulty.

Spontaneous Creation of Life?

By making the most favorable assumptions as to the conditions in which this spontaneous creation of life could have occurred on this earth, we do not come anywhere near the spontaneous assembly of 1500 bits; we can account for perhaps one-tenth that number. Do not shrug this off as being only one order of magnitude off. This involves a factor of 10 in the exponent, and there is a vast difference between the probability of 1 part in 2^{150} and 1 part in 2^{1500}. Then you might say: But it could have happened in many places in our universe, and if it had not happened here, we would not be here to talk about it.

Very well, multiply 2^{150} by the number of stars—that is, by the number of potential solar systems, in the universe—and you obtain 2^{220}, still short of the mark. And yet, life did begin, and looking back in time, we see two mysteries, or at least two highly unlikely events. The first, the creation of the universe, of space, of time, of matter. The second, the creation of life, from which we evolved as a matter of course almost, with such unlikely beings as chemists and engineers in our midst, producing in the laboratory improbable assemblages such as a liter of liquid helium, or saying such unlikely things as what I am now saying to equally unlikely assemblies of molecules as my listeners. We may even have some day an unlikely biochemist who will assemble, radical by radical, an unlikely large molecule which can reproduce itself. But this would not resolve the historical mystery of the creation of the first living molecule.

Two Big Questions of the Future

All I have said so far has been to prepare the ground for two big questions, dealing with what could be called the two basic mysteries of the future.

The first big question is philosophical, and can be stated fairly simply. With his intelligence, with his ability to make experiments and to process information,

does man have the potentiality of ever acquiring full information about the basic laws of our physical universe?

I am sure all of us have asked ourselves this, or a similar question. Some of us believe that the final answer will always escape us, even though every discovery, every extension of present physical theory brings us closer to it. Others of us believe that when we run into integral numbers, such as the number of protons and neutrons in a nucleus, we are approaching the ultimate physical knowledge.

Tied to this first big question, there are other tempting questions. For instance, we have an information theory which has established a measure for the amount of information we can communicate to each other. To be sure it is a brutal measure. To gauge meaningful information in terms of bits—the bits of information Maxwell's demon lacks—would be as meaningless as evaluating a work of art with a yardstick or a weight scale. All the information contained in all the books of the world, some 2^{60} bits, would not suffice for the separation of one milligram of air into its slow and fast molecules, and the information content of a thoughtfully filled time capsule would not suffice for a picogram. Hemmed in as we are by finiteness—the surmised finiteness of our universe, of our brain cells, of our thoughts, and of our life span—we strive for infinitude in the higher values, the intellectual, artistic and spiritual values. We are loath to admit the possibility of a measure of these, and would welcome a proof of the impossibility of such a measure. Should we, some day, have a measure of intelligence, or will intelligence always transcend a definition of itself? And even if we succeed in defining and measuring intelligence, may we eventually prove mathematically the impossibility of intelligence reaching the ultimate truth, just as the mathematician Godel has proved the existence of undemonstrable theorems and the openness, the infinitude of number theory? Shall we perhaps come to the paradoxical proposition that a supreme intelligence should disprove the possibility of its very existence?

I do not want to linger on these speculations, no matter how fascinating they may be. I want to come to the second big question.

While we do not know whether or not we shall be able some day to unravel the last shred of mystery surrounding the truth of the universe we live in, we do know, from the second law of thermodynamics, that the clock cannot run backward, and that our universe is condemned to eventual total decay, to end, as T. S. Eliot has put it, not with a bang but with a whimper. Shall we sit helplessly by watching that process, until even the modest wants of life as we know it can be no longer supplied?

Alternatively, is there a possibility that human intelligence will have the capability of doing something radical about the situation?

At first glance, the answer would seem to be "no"; the second law drives the universe inexorably to eventual decay, and regeneration is ruled out. It is at this point that I would interject a very timid "but." Remember that the world may well have been triggered into existence by a highly intelligent act producing a highly unlikely event—remember that the total energy of the universe may be very small, maybe even zero, the creation of mass having proceeded at the expense of negative gravitational energy. Could it become man's role to be the author of a similar highly intelligent act, before the clock of his universe becomes unwound?

Matter-Negative Gravitational Energy Exchange

I admit this sounds fantastic, because we have today no inkling of the mechanism involved in any trade of positive energy in the form of matter for negative gravitational energy. I must ask you to remember that, so far, physicists have not succeeded in performing a single experiment which connects gravitational phenomena with electrical phenomena, because electrical forces between elementary particles are some 40 orders of magnitude larger than gravitational forces. We are, therefore, at the point where metaphysical arguments must take over from physical arguments. That is, we may assume yet undiscovered mechanisms, while being careful not to violate already established physical principles.

I have pointed out before that we, men, these highly unlikely but intelligent creatures, have produced such unlikely things as a liter of liquid helium, something never produced spontaneously before anywhere in our universe.

Suppose now that our colleagues, the nuclear chemists, were to succeed in engineering a relatively heavy neutral particle, of extremely small volume, and of extremely low probability of spontaneous generation, just like the liter of liquid helium. Keep on supposing that this new particle has sufficient interaction with ordinary matter as we know it, and once produced in some supercosmotron, trickles gently toward the center of the earth, where it coalesces with others like itself into a very small mass of extraordinarily high density. The manufacture of these particles continues, and in a little while this small mass has the size of an electron. Later on, after many more particles have been produced and assembled, this small mass acquires the size of a molecule. But this is an important project, and several million years later (there is a cooling problem) a few millionths of our earth mass have been thus transformed and poured in the ground, to reassemble in the earth's center into a tiny sphere, one wavelength of light in diameter. Some very interesting things could begin to happen by then. Remember that space is curved by mass. Oh, very little. But on the mass surface, this effect is in inverse proportion to the radius of that mass. And I have postulated a very, very small size of extraordinarily high density. By the time our

small but enormously heavy mass has reached a wavelength of light in diameter, it has almost wrapped its own space around itself, and has become very close to what I would call a gravitational "crit." I believe we are about to have a gravitational explosion.

Before it is too late, let us review our calculations. Take a certain mass and distribute it in the physical space of a universe which has the shape of a three-dimensional spherical bubble within a four-dimensional cosmos. Then stipulate that the total mass-energy of the system, which is equal to the initial mass-energy plus the relativistic increase due to the speed of expansion, is also equal to its total negative gravitational energy. This is the same as stipulating that the total energy of the system is zero, and no simpler stipulation can be made. Write this down as an equation, for which we need only the initial mass, the gravitational constant, and the speed of light. Solve this equation and examine the solution you obtain.[1] This solution represents an explosion which proceeds with nearly the speed of light, with a continuously increasing mass but also a continuously decreasing density. And if you substitute the age of the universe today for the time appearing explicitly in this solution you obtain a density of the order of 10^{-30} gram per cc. This is the density of our present universe, within the margin of observational error. And if you like, make the initial mass from which you started, zero, and the solution is hardly affected. No known physical law has been violated in this calculation, but a yet unknown mechanism has been postulated for the trade of positive mass-energy for negative gravitational energy.

This is an intriguing result, which leads to the following picture.

Imagine a two-dimensional plane intersecting our three-dimensional universe within the four-dimensional cosmos I have assumed. This is similar to a plane intersecting a two-dimensional sphere within a three-dimensional space, and if this plane is the blackboard, we have a circle which expands. But we have chosen a plane which passes through the center of the earth, and here there is an increased curvature as we approach our tiny, enormously heavy mass. The experiment continues, the mass increases in weight, the curvature of space increases on both sides, and a critical point is reached when it wraps its own space around itself, shearing itself from its mother-universe, and beginning to expand on its own.

This picture may induce some final soul-searching questions, before fabricating the additional billion tons or so of our heavy particles, which will produce a gravitational crit in the center of our beloved planet.

[1] M. J. E. Golay, "On a connection between Mach's principle and the principle of relativity," *The Observatory*, vol. 79, no. 912, pp. 189–190.

Destruction of Universe Unlikely

Will this supreme experiment destroy our old universe while creating a new one? Probably not. Any annihilation of the universe would require its collapse, and anything resembling a return to the beginning implies an unlikely turnabout of the clock.

Will it create a local disturbance, of the order of a supernova, hardly felt in other solar systems of our galaxy, and barely observed from neighboring galaxies? Or will it produce only a cosmic seed which, wrapping its own space around itself, will make a clean break with the old universe, becoming a new and full-fledged three-dimensional universe of its own, within the four-dimensional cosmos containing all there is? A completely separate new universe, having no physical connection with the old, and producing its own stars and its own living and thinking creatures, who shall know of us no more than we shall know of them, like these ephemeral insects who never coexist with their parents and their offspring.

At this point I would like to ask you not to take too literally some of the things I am saying. I admit their fantasy makes them sound like science fiction literature. I could say nothing about the mechanism involved. In the absence of any physical experiment connecting electrical phenomena with gravitational phenomena, I could only assume the existence of such a mechanism based on the probably nonlinear character of the field equations which should eventually connect electrical and gravitational phenomena, while being careful not to violate known laws; a mechanism which may operate actively only for a few seconds, or even picoseconds, if indeed our concept of time is applicable to it. I have glossed over such serious difficulties as those which arise if we have the possibility of multiple creation, with several junior universes blowing up like smaller soap bubbles within the mother bubble, first interacting and then beginning to interfere with each other. I have not discussed what meaning can be attached to a world mass which consists almost entirely of the incremental relativistic mass of a vanishingly small initial mass. I have no good answer for several sound logical and even embarrassing questions about these and other points. I can only plead for a measure of license, when speculating about a nonrepugnant alternative to a philosophically repugnant once and for all universe, doomed to eventual decay, or to a physically untenable infinite universe stretching indefinitely backward and forward in time.

I said I would not talk about chromatography, and I think I have succeeded in that. I hope to have succeeded also in giving you an idea of the strange lands to which we may be led by communication philosophy, and by speculation about the clock-rewinding task which may challenge the intelligence of man.

An Analysis of the Modes of Operation of a Simple Transistor Oscillator*

J. F. GIBBONS†

Summary—A simple transistor oscillator circuit is analyzed in an illuminating way. The analysis predicts oscillation in either of two modes and provides a means of determining the maximum frequency of oscillation in each. The two modes are identified as "three-terminal" or "two-terminal" according to whether RF current is required in the base lead to produce the oscillations. The relationship between these modes is developed and visualized in a "frequency portrait" for the transistor which serves to unify the principal results of the paper.

Introduction

THE CIRCUIT shown in Fig. 1 is a simple transistor oscillator. Exclusive of biasing networks, it consists of one transistor and two uncoupled impedances. Depending on the frequency of operation required, the two impedances may be LC tanks, transmission lines with sliding shorts, or resonant cavities.

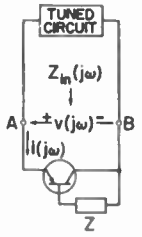

Fig. 1—Basic oscillator circuit.

The circuit has two operating modes: the collector-to-base impedance can be inductive, in which case the transistor is operating as a three-terminal element (*i.e.*, with RF current flowing in all three leads); or the collector-to-base impedance can be an open circuit (to RF), in which case the transistor is operating as a two-terminal element or "transit-time" diode.

An analysis which applies to both of these modes can be constructed on the basis of a polar plot of $(1-\alpha)$ for the transistor, and the maximum frequency for each mode can be obtained from a simple application of trigonometry. The results of this analysis are:

1) The circuit is capable of operating at frequencies up to

$$f_{max} \lesssim \sqrt{f_\alpha / 8\pi r_b' C_c} \qquad (1)$$

in the three-terminal mode with a uniform-base transistor.[1]

2) The circuit may be capable of oscillating at frequencies greater than the f_{max} quoted in (1), when it is operated in the two-terminal mode, if the parasitic impedances in the transistor structure are low enough.

3) At any frequency less than the maximum, approximate circuit Q's required for oscillation in either mode may be obtained.

Both of the results listed in 1) and 2) above have been obtained previously. Pritchard[2] deduced the formula for f_{max} given in (1) by finding the frequency at which the maximum available power gain of a simple transistor amplifier is unity. However, since his analysis is concerned with amplifier gain, it only sets an upper bound on the oscillation frequency and does not suggest an oscillator circuit which is capable of achieving the bound.

Shockley,[3] in an article which was somewhat before its time, recognized the capabilities of a p-n-p structure as a "transit-time" diode and calculated the frequency bands in which various structures of this type would exhibit two-terminal negative resistance. Experimental work at the Bell Telephone Laboratories[4] confirmed his theory, though with a transistor which gave a maximum oscillation frequency of about one megacycle.

The practical significance of the "transit-time" mode seems to have been lost in the onrush of transistor technology until recently, when several experimenters[5] obtained weak oscillations at about 2 kMc from transistors with an f_{max} of about 500 Mc. These results may be satisfactorily explained using a transit-time argument; now, transistors which have been purposely made and mounted to maximize this effect have provided several milliwatts of power at frequencies of 2 kMc and higher.[6]

The analysis of the circuit shown in Fig. 1 is, therefore, of considerable interest since it not only provides design information for the oscillator circuit components but also serves to integrate the existing literature on maximum frequency of oscillation in a simple way.

* Received by the IRE, September 8, 1960; revised manuscript received, March 13, 1961.

† Electronics Labs., Stanford University, Stanford, Calif.

[1] That is, a transistor with uniform doping density throughout the base, and hence no built-in drift field.

[2] Pritchard, R. L., "Frequency Response of Grounded-Base and Grounded-Emitter Transistors," presented at AIEE Winter Meeting, New York, N. Y.; January, 1954.

[3] Shockley, W., "Negative resistance arising from transit-time in semiconductor diodes," *Bell Sys. Tech. J.*, vol. 33, pp. 799–826; July, 1954.

[4] The experimental work was done by G. Weinreich in the latter part of 1954.

[5] For example, V. Vodicka of the Lenkurt Electric Co., San Carlos, Calif. See also Section IV of this paper.

[6] Personal communication from R. Zuleeg, Hughes Semiconductor Div., Hughes Aircraft Co., Newport Beach, Calif.

Some new results on f_{max} for drift transistors are a by-product of the analysis.

The paper is divided into four parts. In Section I, the basic expression to be used in the theoretical development is obtained, and the two special modes of operation mentioned above are distinguished.

Section II contains the theory for the frequency ranges in which the transistor should be used as a three-terminal element. It is highlighted by the proof that the simple circuit shown in Fig. 1 will oscillate at the maximum frequency which a uniform-base transistor will allow for *any* circuit configuration in which RF current flows in all three leads.

Section III contains the theory for the frequency ranges where the transistor should be used as a two-terminal element, or "transit-time" diode. In this mode, no RF current flows in the base lead; hence, r_b' does not appear in the formulas of this section. The maximum frequency of oscillation depends principally upon parasitic resistances in the emitter and collector.

Numerical examples and some experimental results are given in Section IV, along with an interesting division of the frequency scale into bands, each of which is labelled as 1) belonging to the "three-terminal" class, 2) belonging to the "two-terminal" class or 3) being a frequency band over which oscillations cannot be produced with this circuit.

Section I

The attack to be used in developing the theory is to calculate the impedance which the circuit shown in Fig. 1 produces at the terminals AB. The phase of this impedance determines whether the circuit can be made to oscillate at the frequency in question. If

$$| \operatorname{Arg} Z_{in}(j\omega) | = | \operatorname{Arg} [v(j\omega)/i(j\omega)] | > 90°, \qquad (2)$$

then the real part of the impedance seen looking in at the terminals AB is negative, and oscillations can exist (with a tuned circuit of appropriate Q). Whether the inequality can be achieved at any given frequency is a function of both the transistor parameters (principally the ω_α, r_b' and C_e of the transistor model) and the impedance function selected for Z. Of course, even for the optimum choice of Z, there may be a frequency f_{max} beyond which the inequality can no longer be obtained, and this frequency, if it exists, is the "maximum frequency of oscillation."

The manner in which the transistor parameters affect the calculation of f_{max} depends to a large extent upon the model which one chooses to represent the transistor. For example, one may wish to include emitter and collector spreading resistances and lead inductances, as is done in the model of Fig. 2. These parameters play an important role in determining the maximum frequency of oscillation and may be included in the theory. However, for simplicity of exposition, these elements will be initially neglected, and their effects on the formulas estimated at a later point. It will also be assumed at the outset that the emitter transition capacitance C_t

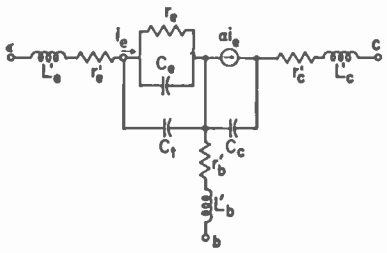

Fig. 2—Possible transistor model for use in calculating $Z_{in}(j\omega)$.

is small compared to C_e, the diffusion capacitance for the emitter-base region. (A moderately large forward bias may be required to achieve this condition in drift transistors.) This latter assumption allows us to consider the r_eC_e parallel combination as being part of the external circuit connecting emitter and collector, and thus to account for the loss associated with the equivalent series resistance of this combination in a simple way.

Under these assumptions, the part of the transistor model as yet unaccounted for is shown in Fig. 3(a). The problem now is to calculate the impedance produced at the terminals CD due to the transistor action. (Terminals CD are equivalent to terminals AB with the approximations given above.) The "calculation" may be done by inspection of Fig. 3(a) and 3(b). It is apparent from these figures that

$$Z_{CD} = (1 - \alpha)Z' \qquad (3)$$

where Z' is defined in Fig. 3(b). The inequality (2) applied to Z_{CD} yields the basic condition for oscillation:

$$| \operatorname{Arg} [(1 - \alpha)Z'] | > 90°. \qquad (4)$$

One important conclusion can be drawn immediately from (4): Since the argument of $(1-\alpha)$ is always less than 90° in magnitude, the argument of Z' and the argument of $(1-\alpha)$ should be of the same sign if it is desired to meet the inequality at all.

To expand upon this point, typical phasor diagrams of α and $(1-\alpha)$ are shown in Fig. 4. The plot of $(1-\alpha)$ is divided into two parts by the solid and dashed segments. For frequencies lying on a solid portion of the curve (*i.e.*, $0<\omega<\omega_1$, $\omega_2<\omega<\omega_3$, $\cdots$), $(1-\alpha)$ has a positive argument; hence Z' should have a positive argument to achieve negative resistance at the terminals CD. For Z' to have a positive argument, however, we must connect an inductive impedance Z between base and collector. In this configuration, RF current flows in all three leads and the maximum frequency of oscillation corresponds closely to the estimate given by Pritchard.[2]

For frequencies lying on a dashed portion of the $(1-\alpha)$ curve (*i.e.*, $\omega_1<\omega<\omega_2$, $\omega_3<\omega<\omega_4$, $\cdots$), a negative argument of Z' is required. This may be readily obtained by making Z an open circuit at the RF frequency, so that Z' is purely capacitive. This achieves the maximum negative argument possible for Z': 90°. In this configuration, no RF current is required in the base lead to produce negative resistance at the terminals CD (though the base lead must still be used for biasing purposes). The transistor is now behaving as a two-

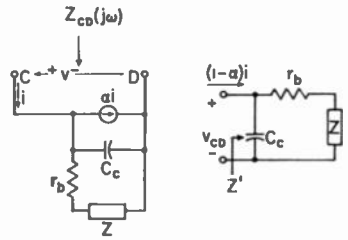

(a) (b)

Fig. 3—Simplified transistor model for calculating $Z_{CD}(j\omega)$.

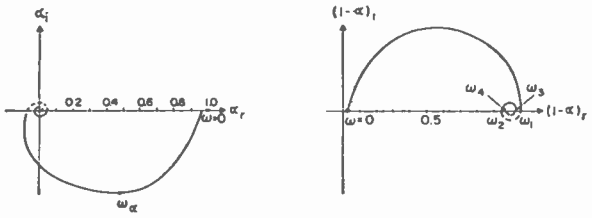

(a) (b)

Fig. 4—Illustrative phasor diagrams of α and $(1-\alpha)$ as a function of frequency (ω). (a) α. (b) $(1-\alpha)$.

terminal negative resistance (with some associated reactance), and the extrinsic base resistance does not directly affect the maximum frequency of oscillation. This is the transit-time mode studied by Shockley.[3]

Phasor diagrams for voltage and current which illustrate the oscillation conditions may be readily constructed from the phasor diagram of $(1-\alpha)$, as in Fig. 5. To study the operation of a three-terminal mode oscillator at frequency ω_a, we construct the plot shown in Fig. 5(a). i is used as the reference (1 ampere at zero phase). The current $(1-\alpha)i$ is the phasor whose end point rests on the $(1-\alpha)$ curve at the frequency ω_a. The voltage V_{CD} is then a phasor of length $|(1-\alpha)Z'|$ at an angle of [Arg Z'+Arg $(1-\alpha)$] from the reference. V_{CD} has a real part V_{CDr} and an imaginary part V_{CDi}. The magnitude of the negative resistance provided at the terminals CD is $|V_{CDr}|$ since i is 1 ampere. The circuit connected to the points CD of Fig. 3 should have a Q of $|V_{CDi}/V_{CDr}|$ for the circuit to oscillate at the frequency ω_a.

Since both Arg Z' and Arg $(1-\alpha)$ decrease as the frequency is increased, V_{CDr} will decrease as the frequency is increased and the circuit will ultimately cease to oscillate. In the absence of parasitic resistances in the emitter and collector, the maximum frequency of oscillation is obtained when [Arg Z'+Arg $(1-\alpha)$] is equal to 90°.

Operation in the two-terminal mode at a frequency ω_b yields the plot shown in Fig. 5(b). Arg Z' for this mode is always −90°, so that V_{CDr} is always finite. The circuit Q which must be presented at the terminals CD is once again $|V_{CDi}/V_{CDr}|$. The maximum frequency of operation for this mode is determined by finding the frequency at which $|V_{CDr}|$ is equal to the parasitic resistances in the transistor's emitter and collector plus the effective series resistance of the external tuned circuit.

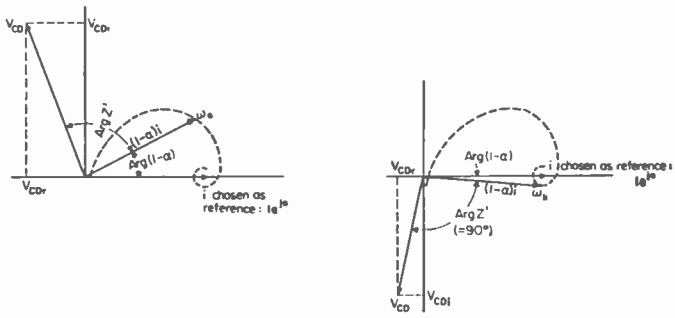

(a) (b)

Fig. 5—Phase plots of V_{CD} and i which meet the requirements for oscillation. (a) Typical plot of V_{CD} and i for three-terminal mode of operation. (b) Typical plot of V_{CD} and i for two-terminal mode of operation.

For both modes of operation, we could postulate a collector voltage which produces an avalanche multiplication factor M at the collector junction. The phasor plot of α is then multiplied by M, and the phasor plot of $1-\alpha$ is replaced by a phasor plot of $1-M\alpha$. This increases the high-frequency capabilities of the circuit, though in a somewhat unsatisfactory way since the stability of the oscillation frequency depends on the constancy of M.[7]

Section II

We now consider in more detail the operation of the transistor as a three-terminal element in the circuit of Fig. 1. In this configuration, the condition for oscillation requires Z' to have a positive phase angle, or, equivalently, it requires Z to be an inductive impedance. When an inductive impedance is connected between base and collector, a phase angle-vs-frequency curve similar to that shown in Fig. 6 will be obtained. The maximum value of $\phi(\equiv \text{Arg } Z')$ is always less than 90°, though it may approach 90° arbitrarily closely at low frequencies. The high frequency maximum of ϕ is severely restricted by the presence of C_c and r_b', and it is this restriction together with the properties of $(1-\alpha)$ which gives rise to a maximum frequency of oscillation for the transistor as a three-terminal element.

It is reasonably obvious that, as long as one remains in a frequency range where a positive angle for Z' is possible, ϕ may be maximized at any given frequency by an appropriate choice for Z. It is also apparent that this choice always requires Z to be a pure reactance, $Z=jX$. In anticipation of a later need, we will now calculate the optimum value for X and the associated maximum phase.

After some manipulation, the reader can verify that the tangent of the phase angle of Z' may be written as

$$\tan\phi = \frac{X(1 - X\omega_0 C_c) - r_b'\omega_0 C_c}{r_b'} \tag{5}$$

[7] A similar proposal has been suggested by H. N. Statz and R. A. Pucel, "Negative resistance in transistors based on transit-time and avalanche effects," Proc. IRE (Correspondence), vol. 48, pp. 948–949; May, 1960.

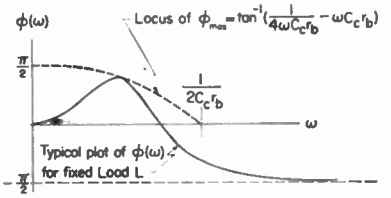

Fig. 6—Illustrative plot of ϕ and ϕ_{max} vs ω.

where X represents the value of the inductive reactance, to be chosen for Z. The maximum positive value of $\tan \phi$ at a given frequency ω_0 is obtained when

$$X = \frac{1}{2\omega_0 C_c} \tag{6}$$

and the maximum is

$$\phi_{\max} = \tan^{-1}\left(\frac{1}{4\omega_0 C_c r_b'} - \omega_0 C_c r_b'\right). \tag{7}$$

The reactance represented by (6) is, of course, not realizable in a fixed inductance except at one frequency. However, for our purposes, it is legitimate to consider "adjusting" L to its optimum value for each frequency ω_0, and thus achieve the $\phi_{\max}$ given by (7) at any given value of ω_0.

We are now in a position to give a simple graphical interpretation of the requirement expressed by (4). Fig. 7(a) shows hypothetical plots of $\phi_{\max}$ and the Arg $(1-\alpha)$ as a function of frequency; when $[\phi_{\max}+\text{Arg}\ (1-\alpha)]$ is greater than $\pi/2$, oscillations can exist.

Of course, the relative positions of the $\phi_{\max}$ and Arg $(1-\alpha)$ curves depend on the relationship between ω_α and the $C_c r_b'$ product. However, for most practical transistor structures, the relationship will be that shown in Fig. 7, where the zero value of $\phi_{\max}$ is well beyond the first maximum of Arg $(1-\alpha)$ on the frequency axis.

To compute the maximum frequency of oscillation for the circuit in general terms, we require an expression for Arg $(1-\alpha)$. Furthermore, this expression need not be accurate for radian frequencies exceeding $1/2C_c r_b'$, since oscillations beyond this frequency are impossible anyway because of the nature of $\phi_{\max}$. Hence, while the hyperbolic secant expression for α is certainly more exact than the one or two pole expressions frequently used, these latter expressions normally provide sufficient accuracy in the range where it is required to justify their use in calculating a maximum frequency of oscillation for three-terminal operation. [See Fig. 7(b).] We therefore illustrate the method of calculating $f_{\max}$ with a single pole expression for α and at the same time produce the standard formula for $f_{\max}$.

Letting α be expressed by

$$\alpha = 1/(1 + j\omega/\omega_\alpha) \tag{8}$$

where ω_α is the radian "cutoff frequency" for α, we obtain

$$\text{Arg}\ (1-\alpha) = 90^\circ - \tan^{-1}(\omega/\omega_\alpha). \tag{9}$$

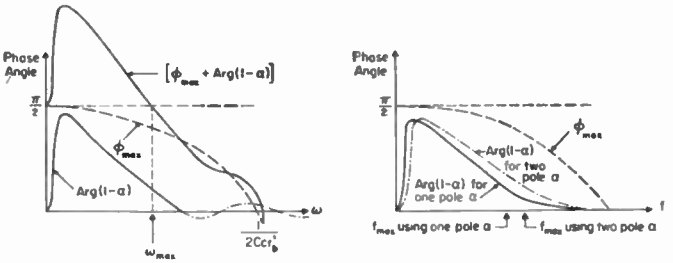

(a) (b)

Fig. 7—Illustrative plots of $\phi_{\max}$ and Arg $(1-\alpha)$ for determining maximum frequency of oscillation in three-terminal mode. (a) $\alpha = \text{sech}\ w/L_p\sqrt{1+j\omega\tau_p}$. (b) One and two-pole approximations to $\alpha = \text{sech}\ w/L_p\sqrt{1+j\omega\tau_p}$.

Using (7) and (9) in the inequality (4), we obtain

$$\tan^{-1}\left(\frac{1}{4\omega C_c r_b'} - \omega C_c r_b'\right) - \tan^{-1}\left(\frac{\omega}{\omega_\alpha}\right) \geq 0 \tag{10}$$

or

$$\frac{1}{4\omega C_c r_b'} - \omega C_c r_b' \geq \frac{\omega}{\omega_\alpha} \tag{11}$$

as an inequality which ω, the desired frequency of oscillation, must satisfy. The maximum frequency of oscillation permitted by the inequality (2) is

$$f_{\max} = \sqrt{\frac{f_\alpha}{8\pi C_c r_b'(1 + \omega_\alpha C_c r_b')}}. \tag{12}$$

For many types of transistors, $\omega_\alpha C_c r_b' \ll 1$, so the expression

$$f_{\max} \cong \sqrt{\frac{f_\alpha}{8\pi C_c r_b'}} \tag{13}$$

is close to the maximum value given by (12). Since the purpose of such calculations is to serve only as a guide to performance, (13) represents a reasonably good estimate, and is frequently used as a figure of merit for a transistor structure. Both of the estimates (12) and (13) fail to account for the equivalent series resistance of the emitter $r_e C_e$ combination, but this precision is usually not justified by the use of a one-pole expression for α.

It is interesting to note that (13) is the same as that obtained by Pritchard using a power gain criterion for establishing $f_{\max}$. It may also be established in other ways, each of which does not rely on a particular circuit configuration for the calculation. Therefore, it follows that with an appropriate selection for Z, the simple circuit shown in Fig. 1 is capable of oscillating at any given frequency up to essentially the maximum allowable in a three-terminal mode.[8]

[8] The phrase "essentially the maximum" is used here to indicate that other circuit configurations which consider the parasitic elements in the circuit design may be capable of producing a slightly higher maximum frequency.

A somewhat more sophisticated and possibly better estimate of the maximum frequency of oscillation than that given by (13) may be obtained by the use of a two-pole approximation for α:[9]

$$\alpha = \frac{1}{\left(1 + j\frac{\omega}{1.17\omega_0}\right)\left(1 + j\frac{\omega}{6.83\omega_0}\right)}. \tag{14}$$

the second factor in the denominator accounting approximately for the so-called "excess phase" of α. The argument of $(1-\alpha)$ may now be written as

$$\text{Arg}\,(1-\alpha) = 90° + \tan^{-1}\frac{\omega}{8\omega_0} - \tan^{-1}\frac{\omega}{1.17\omega_0} - \tan^{-1}\frac{\omega}{6.83\omega_0} \tag{15}$$

Using (15) and (7) in the inequality (4) as before, one obtains

$$\tan^{-1}\frac{\omega}{8\omega_0} + \tan^{-1}\left(\frac{1}{4\omega C_c r_b'} - \omega C_c r_b'\right) \geq \tan^{-1}\frac{\omega}{1.17\omega_0} + \tan^{-1}\frac{\omega}{6.83\omega_0} \tag{16}$$

as the inequality which ω must satisfy. If we assume that

$$\frac{1}{4\omega C_c r_b'} \gg \omega C_c r_b'$$

inequality (16) can be put in the form

$$-\left(\frac{\omega}{\omega_0}\right)^4 - 56\left(\frac{\omega}{\omega_0}\right)^2 + \frac{16}{\omega_0 C_c r_b'} \geq 0 \tag{17}$$

by use of the formula for the tangent of the sum of two angles. Inequality (17) gives

$$f_{\max} \cong \sqrt{\frac{f_\alpha}{7\pi C_c r_b'}}. \tag{18}$$

This result is interesting and possesses a simple interpretation: the extra phase provided by the two-pole approximation for α allows inequality (4) to be maintained to a higher frequency than is indicated by the single pole approximation for α. [Refer again to Fig. 7 (b).]

This fact also leads one naturally to a calculation of the maximum frequency of oscillation for a drift transistor, where the phase characteristic of α is even more favorable for obtaining high frequency oscillation. Once again, the α for three-terminal operation can be moderately well approximated with a two pole function.[9]

[9] For the derivation of this two-pole approximation, see, for example, J. G. Linvill and J. F. Gibbons, "Transistors and Active Circuits," McGraw-Hill Book Co., Inc., New York, N. Y.; 1961.

$$\alpha = \frac{1}{\left(1 + j\frac{\omega}{\omega_1}\right)\left(1 + j\frac{\omega}{a\omega_1}\right)} \tag{19}$$

where the factor a depends on the ratio of the base doping at the emitter to the base doping at the collector, N_{DE}/N_{DC}. If we define

$$\eta = \omega/\omega_1, \tag{20}$$

then

$$\text{Arg}\,Z' + \text{Arg}\,(1-\alpha) = 90° \Rightarrow \eta_{\max}^4 + (a^2 + a + 1)\eta_{\max}^2 - (a^2 + a)/4\omega_1 C_c r_b' = 0. \tag{21}$$

When a and the $\omega_1 C_c r_b'$ product are known, (21) can be solved for $\eta_{\max}$ and hence $\omega_{\max}$.

As an example, the $C_c r_b'$ product for a 2N502 is about 13 $\mu\mu$sec with an f_α of about 290 mc for particular bias conditions. If we assume that $a = 2$ (corresponding to $N_{DE}/N_{DC} = 100$), (19) yields $\omega_\alpha = 0.84\ \omega_1$. Using these values, we have

$$\eta_{\max} = 2.1\omega_1$$
$$f_{\max} = 2.5 f_\alpha = 725 \text{ mc}. \tag{22}$$

Since N_{DE}/N_{DC}, and hence a, depend on the actual base width, one can achieve a relatively wide range of values of $f_{\max}$ by varying the bias conditions. Experimental results on such measurements will be discussed in Section IV.

There is one interesting point in connection with (21) which is worth mentioning. From (19) it is apparent that as $a \to \infty$, α becomes a single-pole function with $\omega_1 = \omega_\alpha$. Eq. (21) yields, as $a \to \infty$,

$$f_{\max} = \sqrt{\frac{f_\alpha}{8\pi r_b' C_c}}.$$

However, for finite values of a, $f_{\max}$ cannot be simply expressed in such a form, and will be smaller than the number one would calculate from the standard expression. Of course, these conclusions rest on the adequacy of a two-pole expression for α, but such a form is sufficiently accurate for many bias conditions to suggest that, at least for the circuit of Fig. 1,

$$f_{\max} = \sqrt{\frac{f_\alpha}{8\pi r_b' C_c}}$$

is not an exceptionally accurate figure of merit for a drift transistor.[10,11]

[10] When the calculation for $f_{\max}$ is artificially cast in such a form for a 2N502, one finds

$$f_{\max} \sim \sqrt{\frac{f_\alpha/n}{8\pi r_b' C_c}}$$

where n is a bias-dependent factor that ranges between 1.5 and 3 for typical conditions.

[11] Excellent phasor plots of α for a 2N502 have been published in J. D. McCotter, N. J. Walker, and M. M. Fortini, "A coaxially packaged MADT for microwave applications," IRE Trans. on Electron Devices, vol. ED-8, pp. 8–12; January, 1961.

To review briefly, (13), (18), and (22) represent estimates of the maximum frequency at which negative resistance may be produced at the terminals CD in Fig. 5; we have loosely labelled these estimates as the maximum frequencies of oscillation for the various transistor models used. For several types of transistors, however, the maximum frequencies thus estimated are seriously in error in that they do not accurately give the maximum frequency at which negative resistance may be produced between emitter and collector terminals; *i.e.*, terminals AB of Fig. 1. Hence, it is appropriate at least to mention the major causes of departure from the first-order theory and to estimate the effects of these departures on f_{max}.

One cause of departure already discussed is the positive resistance introduced by the series equivalent of the emitter resistance r_e. The effect of this resistance may generally be reduced by increasing the dc emitter bias level, though there are obvious limitations on how far this can go. Increasing the emitter bias level also has a salutory effect on the C_e/C_t ratio, which we have assumed to be infinite (see Section I). The effect of emitter bias current is especially noticeable on drift transistors, and indeed the maximum frequency of oscillation in such cases depends in an important way on emitter bias currents when these currents are less than about 3 ma.

Spreading resistance in the emitter (r_e') is also directly in series with the negative resistance produced at terminals CD and thus decreases the actual value of f_{max}. The emitter region is generally doped very heavily, so that this resistance is relatively small, and its effect is of second-order importance. Lead inductance in the emitter circuit is generally also of second-order importance, though the effect of header capacitance from emitter to base magnifies the importance of this parasitic element. Generally speaking, advanced packaging techniques minimize this effect by getting it out of the frequency range of interest.

Since the doping level in the collector may not be high, the resistance associated with the collector body and lead, together with the collector lead inductance, generally represent an important effect. Analysis which accounts for this effect is straightforward but somewhat uninteresting for the purpose of this article. Hence, we shall be content with the observation that to a first approximation reduced values of r_c' and L_c' may be included with Z. The effect of L_c' is thus not particularly important, while the reduced r_c' adds directly to r_b'. For a one-pole α and r_b' equal to r_c', f_{max} is reduced by about 12 per cent from the value given in (13).

Section III

We turn our attention now to the use of a transistor in the "transit-time" mode. To study such operation, it is first necessary to recognize that while a one- or two-pole expression for α is adequate for studying the three-terminal connection for the reasons stated above, these approximations to α do not permit us to study the transit-time mode at all, since neither approximation allows Arg $(1-\alpha)$ to be negative. We must, therefore, resort immediately to the phasor diagrams of α and $(1-\alpha)$ which arise from the distributed transport functions.[12] Two such plots are shown in Fig. 8; part (a) gives the α for a p-n-p drift transistor with a N_D (emitter)/N_D (collector) = 100; part (b) shows $(1-\alpha)$ for the same transistor. The doping gradient in the base is assumed to be exponential, so that a constant drift field is produced. Only drift transistors will be considered since the phase of α for this type is most favorable for transit-time operation.

In Section I it was observed that the phase angle of Z' for this mode of operation could be $-90°$ at any given frequency by merely making Z an open circuit to RF. Hence, the plot of $[\phi_{max}+\text{Arg }(1-\alpha)]$ becomes extremely simple (see Fig. 9), and the condition for oscillation is also simply stated: Whenever Arg $(1-\alpha)$ is negative, oscillations in the transit-time mode are possible (neglecting parasitic losses, of course).

Eq. (3) gives the input impedance at the terminals CD as

$$Z_{CD} = (1-\alpha)Z' = \frac{1-\alpha}{pC_c} \tag{23}$$

which may also be written by inspection from Fig. 3. Since no lateral current is required in the base, r_b' does

[12] The "excess phase" approximation for α does allow the phase of $(1-\alpha)$ to become negative, and can be used for approximate calculations, though considerable accuracy in the Arg $(1-\alpha)$ is required, and the distributed transport functions, or even better, measured data, are preferable.

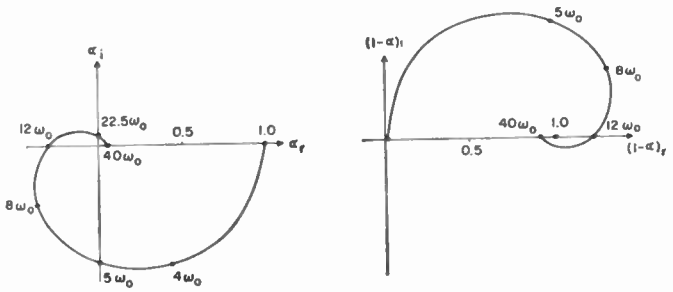

(a) (b)

Fig. 8—Polar plots of α and $(1-\alpha)$ for a drift transistor with $N_{DE}/N_{DC}=100$ and $\omega_0=2D_p/W_b^2$.

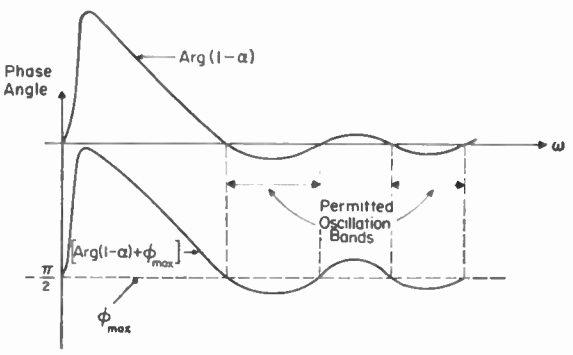

Fig. 9—Illustrative plots of ϕ_{max} and Arg $(1-\alpha)$ for determining oscillation frequency bands in two-terminal mode.

not appear in (23). The calculation of Z_{CD}, therefore, amounts to substitution of the transcendental expression for α which applies for the given biasing conditions.

From a physical viewpoint, we may profitably consider a limiting case of the transistor which serves to emphasize the reason for labelling this mode of operation as the transit-time mode. The limiting case consists of a transistor which has infinite minority-carrier lifetime in the base. Minority carriers are assumed to move across the base by pure drift, reaching the collector in a time τ. Hence,

$$\alpha = e^{-j\omega\tau} \tag{24}$$

and (23) becomes

$$Z_{in} = \frac{1 - e^{-j\omega\tau}}{pC_c} \tag{25}$$

$$= \frac{\tau}{C_c} \frac{\sin \frac{\omega\tau}{2}}{\left(\frac{\omega\tau}{2}\right)} e^{-j(\omega\tau/2)}. \tag{26}$$

Eq. (26) is the familiar form of result for a transit-time diode.[13]

The effect of parasitic elements on this mode of operation is readily visualized. The effect of r_b' is essentially removed. r_e', L_e', r_c' and L_c' are now directly in series with the terminals AB. A bias condition which causes C_e/C_t to be very large is still required, but, given this condition, the r_eC_e combination is also in series with the terminals AB.

Section IV

To clarify some of the points made above, we now give some numerical examples. For these examples we shall suppose that a p-n-p drift transistor with an exponentially graded base and $N_{DE}/N_{DC} = 100$ is to be used in the oscillator circuit shown in Fig. 1. The transistor is assumed to have an f_α of 200 Mc (or an $\omega_0 = 2D_p/W_b^2$ of $2\pi.50$ mc), $C_c = 0.5$ $\mu\mu$f and $r_b' = 30$ Ω.

In a three-terminal mode, the maximum frequency of oscillation of the circuit should be, from (21),

$$f_{max} = 500 \text{ mc}.$$

If the circuit is to be operated at 250 Mc ($5\omega_0$), then from Fig. 8(b) we obtain

$$(1 - \alpha) = 1.2e^{j36°}$$

and from (6) and (7) we obtain

$$X_L = \frac{1}{2\omega C_c} = 640 \ \Omega$$

$$\phi = \tan^{-1}\left(\frac{1}{4\omega C_c r_b'} - \omega C_c r_b'\right) = 59.3°.$$

[13] This is a limiting form of a result derived in Shockley, *op. cit.*, which also may be found in vacuum tube diode literature.

Hence, the impedance seen at the terminals CD of Fig. 4 is

$$Z_{in} = (1 - \alpha)Z = 1.2 \times 1340e^{j95.3°}$$
$$= (-148 + j1600) \ \Omega.$$

A negative resistance of 150 Ω is more than adequate to compensate for the parasitic losses in the transistor and still provide enough negative resistance at the terminals AB to make the circuit oscillate. The circuit Q only needs to be about 10.

For the transit-time mode example, we consider operating at $f = 22.5f_0 = 1.125$ kMc. Z must now be a parallel resonant circuit at this frequency. (Header capacitance will be a part of this tank circuit and will also affect the value of L which will produce 640 Ω of inductive reactance in the preceding example.) Once again we obtain from Fig. 8(b)

$$(1 - \alpha) = 1.05e^{-j40}$$

so that

$$Z_{in} = \frac{(1 - \alpha)}{j\omega C_c} = (-21 - j299) \ \Omega.$$

A negative resistance of -21 ohms would probably be enough to make a transistor with low parasitic resistances oscillate in the transit-time mode. Unfortunately, the 21-ohm figure is somewhat too encouraging, since measured data on several transistor types indicate that the actual phase angle of $(1-\alpha)$ is not as great as that indicated by the computed curves of Fig. 8. However, with circuits of sufficient Q and transistors with low parasitic resistances, oscillations in the 1–2 kMc range can be produced in this mode.

The experimental setup used for verifying the general features of this theory is shown in Fig. 10, and consists of a pair of General Radio coaxial transmission lines provided with sliding shorts and arranged in such a way that the transistor can be mounted directly on a set of brass plugs fitted to the lines. While this arrangement could be improved, it is simple and easy to manipulate and actually serves its purpose quite well.

The formulas in Section II can be checked to some degree with existing transistors. For example, a 2N502, which is roughly equivalent to the hypothetical tran-

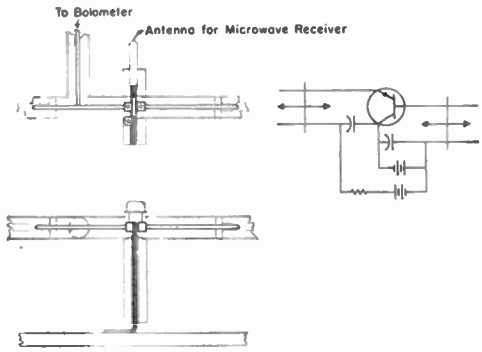

Fig. 10—Experimental arrangement used for verifying the theory.

sistor assumed above, can readily be made to oscillate up to 500 Mc in this setup, some of them continuing to oscillate strongly up to 850 Mc under proper biasing conditions. Using measured parameters for these units, one calculates maximum frequencies of oscillation from (21) which are within 15–30 per cent of those measured.

As a second check, the relevant portion of the phasor diagram for α was measured under various bias conditions, and calculations from these plots were compared with experimental data.[11] The agreement was within about 10 per cent in all cases tested. It is also apparent from these plots that a two-pole approximation for α is reasonably good for some bias conditions and rather poor for others. Hence, the error involved in calculating f_{max} from (21) may be appreciable in some cases.

The transit-time mode is difficult to observe with the setup given in Fig. 10. One important factor contributing to this difficulty is that the measured $(1-\alpha)$ characteristic first has $-4°$ phase at about 2 kMc for the 2N502's used, so that the negative resistance produced should be slightly less than -10 ohms. After accounting for parasitic losses in the transistor, the net negative resistance is quite small and hence a high Q circuit is required to produce oscillations. Operation in the transit-time mode has been observed with this setup, though an improved experimental arrangement is required to produce significant power output at these frequencies.[14]

In addition to operation in either of the two modes just described, the circuit was experimentally found to have a third mode of operation which is of possible technological significance and deserves some comment. The transmission lines can readily be adjusted so that they provide the three-terminal oscillating conditions at some basic frequency, such as 400 Mc, and except for parasitic losses would also provide the oscillating conditions at the fifth harmonic, 2 kMc. In such a case, the power output at 2 kMc may be within 10 db of that at 400 Mc, while all other harmonics are much below this (50–60 db in some cases). This behavior could arise if the 2 kMc mode was almost in an oscillatory condition of its own, so that the fifth harmonic of the 400 Mc signal could produce sustained ringing.[15] The power output at 2 kMc can be several milliwatts; so with some improvements this effect could also provide a small source of power at kilomegacycle frequencies.[16]

Conclusion

It has been shown in this paper that a phasor diagram of $(1-\alpha)$ may be conveniently used to distinguish between the three-terminal and "transit-time" modes of operation for the oscillator circuit of Fig. 1. Furthermore, the phasor diagram of $(1-\alpha)$ together with values for C_c and r_b' are all the information that is required to select appropriate oscillator circuit components. Finally, when mathematical approximations to α are made, estimates of the maximum frequency of oscillation allowed by each approximation are obtained.

A convenient summary of the theory and experiment is given in Fig. 11(a) and 11(b). In this figure, the frequency scale is divided into bands, each band being labelled as belonging to the three-terminal mode, to the two-terminal mode, or being a dead space. Part (a) of the figure is constructed for a hypothetical transistor with all parasitic resistances, including r_b', equal to zero. For such a case, (7) indicates that at any frequency a positive phase angle of $+90°$ is attainable, an intuitively obvious result. The maximum frequencies of oscillation given in Section II are all infinite, although the circuit itself changes its operating mode back and forth between the three- and two-terminal modes.

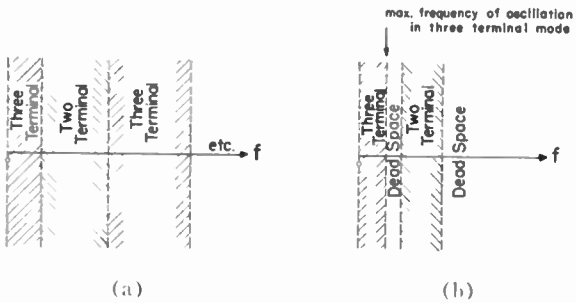

Fig. 11—Illustrating the division of the frequency scale into oscillation bands for the circuit of Fig. 1. (a) Hypothetical transistor with no parasitic resistances. (b) Typical portrait for a real transistor.

A typical transistor will have a protrait more nearly like that shown in Fig. 11(b). There will usually be a dead space separating the first two oscillation bands which is principally due to the effect of r_b' in limiting ϕ_{max}. Parasitic resistances in both the transistor and the external circuit elements will not allow an oscillatory condition in the first part of the first two-terminal band, and the high end of this band will also be limited by these parasitic losses. Transistors which have a high collector body resistance (normal mesa transistors, for example) may never produce oscillations in the transit-time mode, and the first three-terminal frequency band will also cut off at a lower frequency than that expected from a consideration of r_b' alone.

Acknowledgment

The author would like to acknowledge the stimulation he received from V. Vodicka to work on this problem. He also benefited from discussions with his colleagues at Stanford University, and from some comments on the manuscript by an anonymous editorial reviewer. Dr. H. Heffner and A. G. Little also gave generously of their time in the experimental evaluation of the ideas. Space and facilities were provided by a joint-services contract.

[11] The transistors described by Zuleeg, *op. cit.*, are mounted directly in strip transmission line.

[15] This is not the only way to explain such behavior, though it is a promising candidate, and hence, seems to deserve mention in the context of this paper.

[16] The interested reader should see F. A. Brand and G. E. Hambleton who report a similar observation in *Electronic Design*, pp. 148–149; August 17, 1960

Actual Noise Measure of Linear Amplifiers*

K. KUROKAWA†, MEMBER, IRE

Summary—Haus and Adler defined a noise measure M_ϵ and proposed to use the optimum value $M_{\epsilon,\mathrm{opt}}$ of the noise measure as a valid measure of the absolute quality of amplifier noise performance. However, neither M_ϵ nor $M_{\epsilon,\mathrm{opt}}$ includes the contribution from the noise originating in, and reflected back to, the load.

It is the aim of this paper to propose a different noise measure M, which includes the noise contribution from the load, and hence enables us to compare the performance of two different amplifiers which are not necessarily optimized.

It is shown that the optimum value M_{opt} of M is equal to $M_{\epsilon,\mathrm{opt}}$, and most of the conclusions Haus and Adler obtained for $M_{\epsilon,\mathrm{opt}}$ hold equally well for M_{opt}. But the meaning of M is quite different from that of M_ϵ. A detailed discussion about this difference is given in the final section, and it is shown that for practical amplifiers, M is a more appropriate measure of the quality of the noise performance.

I. Introduction

A QUANTITATIVE measure to express the noise performance of an amplifier has been the subject of debate for a long time. First, a rather vaguely defined signal-to-noise ratio at the output was the most popular one, and then the concept of noise figure took its place. In 1958, Haus and Adler[1] extensively studied linear-noisy networks and, as the result, they proposed a newly defined quantity "noise measure" as the most suitable measure for the noise performance of an amplifier. Their excellent treatment clarified a number of important properties of linear-noisy networks, but the proposed noise measure still left some questions.

For an ordinary amplifier with matched input and output circuits, their noise measure fits our intuition very well; on the other hand, for an Esaki-diode amplifier with mismatched input and output circuits, it does not fit our intuition[2] at all. In fact, Penfield[3] recently proved that an amplifier with a noisy-negative resistance has the same value for the noise measure irrespective of the lossless circuit in which the negative resistance is imbedded. This means that, for example, Esaki-diode amplifiers with and without a circulator have the same noise performance. The output noise power of the amplifier without a circulator includes the contribution from the noise originating in, and reflected back to, the load, in addition to the noise from the source and the diode which is common to both amplifiers; hence, the amplifier without a circulator must, in general, be worse than the one with a circulator. This point of view, however, is not reflected in Haus and Adler's noise measure.

This paper proposes a different noise measure, which is of greater practical significance. To distinguish the new noise measure from the old, the old one will be called the "exchangeable noise measure" and expressed by M_ϵ, while the term "actual noise measure" and the symbol M will be used for the new noise measure which will be defined in this paper. This noise measure has a very similar form to the one for the exchangeable noise measure; the meaning, however, is quite different. It enables us to compare the noise performance of two different amplifiers which are not necessarily optimized (corresponding more to the practical case). This was not possible with the exchangeable noise measure.

II. Definition of Actual Noise Measure

An amplifier is a device which amplifies the signal coming from a source with an internal impedance, of which the real part is positive, and delivers the amplified signal to a load which also has a positive real part in its impedance. On this basis, the actual gain G (transducer gain) of an amplifier is defined by[4]

$$G = \frac{\text{Actual signal-output power}}{\text{Available signal-input power}}. \tag{1}$$

Similarly, the actual noise figure F is defined by

$$F = \frac{\text{Actual noise-output power}}{\text{Available noise-input power}} \times \frac{1}{G}, \tag{2}$$

when the noise temperature of the source is standard (290°K). Using (1) and (2), the new noise measure is defined by

$$M = \frac{F - 1}{1 - \frac{1}{G}}. \tag{3}$$

If "actual" is replaced by "available," G and F become the available gain and the conventional noise figure, respectively. Further, if everywhere "available" is replaced by "exchangeable," G, F and M become the exchangeable gain G_ϵ, the extended noise figure F_ϵ, and the exchangeable noise measure M_ϵ, respectively. It is worth noting that when the output of the amplifier is matched, each corresponding definition gives the same value.

* Received by the IRE, May 12, 1961.

† Bell Telephone Labs., Inc., Murray Hill, N. J.

[1] H. A. Haus and R. B. Adler, "Optimum noise performance of linear amplifiers," PROC. IRE, vol. 46, pp. 1517–1533; August, 1958. Also, "Circuit Theory of Linear Noisy Networks," John Wiley and Sons, Inc., New York, N. Y.; 1959.

[2] When evaluating the noise performance of a negative-resistance amplifier, we take the noise contribution from the load into account. However, from the conventional point of view, one may well attribute this to the second stage, if it exists, and evaluate correctly the over-all noise performance of the system. This has been done by Haus (private communication).

[3] P. Penfield, Jr., "Noise in negative resistance amplifiers," IRE TRANS. ON CIRCUIT THEORY, vol. CT-7, pp. 166–170; June, 1960.

[4] Meaning of "actual" will be clear from (7) and (16).

III. Properties of Actual Noise Measure

An amplifier is a noisy two-terminal-pair network and, therefore, after a certain lossless transformation, it can be represented by a "canonical form." This has, at most, two resistances with independent noise voltages. For an amplifier, at least one of the resistances must be negative. For the time being, let us assume that both of them are negative and investigate the possible range of the value of M after the lossless transformation shown in Fig. 1. The lossless network has four ports, and for each port we define

$$a_i = \frac{V_i + Z_i I_i}{2\sqrt{\text{Re } Z_i}}, \tag{4}$$

and

$$b_i = \frac{V_i - Z_i^* I_i}{2\sqrt{\text{Re } Z_i}} \tag{5}$$

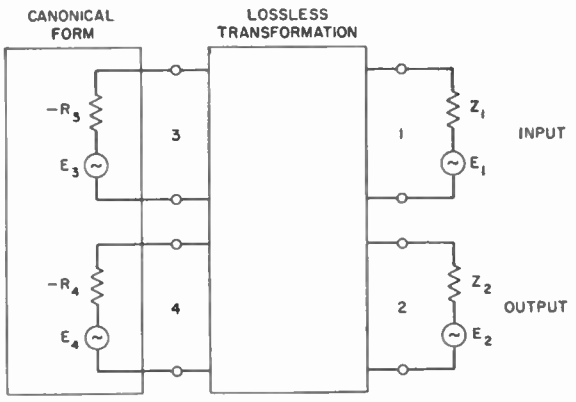

Fig. 1—Lossless imbedding of an amplifier.

Then the lossless transformation is represented by a scattering matrix S connecting a and b by a relation

$$b = Sa, \tag{6}$$

where a and b are column matrices of the four a_i and four b_i, respectively.

The power input to either port 1 or port 2 is

$$|a_i|^2 - |b_i|^2, \qquad i = 1, 2.$$

The available power from the input is $|a_1|^2$, and the power into the output load is $|b_2|^2$. Therefore, the gain G is given by

$$G = \frac{|b_2|^2}{|a_1|^2} = \frac{|S_{21}|^2 |a_1|^2}{|a_1|^2} = |S_{21}|^2. \tag{7}$$

Ports 3 and 4 have negative resistances, and so the power input to port 3 or port 4 is

$$|b_i|^2 - |a_i|^2 \qquad i = 3, 4.$$

The exchangeable power from the noise source at each port is

$$P_{ei} = -|a_i|^2, \qquad i = 3, 4. \tag{8}$$

The total power into the lossless network must be zero, and hence

$$|a_1|^2 + |a_2|^2 - |a_3|^2 - |a_4|^2 - |b_1|^2 - |b_2|^2 + |b_3|^2 + |b_4|^2 = 0. \tag{9}$$

This can be written as

$$a^+Pa - b^+Pb = 0, \tag{10}$$

where $^+$ indicates the transposed conjugate matrix, and P is

$$P = \begin{bmatrix} 1 & 0 & 0 & 0 \\ 0 & 1 & 0 & 0 \\ 0 & 0 & -1 & 0 \\ 0 & 0 & 0 & -1 \end{bmatrix}. \tag{11}$$

Using (6), (10) can be rewritten as

$$a^+(P - S^+PS)a = 0. \tag{12}$$

Since a is arbitrary, we conclude that

$$S^+PS = P. \tag{13}$$

This is the constraint on the scattering matrix of the lossless network. Eq. (13) is equivalent to

$$SP^{-1}S^+ = P^{-1}, \tag{14}$$

of which the 2-2 element is

$$|S_{21}|^2 + |S_{22}|^2 - |S_{23}|^2 - |S_{24}|^2 = 1. \tag{15}$$

We are now in a position to compute the noise measure M. The noise figure F is, by definition,

$$F = \frac{|S_{21}|^2 |a_1|^2 + |S_{22}|^2 |a_2|^2 + |S_{23}|^2 |a_3|^2 + |S_{24}|^2 |a_4|^2}{|S_{21}|^2 |a_1|^2}, \tag{16}$$

so that

$$M = \frac{F - 1}{1 - \frac{1}{G}} = \frac{|S_{22}|^2 |a_2|^2 + |S_{23}|^2 |a_3|^2 + |S_{24}|^2 |a_4|^2}{(|S_{21}|^2 - 1)|a_1|^2}. \tag{17}$$

Using the relation (15), we have finally

$$M = \frac{|S_{22}|^2|a_2|^2 + |S_{23}|^2|a_3|^2 + |S_{24}|^2|a_4|^2}{\{-|S_{22}|^2 + |S_{23}|^2 + |S_{24}|^2\}|a_1|^2} \cdot \quad (18)$$

From (17), we see that M is negative if, and only if, $G = |S_{21}|^2$ is smaller than unity.

Since (15) is the only constraint among the S_{21}'s, $|S_{22}|^2$, $|S_{23}|^2$ and $|S_{24}|^2$ can vary from zero to infinity arbitrarily provided that $-1 \leq \{-|S_{22}|^2 + |S_{23}|^2 + |S_{24}|^2\} \leq \infty$. Here we can assume that $|a_3|^2 \leq |a_4|^2$ without loss of generality. Then, from (18), the range of the value of M is easily found to extend from

$$-\frac{|a_2|^2}{|a_1|^2} \quad \text{to} \quad \frac{|a_3|^2}{|a_1|^2}$$

through infinity, as shown by the solid line in Fig. 2.

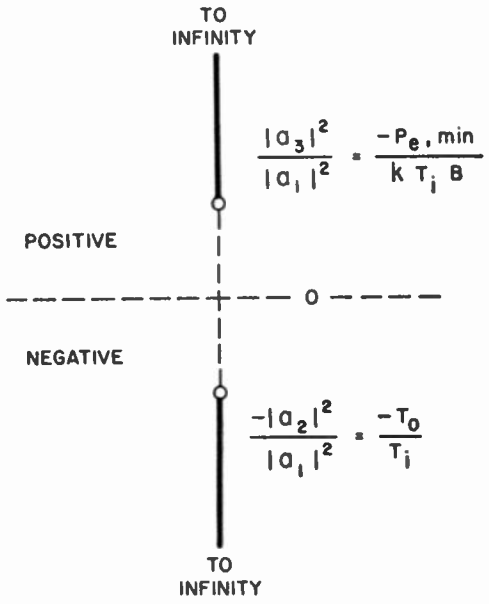

Fig. 2—Range of value of M.

Using the equivalent temperatures T_i (=290°K) and T_o of the input-source resistance and the output-load resistance, respectively, the range becomes from

$$-\frac{T_o}{T_i} \quad \text{to} \quad \frac{-P_{e3}}{kT_iB}$$

through infinity.

Referring to (17), the smaller positive value of M, the better the noise performance. Therefore, the optimum noise measure M_{opt} must correspond to $-P_{e3}/kT_iB$.

It is always possible to achieve M_{opt} with a lossless transformation since the transformation which gives a canonical form is lossless, and in principle a circulator is also lossless; hence, the combination of these two, as shown in Fig. 3, will be lossless, and gives M_{opt} (see Appendix I). Fig. 3 can provide an amplifier system of high gain, positive input and output resistances, and an excess noise figure of M_{opt}.

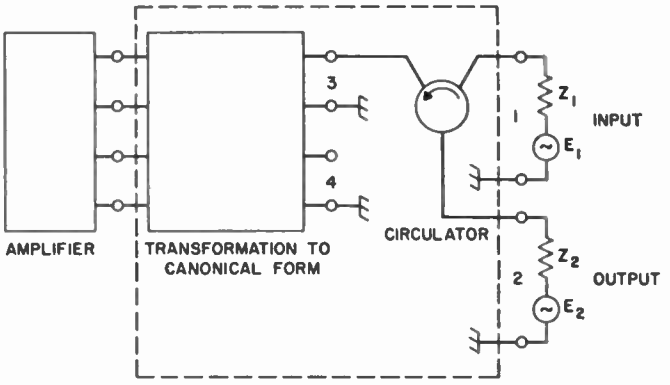

Fig. 3—Realization of M_{opt}.

It is quite straightforward to extend the discussion to the case of the canonical form with one positive and one negative resistance. If we compare the equivalent temperatures of the positive resistance and the load resistance, and designate the lower temperature by T_{min}, then the range of the value of M is from

$$-\frac{T_{min}}{T_i} \quad \text{to} \quad \frac{-P_e}{kT_iB}$$

through infinity, where P_e is the exchangeable noise power of the negative resistance. The rest of the above argument holds equally well in this case. The case of the canonical form with only one negative resistance is obvious from the above discussion and requires no further explanation.

Next, let us consider the interconnection of many amplifiers with an arbitrary passive network. Any passive network can be considered as a combination of a lossless network and positive resistances (Fig. 4). Some of the amplifiers may have a positive resistance in their canonical form. Let the lowest equivalent temperature among all these positive resistances, including the load resistance, be T_{min}, and the largest (smallest in magnitude) exchangeable noise power of the negative resistances in the canonical forms be $P_{e,min}$. Then a similar argument to that used above shows that the range of the value of M is from

$$-\frac{T_{min}}{T_i} \quad \text{to} \quad -\frac{P_{e,min}}{kT_iB}$$

through infinity. The optimum noise measure $M_{opt} = -P_{e,min}/kT_iB$ is achievable by connecting a 3-port circulator to the negative resistance with $P_{e,min}$ in a manner similar to Fig. 3, and effectively disconnecting all other negative resistances.

From the above discussion, we conclude as follows:

1) The smaller the positive value of the actual noise measure, the better will be the noise performance of the amplifier.
2) A negative actual noise measure means that the actual gain is less than unity.

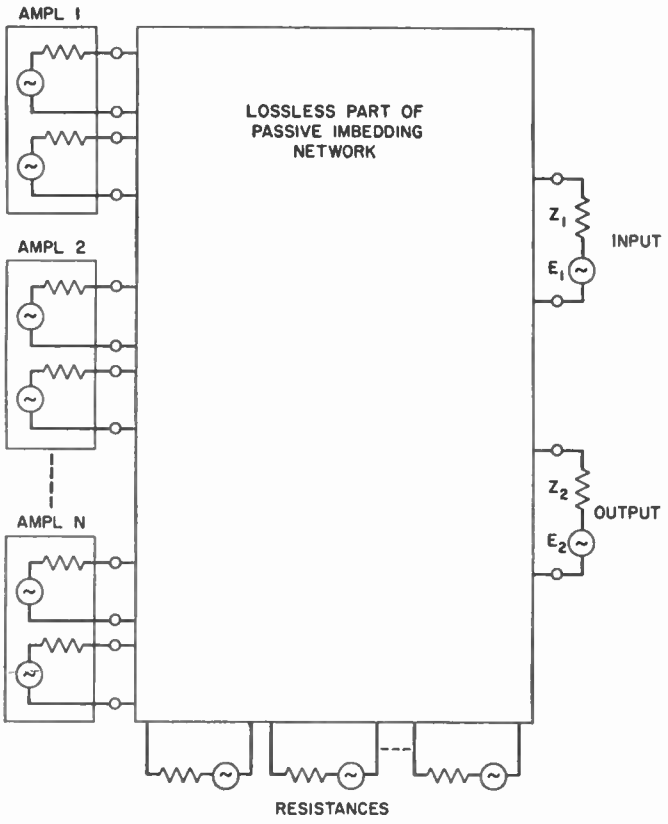

Fig. 4—Passive imbedding of amplifiers.

3) It is always possible to achieve M_{opt} with a lossless transformation.
4) It is impossible to achieve a positive value of M less than M_{opt} with any passive transformation.

A noise figure is meaningful only when the gain is specified beforehand. On the other hand, since an appropriate number of identical amplifiers cascaded through ideal isolators[5] produces an amplifier system with the desired gain and an excess noise figure almost equal to the actual noise measure of the component amplifier, the actual noise measure is meaningful by itself. The gain of the component amplifier determines the number of amplifiers required, but does not affect the over-all noise performance. Because of this fact and the properties listed above, M is a suitable measure of the amplifier-noise performance.

Since M_{opt} of any given two-terminal-pair active network determines the lowest excess noise figure that can be achieved at high gain with the network by a lossless imbedding (no cascade connection is necessary to get a high gain in this case), M_{opt} is a measure of the potentiality of amplifier-noise performance of the given network.

In the numerator of (17), the noise contribution from the source is excluded, whereas the contribution from the load is included. The reason for defining M so is as follows: The noise contribution from the load can be eliminated by using a circulator or other matching circuit. If the noise originating in, and reflected back to, the load makes the amplifier poor, it is the responsibility of the amplifier designer to correct this—the trouble should not be attributed to the load itself. On the other hand, the noise from the source cannot be eliminated by any means available to the designer. Thus, the noise from the source has a quite different property and deserves a different treatment, even though both source and load are usually given beforehand in the design of an amplifier.

M is a quantity normalized by kT_iB, but this normalization is not necessary. For example, the equivalent noise temperature of an amplifier can be defined as

$$T_{eq} = MT_i.$$

For an evaluation of space-communication systems, this may be more convenient than the noise measure itself.

IV. Comparison Between the Two Noise Measures

The value of M_{opt} is equal to $-P_{e,min}/kT_iB$, which is also the value of $M_{e,opt}$. Hence, most of the conclusions Haus and Adler obtained for $M_{e,opt}$ hold equally well for the M_{opt} discussed in this paper. In addition, the definition of M is very similar to that of M_e. It is therefore desirable to make the difference between M and M_e clear.

M is a measure of the noise performance of an amplifier when we include not only the input circuit but also the output load as part of the amplifier, while M_e completely excludes the effect of the load circuit.

Now suppose that a source, a load and a two-terminal-pair active network are given. Let us now connect the source to port 1 and the load to port 2 of the two-terminal-pair network, and examine the noise performance of this system. By noise performance, we understand that, if we have two systems with the same signal-to-noise ratio at the output, the system with a smaller gain is the less desirable one, since with it the noise contribution of the following stages will be greater. On this basis, the definition of the noise measure M was proposed. Then we asked, "Is it possible to reduce the value of M by disconnecting the source and the load from the two-terminal-pair network, imbedding the network in a passive network and reconnecting the source and the load to the resultant network?" In this procedure, it is understood that the inside of the two-terminal-pair network cannot be changed. The answer was, "There is an optimum value of M designated by M_{opt}; it is possible to achieve M_{opt} by a lossless imbedding, but it is impossible to achieve a positive M less than the M_{opt} by any passive imbedding." No such statement can be made about the noise figure; thus, the

[5] The isolators are introduced to secure the positive real part in the source and load impedances of the component amplifier (see Appendix II).

proposed M is superior as a measure of amplifier-noise performance. This is effectively what we did in the previous sections.

Next, let us consider in our language what Haus and Adler did. First, a source and a two-terminal-pair network are given. The source is connected to port 1 of the two-terminal-pair network, leaving us with a one-port network. For simplicity, let us assume for a moment that this one-port network has an output impedance of which the resistive part is positive. We now connect a load and change it in various ways to obtain the largest amount of output-signal power. During this process, the output signal-to-noise ratio becomes a maximum, since the output signal-to-noise ratio attributable to the source and the two-terminal-pair network remains constant, but the noise originating in, and reflected back to, the load becomes zero. The exchangeable (available) noise measure M_e is defined to express the noise performance of this final system. In other words, M_e expresses a quantity already optimized, and is not a measure of the quality of the noise performance of a given amplifier which consists of a source, a two-terminal-pair active network, and a load. This is the reason why M_e cannot be used as a measure of the quality of a given amplifier. If the resistive part of the output impedance of the one-port network is negative, the above procedure runs into the difficulty that it leads to an infinite amount of output-signal power. They accordingly replaced the "largest amount" of the output-signal power by its "stationary value," and allowed the use of a negative resistance in the load to get this stationary value. The interpretation of this extension of the definition is difficult in our language, since we assumed from the start that the load has a positive resistance. However, they did extend the definition in this way and asked, "Is it possible to improve M_e by means of a passive transformation?" The answer was expressed by $M_{e,\mathrm{opt}}$, which gives the same value as our M_{opt}.

Two different optimizations are made to get $M_{e,\mathrm{opt}}$, namely, a load adjustment and a lossless imbedding. The first of these is unnecessary in our case, for the second one covers the first.

As the frequency goes up, it becomes increasingly more difficult to make a matching circuit without introducing an appreciable amount of loss, and hence an additional source of noise. The extent to which one succeeds in making the matching circuit with low loss is in practice reflected in the over-all noise performance, and accordingly the noise measure should really take this into account; this the quantity M_e fails to do. For example, for an Esaki-diode amplifier, once the diode is given, in principle all one has to do is to make lossless-matching circuits for the input and output; in practice this is a major difficulty, but M_e does not reflect the degree of success in making these matching circuits lossless. In other words, the quantity M_e provides no measure of the achievements of the circuit engineer who builds the amplifier. To correct this was the motivation of the present work, but it must be emphasized that there is nothing wrong with the work of Haus and Adler—it is only the point of view which is different.

V. Conclusion

A new noise measure M is proposed to evaluate the noise performance of an amplifier; it includes the effect of the noise originating in, and reflected back to, the load. In terms of M, it becomes possible to compare the noise performance of amplifiers which are not necessarily optimized.

It is shown that there is an optimum value M_{opt} which is achievable by a lossless transformation, but not surpassable by any passive imbedding.

In designing a practical amplifier, M can be used as a measure of the quantity of the amplifier's noise performance. The circuit engineer should not, however, necessarily be satisfied with achieving M_{opt}, since the possibility may exist of obtaining a better M by using the same components, but changing the connections inside the two-terminal-pair active network; furthermore, sometimes better components may be available.

Appendix I

Examples

For a comparison of the quality of two different amplifiers, we have to consider the gain, noise performance, bandwidth, stability, complexity, etc. For the noise performance, we can use either the noise measure or the noise figure; the noise measure, however, is superior since the noise figure is meaningful only when the gain is specified beforehand. This point of view, and the difference between M and M_e, will perhaps be clearer after discussing some illustrative examples.

Let us consider an Esaki-diode amplifier with a circulator as shown in Fig. 5. In Fig. 5, $-g$ is the negative conductance of the diode, b is the remaining susceptance, P_e is the exchangeable noise power of the diode, g_0 is the characteristic admittance of the circulator arm; the source g_s and the load g_L are assumed to be matched and to have the same standard noise temperature T ($=290°\mathrm{K}$).

The actual gain of the amplifier is found to be

$$G = \frac{(g_0 + g)^2 + b^2}{(g_0 - g)^2 + b^2}. \tag{19}$$

The actual noise figure is

$$F = 1 + \left(\frac{-P_e}{kTB}\right)\frac{4g_0 g}{(g_0 + g)^2 + b^2}, \tag{20}$$

whereas the actual noise measure is given by

$$M = \frac{-P_e}{kTB}. \tag{21}$$

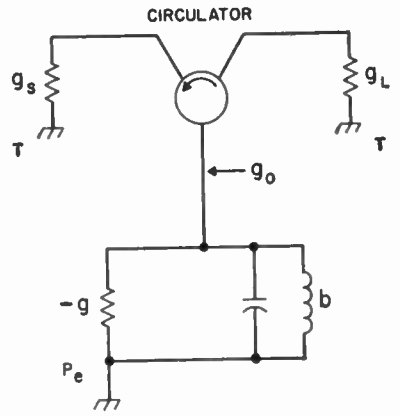

Fig. 5—Esaki-diode amplifier with a circulator.

The noise measure M is equal to its optimum value irrespective of the value of b. One may well ask then why we do not use a detuned amplifier. The reason is that this would reduce the gain G of the amplifier. Admittedly, one could build a high-gain amplifier system by connecting a number of the detuned amplifiers in cascade, but this adds unnecessary complexity (and cost). So we see that the gain, noise measure, and complexity serve as independent variables when considering the quality of an amplifier. As b increases, the noise-figure F decreases, suggesting improved quality. However, this is definitely in the wrong direction. When b becomes large, the gain drops and the noise contribution from succeeding stages, which are necessary to restore the gain, increases; this effect is so predominant that the noise figure fails to represent the noise performance properly.

For this particular example, the input and output circuits were assumed to be matched, and thus, as mentioned in the text, it makes no difference whether one uses M or M_t.

Next, let us consider an Esaki-diode amplifier without a circulator. The equivalent circuit is shown in Fig. 6. The actual gain is given by

$$G = \frac{4g_s g_L}{(g_s - g + g_L)^2 + b^2}. \tag{22}$$

The actual noise figure is

$$F = 1 + \frac{(g_s - g - g_L)^2 + b^2}{4g_s g_L} + \frac{g}{g_s}\left(\frac{-P_e}{kTB}\right), \tag{23}$$

and the actual noise measure is

$$M = \frac{\dfrac{(g_s - g - g_L)^2 + b^2}{4g_s g_L} + \dfrac{g}{g_s}\left(\dfrac{-P_e}{kTB}\right)}{1 - \dfrac{(g_s - g + g_L)^2 + b^2}{4g_s g_L}}. \tag{24}$$

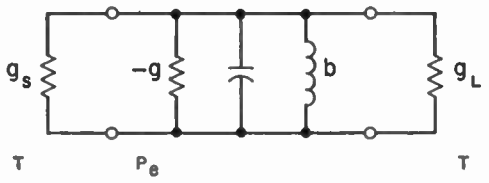

Fig. 6—Esaki-diode amplifier without a circulator.

We shall confine ourselves to the case $G>1$. If we keep the g's constant, $b=0$ gives the smallest noise measure, and we therefore set b equal to zero. Then, M becomes

$$M = \frac{\dfrac{(g_s - g - g_L)^2}{4g_s g_L} + \dfrac{g}{g_s}\left(\dfrac{-P_e}{kTB}\right)}{1 - \dfrac{(g_s - g + g_L)^2}{4g_s g_L}}. \tag{25}$$

Since

$$(g_s - g - g_L)^2 \geq 0 \tag{26}$$

is equivalent to

$$\frac{\dfrac{g}{g_s}}{1 - \dfrac{(g_s - g + g_L)^2}{4g_s g_L}} \geq 1 \tag{27}$$

provided $G>1$, we conclude that the smallest positive value of M is obtained when, and only when,

$$g_s = g + g_L \quad \text{and} \quad b = 0. \tag{28}$$

The optimum value of M is

$$M = \left(\frac{-P_e}{kTB}\right) = M_{\text{opt}}. \tag{29}$$

Large gain is compatible with this optimum noise measure ($g_L \to 0$, $G \to \infty$), but the bandwidth and the stability become poor; for this reason, the Esaki-diode amplifier without a circulator is not generally considered to be as good.

The value of M_t for this amplifier is $-P_e/kTB$ irrespective of the circuit constants. Thus M_t gives no guidance on how to improve the noise performance of a given amplifier, while M does, as is shown above. This is a major difference between M and M_t.

Appendix II

Cascade Connection

Let us consider a cascade connection of two amplifiers through an ideal isolator as shown in Fig. 7. In this figure Z_g and Z_L are the source and load impedances, respectively. The real part of these impedances is assumed to be positive. Since the isolator provides a positive real part in the load and source impedances of the amplifiers 1 and 2, respectively, the values of M and G for each amplifier can be clearly defined. The over-all actual gain is given by

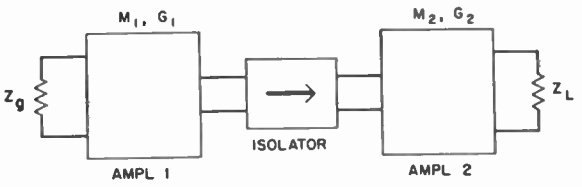

Fig. 7—Cascade connection through isolator.

$$G = \frac{\text{Actual signal power to } Z_L}{\text{Available signal power from } Z_g} = \frac{\text{Actual signal power to isolator}}{\text{Available signal power from } Z_g} \times \frac{\text{Actual signal power to } Z_L}{\text{Available signal power from isolator}} = G_1G_2, \tag{30}$$

where we used the fact that, in the forward direction, the available power from an ideal isolator is equal to the actual power into the isolator. Similarly, the over-all actual noise figure is given by

$$F = \frac{\text{Actual noise power to } Z_L}{kT_iBG} = \frac{\text{Available noise power from isolator} \times G_2 + kT_iBG_2(F_2 - 1)}{kT_iBG}$$

$$F = \frac{kT_iBG_1F_1 \times G_2 + kT_iBG_2(F_2 - 1)}{kT_iBG} = F_1 + \frac{1}{G_1}(F_2 - 1). \tag{31}$$

Therefore,

$$M = \frac{F - 1}{1 - \frac{1}{G}} = \frac{M_1\left(1 - \frac{1}{G_1}\right) + M_2\left(1 - \frac{1}{G_2}\right)}{1 - \frac{1}{G}} = M_1 + (M_2 - M_1)\frac{G_2 - 1}{G_1G_2 - 1}. \tag{32}$$

Eq. (32) gives the over-all actual noise measure for the cascade connection of two amplifiers through an isolator. Note that if the two amplifiers have the same value of M, then the resultant amplifier also has this value of M, but with a gain of G_1G_2. Thus, by connecting a number of identical amplifiers in cascade through isolators, one can obtain a high-gain amplifier with a value of M equal to that of the component amplifiers.

For the case where the input and output frequencies of an amplifier are different, the lossless imbedding discussed in Section III, and hence most of the results obtained there, have little meaning. However, the definition of M is still applicable for this case, and (30) and (32) hold equally well for the cascade connection of such amplifiers through an ideal isolator.

In many cases, the second amplifier is already built in such a way as to provide an adequate gain and the best noise measure when the source impedance is equal to the characteristic impedance of the input connector. The function of the first amplifier is to improve the over-all noise performance. Let us consider how to adjust the first amplifier to get the best over-all noise performance.

1) If the output impedance of the first stage has a positive real part (for instance, upper sideband up-converters), the best procedure is to insert an isolator matched to the input connector of the second amplifier and to adjust the first stage to give the smallest positive value of

$$M = M_1\left(1 - \frac{1}{G_1}\right) + \frac{M_2}{G_1}, \tag{33}$$

which corresponds in (32) to the over-all actual noise measure with large G_2. The output impedance of the first stage is then automatically matched[6] to the isolator and the noise originating in the isolator makes no contribution to the noise output of the resultant amplifier. Therefore, elimination of the ideal isolator would not result in any better noise performance, and we see that the best over-all noise performance is always obtainable with the above adjustment.

2) If the output impedance of the first stage has a negative real part (for instance, lower sideband up-converters), the adjustment of the first stage has to be made to give the smallest positive M_1 and infinite G_1. To obtain the smallest positive M_1, it may be necessary to cool the isolator to 0°K. One would not expect to obtain a better over-all noise performance by any other adjustments, since the above adjustment eliminates all noise contributions except that from the first stage, and this is adjusted to be the best. In practice, even if the isolator is at room temperature, the over-all noise performance is improved through the use of the isolator, since the equivalent noise temperature of the input impedance of the second stage is generally higher than room temperature because of the shot noise involved.

Acknowledgment

Acknowledgments are due to H. Seidel, K. D. Bowers and M. Uenohara for their continued encouragement and helpful criticism. The author wishes to thank Professor H. A. Haus for his criticisms about this new noise measure, and Professor P. Penfield, Jr., for the discussions of low-noise parametric amplifiers, and for the preprint of the paper referred to in the text. The first half of Section III is based on his paper.

[6] If this were not so, then, by inserting a matching circuit, a smaller value of M could be obtained, since G_1 becomes larger and

$$M_1\left(1 - \frac{1}{G_1}\right) = F_1 - 1$$

becomes smaller.

IRE Standards on Radio Interference: Methods of Measurement of Conducted Interference Output to the Power Line from FM and Television Broadcast Receivers in the Range of 300 kc to 25 Mc, 1961*

(61 IRE 27.S1)

Committee Personnel

Subcommittee on Radio and TV Receivers
1958–1959

R. J. FARBER, *Chairman* 1958–1959
F. R. WELLNER, *Chairman* 1959
F. G. COLE, *Chairman* 1960–1961

J. C. Achenbach
A. F. Augustine
E. D. Chalmers
E. W. Chapin
M. S. Corrington
E. C. Freeland
R. O. Gray
W. R. Koch
S. Mazur
W. G. Peterson
F. Stachowiak
D. G. Thomas
A. E. Wolfram
R. S. Yoder

Radio Frequency Interference Committee
1959–1961

R. J. FARBER, *Chairman* 1959–1961
S. J. BURRUANO, *Vice Chairman* 1959–1961

H. R. Butler
E. W. Chapin
J. F. Chappell
K. A. Chittick
L. E. Coffey
S. I. Cohn
F. G. Cole
H. E. Dinger
E. C. Freeland
C. W. Frick
W. F. Goetter
G. G. Hall
V. J. Mancino
J. B. Minter
W. E. Pakala
W. A. Shipman
R. M. Showers
F. R. Wellner

Standards Committee
1960–1961

C. H. PAGE, *Chairman*
J. G. KREER, JR., *Vice Chairman*
H. R. MIMNO, *Vice Chairman*
L. G. CUMMING, *Vice Chairman*

J. H. Armstrong
J. Avins
G. S. Axelby
M. W. Baldwin, Jr.
W. R. Bennett
J. G. Brainerd
A. G. Clavier
S. Doba, Jr.
R. D. Elbourn
G. A. Espersen
R. J. Farber
D. G. Fink
G. L. Fredendall
E. A. Gerber
A. B. Glenn
V. M. Graham
R. A. Hackbusch
R. T. Haviland
A. G. Jensen
R. W. Johnston
I. Kerney
E. R. Kretzmer
W. Mason
D. E. Maxwell
R. L. McFarlan
P. Mertz
H. I. Metz
E. Mittelmann
L. H. Montgomery, Jr.
S. M. Morrison
G. A. Morton
R. C. Moyer
J. H. Mulligan, Jr.
W. T. Wintringham
A. A. Oliner
M. L. Phillips
R. L. Pritchard
P. A. Redhead
C. M. Ryerson
G. A. Schupp, Jr.
R. Serrell
W. A. Shipman
H. R. Terhune
E. Weber
J. W. Wentworth

Measurements Coordinator

J. G. KREER, JR.

* Approved by the IRE Standards Committee, February 9, 1961. Reprints of IRE Standard 61 IRE 27.S1 may be purchased while available from The Institute of Radio Engineers, Inc., 1 East 79 Street, New York 21, N.Y., at $.60 per copy. A 20 per cent discount will be allowed for 100 or more copies mailed to one address.

1. Introduction

FM and television broadcast receivers are frequently potential sources of interference to other FM and television broadcast receivers as well as to receivers in other services. In the range of 300 kc to 25 Mc, this interference can arise from high-level receiver signals such as the IF and, in television receivers, the horizontal deflection system. This standard defines a method for obtaining a measure of the interference conducted by the power line from these various interference sources in the frequency range of 300 kc to 25 Mc. It supersedes and replaces the following three standards: "IRE Standards on Receivers: Methods of Measurement of Interference Output of Television Receivers in the Range of 300 to 10,000 kc, 1954" (54 IRE 17.S1), "IRE Standards on Methods of Measurement of the Conducted Interference Output of Broadcast and Television Receivers in the Range of 300 kc to 25 Mc, 1956" (56 IRE 27.S1), and "Supplement to IRE Standards on Receivers: Methods of Measurement of Interference Output of Television Receivers in the Range of 300 to 10,000 kc, 1954 (54 IRE 17. S1)" (58 IRE 27. S1).

This standard describes standard input signals, the equipment set-up and measurement techniques.

2. Equipment Required and Method of Installation

2.1 Equipment Required

To perform the measurements described in this standard, the following equipment is required: screen room (2.1.1), power line impedance network (2.1.2), source of RF signal (2.1.3), a tuned voltmeter (2.1.4), and, for television receivers only, a picture carrier IF signal source (2.1.5).

2.1.1 A screen room large enough to meet the requirements of Section 2.2.1 with adequate shielding and filtering to eliminate external interference. A typical size is 7 feet high by 7 feet wide by 10 feet long.

2.1.2 A power line impedance network. The purpose of this network is to present a standard value of power line impedance to the receiver under test regardless of the local power line conditions.

2.1.2.1 The line impedance network is schematically illustrated in Fig. 1. The purpose of the one-ohm (nonreactive) resistor is to limit any possible resonance effects of the series circuit of the 5-μh inductor and the 1.0-μf capacitor. The purpose of the 1000-ohm resistors is to limit the line voltage that may appear at the coaxial connectors.

2.1.2.2 The impedances of the line network measured from each side of the receiver receptacle to chassis must conform within ± 5 per cent to the characteristic shown in Fig. 2. (For this requirement the power plug is open-circuited and both measurement outlets terminated in 50 ohms as shown in Fig. 3.)

2.1.2.3 A suitable method of measuring the magnitudes of impedances is shown in Fig. 3. This measurement technique is a substitution method. The reference resistor is chosen so that the voltage drop across this resistor is equal to the voltage across the line-impedance network at each frequency of measurement. The value of the resistor is then taken as the absolute value of the impedance. Since the impedance of the line network is considerably less than that of the 470-ohm resistor, the generator impedance has a negligible effect on the measurements. The accuracy of the voltmeter is unimportant since it is only used to hold the voltage constant when the switch is changed. It is important to keep the lead lengths as short as possible.

2.1.2.4 To minimize variations which might occur among different line impedance networks and to permit more uniformity in test facilities, detailed construction drawings of a suitable network, of which assembly drawings are shown in Fig. 4(a) and (b), have been pre-

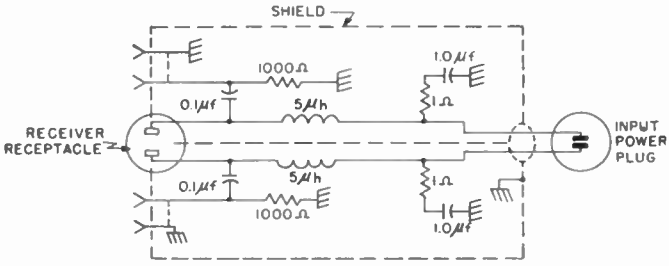

Fig. 1—Power-line impedance network schematic.

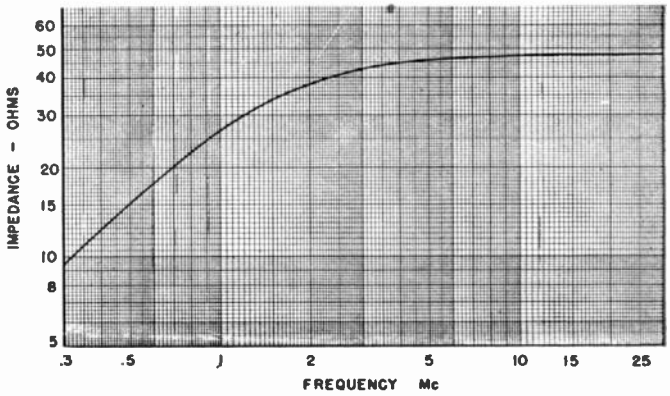

Fig. 2—Impedance magnitude characteristic of line measured from either side of the receiver receptacle to chassis.

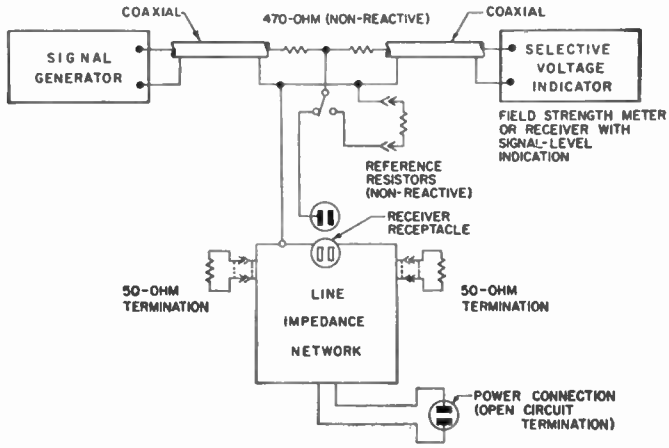

Fig. 3—Circuit for measurement of impedance.

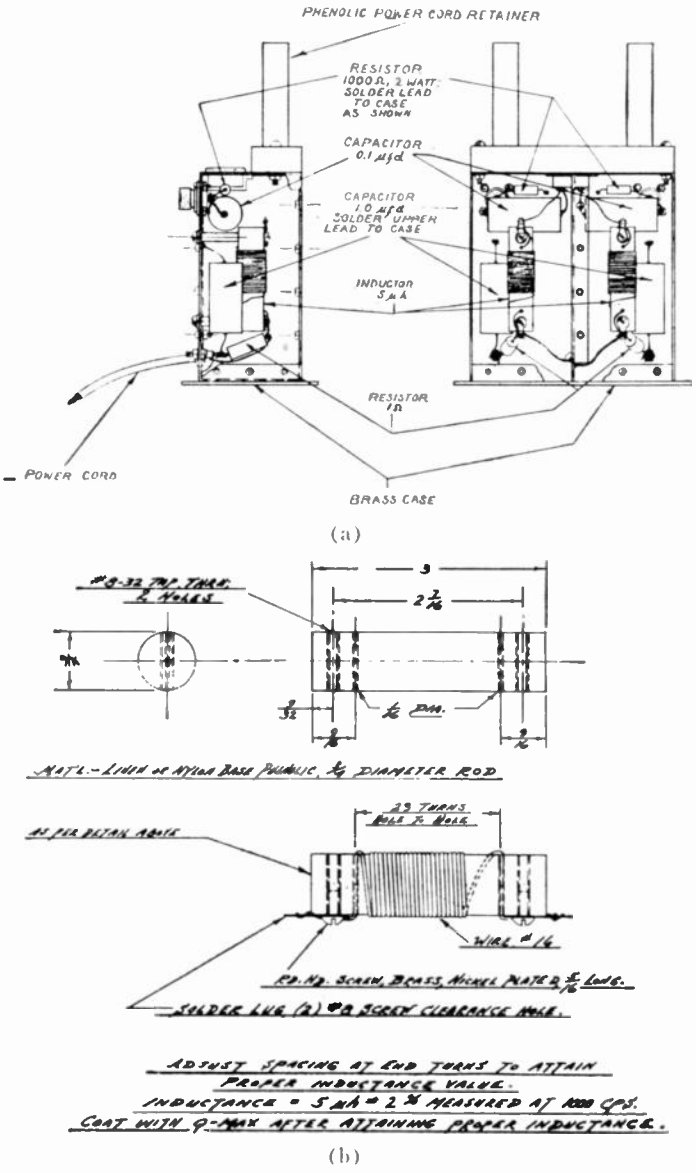

Fig. 4—(a) Line impedance assembly. (b) Inductor 5 μh.

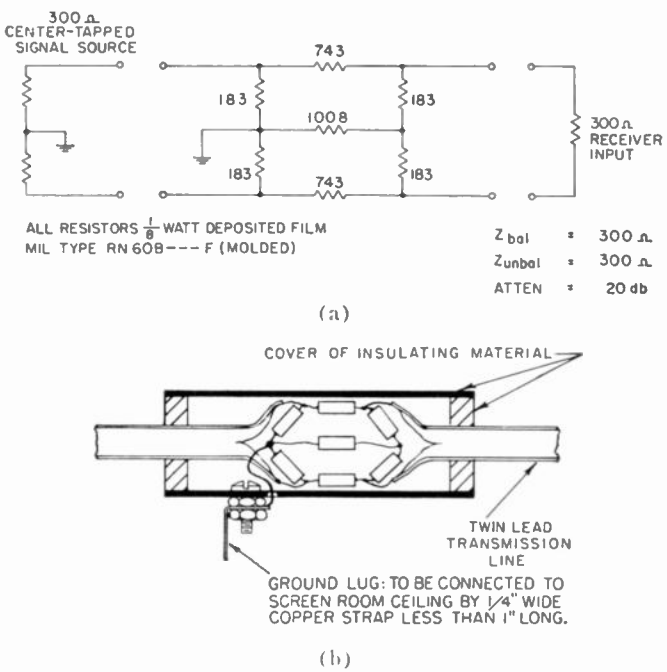

Fig. 5—Antenna coupling pad. (a) Schematic diagram. (b) Drawing of typical construction.

pared.[1] A network constructed according to these drawings should nevertheless be tested in order to insure that it meets the requirement of Section 2.1.2.2.

2.1.3 A source of a standard RF input signal.

2.1.3.1 The RF signal shall be supplied to the receiver under test through a 20-db 300-ohm antenna coupling pad. This network, details of which are shown in Fig. 5, is designed to have an impedance of 300 ohms balanced, and 300 ohms unbalanced (impedance between the two output terminals connected together and ground). If the signal generator is not located within the screen room, adequate filters should be installed at the signal input to the screen room to exclude undesired signals in the frequency band of interest.

If the receiver has a built-in antenna, it shall be disconnected from the antenna terminals during these tests. If the signal generator does not have a nominal 300-ohm center-tapped output impedance, a suitable matching network shall be provided between the signal generator and the pad.

If the receiver is designed for use with an unbalanced shielded transmission line, a line having the characteristics recommended by the receiver manufacturer shall be used in place of the twin-lead in Figs. 5 and 7. The input terminals of the transmission line are connected to the output terminals of the pad. In addition, a resistor is connected in shunt with the output terminals of the pad so that the combination of pad and resistor matches the nominal input impedance of the receiver.

2.1.3.2 For a television receiver, the input signal shall consist of simulated sound and picture signals on any standard television channel.

2.1.3.2.1 The modulation of the picture signal shall consist of the mixture of the following signals as shown in Fig. 6 (observed on a double-sideband detector or equivalent, with a video frequency response that is uniform within ±0.5 db up through 3.58 Mc):

a) Pulses of 5 μs width at a repetition rate of 15,750 pulses per second to represent horizontal synchronizing pulses. The pulse amplitude shall be sufficient to modulate the picture carrier so that the level between pulses is 37.5 per cent of the peak level during the pulses.

b) A sine wave of 2.0 Mc to represent video modulation. The amplitude of this modulation shall be sufficient to produce 1 per cent peak-to-peak modulation during the time interval between the synchronizing pulses. This sine wave may be allowed to run through the synchronizing pulse period. (A method of obtaining 1 per cent modulation is to adjust the modulation level for 10 per cent to permit observation on an oscilloscope and then to reduce the modulating 2.0 Mc signal by 20 db.)

[1] These drawings may be purchased from The Institute of Radio Engineers, Inc., 1 East 79 Street, New York 21, N. Y., at a cost of $2.00 per copy. In ordering, refer to "61 IRE 27.S1-A, Construction Drawings of IRE Line Impedance Network."

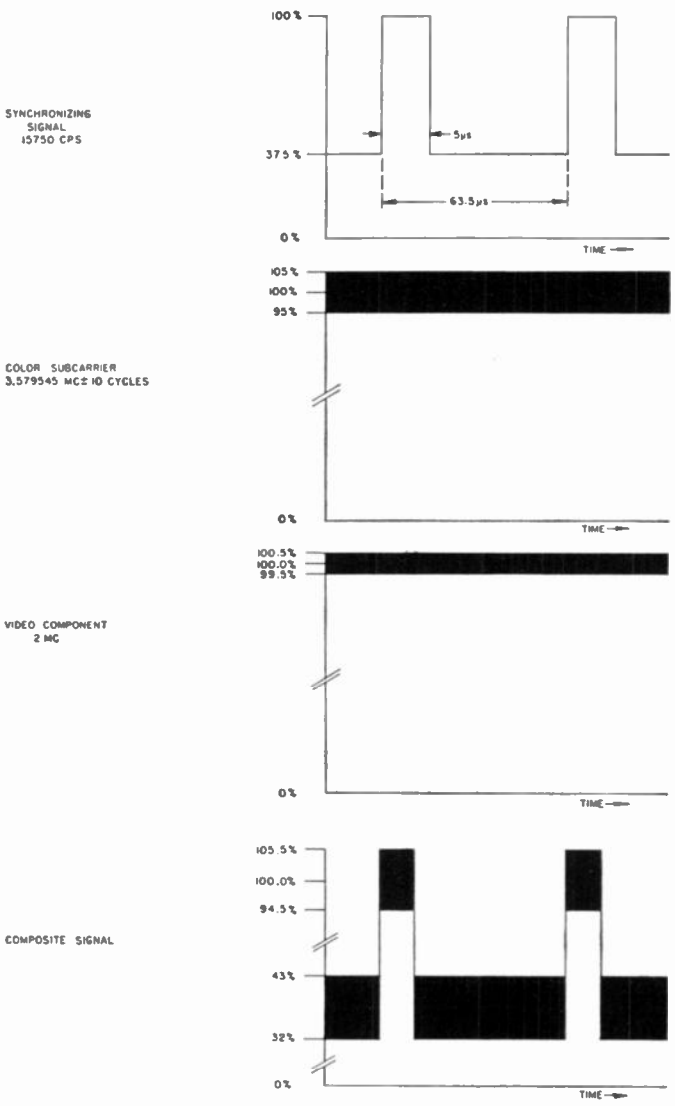

Fig. 6—Modulation of picture signal (see Section 2.1.3.2.1).

c) A sine wave of 3.58 Mc to represent color signal modulation. The amplitude of this modulation shall be sufficient to produce 10 per cent peak-to-peak modulation between the synchronizing pulses. This sine wave may be allowed to run through the synchronizing pulse period.

2.1.3.2.2 No modulation of the sound signal is employed.

2.1.3.2.3 The peak level of the picture carrier delivered at the output terminals of the 300-ohm antenna coupling pad shall be nominally 3200-μv rms open circuit. The open circuit sound carrier level shall be 3 db below the peak level of the modulated picture carrier.

2.1.3.3 For an FM broadcast receiver, the input signal shall be delivered from the 300-ohm antenna coupling pad at a nominal open circuit level of 1000-μv rms at a frequency of 98 Mc. No modulation will be employed.

2.1.4 A suitable tuned voltmeter (field strength meter.)

2.1.4.1 The tuned voltmeter shall have a nominal 50-ohm input impedance and be tunable over at least the frequency range of interest. The nominal bandwidth of the voltmeter shall not exceed 10 kc. Means shall be provided for either internal or external calibration. The instrument shall be adequately shielded and the power leads filtered to prevent spurious pick-up.

2.1.4.2 The tuned voltmeter shall indicate the rms carrier level of the signal to which it is tuned. This measurement position is normally designated as "field intensity" or "carrier."

2.1.5 For television receivers, a reference picture IF signal source. This shall consist of a signal source at the nominal picture carrier intermediate frequency. The signal is injected into the television receiver as a reference to facilitate the proper tuning of the receiver as described in Section 3.1.1.

2.1.6 A regulated source of primary input power. Unless otherwise specified, the line voltage at the receiver receptacle shall be maintained at 117 volts $\pm$ 2 volts. The harmonic content of this line voltage shall be less than 5 per cent.

2.2 Installation of Equipment

2.2.1 All portions of the receiver under test shall be at least 30 inches from the wall of the shielded enclosure. Floor model receivers shall be placed on a nonmetallic platform 18 inches above the metallic floor of the shielded enclosure, and table models placed on a nonmetallic platform 30 inches above the floor. If the receiver is equipped with remote cables, these should be connected to the receiver and terminated either with the normal equipment or with a dummy load. They should be coiled up and located on top of the receiver.

2.2.2 The power-line impedance network shall be located on the floor of the screen room directly below the back of the cabinet of the receiver under test. The center line of the power line impedance unit shall be coincident with the center line of the receiver back. Similarly, the RF signal coupling pad shall be mounted at the ceiling of the screen room directly above the power line impedance network. The standard arrangement is shown in Fig. 7.

2.2.3 The power-line impedance network shall be connected to the metallic floor by means of four solid copper straps as shown in Fig. 8. The width-to-length ratio of each strap shall be at least 1 to 5, and the thickness of the strap shall be at least 0.025 inch. In the unit shown in Fig. 8, four holes have been provided for this purpose. The connection from the power-line impedance network to the power source should be kept close to the walls or floor of the shielded room when inside the enclosure.

2.2.4 A 50-ohm resistive load shall be connected to each of the two coaxial connectors of the line impedance network at all times. The voltages developed across these loads represent the conducted-interference output of the receiver. A 50-ohm nonreactive resistor, a 50-ohm input impedance field-strength meter, or any combination of field-strength meter and external resistor to equal 50 ohms can be used as the resistive load.

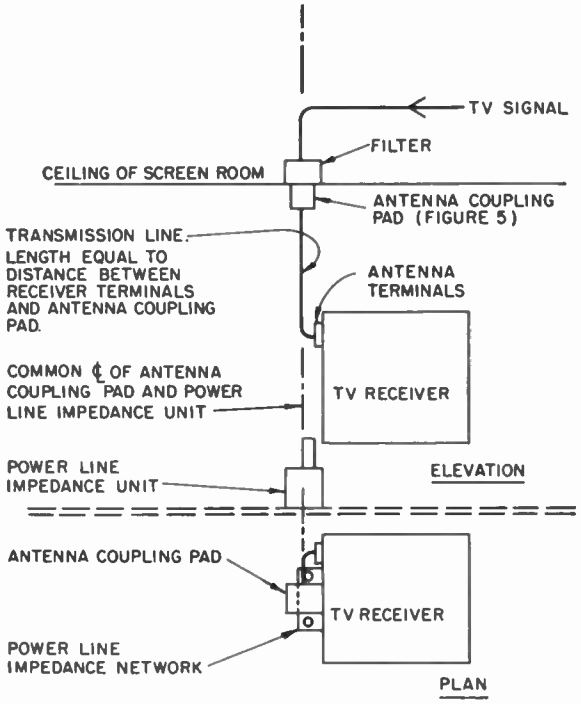

Fig. 7—Signal input system.

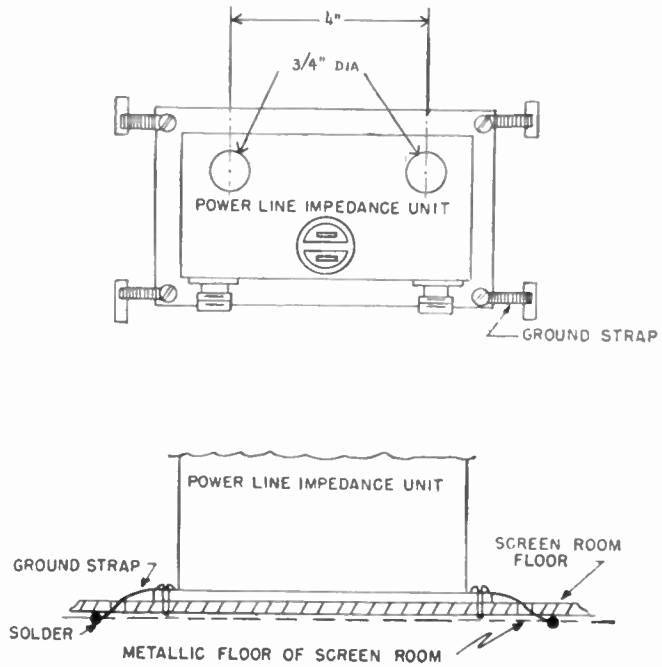

Fig. 8—Suggested method for grounding the power-line impedance unit to the screen room.

2.2.5 The power line cord from the receiver under test shall be dressed to the power line impedance network through the shortest possible path. The excess cord length shall be taken up by wrapping the cord in a figure-eight pattern around the two posts provided on the top of the unit. The receiver power line cord shall be plugged into the receptacle provided in the power line impedance network. This is shown in Fig. 9.

The disposition and length of the RF transmission line between the antenna coupling pad and the receiver are also important. As shown in Fig. 7, the length of

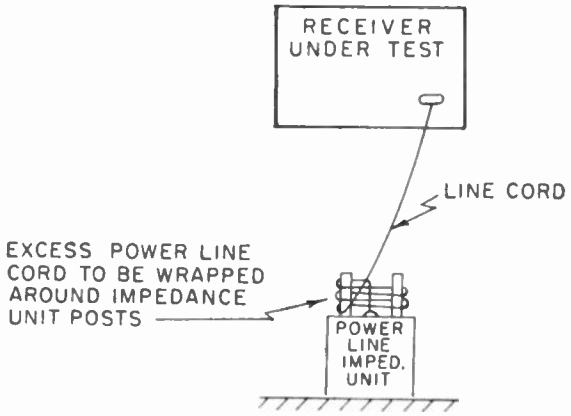

Fig. 9—Method of dressing the receiver power line cord.

transmission line shall be just sufficient to connect the receiver antenna terminals to the antenna coupling pad.

3. Measurement Procedure

3.1 Equipment Assembly and Initial Adjustments

The equipment is assembled in the prescribed manner, and the receiver under test is tuned to the appropriate input signals.

3.1.1 For a television receiver, the correct tuning is determined by injecting a signal at the nominal intermediate picture carrier frequency and tuning the receiver local oscillator for a zero beat with the converted input picture carrier. This tuning point simulates normal operation and the interference developed under normal operating conditions. If the receiver employs automatic local oscillator tuning means, the frequency of the converted IF picture carrier shall be recorded. If both manual and automatic tuning are provided, measurements shall be recorded for both conditions.

3.1.2 For an FM receiver the tuning is adjusted for maximum measured interference.

3.2 Interference Voltage Measurement

With the tuned voltmeter connected to one 50-ohm output of the power line impedance network, the voltage between this side of the power line and ground is measured at the frequencies of interest. The measurement is repeated with the voltmeter connected to the other 50-ohm terminal of the power line impedance network.

3.3 Adjustment of Operating Controls

The customer-operated controls of the receiver, with the exception of the tuning adjustments, may be placed at any setting. In general, the range of these controls should be searched to determine the setting that produces the maximum interference value at each frequency of interest.

3.4 Recording of Measured Data

The interference voltage is recorded separately for each side of the power line at each frequency of interest.

The Delay-Lock Discriminator—An Optimum Tracking Device*

J. J. SPILKER, JR.†, MEMBER, IRE, AND D. T. MAGILL†, MEMBER, IRE

Summary—**The delay-lock discriminator described in this paper is a statistically optimum device for the measurement of the delay between two correlated waveforms. This new device seems to have important potential in tracking targets and measuring distance, depth, or altitude. It operates by comparing the transmitted and reflected versions of a wide-bandwidth, random signal. The discriminator is superior to FM radars in that it can operate at lower power levels; it avoids the so-called "fixed error," and it is free of much of the ambiguity inherent in such periodically modulated systems. It can also operate as a tracking interferometer.**

The discriminator is a nonlinear feedback system and can be thought of as employing a form of cross-correlation along with feedback. The basic theory of operation is presented, and a comparison is made with the phase-lock FM discriminator. Variations of performance with respect to signal spectrum choice, target velocity, and signal and interference power levels are discussed quantitatively. The nonlinear, "lock-on" transient and the threshold behavior of the discriminator are described. Performance relations are given for tracking both passive and actively transmitting targets. Results of some experimental measurements made on a laboratory version of the discriminator are presented.

Introduction

In many problems of position measurement, interferometry, and tracking, it is necessary to measure the delay difference between two versions of the same signal, *e.g.*, the transmitted signal and the returned signal reflected from a target. In the domain of pulse radar, emphasis in recent years has been placed on the improvement of positioning accuracy in the presence of noise, and this effort has led to the development of advanced, matched-filter and pulse-compression techniques.[1,2]

The purpose of this paper is to present an improved delay estimation technique which operates on wide-bandwidth, continuous signals in the presence of interfering noise. The delay-lock discriminator, which is described herein, provides an optimum, continuous measurement of delay by operating on a wide-bandwidth, random, continuous signal. Throughout most of this paper, the signal is considered to be either filtered Gaussian random noise, or a sine wave randomly modulated in frequency. The signals are usually nonperiodic. Operation with pulsed signals is also possible, although this possibility is not treated specifically.

The delay-lock discriminator is shown as it might be used in tracking Fig. 1. This tracking problem differs from the conventional pulse radar problem in that only a single target is to be tracked by each discriminator. (There may, however, be several discriminators.) The target is tracked continuously as a function of time rather than at periodic intervals. (Dispersive effects in the target return are to be neglected in this discussion.)

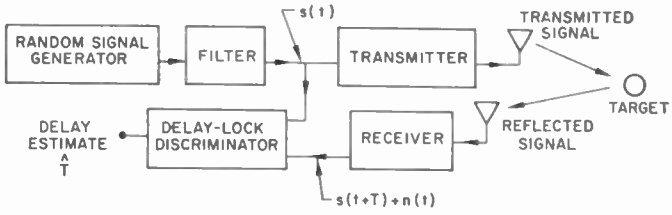

Fig. 1—Use of the delay-lock discriminator in tracking.

Although this radar uses a continuous signal, it differs from ordinary FM radars[3,4] in that, first, it avoids the so called "fixed error"; secondly, it is free of much of the ambiguity inherent in such periodically modulated systems; and finally, it can operate with multiple targets present at the same bearing from the antenna, thus providing range discrimination. The discriminator can be used in a second type of application: it can operate on a signal transmitted from the target which arrives via two separate receiving antennas. The delay difference in the two received signals is then measured by a method similar to that of a tracking interferometer.

Random-signal distance-measuring systems in themselves are not new. It is well known that when cross-correlations are made between the transmitted and received waveforms, the time difference can be accurately ascertained, if the received signal is sufficiently free of interference. These techniques have limitations, however, in that if the target is moving rapidly, the cross-correlation operation has limited useful integration time.

A somewhat different form of distance measuring technique employing random signals has been described by B. M. Horton[5] and was proposed for use as an altim-

* Received by the IRE, March 23, 1961; revised manuscript received, June 23, 1961.

† Commun. and Controls Res., Lockheed Missiles and Space Co., Palo Alto, Calif.

[1] C. E. Cook, "Pulse compression—key to more efficient radar transmission," PROC. IRE, vol. 18, pp. 310–316; March, 1960.

[2] Matched Filter Issue, IRE TRANS. ON INFORMATION THEORY, vol. IT-6, pp. 310–413; June, 1960.

[3] D. G. C. Luck, "Frequency Modulated Radar," McGraw-Hill Book Co., Inc., New York, N. Y.; 1949.

[4] M. A. Ismail, "A precise new system of FM radar," PROC. IRE, vol. 44, pp. 1140–1145; September, 1956.

[5] B. M. Horton, "Noise-modulated distance measuring system," PROC. IRE, vol. 47, pp. 821–828; May, 1959.

eter. This technique simply involves the direct multiplication of the transmitted and received signals, followed by a frequency-discrimination operation. Basically, this is a special type of correlation technique which is capable of operating over a relatively small range of delay. However, this system has a limitation on the dynamic range of delay which for many purposes would be overly restrictive.

Correlation techniques can be extended to cope better with time varying delays as shown in Fig. 2. A single element in the simple cross-correlation process is shown in Fig. 2(a). The fixed delay T_m is one of a large set of delays to be tested for maximum cross-correlation. (Notice that the time shift T is negative for a real delay.) The delay which produces the largest cross-correlation voltage V_m is considered the best estimate over a given interval of time. However, the integration time τ is limited to relatively short periods of time over which the delay $T(t)$ does not fluctuate enough to change the cross-correlation significantly. This restriction on integration time can, in some situations, cause severe limitations on the accuracy of the delay estimate in the presence of interference.

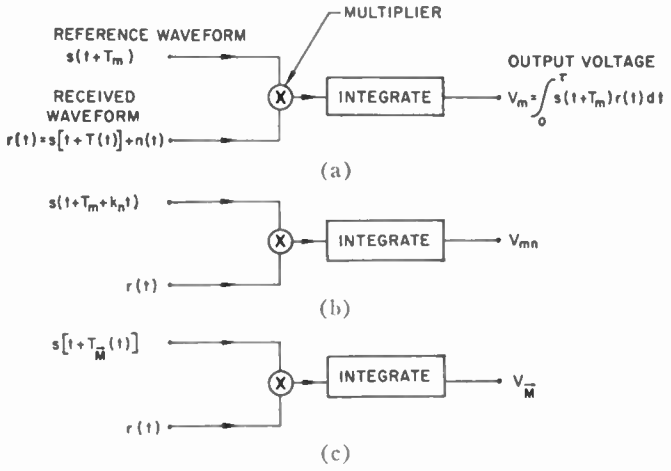

Fig. 2—Use of cross-correlation in delay estimation. Reference waveforms have: (a) Fixed delays T. (b) Fixed, plus linearly varying delays $T_m+k_m t$. (c) Time varying delay, $T_{\vec{M}}(t)$ chosen from a set of time functions τ sec long with bandwidth W.

A modified cross-correlation process is shown in Fig. 2(b). Here comparisons are made between the received signal and a two-dimensional set of fixed, plus linearly varying delays, and the integration time can be increased to time intervals over which the time delay is well approximated by a member of this set. Matched filter analogs to this technique have been discussed in the literature.[6]

The final stage of accuracy that can be achieved is shown in Fig. 2(c), where a multidimensional set of delay functions $T_{\vec{M}}(t)$ of length τ sec and bandwidth W are used as comparison delay functions. It is clear, however, that to use large dimensions for $\vec{M}$ would be unfeasible in most practical problems.

The delay-lock discriminator provides an approximation to this last technique by generating its own comparison delay function $T_{\hat{M}}(t)$ through the use of cross-correlation and error feedback.

Delay-Lock Discriminator

A block diagram of the delay-lock discriminator is shown in Fig. 3. As the figure shows, the discriminator is basically a nonlinear feedback system employing a multiplier, linear filter, and a controllable delay line.[7] The controllable delay line can have a number of implementations, *e.g.*, a ferrite-core delay line with magnetically controlled permeability and delay, or a servo-controlled electric or ultrasonic delay line. The ultrasonic lines are preferable for delays in the millisecond range or greater. In practice, it is often desirable to have an automatic gain control or limiter to maintain constant power at the discriminator input.

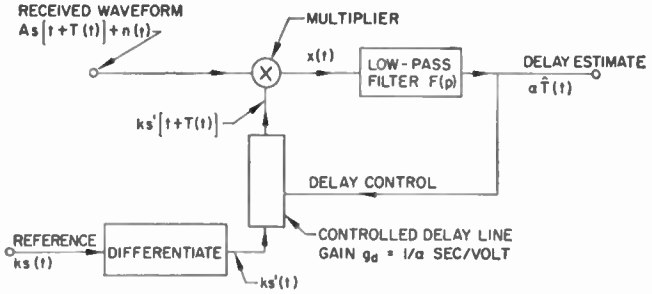

Fig. 3—Block diagram of the delay-lock discriminator. The symbols k, α, are constants.

Through an analysis similar to that used by Lehan and Parks,[8] this discriminator, or a slightly modified version of it, can be shown to be optimum in that it provides the maximum likelihood (*a posteriori*, most probable) estimate of the delay. This derivation has been made by Spilker in unpublished work under the assumption of Gaussian random delay and interfering noise. In general, the truly optimum discriminator contains a second feedback loop which serves to reduce the effects of intrinsic or self-noise described in this section. It should be pointed out, however, that the maximum likelihood discriminator taking the form shown in Fig. 3 requires a nonrealizable loop filter $F(p)$. In this paper the configuration of elements of Fig. 3 is retained, but the loop filter is constrained to be realizable and is optimized for an important class of target delay functions;

[6] R. M. Lerner, "A matched filter detection system for complicated Doppler shifted signals," IRE Trans. on Information Theory, vol. IT-6, pp. 373–385; June, 1960.

[7] The output of a passive, lossless, delay line with an input $f(t)$ is actually $\sqrt{1+dT(t)/dt}\,f[t+T(t)]$ rather than just $f[t+T(t)]$ as shown in Fig. 3. The square root term is present to keep the output energy equal to the input energy. However, in most practical problems we have the relationship $dT(t)/dt \ll 1$, and this effect can be ignored.

[8] F. W. Lehan and R. J. Parks, "Optimum demodulation," 1953 IRE National Convention Record, pt. 8, pp. 101–103.

delay functions which can be approximated by a series of ramps fall into this class.

The operation of the discriminator can be analyzed by examining the multiplier output $x(t)$. The delay error may be defined as $\epsilon(t) = T(t) - \hat{T}(t)$. We can then write the Taylor series for the delayed signal

$$s(t + T) = s(t + \hat{T}) + \epsilon s'(t + \hat{T}) + \frac{\epsilon^2}{2} s''(t + \hat{T}) + \cdots$$

where the primes refer to differentiation with respect to the argument, and all derivatives of $s(t)$ are assumed to exist.[9] Initially, the delay error $\epsilon(t)$ is assumed to be small so that the Taylor series expansion of $s(t+T)$ about $s(t+\hat{T})$ converges rapidly. The multiplier output then has the series expansion

$$\frac{x(t)}{k} = A\left[s(t + \hat{T})s'(t + \hat{T}) + \epsilon(t)[s'(t + \hat{T})]^2 + \frac{\epsilon^2(t)}{2!} s''(t + \hat{T})s'(t + \hat{T}) + \cdots\right] + n(t)s'(t + \hat{T}). \quad (1)$$

For convenience, $s(t)$ is normalized to have unity power, and thus the received signal power is $P_s = A^2$. The term $(s')^2$ has a nonzero average value which will be defined as P_d, the power in the differentiated signal, and is dependent only upon the shape of the signal spectrum. We can then write $[s'(t)]^2 \triangleq P_d + s_2(t)$ where $s_2(t)$ has a zero mean. By making use of this last definition, we can rewrite (1) as

$$\frac{x(t)}{k} = A P_d \epsilon(t) + n_e(t), \quad (2)$$

where the first term is the desired error correcting term, and the second term $n_e(t)$ is an equivalent noise term caused by the interfering noise $n(t)$ and the remainder of the infinite series (distortion and intrinsic noise effects). If ϵ is small, $n_e(t)$ has little dependence upon $\epsilon(t)$.

The delay tracking behavior is evident from (2). Suppose that the input delay $T(t)$ is suddenly increased by a small amount. The error $\epsilon(t)$, assumed initially small, will also suddenly increase; the multiplier output will increase, and therefore the delay estimate $\hat{T}(t)$ will increase and tend to track the input delay. The discriminator output is indeed an estimate of the delay.

The representation of the multiplier output given in (2) permits the use of the partially linearized equivalent network shown in Fig. 4. The closed-loop transfer function $H(p)$ is

$$H(p) = \frac{F(p)}{1 + kAP_dF(p)/\alpha} \quad (3)$$

[9] RC filtered white noise for example is nondifferentiable. It seems, however, that for most physical systems parasitic effects cause the signal functions to be differentiable. See S. O. Rice, "Mathematical Analysis of Random Noise," in "Noise and Stochastic Process," edited by N. Wax, Dover Publications, New York, N. Y., pp. 193–195; 1954.

where p is the complex frequency variable. This representation is equivalent to that shown in Fig. 3 because the input to the loop filter $F(p)$ is the same in both instances. The delay estimates thus obtained are identical.

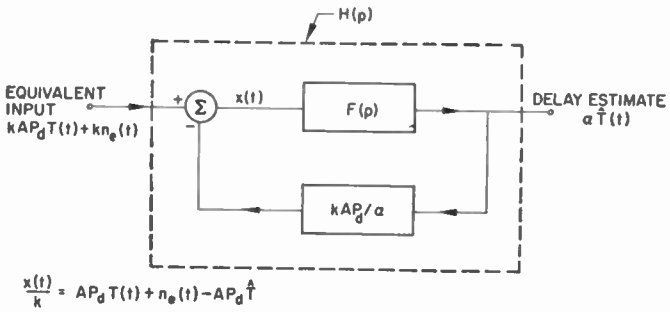

Fig. 4—Partially-linearized equivalent circuit for the delay-lock discriminator.

Notice that the equivalent transfer function $H(p)$ is still nonlinear because it is dependent upon the input signal amplitude A. In the initial part of this discussion, A is assumed constant, and $H(p)$ is assumed linear. In a later paragraph, the effect of AGC or limiting the input signal on the loop transfer function is discussed.

The equivalent input noise $n_e(t)$ is dependent upon $\hat{T}(t)$. However, it can be seen that under conditions of small delay error, this effect can be neglected. This linearized equivalent circuit, then, has its greatest use under conditions of small delay error, *i.e.*, "locked-on" operation. Notice that if $n(t)$ is "white," the interfering noise component of $n_e(t)$ is also white.

To provide a relatively simple yet useful and rather general analysis of the discriminator operation, the signal $s(t)$ will be assumed to have the form of a random frequency, modulated sine wave

$$s(t) = \sqrt{2} \sin [\omega_0 t + \phi(t)] = \sqrt{2} \sin \left[\omega_0 t + \int_0^t \omega_i(t')dt'\right]. \quad (4)$$

The spectrum of this signal can have a wide range of shapes[10] depending upon the statistics of $\omega_i(t)$, but for convenience in calculation, the spectrum of $s(t)$ will be taken to be rectangular with bandwidth B_s and center frequency f_0 as shown in Fig. 5. (It is assumed that $B_s < 2f_0$ and that $\omega_i(t)$ has a zero average value.) Then we can write the expressions:

$$s'(t) = \sqrt{2}\, \omega_s(t) \cos [\omega_0 t + \phi(t)]$$

$$P_d = (2\pi)^2 \left[f_0^2 + \frac{1}{3}\left(\frac{B_s}{2}\right)^2\right], \quad (5)$$

[10] D. Middleton, "An Introduction to Statistical Communication Theory," McGraw-Hill Book Co., Inc., New York, N. Y., pp. 604–625; 1960.

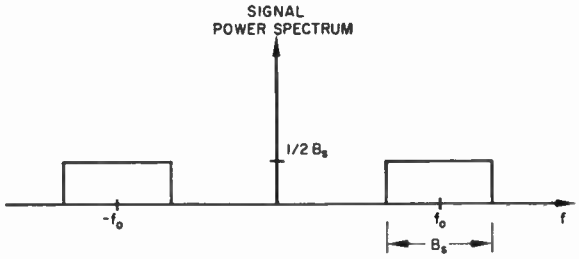

Fig. 5—Power spectral density of $s(t)$.

where we have defined $\omega_s(t) = \omega_0 + \omega_i(t)$.

Define the quantities $a_n = E[s'(t)s^{(n)}(t)]$. Note that $a_n = 0$ if n is even.

In general, the input to the linearized equivalent circuit can be written as the sum of the equivalent inputs to the discriminator, signal and three types of interference noise terms,

$$\text{Signal term} = kAP_d\epsilon(t)$$

$$\text{Noise term} = kn_e(t) = k[n_d(t) + n_i(t) + n_n(t)] \quad (6)$$

where $n_d(t)$ represents a nonlinear distortion term (it is small for small ϵ); $n_i(t)$ is an intrinsic or self-noise term, which is dependent upon the carrier characteristics, and $n_n(t)$ is an external interference term, which is dependent upon external noise at the discriminator input. By making use of (4) and (5), these noise terms can be evaluated as

$$n_d(t) = A\left[a_3\frac{\epsilon^3(t)}{3!} + a_5\frac{\epsilon^5(t)}{5!} + \cdots\right]$$

$$n_i(t) = A\left\{\epsilon(t)[(s'(t+\hat{T}))^2 - a_1] + \frac{\epsilon^2(t)}{2!}s'(t+\hat{T})s''(t+\hat{T}) + \frac{\epsilon^3(t)}{3!}[s'(t+\hat{T})s'''(t+\hat{T}) - a_3] + \cdots\right\}$$

$$n_n(t) = n(t)s'(t+\hat{T}) = \sqrt{2}\,n(t)\omega_s(t+\hat{T})\cos[\omega_0 t + \phi(t+\hat{T})]. \quad (7)$$

The distortion terms are taken as those terms of the form ϵ^n for $n \neq 1$.

The terms in the multiplier output with spectra centered about $\omega = 2\omega_0$ have been neglected because they will be assumed to be above the passband of the loop filter. This is not possible for low-pass spectra, of course.

The importance of the intrinsic noise term in determining the performance of the discriminator is dependent upon how much of its spectrum passes through the low-pass loop filter. Notice that the intrinsic noise terms are present even if the interference $n(t)$ is absent. It can be seen from (6) and (7) that the intrinsic noise effect is relatively small for this type of signal if

$$|\omega_i(t)|/\omega_0 \leq B_s/2\omega_0 < 1,$$

and the bandwidth of the instantaneous frequency $\omega_i(t)$ is large compared to the closed-loop bandwidth. It should be pointed out that the operation of the discriminator is not restricted to the use of fixed envelope signals. However, the intrinsic noise contributions will generally increase if envelope fluctuations of the signal are allowed.

Comparison with the Phase-Lock FM Discriminator

The operation of the delay-lock discriminator is analogous, in several respects, to the operation of the phase-lock FM discriminator (see Fig. 6 for a diagram of the phase-lock loop). It is desirable to investigate the differences and similarities of these two devices.

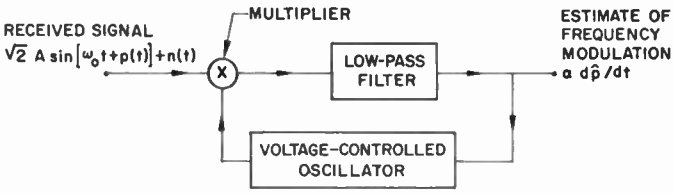

Fig. 6—Block diagram of the phase-lock discriminator.

For pure sine wave carriers (unmodulated carrier bandwidth of zero), delay modulation has a corresponding modulation in phase, *i.e.*,

$$\sin[\omega_0 t + \phi(t)] = \sin\omega_0[t + T(t)] \text{ if } \phi(t) = \omega_0 T(t).$$

Thus, if pure sine wave carriers are used, the delay line and its reference carrier input can be replaced by a differentiator and voltage-controlled oscillator. The differentiator can be lumped into the loop filter of the phase-lock loop. Theoretically, therefore, for the special case of a pure sine wave carrier, the delay-lock discriminator functions exactly as a phase-lock loop.[11]

The delay-lock discriminator normally operates with a wide bandwidth signal when used as a tracking device, and with this type of signal there is no longer a direct correspondence with the phase-lock discriminator operation. As might be expected, however, there are analogous features in both discriminators. For example, the delay-lock discriminator has a threshold error and lock-on performance which are analogous to those in the phase-lock loop.

Discriminator Operating Curve

Thus far, it has been indicated that the discriminator will tend to track the delay variations of an incoming signal provided that the delay error magnitude, $|\epsilon| = |T - \hat{T}|$, is small. In this section we seek to determine how small this error must be and what occurs as the error becomes larger.

[11] In practice, the delay-lock discriminator uses a delay line with restricted dynamic range of delay. Thus, it can be operated only with the sine wave carriers having a limited peak phase deviation.

Assume that $s(t)$ is a stationary (wide sense), ergodic, random variable with zero mean, and that the delays $T(t)$ and $\hat{T}(t)$ are constant or slowly varying with time. Under these conditions, the loop filter when properly optimized forms the average of the multiplier output to obtain:

$$E[x(t)] = E_t\{[As(t+T) + n(t)]ks'(t+\hat{T})\}$$
$$= -kAR_s'(T-\hat{T})$$

where $n(t)$ and $s(t)$ are assumed independent, and $R_s'(\tau) = d/d\tau[R_s(\tau)]$, the derivative of the autocorrelation function of $s(t)$. The important component in the multiplier output is not always linearly dependent upon the delay error, but, more generally, is functionally dependent upon the error through the differentiated autocorrelation function, and thereby causes changes in the effective loop gain.

The multiplier output can be written using (6) and (7) as

$$\frac{x(t)}{k} = -AR_s'[\epsilon(t)] + n_i(t) + n_n(t) \tag{8}$$

where we have used the relationship

$$R_s'(\epsilon) = \sum_{n=1}^{\infty} a_n \epsilon^n / n!.$$

A further general statement can be made with respect to the effective loop gain for small $|\epsilon|$. The correction component of the multiplier output for small $|\epsilon|$ is $kA\epsilon(t)a_1$ where a_1, in general, is given by

$$a_1 = \int_{-\infty}^{\infty} \omega^2 G_n(f)df$$

and depends only on the shape of the signal spectrum.

Threshold Error

To illustrate the nonlinear behavior of the discriminator, some exemplary signal spectra are shown in Fig. 7 along with their corresponding discriminator characteristics. If $s(t)$ is taken to have a rectangular band-pass spectrum as shown in Fig. 7(a), then, in the region $|\epsilon| < \frac{1}{4}f_0$, the discriminator curve is approximately linear and has a positive slope. However, if the error exceeds the threshold error[12] ϵ_T, the point at which the slope of the discriminator curve first becomes zero, the slope becomes negative, and further small incremental increases in ϵ in this region produce decreases in $\hat{T}$. Thus, the discriminator is unlocked and temporarily unstable with respect to small noise perturbations. Notice that in Fig. 7(a) there are several possible positive-slope lock-on regions, a characteristic of band-pass signal spectra. The effective loop gain, however, dependent upon the magnitude of the slope in these regions, decreases considerably as the delay error moves several inverse bandwidths away from the origin.

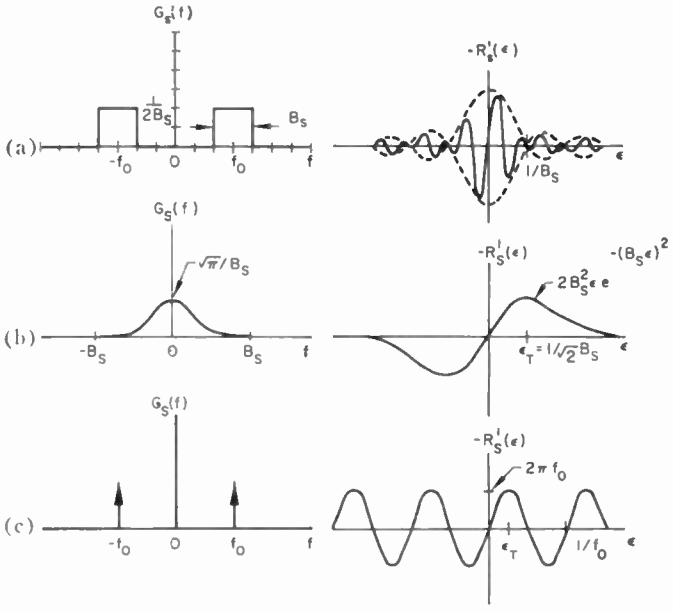

Fig. 7—Signal-power spectral density (unity-signal power) and the corresponding discriminator characteristics. (a) Rectangular band-pass spectrum $\epsilon_T = 1/4f_0$. (b) Gaussian low-pass spectrum $G(f) = (\sqrt{\pi}/B_s)\exp -(\pi f/B_s)^2$, $\epsilon_T = 1\sqrt{2}B_s$. (c) Pure sine-wave signal.

A Gaussian shape of low-pass signal spectrum is shown in Fig. 7(b). The discriminator curve for this signal spectrum has only one lock-on region, a characteristic which is also obtained using white noise passed through low-pass filters with poles on the negative real axis in the p plane. The threshold error for this Gaussian spectrum is $\epsilon_T = 1/\sqrt{2}B_s$. These signals with low-pass spectra are, of course, assumed to be detected (AM, FM, or PM) versions of the actual transmitted RF waveform.

The last spectrum, Fig. 7(c), corresponds to a pure sine wave carrier and phase-lock loop type of operation. Obviously, there are an unlimited number of indistinguishable lock-on regions here, and each has the same loop gain and threshold error. The use of this type of carrier in a tracking problem has limitations unless the delay variations are restricted to values less than $1/f_0$.

Dynamic Range

The dynamic range of the delay-lock discriminator is defined to be the maximum delay excursion of the controlled delay line, and is determined by the largest delay line control input voltage and the delay line gain. The maximum control input voltage in turn is determined by the signal amplitude, the loop filter dc gain, and the

[12] In general, the threshold error ϵ_T in the fundamental lock-on region about $\epsilon = 0$ is given by the smallest value of ϵ which can satisfy the equation

$$\int \omega^2 G_n(\omega) \cos \omega\epsilon d\omega = 0.$$

peak value of the discriminator curve. Thus, the dynamic range[13] ΔT is

$$\Delta T = kg_d AF(0)R'_{s\,\text{peak}} = gR'_{s\,\text{peak}}/P_d \qquad (9)$$

where $g \triangleq kg_d P_d AF(0)$ is the dc loop gain. This value of ΔT relates to the fundamental lock-on region. The values for other regions, if they exist, will be correspondingly less.

Delay Ambiguities and Interference from Other Targets

If a signal having a band-pass spectrum is used, there will exist ambiguities, in many situations, as to which lock-on zone the discriminator is using. An exception to this statement occurs if the ambiguity can be resolved by other means (such as knowledge of the exact target position at a certain instant of time, as might be the situation in tracking a rocket from its firing position). A means for resolving this ambiguity could be to control externally the bias on the controlled delay line and to observe some characteristic of the discriminator curve, *e.g.*, its slope or peak amplitude in a given lock-on region. The problem, then, is analogous to the resolution problem of radar.

Woodward[14] has defined a measure of time ambiguity for radar signals called the time resolution constant T_c. This constant is a measure of the width of the envelope of the discriminator characteristic; and for a rectangular signal spectrum, this time ambiguity has the value $T_c = 1/B_s$. It is difficult to determine the correct lock-on region from others that are separated in delay from it by less than $1/B_s$.

Of course, if a properly chosen low-pass signal spectrum is used, multiple lock-on regions will not exist, and hence ambiguities of this sort do not occur.

Considerations of a similar nature arise when one attempts to compute the interference caused by the presence of multiple targets. Suppose that the discriminator is locked on to a target with delay T, and an interfering target comes into view with delay T_i and returned signal amplitude A_i. Then the multiplier output in the discriminator is $-[AR'_s(T-\hat{T})+A_iR_s(T_i-\hat{T})]$, and the discriminator will operate so as to minimize the sum of these two terms rather than the desired term $-AR'_s(T-\hat{T})$ alone. If the relative effect of the interfering target is to be small, then it is necessary to have the ratio $|A_iR'_s(T_i-\hat{T})/AR_s(T-\hat{T})|$ small for the desired accuracy maximum error $|T-\hat{T}|$. Thus, if a small effect only is to be caused by the second target, it must be separated from the desired target by a delay $|T_i-T| \gg 1/B_s$. It is also desirable that $R_s(\tau)$ decrease rapidly with increasing τ to make up for the differences in path attenuations from the target returns caused by a relatively close undesired target. Spectra with gradual cutoffs are therefore desirable because of the rapid falloffs of $R_s(\tau)$ for large τ, *e.g.*, if $G_s(\omega) \sim \exp -(\omega/2B_s)^2$, then $R_s(\tau) \sim \exp -(B_s\tau)^2$.

Lock-on Performance

Before a target can be tracked, the discriminator must lock on to the target delay so that the discriminator is operating in its linear region. This operation can be performed in practice by manually or automatically sweeping the bias on the delay line control throughout the expected range of the target delay. An alternative approach is to set the delay to correspond to the perimeter of some circular region surrounding the radar. Then targets will be tracked as they enter this region. In this subsection a short analysis is made of the nonlinear lock-on transient when the signal is first applied to the discriminator.

Two discriminator curves are shown in Fig. 8, one for a band-pass spectrum, the other for a low-pass spectrum. Both spectra have Gaussian shapes. If we assume that the received signal has a fixed delay T, and that the quiescent discriminator delay is zero, the steady-state conditions of the discriminator must then satisfy the equation

$$-gR'_s(T-\hat{T})/P_d = \hat{T} = (T-\epsilon). \qquad (10)$$

It can be seen that solutions to this equation are given by the intersections of $-R'_s(\epsilon)$ and the straight line in Fig. 8. Recall that only the positive slope regions are stable zones with respect to noise perturbations.

A typical lock-on transient for the signal with a low-pass spectrum is as follows: when the input signal is first applied to the discriminator at $t=0$, the error $\epsilon(t)$ has its initial value $\epsilon(0+)=T$. As a result of this error, the loop filter input takes on a positive value, and $\hat{T}$ will begin to increase from zero and rise towards T. To describe the exact behavior of the loop, the loop filter must be specified.

If a simple low-pass RC filter is used as the loop filter, the lock-on transient is described by a first-order nonlinear differential equation. Referring to Fig. 3 and (8), and neglecting noise effects, one readily finds the differential equation to be

$$\left[\frac{1}{\omega_f}\frac{d\hat{T}}{dt} + \hat{T}\right] = \frac{F(0)}{\alpha}x(t) = -gR'_s(T-\hat{T})/P_d \qquad (11)$$

where $\omega_c \triangleq 1/RC$. If $T(t)=T$ is a constant, and $\hat{T}(0)=0$, then the transient response can be obtained by integrating

$$dt = d\hat{T}/\omega_f[-gR'_s(T-\hat{T})/P_d - \hat{T}(t)]. \qquad (12)$$

[13] Notice that this dynamic range restriction is different from that encountered with phase-lock discriminators. Here it is the maximum delay excursion which is limited, whereas, with the phase-lock loop, the maximum frequency excursion is the quantity limited. The reason for this difference is that in the phase-lock loop, the multiplier output controls the *frequency* of the VCO.

[14] P. M. Woodward, "Probability and Information Theory with Applications to Radar," McGraw-Hill Book Co., Inc., New York, N. Y., pp. 115–118; 1953.

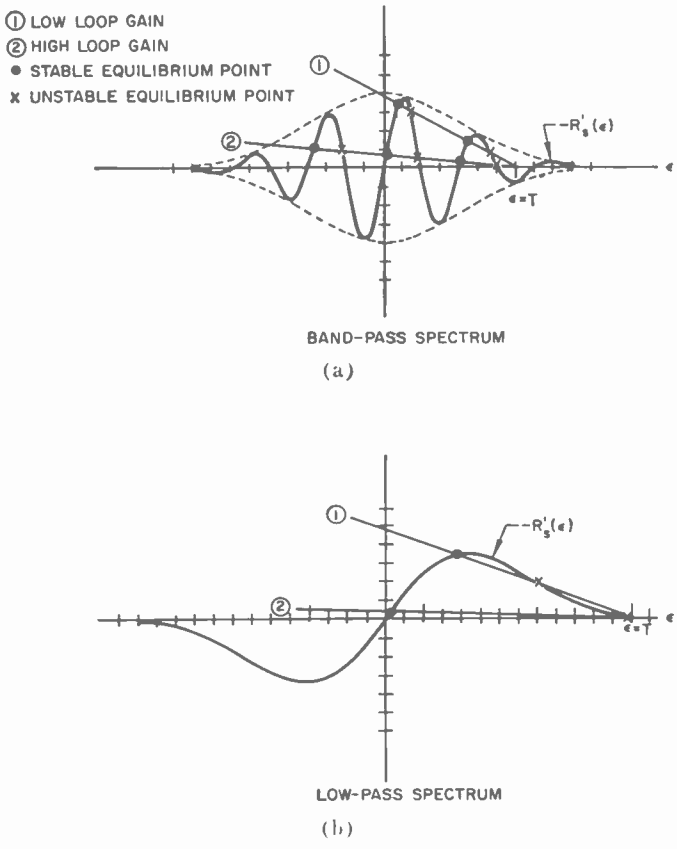

Fig. 8—Possible steady-state conditions. (a) Band-pass signal spectrum. (b) Low-pass signal spectrum.

Notice that the slope $d\hat{T}/dt$ is proportional to the difference between $-R_s'(T-\hat{T})$ and the straight line as shown in Fig. 8. Thus the slope becomes zero whenever the two curves cross. Of course if there are any zero slope points in negative discriminator slope regions, they are still unstable because of noise considerations neglected in (12).

If the Gaussian low-pass spectrum of Fig. 7(b) is assumed for the signal, and the loop gain is sufficient so that only one zero slope point exists, then the time τ required for the error to change from $\epsilon(0)=T$ to $\epsilon(\tau)=\epsilon_T$, the threshold condition, is given by

$$\tau = \int_0^{\tau} dt = \int_0^{T-\epsilon_T} \frac{d\hat{T}}{\omega_f\left[-gR_s'(T-\hat{T})/P_d - \hat{T}\right]}$$

$$\approx \int_0^{T-\epsilon_T} \frac{P_d\, d\hat{T}}{-\omega_f g R_s'(T-\hat{T})} \qquad (13)$$

where the last expression assumed $-gR_s'(T-\hat{T}) \gg P_d\hat{T}$ in the region of interest. For the Gaussian spectrum (13) becomes

$$\tau = \hat{T}\int_{\epsilon_T} \frac{P_d e^{(B_s\epsilon)^2} d\epsilon}{\omega_f g 2B_s^2 \epsilon} = \frac{P_d}{2B_s^2\omega_f g}\left[\ln y + \sum_{n=1}^{\infty} \frac{y^{2n}}{2n(n!)}\right]\Bigg|_{\epsilon_T B_s}^{TB_s}$$

where $y \triangleq B_s\epsilon$.

Now, by making use of the series representation

$$\frac{1}{2y^2}(e^{y^2}-1) = \frac{1}{2}\sum_{n=0}^{\infty}\frac{y^{2n}}{(n+1)!}$$

and the approximation $n(n!)\approx(n+1)!$ for $n\gg 1$, then for $y>1$ we have

$$\tau \approx \frac{P_d}{4B_s^2\omega_f g}\left[\frac{1}{y^2}(e^{y^2}-1-y^2)\right]\Bigg|_{\epsilon_T B_s}^{TB_s} \qquad (14)$$

Thus, with sufficiently large loop gain and the absence of interfering noise, the discriminator will eventually lock on even if the initial delay error is large. However, if $\epsilon(0)=T\gg 1/B_s$, the lock-on time will become extremely large and interfering noise effects will become of dominant importance.

Referring to (13) one sees that low-pass signals with autocorrelation functions which decrease rapidly with delay for large delays (desirable because of the effects of multiple targets) have lock-on times which increase extremely rapidly with initial delay error for large initial errors, *e.g.*, from (14),

$$\tau \sim e^{(TB_s)^2}/(TB_s)^2$$

for large TB_s with the Gaussian signal spectrum.

Accuracy of the Discriminator

In this section we return to the investigation of linear discriminator operation and the linearized equivalent representation shown in Fig. 4. The objective of this section is to determine the accuracy of the discriminator and the threshold value of input SNR. Intrinsic noise effects are assumed negligible compared to those caused by other error terms. Both band-pass and low-pass signal spectra are considered. The input signal amplitude is assumed fixed.

The target delay to be used is a ramp of delay beginning at $t=0$ and corresponds to a sudden change in velocity, *i.e.*,

$$T(t) = 0 \qquad \text{for } t<0$$

$$= \frac{2v}{c}t \qquad t\geq 0,$$

where v is the target velocity, and c the velocity of light. The Laplace transform of the delay is $T(p)=2v/cp^2$. Although real targets, of course, cannot change velocity instantaneously in this manner, they can approximate this ramp well enough to make the results of this analysis useful. This sudden ramp of delay is also important in studying the discriminator response when the return from a constant velocity target is suddenly applied to the input. Furthermore, the general behavior of the transient errors and the steady-state errors with velocity inputs are of interest by themselves. The linearized analysis used here applies only if the delay error at the beginning of the transient $\epsilon(0)$ is much less than the threshold error.

Two loop filters are shown in Fig. 9. The first of these, a simple integrator, produces a closed-loop transfer function [obtained from (3)] which is given by

$$H(p) = \frac{\alpha}{kAP_d}\left(\frac{1}{1 + p/p_0}\right). \tag{15}$$

This filter has zero steady-state error to step inputs of delay, but a finite nonzero steady-state error to ramp inputs. The second loop filter, shown in Fig. 9(b), is composed of an integrator and an RC filter. The closed-loop transfer function for this filter is

$$H(p) = \frac{\alpha}{kAP_d}\,\frac{1 + \sqrt{2}\,p/p_0}{1 + \sqrt{2}\,p/p_0 + (p/p_0)^2}. \tag{16}$$

This loop filter has been shown optimum for ramp inputs in the presence of white noise, in that it minimizes the total squared transient error plus the mean square error caused by interfering noise.[15] The frequency p_0 would then be chosen by relative weighting of the two types of errors. The frequency here will be chosen from other considerations, namely, to keep the peak transient error below a set value. This filter produces zero steady-state error in response to a ramp input.

The transient error is defined as the delay error $T(t) - \hat{T}(t)$ for a given delay function $T(t)$ in the absence of discriminator interference $n_i(t)$. The transient error for the simple integrator type of loop filter [Fig. 9(a)] with a ramp of delay as the input is shown in Fig. 10(a). The corresponding closed-loop frequency response is shown in Fig. 10(b). Notice that the error rises to a final steady-state value $\epsilon_t(\infty) = 2v/cp_0$ for a target radial velocity v, and a corresponding steady-state target position error $2v/p_0$. It is obviously desirable to have $\epsilon_t(\infty) < \epsilon_T$ and the position error small enough to obtain the required position accuracy. Suppose, then, that we choose p_0 to obtain the desired small steady-state transient error $\epsilon_t(\infty)$, *i.e.*, $p_0 = 2v/c\epsilon_t(\infty)$.

For this value of p_0, what is the lowest input SNR for which we can keep the delay errors below the threshold value ϵ_T most of the time? If the equivalent input noise, $n_e(t)$, is assumed Gaussian, and produces an rms error σ_{ϵ_n} in the delay estimate, then a reasonable condition for the discriminator to be said to operate above threshold is that $\sigma_{\epsilon_n} \leq \epsilon_T/3$. For delay errors which are approximately Gaussian (transient errors are assumed much less than ϵ_T), this condition corresponds to a probability of $|\epsilon| \geq \epsilon_T$ of less than or equal to 0.27 per cent at any instant of time.

The rms value of noise error for white noise inputs can be found from the expression

$$\sigma_{\epsilon_n}^2 = \int_{-\infty}^{\infty} k^2 G_{n_n}(f)\,|\,H(j\omega)/\alpha\,|^2 df = G_{n_n}(0)p_0/2(AP_d)^2$$

[15] R. Jaffe and E. Rechtin, "Design and performance of phase-locked circuits capable of near optimum performance over a wide range of input signal levels," IRE TRANS. ON INFORMATION THEORY, vol. IT-1, pp. 66–72; March, 1955.

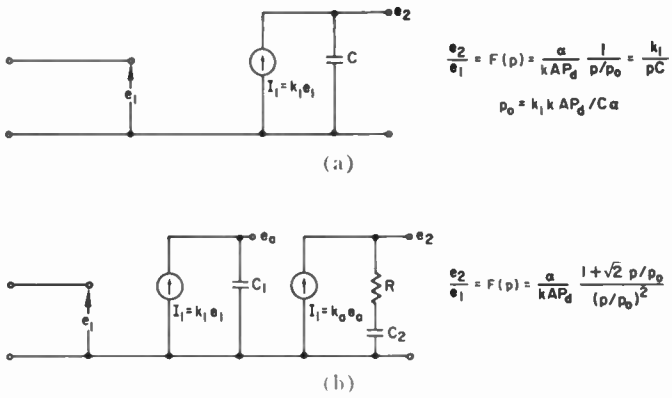

Fig. 9—Two loop filters and their transfer functions.

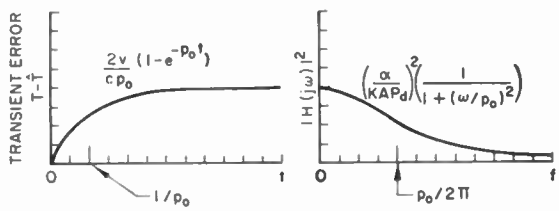

Fig. 10—Discriminator performance with the loop filter of Fig. 9(a). (a) Transient error in response to a ramp of delay. (b) Closed-loop frequency response.

where $G_{n_n}(f)$ is the power spectral density of the noise term $n_n(t)$. For the value of p_0 chosen, we have

$$\sigma_{\epsilon_n}^2 = \frac{G_{n_n}(0)v}{c\epsilon_t(\infty)(.1P_d)^2}. \tag{17}$$

The threshold occurs, then, when $G_{n_n}(0)$ has the value $c\epsilon_T^2\epsilon_t(\infty)(.1P_d)^2/9v$. The power spectral density $G_{n_n}(0)$ is in turn related to the input noise spectral density. For white input noise $n(t)$ and a signal spectrum which is rectangular or Gaussian in shape, the spectrum of $G_{n_n}(f)$ is also white.

For white interfering noise $n(t)$ with power P_n in a bandwidth $2B_s$ (both positive and negative frequency regions are used throughout this paper), the amplitude of this power spectral density is[16]

$$G_{n_n}(f) = P_d G_s(f) * G_n(f)$$

and

$$G_{n_n}(0) = P_d P_n/2B_s. \tag{18}$$

This last relation is valid regardless of the shape of the spectrum of $s(t)$ and has assumed that the spectrum of $s'(t+\hat{T})$ is the same as that of $s'(t)$.

Now by combining (17) and (18), the threshold input SNR can be found

$$(\mathrm{SNR})_{\mathrm{threshold}} = \left[\frac{A^2}{P_n}\right]_{\mathrm{threshold}} = \frac{4.5(v/c)}{B_s P_d \epsilon_T^2 \epsilon_t(\infty)}. \tag{19}$$

[16] The use of the asterisk indicates convolution in the frequency domain.

It is seen that, in general, the threshold SNR increases as the transient error ϵ_t is made smaller for fixed velocity v, just as expected.

To evaluate this expression, the power spectrum of $s(t)$ must be specified so that ϵ_T and P_d can be determined. If $s(t)$ has a Gaussian low-pass spectrum,

$$G_s(f) = \frac{\sqrt{\pi}}{B_s}\exp -(\pi f/B_s)^2, \qquad \sigma \text{ is } \frac{B_s}{\sqrt{2}\pi}$$

for this spectrum, then

$$\epsilon_T = 1/\sqrt{2}B_s, \qquad P_d = (2\pi\sigma)^2 = 2B_s^2.$$

Thus the threshold SNR is

$$(\mathrm{SNR})_{\text{threshold}} = \frac{4.5(v/c)}{B_s\epsilon_t(\infty)} \tag{20}$$

As an example, suppose $B_s = 1$ Mc, which makes $\epsilon_T = 0.707$ μsec, $\epsilon_t(\infty) = 0.1$ μsec (98.4 ft. transient error), $v = 2000$ mph, and $(v/c = 2.99\times10^{-6})$, then the threshold SNR is 1.36×10^{-4} or -38.6 db.

The transient error for the loop filter depicted in Fig. 9(b) in response to the same ramp input of delay $T(t) = 2(v/c)t$ is shown in Fig. 11(a). The closed-loop frequency response is shown in Fig. 11(b). The peak transient error for this filter is $\epsilon_t(t_{\text{peak}}) = 0.91\ (v/cp_0)$ and occurs at time $t_{\text{peak}} = 1.11/p_0$. Because the transient error is significant over a limited time interval only (about $2t_{\text{peak}}$) and has a limited rise time, it can be seen that in order to have the peak transient error from a real target be well approximated by that given in Fig. 11(a), the actual change in target velocity must occur over a time interval less than t_{peak}. In other words, the maximum target velocity transient considered here is the velocity change that can occur in a period of time t_{peak}.

The peak transient error will be set at $\epsilon_T/3$, *i.e.*, $p_0 = 2.72v/c\epsilon_T$. Threshold will be said to occur when the delay error caused by noise ϵ_n has an rms value $\sigma_{\epsilon_n} = \epsilon_T/3$. For Gaussian ϵ_n, this condition corresponds to a probability of $|\epsilon| \geq \epsilon_T$ of 0.27 per cent when there is no transient error. The probability of $|\epsilon| \geq \epsilon_T$ at peak transient error is 2.3 per cent.

The mean square delay error caused by a white interfering noise input can be found using (16) as[17]

$$\sigma_{\epsilon_n}^2 = \int_{-\infty}^{\infty} k^2 G_{n_n}(f)\,\left|H(j\omega)/\alpha\right|^2 df$$

$$= 1.06 G_{n_n}(0)p_0/(AP_d)^2 = (\epsilon_T/3)^2. \tag{21}$$

Now by using (18), (21) and the relation for p_0, the threshold input SNR can be found as

$$(\mathrm{SNR})_{\text{threshold}} = \left(\frac{A^2}{P_n}\right)_{\text{threshold}} = \frac{13.0(v/c)}{B_s P_d \epsilon_T^3}. \tag{22}$$

[17] This integral has been evaluated using D. Bierens de Haan, "Nouvelles tables d'intégrales définés," Hafner Publishing Co., New York, N. Y., p. 47; 1957.

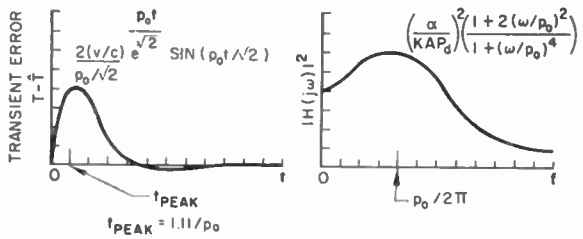

(a) (b)

Fig. 11—Discriminator performance with the loop filter of Fig. 9(b). (a) Transient error in response to a ramp of delay. (b) Closed-loop frequency response.

If the signal spectrum has a Gaussian shape as before $\sigma = B_s/\sqrt{2}\pi$, then (22) becomes

$$(\mathrm{SNR})_{\text{threshold}} = 18.4(v/c). \tag{23}$$

As a second example, suppose $v = 2000$ mph $(v/c = 2.99\times10^{-6})$. Then the threshold (SNR) is 5.5×10^{-5} or -43 db, an improvement of more than 4 db over that provided by the first filter.

Tracking an Actively Transmitting Target

One of the more important applications of the delay-lock discriminator is to track a target which is itself transmitting a wide-bandwidth, random signal. Information on the target position can be obtained by estimating the delay difference $T(t)$ between the signals as they arrive at the two antennas as shown in Fig. 12. The signal received from one antenna is fed into the discriminator as the reference, and the other received signal is fed into the input. By comparing the delay differences for three such pairs of antennas, the target position (including range) can be determined as the intersection point of three hyperboloids.[18] Two pairs of antennas are sufficient to provide angular information.

As it concerns the operation of the delay-lock discriminator, this problem differs from the one just discussed only in that the noise-perturbed signal received in one antenna is used as the reference. As a result, a corresponding degradation in accuracy at low input SNR is to be expected. By referring to Fig. 13 and (2), one can write the low-frequency terms of the multiplier output as

$$x(t) = A_1A_2P_d\epsilon(t) + n_e(t) \tag{24}$$

where $n_e(t)$ is the equivalent linearized interference and has the representation

$$n_e(t) = A_1A_2[n_d(t) + n_i(t)] + A_1s(t+T)n_2'(t+\hat{T})$$

$$+ A_2s'(t+\hat{T})n_1(t) + n_1(t)n_2'((t+\hat{T}), \tag{25}$$

[18] Actually, there are two intersections of the three hyperboloids, one on each side of the plane of the antennas. However, if the antennas are on the ground, it is usually easy to decide which point is correct.

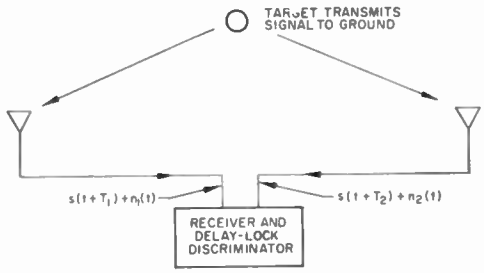

Fig. 12—Tracking a target which is transmitting a wide bandwidth signal.

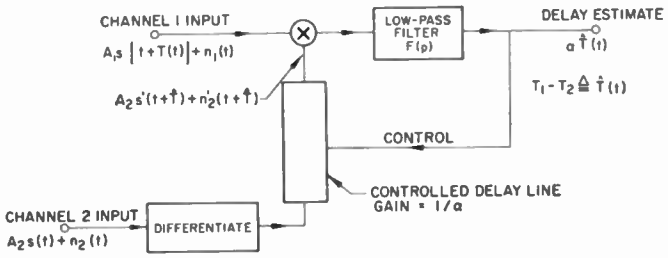

Fig. 13—Operation of the delay-lock discriminator with a noise perturbed reference.

where $n_d(t)$, $n_i(t)$ are the distortion and intrinsic noise components, respectively. Notice that in addition to the noise terms of (6) there are now two additional noise terms, another $S\times N$ term (signal times noise term) and a $N\times N$ term.

In many situations the dominant noise terms are generated in the two receiver amplifiers, and the noise terms $n_1(t)$ and $n_2(t)$ are independent of one another. If the spectra of the signal and these noise components have bandwidths much greater than the closed loop bandwidth of the discriminator, then $n_e(t)$ can be considered to have an approximately white spectrum, and the results of the previous section can be used to obtain the performance of this discriminator. Of course, if $n_1(t)$ and $n_2(t)$ contain components which are not independent, any dc and low-frequency noise components which might then exist must be taken into account.

If, for example, we take the signal and independent noise components to have rectangular spectra with bandwidths B_s, then the equivalent noise spectrum in the low-frequency region is

$$G_{n_n}(0) = \frac{1}{2B_s}(A_1^2P_{dn_2} + A_2^2P_dP_{n_1} + P_{dn_2}P_{n_1})$$
$$= \frac{A_1^2A_2^2P_d}{2B_s}(r_1 + r_2 + r_1r_2) \qquad (26)$$

where P_{n1}, P_{dn2} are the average powers in $n_1(t)$, $n_2'(t)$, and r_1, r_2 are the noise-to-signal power ratios on channels 1 and 2, respectively.

If intrinsic noise effects are negligible, then threshold input SNR can be obtained by combining (26) with either (17) or (21), depending on which loop filter is used. Notice that constant k in (15) and (16) now becomes A_2. Consider that the loop filter of Fig. 9(b) is used. Then by using (21), (26) and assuming equal SNR on both channels, the threshold SNR can be evaluated as

$$(\mathrm{SNR})_{\mathrm{threshold}} = h + \sqrt{h + h^2} \qquad (27)$$

where

$h \triangleq 13.0(v/c)/B_sP_d\epsilon_T^3$, and v is the radial velocity difference to the antennas. For $h \ll 1$, this relation becomes $(\mathrm{SNR})_{\mathrm{threshold}} = \sqrt{h}$. As an example, suppose that $v = 2000$ mph. If the signal spectrum is low-pass and rectangular, then $\epsilon_T \cong \frac{1}{2}B_s$, $P_d = (2\pi B_s)^{2/3}$, and the threshold SNR is 4.85×10^{-3} or -23 db.

Effect of AGC or Limiting on the Discriminator Performance

As pointed out earlier, to control the discriminator loop gain it is desirable to feed the received data through a limiter or an amplifier with strong AGC. The use of an ideal AGC serves to maintain a constant average input power for the discriminator and has a relatively simple effect. Thus, the ideal AGC acts as a variable attenuator which produces no distortion of the input, but attenuates the amplitude of the signal component in its output. Its only effect is to vary the discriminator loop gain as a function of the input SNR. If the total input power to the discriminator is A_t^2 and only one channel has noise added and AGC control, then the effective loop gain is

$$\text{loop gain} = g = \frac{kA_tP_dg_dF(0)}{\sqrt{1 + P_n/P_s}}. \qquad (28)$$

The change in the loop gain, however, is important because it affects both the dynamic range of the discriminator and the closed-loop bandwidth. Here we encounter the problem: if a time invariant loop filter is to be used, what value of the loop gain should be assumed in designing the loop filter?

Once the discriminator has locked onto the signal, the most critical phenomenon is the occurrence of the threshold or loss of lock condition. While the discriminator is operating well above threshold at a fixed SNR, there is a linear relationship—the closed-loop transfer function $H(j\omega)$—between the true delay and the delay estimate. Thus we can follow the discriminator with a linear filter with a transfer function $H_2(j\omega)$, and the product $H_T(j\omega) = H(j\omega)H_2(j\omega)$ can be chosen so that it is optimum in some sense, *e.g.*, $H_T(j\omega)$ can be chosen as the realizable Wiener filter which allows some particular value of delay (negative, if a predictor is desired) in forming the estimate of the target delay. Consequently, one reasonable approach to this is to optimize the loop filter using the threshold value of loop gain, and then to choose a time invariant filter $H_2(j\omega)$, so that $H_T(j\omega)$ is optimum in the Wiener sense at large input SNR.

Now, if we consider that the single noisy channel has a limiter preceding the discriminator, it can be shown that the dominant effect is the change in the loop gain. However, the exact dependence of loop gain on input SNR is not always exactly the same as with perfect

AGC, because the limiter input and output SNR are not always equal. For example, Davenport[19] has shown that the signal power output of an ideal band-pass limiter for sine wave plus Gaussian noise inputs is related to the total limiter output power by the expression

$$P_{s\,\text{out}} = \frac{P_T}{1 + b(P_n/P_s)}$$

where P_T is the band-pass limiter output power, $\pi/4 \leq b \leq 2$, and b depends on the input SNR P_s/P_n. The loop gain varies with $P_{s\,\text{out}}$ roughly in the same manner as with AGC.

If the input to an ideal limiter is a Gaussian signal plus independent Gaussian noise, then the discriminator operating curve can be obtained using the results of Bussgang[20] which show that the cross-correlation between the input and output of the limiter is proportional to the autocorrelation function of the input. The discriminator operating curve can thus be shown to be

$$-R'(\tau) = \sqrt{P_s P_T}\,\frac{-R_s'(\tau)}{\sqrt{1 + r}}$$

where P_T is the limiter output power, P_s is the signal power, and $R_s(\tau)$ is the autocorrelation function of the signal which has been normalized to unity power. In this way the loop gain is changed exactly as it was with the AGC. The loop gain change may not be the only effect, because in passing through the limiter the noise statistics change and harmonics of the signal are generated. In practice, however, the limiting operation can usually be done at an IF or RF frequency (before detection if $s(t)$ is to be low-pass) so that harmonic content is removed by band-pass filters and is of little concern.

It is sometimes convenient to limit both received data channels at the multiplier inputs; the reference channel is differentiated and delayed before amplitude limiting. With this type of operation the multiplier inputs are both binary random variables, and the multiplier circuit can be implemented by using an AND circuit. If both inputs to the receiver have stationary Gaussian statistics and the noise-to-signal power ratios on the two channels are r_1 and r_2, then the discriminator characteristic can be shown to be[21]

$$\frac{2}{\pi} P_T \sin^{-1}\left[R_s'(\tau)/\sqrt{(1 + r_1)(1 + r_2)R_s(0)R_s''(0)}\right]$$

where P_T is the output power of each of the limiters, and $R_s(\tau)$ is the autocorrelation function of the signal. The ratio $R_s'(0)/\sqrt{R_s(0)R_s''(0)}$ is less than unity as can be shown using the Schwarz inequality. This discriminator characteristic is of roughly the same shape as obtained without limiting since $\sin^{-1}x \approx x$ for $|x| < 1$. The peak value of the loop gain varies in proportion to $[(1+r_1)(1+r_2)]^{-1/2}$.

If a band-pass limiter is used on both received input channels, then using Price's[22] (6) we can show that the cross-correlation is given by

$$R_{12}(\tau) = \frac{\left(\frac{\pi}{8}\right)P_T R_s(\tau)}{\sqrt{(1 + r_1)(1 + r_2)}}\left\{1 + \sum_{m=1}^{\infty} \cdot \frac{\left[\left(\frac{1}{2}\right)\left(\frac{3}{2}\right)\cdots\left(\frac{2m-1}{2}\right)\right]^2}{m!(m-1)!}\,\frac{\rho_s{}^{2m}(\tau)}{\sqrt{(1 + r_1)(1 + r_2)}}\right\}$$

where $R_s(\tau) \triangleq \rho_s(\tau)\cos[\omega_0\tau + \lambda(\tau)]$, *i.e.*, $\rho_s(\tau)$ is the envelope of $R_s(\tau)$. The discriminator characteristic, $-R_{12}'(\tau)$, is not greatly different in shape from $-R_s'(\tau)$. The loop gain is again attenuated by both noise-to-signal ratios r_1 and r_2.

Experimental Version of the Discriminator

A laboratory model of the delay-lock discriminator has been constructed and tested. The objective of the experimental work was to demonstrate the basic principles of operation and to provide experimental verification of some of the theory of linear operation. Ferrite-core delay lines with magnetically controlled permeability[23] were used in these particular experiments as the variable delay elements.

A block diagram of the experimental delay-lock discriminator is shown in Fig. 14. In this experimental equipment, the reflection and transmission from the target were simulated by another delay line similar to the one used in the discriminator. An AGC amplifier was provided in the signal input channel to maintain constant input power to the discriminator. The loop filter $F(p)$ consisted of a RC low-pass filter with a time constant of 8.8 msec.

The phase delay vs control current characteristic of the delay lines used in the experimental discriminator is shown in Fig. 15. Note the nonlinearity and hysteresis effect present even for relatively small delay variations. Additional measurements have shown the slope of the curve (*i.e.*, the delay line gain) to vary as a function of carrier frequency approximately ± 10 per cent of the value shown. The group delay (slope of the phase shift vs frequency curve) is expected to vary by about this same amount from the values shown.

The amplitude spectrum of the carrier measured at the output of the AGC amplifier is shown in Fig. 16(a).

[19] W. B. Davenport, Jr., "Signal-to-noise ratios in bandpass limiters," *J. Appl. Phys.*, vol. 24, pp. 720–727; June, 1953.

[20] J. J. Bussgang, "Cross-correlation functions of amplitude-distorted Gaussian signals," Mass. Inst. Tech., Cambridge, Mass., RLE TR No. 216, pp. 4–13; March, 1952.

[21] If x_1 and x_2 are limited forms of $y_1 \triangleq s + n_1$ and $y_2 \triangleq s' + n_2$, respectively, then it can be shown that $R_{x_1x_2}(\tau) = P_T\{4\,\Pr[y_1(t) > 0, y_2(t+\tau) > 0] - 1\}$, where $\Pr(y > 0)$ is the probability that $y > 0$. This probability can be evaluated by integrating the bivariate normal distribution to obtain the above result.

[22] R. Price, "A note on the envelope and phase-modulated components of narrow-band Gaussian noise," IRE Trans. on Information Theory, vol. IT-1, pp. 9–12; September, 1955.

[23] H. W. Katz and R. E. Schultz, "Miniaturized ferrite delay lines," 1955 Natl. IRE Convention Record, pt. 2, pp. 78–86.

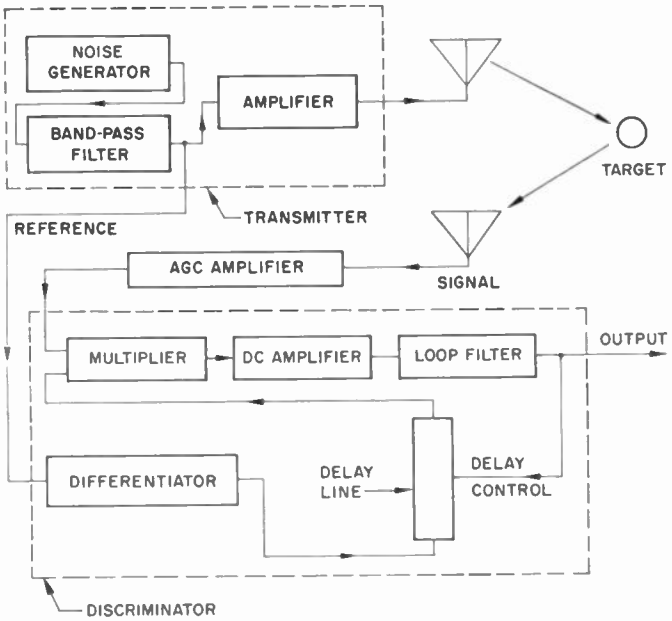

Fig. 14—Experimental system-block diagram.

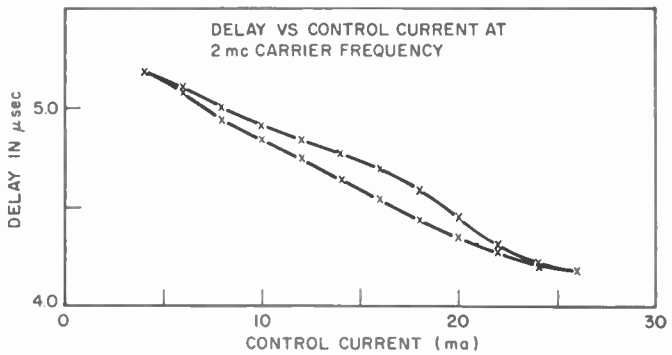

Fig. 15—Discriminator delay-line characteristic.

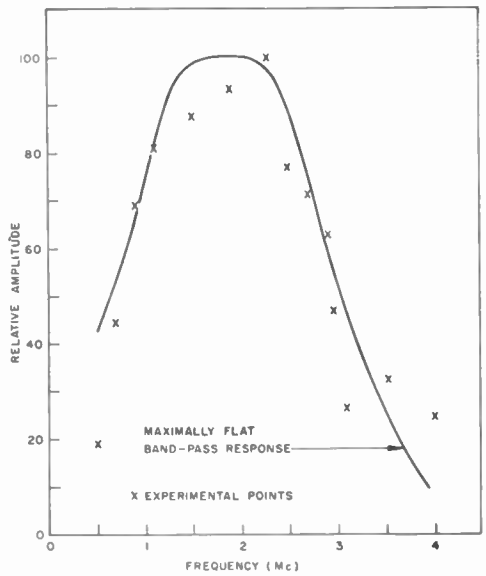

(a)

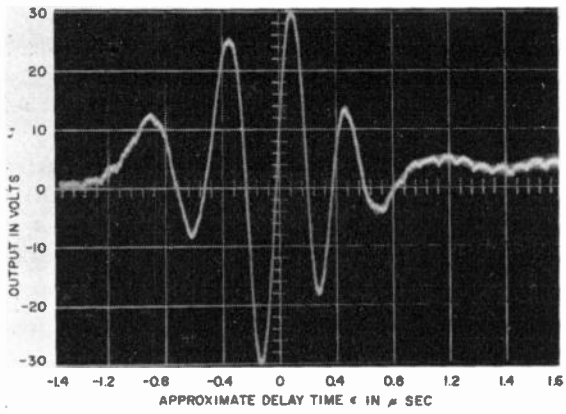

(b)

Fig. 16—(a) Amplitude spectrum of carrier. (b) Oscillogram of discriminator characteristic.

A maximally flat band-pass spectrum with the same 3 db points as the experimental data is plotted for comparison. This spectrum has a center frequency of 1.85 Mc.

The discriminator characteristic obtained from the experimental system is shown in Fig. 16(b). The horizontal axis is labelled "approximate delay" since much nonlinear distortion was produced by the delay line. Note that the delay variation presented is about $2\frac{1}{2}$ times that shown in Fig. 15. It should be pointed out, however, that the operating range for the measurements presented is the main lock-on region at the center of the oscillogram. This portion of the discriminator characteristic, which is quite linear, extends ± 0.12 μsec about the $\epsilon = 0$ position. This wave corresponds to a center frequency of approximately 2.1 Mc for a symmetrical band-pass spectrum. Thus, the major linear region of the characteristic extends over a range of delay error ϵ that agrees to within 13 per cent of the value predicted by the maximally flat band-pass approximation to the experimental spectrum.

Measured open-loop and closed-loop amplitude responses are plotted in Figs. 17(a) and 17(b), respectively. The measured open-loop response coincides well with the theoretical response of an RC low-pass loop filter with a cutoff frequency of 18 cps. Using a linearized equivalent circuit similar to Fig. 4, we see that for such a simple filter the only effect of the feedback will be to multiply the cutoff frequency by a factor of $1+g$. The measured loop gain was $g=11$. The theoretical closed loop response plotted in Fig. 17(b) is that of a single real-axis pole with a cutoff frequency of 216 cps. The measured closed-loop response, plotted also in Fig. 17(b), again matches the theoretical curve closely.

Another check on the theory of linear operation of the delay-lock discriminator can be made by measuring the transient error for a triangular wave input. Figs. 18(a) and 18(b) show the discriminator responses for 13 ma, peak-to-peak inputs of frequencies 24 cps and 240 cps, respectively. Since a triangular wave is a summation of an infinite number of ramps, the transient error to a triangular wave can be found from the error to a ramp.

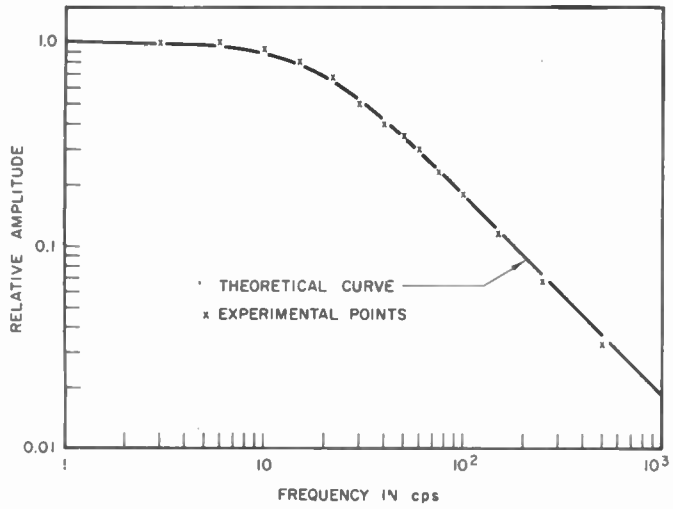

(a)

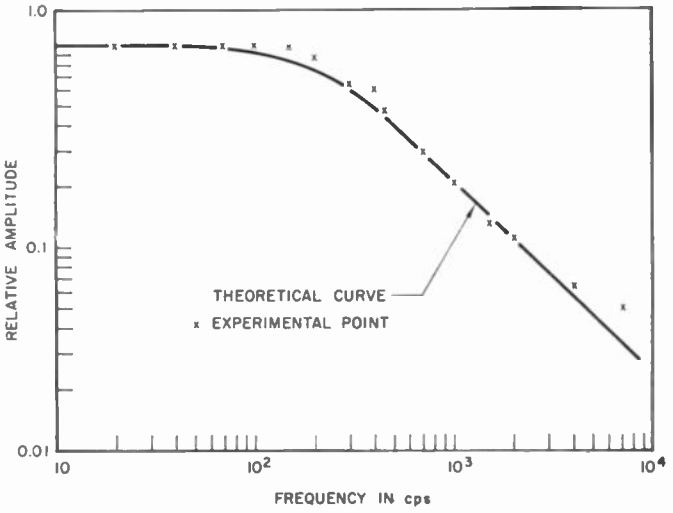

(b)

Fig. 17—(a) Open-loop amplitude response. (b) Closed-loop amplitude response.

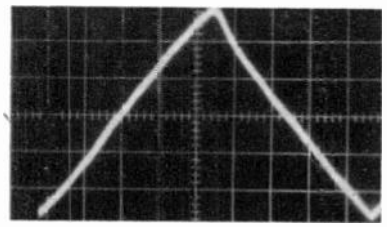

(a)

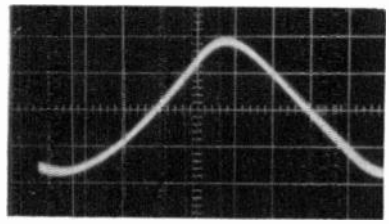

(b)

Fig. 18—Oscillograms of discriminator delay-line, control current for triangular wave control current in modulating delay line. (a) 24 cps input. Vertical scale is 2 ma per division, while the horizontal scale is 5 msec per division. (b) 240 cps input. Vertical scale is 2 ma per division, while the horizontal scale is 500 μsec per div.

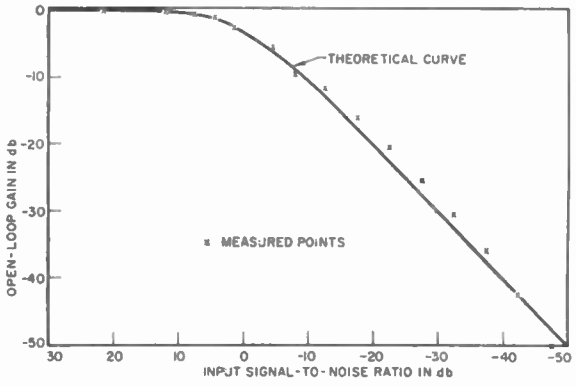

Fig. 19—Loop gain vs input signal-to-noise power ratio.

From elementary control theory, using a linearized equivalent circuit similar to Fig. 4, it is possible to find a simple expression for the delay error $\epsilon(t)$ to a ramp input of delay.

$$\epsilon(t) = \frac{at}{(1+g)} + \frac{agRC}{(1+g)^2}\left(1 - e^{-(1+g)t/RC}\right) \qquad (29)$$

where the input is

$$T(t) = at, \qquad t \geq 0$$
$$= 0, \qquad t < 0.$$

If we define ϵ' as the peak-to-peak output error in response to a triangular wave input, then it can be shown that[24]

$$\epsilon' = 2\epsilon(t = T_0/2) \qquad (30)$$

[21] Choose the time origin so that the input function is an even function of time.

where T_0 is the period of the triangular wave input. Further calculations using (29) and (30) predict a peak-to-peak amplitude of 11.6 ma for the 24 cps input, and a peak-to-peak amplitude of 8.0 ma for the 240 cps input. These predictions are in good agreement with the oscillograms of Figs. 18(a) and 18 (b).

The measured loop gain as a function of input, SNR power ratio, is plotted in Fig. 19. A theoretical curve based on (28) is plotted in the same figure and corresponds closely with the experimental points. This curve of loop gain is an indirect indication of closed-loop discriminator dynamic range and closed-loop bandwidth. A version of this discriminator, with a higher dc loop gain than that described here, has operated at input SNR ratios as low as −40 db.

Discussion

On the basis of these results, the delay-lock discriminator appears to have good potential in tracking rapidly

moving targets while using very low, received, SNR ratios. It is especially suited to tracking problems where the initial target position is known or where tracking is to begin only when the target enters a fixed perimeter. However, by the use of search techniques, targets of unknown initial position can be tracked.

By properly choosing the signal spectrum shape and bandwidth, good performance can be obtained with respect both to reducing the ambiguity in target position and discriminating against undesired targets.

In practice, where tracking is required over moderately long distances, the use of servocontrolled ultrasonic delay lines seems attractive. Delays in the millisecond range are attainable using such lines, and the linearity of delay vs control voltage can be made quite good. However, the response of the servosystem has to be taken into account in computing the closed-loop response. The presence of this servomotor within the loop may require some modification of the loop filter depending on the speed of response desired. Other delay techniques using such devices as magnetic recorders or shift registers might also be useful where long delays are desired.

The delay line also restricts the signal frequency spectrum that can be used because of its delay-bandwidth product limitations. At present, quartz delay lines can function at frequencies up to 100 Mc. However, the state of the art prevents direct discriminator operation at frequencies much above this with delays in the millisecond region. If transmission frequencies above this are to be used (a likely requirement) and delays are large, the transmitted signal can be formed by amplitude or frequency-modulating an RF sine wave with low-pass random energy. The low-pass random waveform can then be synchronously (or nonsynchronously) detected at the receiver, and the detected signal fed into the delay-lock discriminator. If synchronous detection is to be used, it should be noted that the phase of the local oscillator used for detection must follow the phase modulation of the carrier caused by the reflection from the moving target.

It is also possible to devise modified versions of the delay-lock discriminator which can operate directly on FM deviated signals and use video delay lines. Nonsynchronous forms of the discriminator can provide delay estimates which are free of the possible ambiguities caused by the fine structure of the signal autocorrelation function. In essence, this type of operation is made possible by ignoring the fine structure and working only with the envelope of the autocorrelation function. If the delay-lock discriminator is to be used in an interferometer, the delay variations generally are in the microsecond region or less, and the frequency limitations of the delay lines become greatly relaxed.

Further work is being carried out on the problems of locking-on and unwanted target discrimination. For example, reflections from undesired targets can be discriminated against in both range and velocity by making the closed-loop bandwidth relatively small. Then, if the undesired target passes rapidly enough through the range of the target to which the discriminator is locked, the interfering transients which result occur too rapidly to affect materially the discriminator output. Adaptive filtering techniques seem to be appropriate here; one loop filter can be employed during the lock-on transient, and another can be used after lock-on is established.

List of Symbols

A = signal amplitude
B_s = signal bandwidth (cps)
c = velocity of light (or of sound if sonic propagation is considered)
$e = 2.718$
E = expected value of a random variable
f = frequency (cps)
f_0 = center frequency of the signal
$F(p)$ = loop filter transfer function
g = loop gain
$G_s(f)$, $G_n(f)$ = signal, noise, power, spectral densities
h = a constant
$H(p)$ = linearized equivalent transfer function
k = reference signal amplitude
$n(t)$ = input noise waveform
$n_e(t)$ = equivalent noise
p = complex frequency
p_0 = filter cutoff frequency in rad/sec
P_s, P_n = signal, noise-average power
r = input noise-to-signal power ratio
$R_s(\tau)$, $R_n(\tau)$ = signal, noise autocorrelation functions
$s(t)$ = signal waveform (unity power)
t = the variable time
$T(t)$ = delay
$\hat{T}(t)$ = estimate of delay
v = velocity of the target
$x(t)$ = multiplier output
y = a variable
α = relative amplitude of the delay estimate
$\delta(f)$ = Dirac delta function
ΔT = dynamic range of the discriminator
$\epsilon(t)$ = delay error $T(t) - \hat{T}(t)$
ϵ_T = threshold delay error
$\rho(\tau)$ = envelope of the normalized autocorrelation function
σ = standard deviation of a random variable
τ = a variable representing time
$\phi(t)$ = phase function
ω = angular frequency
$\omega_i(t)$ = instantaneous angular frequency

Acknowledgment

The authors would like to acknowledge the valuable comments and suggestions of their associates in Communications Research at Lockheed Missiles and Space Company. Special thanks are expressed to M. R. O'Sullivan for his interesting and rewarding comments.

A Sequential Detection System for the Processing of Radar Returns*

AARON A. GALVIN†, MEMBER, IRE

Summary—**This paper describes a system which permits a substantial reduction in the amount of equipment required for the detection of narrow-band radar returns which may fall into any part of a wide, noisy Doppler band. The system utilizes a two-step process; the first providing a coarse, high false-alarm indication of range and Doppler, and the second providing high-quality detection and parameter estimation.**

The basic principles are discussed, followed by a description of an experimental prototype system.

Experimental results are presented.

Introduction

WHEN no *a priori* knowledge is available about the Doppler frequency or time of occurrence of a narrow-band return falling in a wide-band noisy spectrum (see Fig. 1), an optimum method for real-time detection is to survey the spectrum with a parallel bank of a large number of matched filters arranged as a comb in frequency, and to observe whether the output of one or more filters exceeds a preset threshold. In order to be sure that at least one of the filters in the comb is approximately matched to the return, a sufficient number of the filters must be used to guarantee that one will be excited near its center frequency. The number of filters required to do this for a single receiver can get into the thousands.

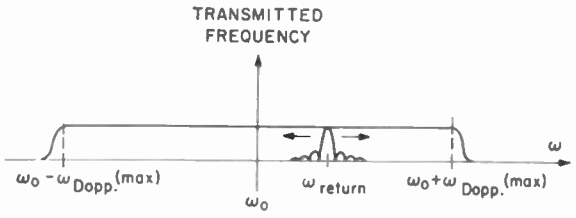

Fig. 1—Problem: detection of narrow-band radar return in noisy, wide-Doppler-band environment.

For an example, consider a radar with a 1-msec pulse, operating at 9000 Mcps, and equipped to handle a range of target velocities of ±18,000 nautical mph. A comb set of matched filters for this radar would contain approximately 2000 filters.

In recent years, the problem of providing matched filtering for radars has become increasingly difficult because of the tendency for advanced radars to: 1) operate at higher-carrier frequencies, which results in a larger Doppler band for a given range of target velocities, 2) be designed to handle a larger range of target velocities, 3) use long-duration, narrow-band signals to achieve high-energy per pulse, and 4) have multiple simultaneous beams, each of which must be optimally processed.

Because of the increased cost per incremental db of system sensitivity in advanced radars, it is essential to use a processing system which provides as close to optimum-signal detectability as is technically feasible.

Detection Techniques

A. Detector Plus Video Filter

The simplest method for achieving reasonably high detectability on a simple-pulsed return in noise is to feed the IF output into a diode detector whose output then feeds a video low-pass filter, matched (or nearly matched) to the envelope of the return (see Fig. 2). At high IF input signal-to-noise ratios, the detector plus video filter very nearly approximates an IF coherent-matched filter which has been centered on the frequency of the return. When the input signal-to-noise ratio is reduced, the efficiency of the detector begins to fall off, and at an input signal-to-noise ratio of about +3 db the rate of signal degradation approaches a point below which the use of this technique becomes questionable. No information on the Doppler of the signal can be obtained during this process since this information is destroyed by the initial detection.

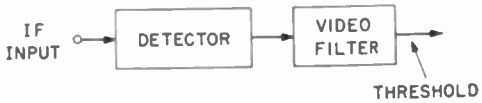

Fig. 2—Simple method for detection, good at high *S/N*.

B. Medium-Bandwidth Filters Plus Detectors Plus Video Filters

The inability of the detector-plus-video-filter combination to function properly at low signal-to-noise ratios can be circumvented by using it in a filter system which guarantees that, for signals of interest, the detector will always be presented with a high signal-to-noise ratio. A comb set of medium-bandwidth predetection filters (IF filters whose bandwidths are large when compared to the signal-spectral width, but small when compared to the total Doppler coverage band) raises the input signal-to-noise ratio to a value at which the detectors can efficiently operate. It is then possible to per-

* Received by the IRE, March 17, 1961; revised manuscript received, June 19, 1961.

† Lincoln Lab., Mass. Inst. Tech., Lexington, Mass.

form the remainder of the narrow banding with the use of a simple set of video filters as shown in Fig. 3.

An incidental benefit to the use of this technique is that it is possible to get an approximate indication of the Doppler of the signal, as will be shown later in this paper.

C. Bank of Narrow-Band Filters

A filtering technique that is able to achieve good performance at low-input signal-to-noise ratios is that shown in Fig. 4, a comb set of IF coherent matched (or nearly matched) filters. It should be noted, however, that this method requires a considerably larger number of filter channels than does the technique described in the preceding paragraph for the same total Doppler band.

D. Millstone Hill[1] Detection Technique

The Millstone Hill radar represents an early example of a radar in which the occurrence of a wide Doppler band and a narrow-signal spectrum combine to cause a somewhat difficult problem in the processing of the receiver data.

The following is a list of the parameters of the Millstone Hill radar which, in part, determine the parameters of the detection equipment:

Operating Frequency:	440 Mc/sec
Type of Modulation:	rectangular pulse, noncoded
Repetition Rate:	30 pulses per second
Pulse width (τ):	2 msec
$1/\tau$:	50 cps.
Range of target velocities:	$\pm$18,000 nautical mph
Corresponding Doppler band:	$\pm$25 kcps.

The matched filter for Millstone's two-millisecond pulsed sinusoid is a filter with the familiar $\sin x/x$ selectivity characteristic, centered at the frequency of the target return, with a $\pm$500 cps first null. In order to provide matched filtering over the entire 50 kcps of Doppler, a large set of $\sin x/x$ filters could be arranged as a comb in frequency as shown in Fig. 4. Based on the Millstone parameters, the matched filters could be spaced by 250 cps at the cost of a 1-db loss in signal detectability if the return falls midway between two filters. If this spacing is chosen, a total of 200 filters are required per receiver polarization in order to obtain full coverage in Doppler. Although this number of filters is not unreasonable if one uses a simple filter, the amount of equipment becomes prohibitive if one considers using this number of matched filters, each of which is highly complex. In order to permit a system which is feasible from an equipment standpoint, some deviation from the optimum filter must be allowed.

[1] Lincoln Lab. tracking-radar field site, Westford, Mass.

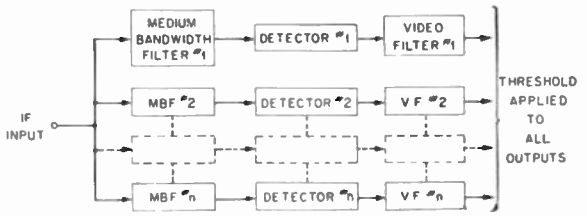

Fig. 3—Method for detection good at medium S/N.

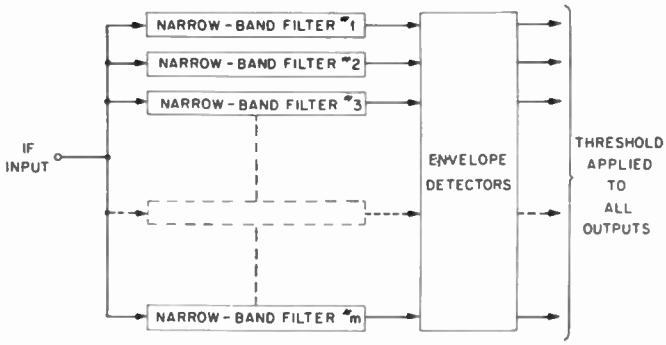

Fig. 4—Method for detection good at low, medium, and high S/N.

A small deviation (less than 1 db) from the optimum filter is allowed in the Millstone Hill detection equipment by the use of a single-tuned approximation. These filters are simple and relatively inexpensive, but a large number of them are still required in order to guarantee that one will be excited near its center frequency for any signal frequency.

Although a spacing on the order of 250 cps could be used between the filters at Millstone, it was decided to reduce this spacing to 160 cps for two reasons: 1) to reduce the peak-signal loss which occurs in the mid-range between two filters, and 2) to provide a better indication of where in frequency the return fell, without requiring the additional complexity of frequency-interpolation equipment.

Fig. 5 shows the peak CW response and the response at the end of a 2-msec pulsed input for two adjacent Millstone filters. It should be noted that although the CW filter response has a half-power bandwidth of 200 cps (the optimum single-tuned bandwidth for processing a 2-msec pulsed sinusoid in noise) the pulse-response characteristic exhibits an effective bandwidth greater than 450 cps.

Fig. 6 shows part of Millstone's 628-filter (314 filters per receiver polarization) comb set and some associated digital-encoding equipment.

Although the Millstone filtering technique offers conceptual simplicity (an important factor in the consideration of equipment which might be used in a production-model field radar, to be maintained by relatively untrained operating personnel) a rather large amount of equipment is required for its implementation. Certainly, if the Doppler band were a few times larger or the signal bandwidth a few times narrower, this technique would have to be abandoned.

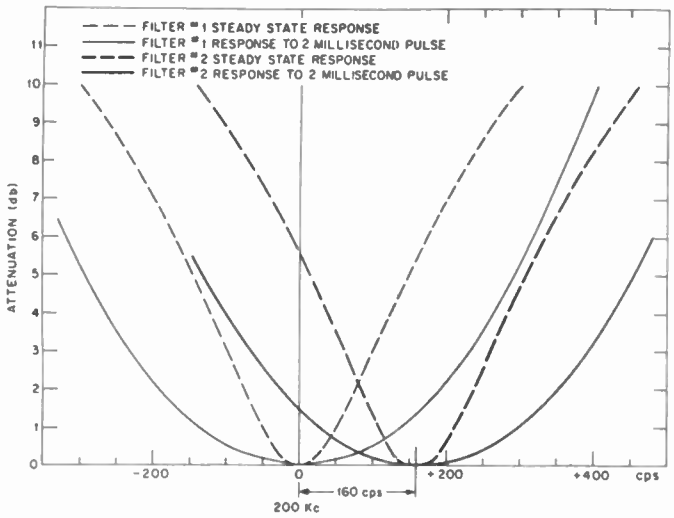

Fig. 5—Steady-state and transient-selectivity characteristics of two adjacent Doppler filters.

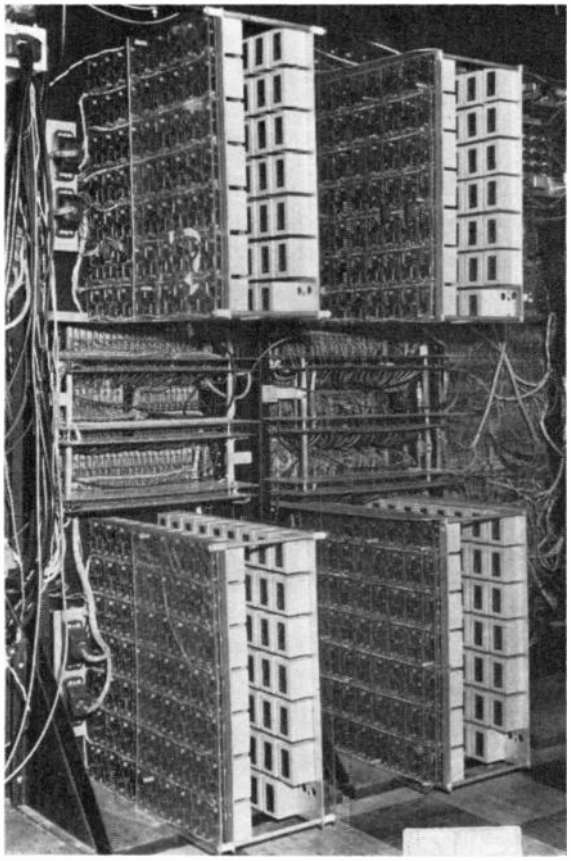

Fig. 6—Section of Millstone filter bank.

Sequential Detection and Processing Technique

It was found that considerable economy could be realized by a two-step detection process; *i.e.*, by first performing the job of detection in a coarse, high false-alarm manner and then taking the stored IF input and routing it to a small comb set of narrow-band filters covering a bandwidth only as large as that required to find the signal with the aid of the original coarse measurements. Fig. 7 shows a block diagram of this sequential technique. When the output of the coarse detection equipment exceeds the first threshold, it initiates a selection of one of a bank of crystal oscillators. At the same time it gates the stored IF output into a converter which is fed by a mixing oscillator whose frequency is selected to place the converted signal within the band embraced by the fine-detection equipment. If the output of the fine detector does not exceed the second threshold, the original coarse detection is assumed to have been a false alarm and it is neglected. If the threshold is exceeded, a legitimate hit is assumed to have occurred and precision parameter-estimation equipment is then put into action.

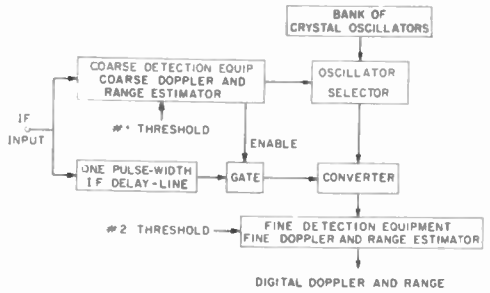

Fig. 7—Sequential detection and processing system.

In addition to using the knowledge of Doppler, gained in the first step of the detection process, it is also possible to utilize the coarse-range measurement. Instead of allowing the fine narrow-band filters to be fed with IF noise at all times (even when the signal is not present) the delayed signal can be gated into the fine filters using a gating signal which encloses the delayed IF signal. This noise-gating process reduces the contribution of the presignal noise to the total output noise. The experimental sequential processor, to be described later, utilizes this technique.

A. Coarse-Detection Equipment

The practicability of the sequential approach depends rather strongly on the availability of a simple device for performing the job of coarse detection. That is, there must be available a simple piece of equipment which can operate over the entire Doppler band with a probability of detection very nearly the same as a set of matched filters, at the price of a high false-alarm rate. At the same time, the equipment must be able to give a coarse indication of the Doppler frequency and the range of the return for use in the second step of the detection process.

For a simple, rectangular, pulsed-sinusoidal signal this can be done as shown in Fig. 8.

The equipment primarily consists of a set of the filters shown in Fig. 3. The outputs of the video low-pass filters feed a set of diodes all of which have a common load. The output of this diode load then consists of the instantaneous maximum of the output of any one of the video filters. The voltage out of the diode network then feeds a range estimator which produces a trigger at the trailing edge of the return. This trigger is fed into the

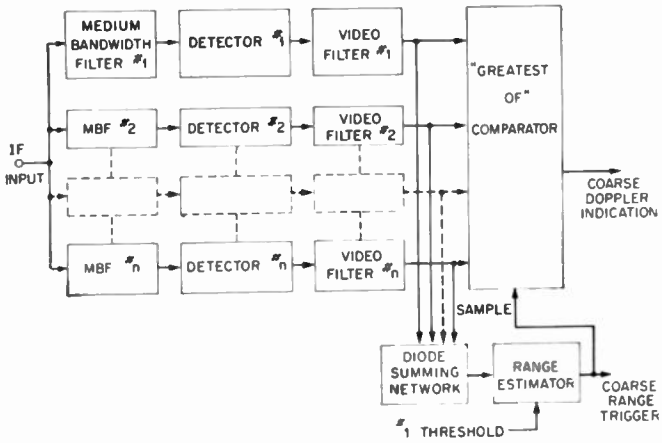

Fig. 8—Coarse detection equipment, course Doppler and range estimator.

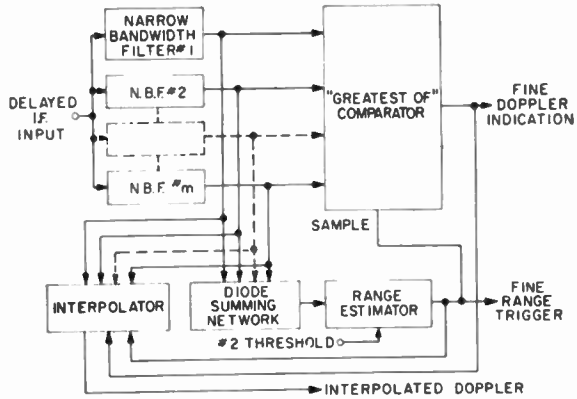

Fig. 9—Fine detection equipment, fine Doppler and range estimator.

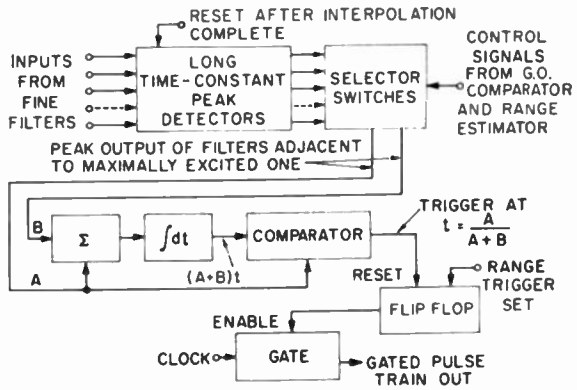

Fig. 10—Doppler interpolator.

"sample" input of the "greatest of" comparator, which determines which of the inputs has the highest instantaneous-voltage value. When the "sample" pulse is removed, the output corresponding to the highest input stores a positive dc voltage, which is used to select a local oscillator for use in the conversion of the signal frequency into the band covered by the fine-detection filters.

Based on the Millstone Hill parameters it is possible to do the complete job of coarse Doppler and range estimation with about one five-inch subrack of transistorized equipment.

B. Fine-Detection Equipment

The fine-detection equipment primarily consists of a set of the filters shown in Fig. 4. The outputs of the narrow-band filters are handled in much the same way as were the filters in the coarse-detection equipment, except that the filter outputs also drive an interpolator.

The stability requirements on the center frequencies, bandwidths, and insertion losses of the narrow-band filters are very stringent since in this system these stabilities, in conjunction with the operation of the interpolator, determine the basic limits of the no-noise Doppler accuracy.

Two of the blocks in Fig. 9 are not self-explanatory and deserve further discussion: the Doppler interpolator and the range estimator.

C. Doppler Interpolator

The Doppler interpolator is a device which reduces the Doppler measurement quantum to a value below that which would be obtained by encoding only the fact that the signal fell in a particular filter. As shown in Fig. 10 it is a partially analog, partially digital device. A set of selector switches, controlled by signals from the fine "greatest of" comparator and range estimator, cause a gating into some analog circuitry of the peak-voltage output of the two filters (labeled A and B) adjacent to the maximally excited one. This circuitry produces a trigger at a time proportional to the ratio of the amplitude out of filter A to the amplitude out of filter A plus filter B. The time between this generated trigger and the time of application of the two input voltages can be shown to be proportional to the frequency difference between some known frequency in the mid-range between filters A and B, and the best estimate of the place where the return fell. By choosing the proper clock rate it is possible to obtain a gated-pulse train in which each pulse represents one cycle per second of Doppler shift.

D. Range Estimator

The purpose of the range estimator, shown in Fig. 11, is to make an accurate estimate of the time of occurrence of the return, even though the video output which feeds the device has a very long time duration.

Before the range estimator will put out a range trigger, four different criteria must be met simultaneously: the input must exceed a certain preset amplitude threshold; a digital range-enable pulse must be positive; the slope of the input waveform must be negative; and the "centroid" of the input waveform must be nearly centered in a video delay-line, which is a means of avoiding gross errors in the estimate of the position of the range pulse at very low signal-to-noise ratios. At high SNR this geometric criterion would not be necessary since it would be impossible to get a negative slope at any place other than the trailing edge of the target return.

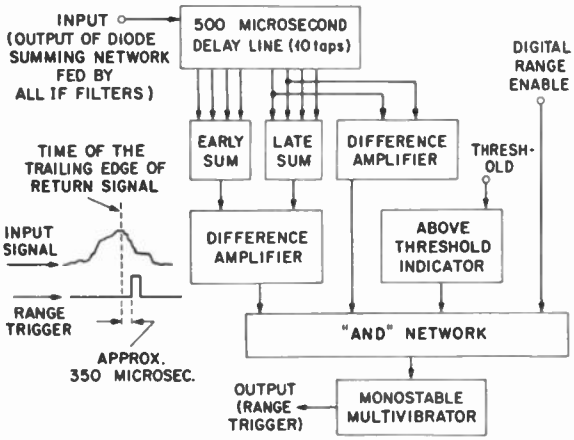

Fig. 11—Range estimator (for 2-msec pulse).

E. Doppler Summarizer

The Doppler summarizer, shown in Fig. 12, is a digital device which accepts inputs from the fine and coarse "greatest of" comparators and the Doppler interpolator and encodes and combines these to form a resultant digital-Doppler word.

Experimental System

Fig. 13 shows a block diagram of an experimental sequential-Doppler processor which has been implemented using the Millstone Hill radar signal parameters in order to provide a means of testing it in actual target tracking operations.

The following is a description of the system:

The input is fed at 30 Mc from the radar receiver. Two channels are driven in parallel; one undelayed and one delayed by 2.5 msec using an ultrasonic crystal delay-line. The undelayed channel is converted down to 200 kcps to feed the 13 filters of the coarse detector, and the delayed channel is converted (with a local-oscillator frequency selected by the coarse-detection equipment) down to a frequency which will place any target into a 5-kcps band centered at 200 kcps. The output of the delayed channel is then gated into a set of 21 narrow-band filters. If the output of any one of these filters exceeds a preset threshold, a legitimate echo is assumed to have occurred. The "greatest of" comparator then determines which of the filters has the highest peak response and controls the Doppler interpolator, which samples the amplitudes of the two filters adjacent (higher and lower frequencies) to the maximally-excited filter and converts this to a digital indication of where in the response of the center filter the return fell.

The results of the coarse, fine, and interpolation measurements are summed in the Doppler summarizer and then stored in a 16-bit accumulator.

The following is a discussion of some of the rationale behind the choice of the particular type, numbers, bandwidths, and spacings of the filters in the coarse and fine filter banks:

The first step was to choose the type, bandwidth, and

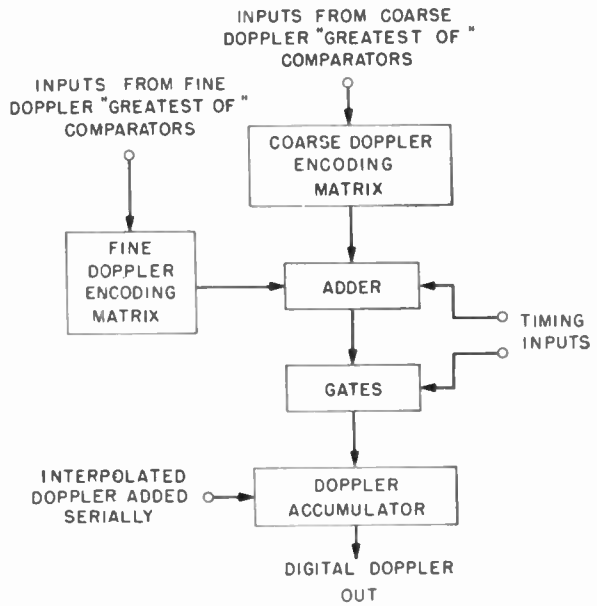

Fig. 12—Doppler summarizer.

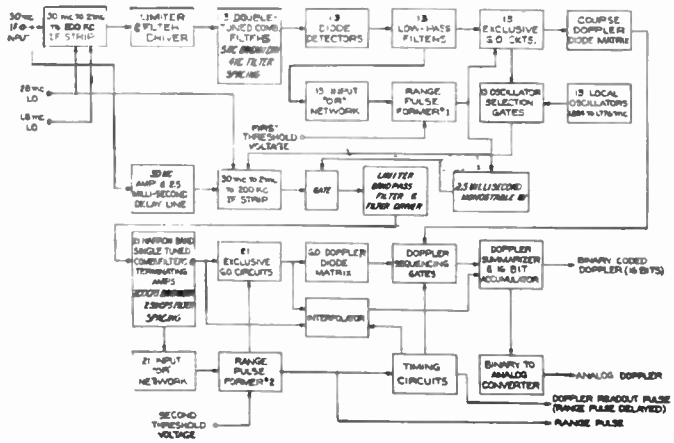

Fig. 13—Experimental sequential processor for 2-msec pulse and 50-kc Doppler band. (Note: only one polarization shown.)

spacing of the filters in the fine filter bank. For simplicity, single-tuned filters were chosen, and since the signal pulsewidth was 2 msec, 200-cps filter bandwidths were used. A 250-cps filter spacing was chosen in order to provide a small total number of fine filters with an acceptable loss in signal midway between filters.

The second step was to choose the operational fine-filter threshold, and then to calculate the required IF input signal-to-noise ratio to yield a threshold crossing. In order to yield a high probability of detection, in excess of 95 per cent, and a reasonably low false-alarm rate, less than one per minute, an output signal-to-noise ratio of approximately 14 db was required. A 200-cps single-tuned filter in a 50-kc IF bandwidth will yield a 14-db output signal-to-noise ratio when the input is approximately minus 5 db.

The third step was to determine the required medium-band filter pre-detection signal-to-noise gain at an input

signal-to-noise ratio of −5 db. An 8-db signal-to-noise gain above IF was required to guarantee that the signal would present the detector with a plus 3-db input signal-to-noise ratio; however, in order to be more conservative, the requirement was set at a 9.5-db predetection gain.

The fourth step was to choose the type of medium-band filter. Since the type is not critical once one gets above a single-pole filter, a second-order Butterworth filter was chosen.

Once the type of medium-band filter was chosen, the required bandwidth and spacing could be determined. To achieve a 9.5-db signal-to-noise improvement, a bandwidth of 5 kcps was required, and in order to yield a low loss between filters a 4-kcps spacing was chosen.

The last step was to choose the total number of coarse and fine filters. Since the coarse filters had to cover the entire 50 kcps of Doppler with 4-kc spacing, a total of 13 filters were required. Since the fine filters only needed to cover a region of frequency slightly larger than the spacing between coarse filters only about 17 fine filters were required, but in order to reduce the stability requirements on the coarse-filter banks, 21 fine filters were used in the experimental system.

The block diagram of Fig. 13 shows only a single IF input. The experimental system, however, accommodates two IF inputs, one for each of two orthogonal-receiver polarizations.

The additional polarization is processed as follows:

A duplicate coarse-filter bank and crystal delay-line is driven by the other polarization receiver. A comparison of the amplitudes out of the coarse filters from the two polarizations gates the stored IF from the polarization with the greater signal into the fine processor.

The procedure is, in essence, to set up the coarse-detection equipment in such a way that it provides information on the relative strengths of the signals in each polarization in addition to performing its basic functions.

For aid in testing the sequential processor, two binary-to-analog converters, one for the first 8 bits of Doppler and another for the next 8 bits, were included in the equipment to provide visual indications of Doppler on meters or analog recording devices.

The system can handle multiple targets (nonoverlapping in range, or overlapping, but in the same coarse-frequency region) and provides single-pulse measurements, quantized to the nearest one foot per second, to signal-to-noise ratios as low as −6 db (at IF).

Figs. 14 and 15 show a front and rear view of the experimental system.

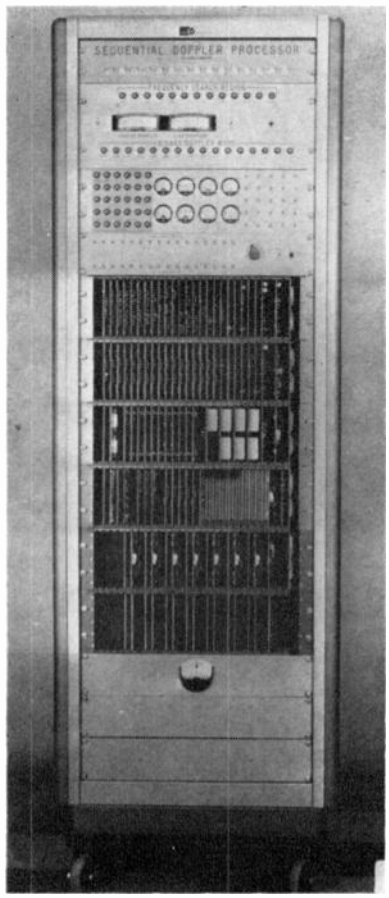

Fig. 14—Front view of experimental sequential processor.

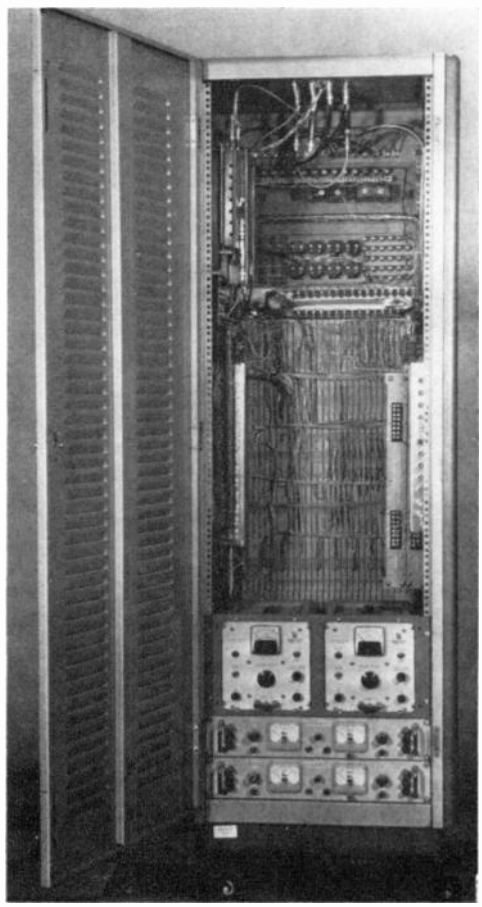

Fig. 15—Rear view of experimental sequential processor.

Experimental Results

Tests were run during satellite tracking operations using the sequential processor and the Millstone filter bank in parallel in order to obtain a comparison between the performance of the two systems. A digital computer accepted the data from both systems in real time and plotted the hit-by-hit output data. A detailed examination of these hit-by-hit data indicated that the sequential processor operated with essentially the same probability of detection, and false-alarm rate as the full filter bank, in spite of the fact that the satellite returns were scintillating rather strongly and both systems experienced a wide range of input signal-to-noise ratios.

Fig. 16 shows a segment of data taken from the sequential processor during the tracking of a satellite. The data was taken using a moving-pen recorder with one pen connected to a digital-to-analog converter fed by the eight most significant bits of digital-Doppler output and the other pen, the eight least significant bits. Noise-induced jitter in the Doppler measurements can be seen modulating the bottom analog recording.

Computer plots of Doppler-report distributions for matched-filter output signal-to-noise ratios of 16 db and 49 db (IF signal-to-noise ratios of approximately −4 db and +29 db, respectively) are shown in Fig. 17. The horizontal baselines of the photographs are 1000 feet per second, representing two per cent of the entire Doppler-coverage band.

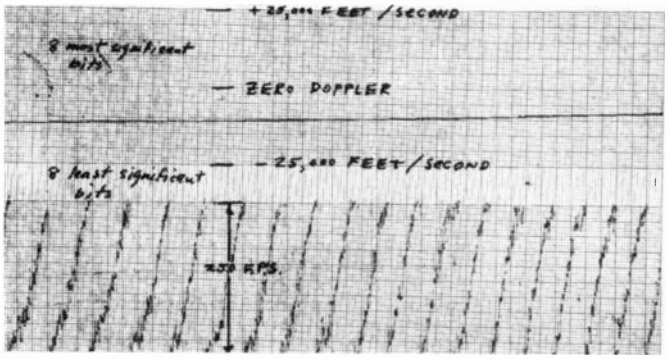

Fig. 16—Analog conversions of digital-Doppler reports obtained while tracking a satellite.

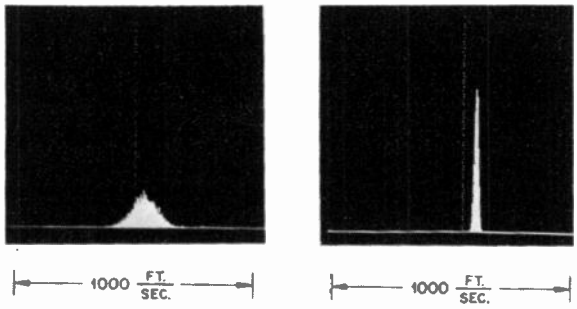

Fig. 17—Measured distributions of Doppler reports for signal-to-noise ratios of 16 db (left) and 49 db (right).

Fig. 18 shows a plot of the measured standard deviations of Doppler-report distributions as a function of $2E/N_0$ (where E is the signal energy and N_0 is the noise power per cycle) for the sequential processor. Although the experimental curve was plotted from 15 points, with each point calculated from a 5000-sample distribution, the use of the Millstone computer in real time permitted the entire experiment to be run and the curve to be drawn in approximately one hour.

A plot of R. Manasse's formula for maximum-theoretical Doppler accuracy[2] is shown for comparison with the experimental results. The discrepancy between the two curves has not as yet been fully explained and is presently under investigation.

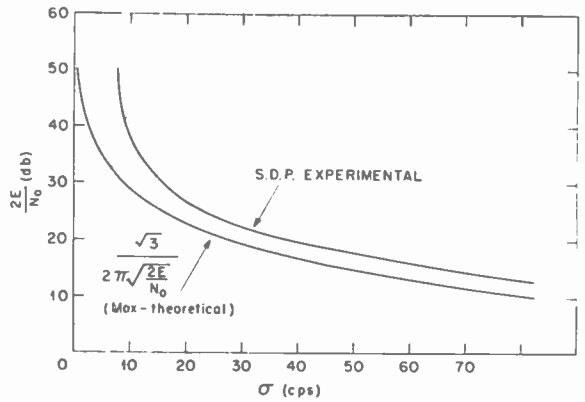

Fig. 18—Standard deviation of Doppler-report distribution vs $2E/N_0$.

Concluding Remarks

The experimental prototype system succeeded in simulating a set of four-hundred filters with only forty-seven filters, and operated with essentially no sacrifice in performance when compared to the many-filter method of detection. The techniques should be applicable to an extrapolated version of this system for the simulation of a much larger filter bank. A sequential processor is presently being designed to process 10 msec simple, rectangular pulses (±100 cps sin x x first null) in a Doppler band 1.5 mcps wide; a problem which, with the use of a conventional narrow-band comb set, would require 30,000 filters for its solution.

Acknowledgment

The author wishes to acknowledge the help of E. L. Key, formerly of the Lincoln Laboratory, in the design of the Doppler interpolator, and the work of D. R. Bromaghim, W. H. Drury and W. F. Kelley, of the Lincoln Laboratory, in the detailed design and testing of the experimental system.

[2] R. Manasse, "Summary of Maximum Theoretical Accuracy of Radar Measurements," Mitre Corp., Bedford, Mass., Tech. Ser. Rept. No. 2; 1960.

Correspondence

Minimum Time for Turn-Off in Four-Layer Diodes*

It has been shown[1] that the minimum time τ_t required to turn off a four-layer diode by a linearly-decreasing terminal current does not depend on the rate of decrease of this current. The period τ_t, rather, depends exclusively on the dimensions of the two base regions and the minority-carrier constants in these regions as may be seen from the following equations:

$$\tau_t = \tfrac{1}{2}\tau_p\tau_n(\xi + 1)/(\tau_n\xi + \tau_p), \quad (1)$$

where

$$\xi = -(D_pA_p)/(D_nA_n). \quad (2)$$

$$A_p = (m/\Delta)(16q^2D_n^2p_nL_p/\tau_t\tau_n n_pL_n) \cdot \{|1 - \cosh(w_p/L_n)|\sinh(w_n/L_p) - (n_pL_n\tau_p/p_nL_p\tau_n)\sinh(w_p/L_n)\}. \quad (3)$$

$$A_n = (m/\Delta)(16q^2D_p^2D_n/\tau_p\tau_n) \cdot \{|\cosh(w_n/L_p) - 1|\sinh(w_p/L_n) + (p_nL_p\tau_n/n_pL_n\tau_p)\sinh(w_n/L_p)\}. \quad (4)$$

$$\Delta = -32(q^3D_n^2D_p)/(\tau_p\tau_n n_pL_n) \cdot [(n_pL_n/\tau_n)\sinh(w_p/L_n)\cosh(w_n/L_p) + (p_nL_p/\tau_p)\sinh(w_n/L_p)\cosh(w_p/L_n)]. \quad (5)$$

The constant m is the rate of decrease of the device terminal current. The constants w_p and w_n are the widths of the p-type and n-type base regions, respectively, and all other symbols have their usual meanings.

The above expression for τ_t is somewhat complicated. The purpose of this note is to express τ_t in an approximate simple form, and to plot the dependence of τ_t on the device constants.

In the on mode, the sum of the transport factors in the base regions is higher than unity[2] and less than two. If each of the two transport factors is sufficiently close to unity, then

$$\left.\begin{aligned} w_p/L_n &\ll 1 \\ w_n/L_p &\ll 1 \end{aligned}\right\}. \quad (6)$$

Conditions (6) allow us to write

$$\left.\begin{aligned} \sinh(w_p/L_n) &\cong (w_p/L_n) \\ \cosh(w_p/L_n) &\cong 1 \end{aligned}\right\}. \quad (7)$$

Similar approximations may be made for $\sinh(w_n/L_p)$ and $\cosh(w_n/L_p)$. In view of these approximations and (1)–(5), there results:

$$\tau_t/\tau_p = \frac{1}{2}\left[\frac{1 + (\tau_n/\tau_p)x}{1 + x}\right], \quad (8)$$

where

$$x = (p_nw_n\tau_n)/(n_pw_p\tau_p). \quad (9)$$

Eq. (8) is plotted in Fig. 1 for a number of values of (τ_n/τ_p). It may be observed from (8) that for small values of x, (τ_t/τ_p) approaches 0.5; and for large values of x, (τ_t/τ_p) approaches $(\tau_n/2\tau_p)$ or (τ_t/τ_n) approaches 0.5.

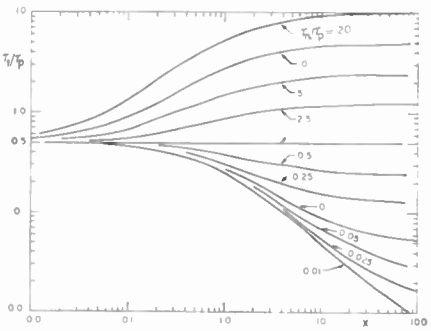

Fig. 1—Plots of the ratio (τ_t/τ_p) vs x for different values of (τ_n/τ_p).

M. A. Melehy
Elec. Eng. Dept.
University of Connecticut
Storrs, Conn.

Microwave Amplification in Electrostatic Ring Structures*

The possible use of spatially periodic electrostatic or magnetic structures to amplify cyclotron waves on electron beams is now established. Both quadrupolar[1] and axially-symmetric structures[2,3] have been considered. The former amplify by producing coupling between the fast and slow cyclotron waves; these have both opposite power flow and opposite polarizations. The latter amplify by coupling a cyclotron wave with the synchronous wave of opposite power flow; this has the same polarization. In this case, the axially-symmetric pump fields produce equal rotational energy and displacement changes on all electrons of an input cyclotron wave. An output coupler will remove all the rotational energy of all electrons and, hence, leave the beam monoenergetic. By collector potential depression the conversion efficiency of such devices may, therefore, be very high.

This note describes the main features and some experimental results on amplification in the electrostatic ring system of Fig 1 (see also Gould and Johnson).[4] The equations of motion for a paraxial electron in the fundamental component of the electrostatic pump fields and the axial magnetic field $B_z = \omega_c/\eta$ are:

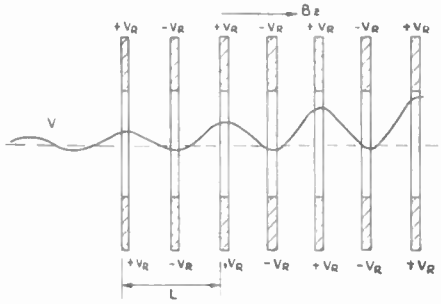

Fig. 1—Electrostatic ring amplifier.

$$\frac{d^2x}{d\theta^2} + \frac{dy}{d\theta} - \mu\sin\beta z \cdot x = 0 \quad (1a)$$

$$\frac{d^2y}{d\theta^2} - \frac{dx}{d\theta} - \mu\sin\beta z \cdot y = 0 \quad (1b)$$

$$\frac{d^2z}{d\theta^2} - \frac{2\mu}{\beta}\cos\beta z = 0 \quad (1c)$$

where $\theta = \omega_c t$, $\mu = \eta\beta^2A_1V_R/2\omega_c^2$, $\beta = 2\pi/L$, and A_1 is an amplitude coefficient. For amplification, the electron transit time over one structure period must equal a cyclotron period. Hence, for small pump strengths, $\sin\beta z = \sin\theta$. A simplified solution of (1a) and (1b) gives the subsequent displacement of an electron in a filamentary fast or slow cyclotron wave entering the structure at r, ϕ as

$$x = r\left[\cosh\frac{\mu\theta}{2}\cos(\theta+\phi) - \sinh\frac{\mu\theta}{2}\cos\phi\right] \quad (2a)$$

$$y = r\left[\cosh\frac{\mu\theta}{2}\sin(\theta+\phi) - \sinh\frac{\mu\theta}{2}\sin\phi\right]. \quad (2b)$$

These equations show that its motion is that of an electron in a cyclotron wave growing as $\cosh\mu\theta/2$, coupled with that of an electron in a similarly polarized synchronous wave growing as $\sinh\mu\theta/2$. The profile of the resultant off-centered expanding helical trajectory of any electron in the beam is shown in Fig. 1. The cyclotron wave gain is given in decibels as 20 log $\cosh[A_1V_R\pi N/8V_0]$ for an N-electrode structure whose synchronous voltage is V_0 at zero ring voltage. The axial fields produced by an applied ring

* Received by the IRE, April 5, 1961. This work was sponsored by Hamilton Standard Div., United Aircraft Corp., Broadbrook, Conn., and was conducted at the University of Connecticut, Storrs.

[1] M. A. Melehy, "Theory of turn-off in four-layer diodes," to be published in IRE TRANS. ON ELECTRON DEVICES.

[2] For an explanation, see J. L. Moll, M. Tanenbaum, J. Goldey, and N. Holonyak, "*P-N-P-N* transistor switches," PROC. IRE, vol. 44, pp. 1174–1182; September, 1956.

* Received by the IRE, June 7, 1961.

[1] E. I. Gordon, "A transverse-field travelling-wave tube," PROC. IRE, vol. 48, p. 1156; June, 1960.

[2] T. Wessel-Berg and K. Blötekjaer, "Some Aspects of Cyclotron Wave Interaction in Time Periodic and Space Periodic Fields," presented at Internatl. Conf. on Microwave Tubes, Munich, Germany; June, 1960.

[3] E. I. Gordon, "Charged particle orbits in varying magnetic fields," *J. Appl. Phys.*, vol. 31, pp. 1187–1190; July, 1960.

[4] R. W. Gould and C. C. Johnson, "Coupled mode theory of electron-beam parametric amplification," *J. Appl. Phys.*, vol. 32, pp. 248–258; February, 1961.

voltage V_R lengthen the electron transit time over a structure period and the necessary input beam velocity u (voltage V) to give correct synchronism is found by integration of (1c) as

$$u = \frac{2u}{\pi\sqrt{1 + A_1V_R/V}} \cdot K\left[\frac{\pi}{2}, \sqrt{\frac{2A_1V_R}{A_1V_R + V}}\right]. \quad (3)$$

K is a complete elliptic integral. This expression decreases to u_0 as A_1V_R goes to zero. Since this amplifier couples synchronous waves with cyclotron waves an input beam of finite thickness expands periodically as exp $(\mu\theta/2)$ even in the absence of a signal wave. The tube must be designed to accommodate this expansion.

The experimental results were obtained at a frequency of 1100 Mc using a tube incorporating Cuccia couplers designed as capacitive terminations of balanced and screened resonant-transmission lines, each with 1.5 db minimum coupling loss to the beam. The ring structure comprised twelve thin disks. Its synchronous voltage V_0 was 300 v. Structure gain is plotted in Fig. 2 for

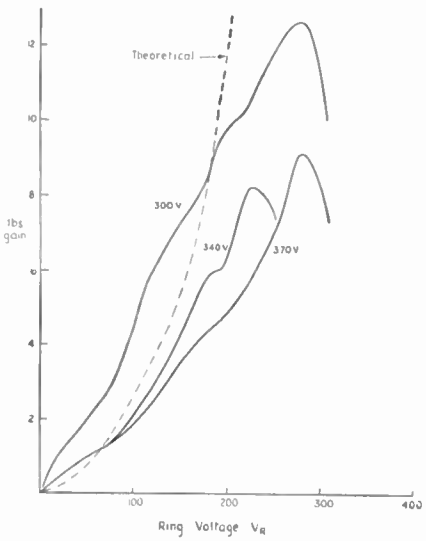

Fig. 2—Ring-structure gain.

various fixed beam voltages and its theoretical gain curve shown. This curve should represent the maximum attainable gain at any value of ring voltage and beam voltage. The turnover points of the different gain curves coincide with substantial current interception on the output coupler and the differences in turnover point for difference beam velocities can be correlated with electron rotation produced by the gun anodes. This can reduce or enhance beam spread according to entry conditions at the structure. The amount of spread is in agreement with theory.

The author wishes to thank Dr. T. E. Allibone, C.B.E., F.R.S., Director of the Laboratory for permission to publish this note.

J. C. Bass
Research Lab.
Associated Electrical Industries, Ltd.
Aldermaston, England

Diode Reverse Characteristics at Low Temperatures*

The low-temperature reverse current characteristics of a junction diode are found to exhibit inductance, negative resistance, and multiple crossings of different ambient temperature curves. These phenomena may be explained in terms of the diode's self-heating and the voltage drop across the bulk region of the sample external to the junction. The observed negative resistance differs from previous types of thermal "turnover"[1] in its origin and in the temperature range in which it occurs.

Fig. 1 shows the current-voltage characteristics of the diode (1N696) at ambient temperatures of 35°K, 78°K (liquid nitrogen) and, for the sake of comparison, room temperature. The turnover region is not shown. At low voltages, the current is simply the sum of the junction saturation and leakage currents, both of which increase with temperature; hence, in this region, the diode current rise with temperature is monotonic. The curves, however, intersect at 37 v and again at 48 v (a third intersection at a higher current will subsequently be discussed). The first crossing results from carrier multiplication[2] setting in earlier in the "colder" diode. The second intersection is brought about by the temperature dependence of the sample's bulk region resistance, as becomes evident by comparing the high current slopes of the two curves.

Large current characteristics (above 10^{-1}a) are plotted in Fig. 2 for ambient temperatures of 4°K and 40°K. For the latter temperature, two curves are given, illustrating the effect of the diode's internal heating. The observed negative resistance disappears when, for higher currents, the ambient temperature is lowered to compensate for the sample's own heating, thereby locally restoring the 40°K environment.

With the sample immersed in liquid helium, the negative resistance is more pronounced, as is shown in Fig. 2. A large inductance of thermal origin may also be identified in the turnover region. No turnover effects were found at temperatures above 55°K.

The explanation of the negative resistance and accompanying inductance is contained in Fig. 3(a) which illustrates two low-temperature isothermal current-voltage curves. The carrier multiplication regions and high current slopes are sketched as previously discussed. A pulse which shifts the load line from A-A to B-B initially moves the operating point from a to a'. However, the added dissipation in the sample increases its temperature resulting in a final operating point, b. This behavior is incorporated in the small-signal equivalent circuit of Fig. 3(b).

For operation in a helium bath, the inductance and negative resistance are quite stable and reproducible, since the sample is not subjected to air currents or ambient temperature variations. Presumably these turnover effects may be enhanced by constructing a sample with a long bulk region. Appreciable negative resistance and inductance may then be expected in a more convenient environment such as liquid nitrogen.

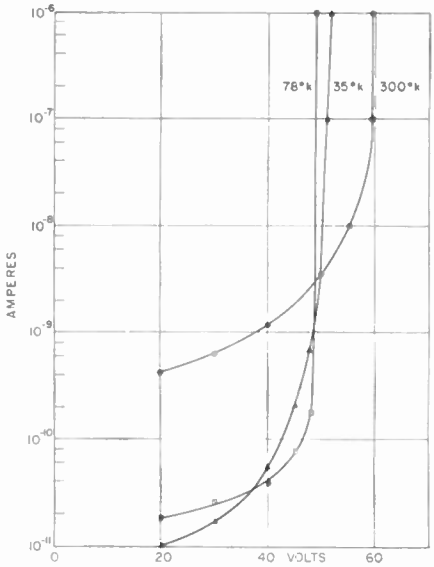

Fig. 1—Reverse current vs voltage.

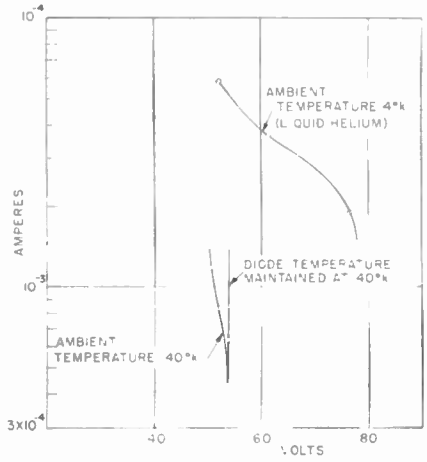

Fig. 2—Turnover region characteristics.

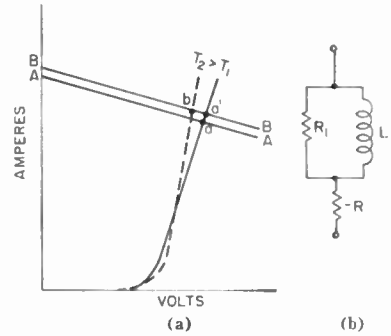

Fig. 3—Pulse behavior of diode in turnover region.

* Received by the IRE, June 21, 1961.
[1] See, for example, A. W. Matz, "Thermal turnover in germanium p-n junctions," *Proc. IEE*, vol. 104, pp. 555–564; May, 1957.
[2] K. G. McKay, "Avalanche breakdown in silicon," *Phys. Rev.*, vol. 94, pp. 877–884; May 1954.

Hence, useful applications of these phenomena appear possible at low frequencies.

ACKNOWLEDGMENT

The author gratefully acknowledges the contributions of W. T. Easter to this investigation.

ALVIN S. CLORFEINE
Dept. of Elec. Engrg.
Carnegie Inst. of Tech.
Pittsburgh, Pa.

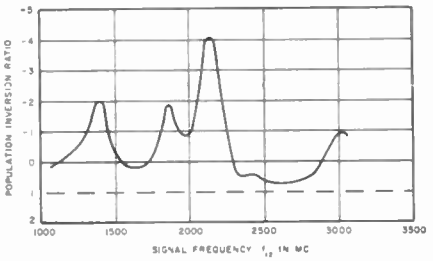

Fig. 1—Population-inversion ratio as a function of signal frequency for a fixed pump frequency $f_p = 12{,}465$ Mc.

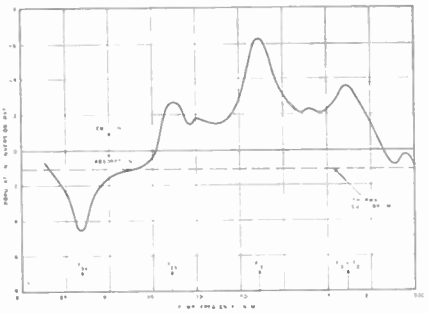

Fig. 2—Population-inversion ratio as a function of pump frequency for fixed signal frequency $f_{12} = 1055$ Mc and fixed magnetic field.

Maser Action in Ruby by Off-Resonance Pumping*

Strong microwave maser action has been obtained in ruby by pumping in the far wings of the pump transition as much as 1400 Mc from its center frequency. In a systematic investigation of the variation of population inversion with pump frequency, several anomalous inversion peaks were observed as the applied pump frequency was moved from the pump transition line center into the wings. For a fixed signal frequency of 1055 Mc, population inversion was maintained for a variation in pump frequency of 2500 Mc.

The investigation was made at 4.2°K for pink ruby (nominally 0.06 per cent Cr^{+++} by weight) whose C axis was oriented at 90° to the applied magnetic field. The experimental structure was similar to that of Geusic, *et al.*[1] This structure permits the direct determination of the population inversion ratio by measuring the magnetic emission (pump on) and magnetic absorption (pump off) over a range of signal frequencies.

Constant Pump Frequency Measurements: A number of measurements were made of the population inversion ratio while keeping the pump frequency constant, and varying the signal frequency f_{12} from 800 to 3400 Mc. (The notation f_{xy} refers to the frequency spacing between energy levels x and y numbered in order of increasing energy.) The incident pump power was kept constant near 200 mw. The applied magnetic field was changed for each signal frequency to correspond to the value required for normal three-level maser operation. Fig. 1 shows the population inversion ratio as a function of signal frequency for a fixed pump frequency $f_p = 12{,}465$ Mc. In addition to the peak at $f_{12} = 2150$ Mc, which corresponds to normal three-level maser operation, two new, relatively strong, inversion peaks are noticed at lower signal frequencies. Another inversion peak is observed near $f_{12} = 3000$ Mc. This operating point, where $f_p \approx f_{34}$, was shown to give significant gain in a traveling-wave maser.[2]

Constant Signal Frequency Measurement: An interesting measurement of population-inversion ratio as a function of pump frequency was obtained for a fixed signal frequency $f_{12} = 1055$ Mc. The applied magnetic field was kept fixed at its optimum value for normal three-level maser operation. Inversion was maintained for pump frequencies from 9600 to 12,100 Mc—a 2500-Mc range corresponding to more than 40 line widths (Fig. 2). The central peak corresponds to normal three-level operation ($f_p = f_{13}$). The inversion peak at $f_p = 9700$ Mc corresponds to $f_p = f_{23}$, which causes saturation of the f_{14} line via harmonic spin-coupling[3-5] since $f_{14} = 2f_{32}$ here. The refrigeration valley at 8700 Mc is due to $f_p = f_{34}$, and can be accounted for by harmonic spin-coupling ($f_{11} = 2f_{23}$). A strong anomalous inversion peak is observed at $f_p = 11{,}730$ Mc.

These and other measurements are summarized in Fig. 3, where pump frequency is plotted as a function of signal frequency f_{12}. The inversion *peaks* from the various measurements are shown as solid points. We have superimposed lines corresponding to the computed energy levels for ruby.[6] Inversion was obtained at pump frequencies removed as much as 1400 Mc (23 line-widths) from the f_{13} (or any other) resonance line.

In order to interpret the observed anomalous inversion peaks, other theoretical lines corresponding to pump frequencies equal to 1) $f_{13}+f_{12}$ and 2) $f_{34}+f_{12}$ have been superimposed on Fig. 3. The fit between these lines and the experimentally observed inversion peaks is very good. Calculation of the expected inversion, on the basis of a Lorentzian line shape[7] for the pump transition, accounts for the small inversion ratio obtained between the peaks. The anomalous

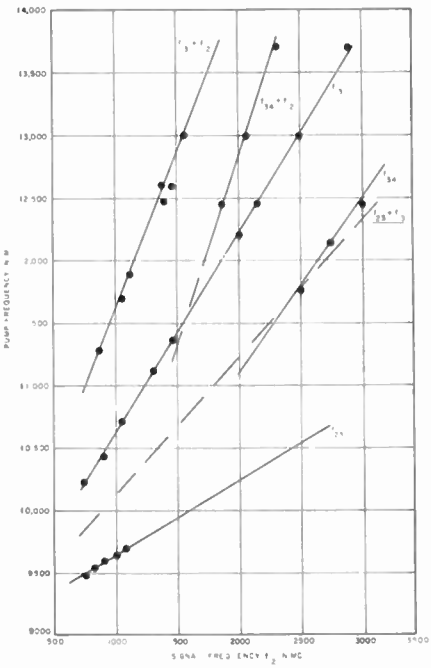

Fig. 3—Inversion peaks and their correlation with computed energy levels and anomalous lines $f_p = f_{13} + f_{12}$ and $f_p = f_{34} + f_{12}$.

peaks correspond very closely to frequencies at which there is a high probability of multiple spin-flip processes that conserve Zeeman energy and involve several energy levels. We believe these processes to be similar in nature to cross-relaxation processes discussed by Bloembergen *et al.*,[8] for LiF, and analyzed by Van Vleck for crystals with two magnetic species.[9] The predominant, simultaneous triple spin-flip processes corresponding to the anomalous peaks are: For $f_p = f_{13} + f_{12}$, a downward spin-flip at the off-resonance pump frequency, and upward spin-flips from level 1 to 3 and 1 to 2. For $f_p = f_{34} + f_{12}$, a downward spin-flip at the off-resonance pump frequency and upward spin-flips from level 3 to 4, and 1 to 2. These spin-flips are the most probable at that frequency in the wings where energy transfer can occur to the line *centers* while conserving Zeeman energy. A phenomenological treat-

* Received by the IRE, May 4, 1961; revised manuscript received, June 5, 1961. This is part of a Doctoral Dissertation performed at the Polytechnic Institute of Brooklyn, N. Y. The support of the Airborne Instruments Lab., Melville, N. Y., is gratefully acknowledged.

[1] J. Geusic, E. Schulz-DuBois, R. DeGrasse, and H. Scoril, "Three-level spin refrigeration and maser action at 1500 Mc/sec," *J. Appl. Phys.*, vol. 30, pp. 1113–1114; July, 1959.

[2] S. Ahern, private communication. Also, J. Walling and P. A. Gould, Mullard Res. Labs., Salfords, Surrey, Eng. Rept. 2312; December, 1960.

[3] F. Arams, "Maser operation at signal frequencies higher than pump frequency," IRE TRANS. ON MICROWAVE THEORY AND TECHNIQUES, vol. MTT-9, pp. 68–72; January, 1961.

[4] W. H. Higa, "Excitation of an L-band ruby maser," in "Quantum Electronics," Columbia University Press, New York, N. Y., p. 298; 1960.

[5] J. E. Geusic, "Harmonic spin coupling in ruby," *Phys. Rev.*, vol. 118, pp. 129–130; April, 1960.

[6] W. S. Chang and A. E. Siegman, "Characteristics of Ruby for Maser Applications," Electron Devices Lab., Stanford Univ., Stanford, Calif., Tech. Rept. 156-2, Figs. 14, 15; September 30, 1958. Also J. Weber, "Masers," *Rev. Mod. Phys.*, vol. 31, pp. 681 710; July, 1959.

[7] C. Kittel and E. Abrahams, "Dipolar broadening of magnetic resonance lines in magnetically diluted crystals," *Phys. Rev.*, vol. 90, pp. 238–239; April, 1953.

[8] N. Bloembergen, S. Shapiro, P. Pershan, and J. Artman, "Cross-relaxation in spin systems," *Phys. Rev.*, vol. 114, pp. 445–459; April, 1959.

[9] J. H. Van Vleck, "Dipolar broadening of magnetic resonance lines in crystals," *Phys. Rev.*, vol. 74, pp. 1168–1183; November, 1948.

ment, based upon inclusion in the rate equations of the cross-relaxation terms, shows the enhancement in inversion to be expected. Reasonable values for the cross-relaxation times give calculated results in semiquantitative agreement with the measurements.

The experiments reported here provide further evidence of the important role played by cross-relaxation in the attainment of population inversion in masers. Such data may also yield information on cross-relaxation line shape (since the magnetic field can be held constant) and higher-order spin-flip processes that give fine structure. By using a pulsed pump it may be possible to measure the relaxation times of various competing energy transfer processes.[10,11] Furthermore, the maser technique described here appears to be a sensitive tool for studying spin-spin processes and the behavior of paramagnetics in the far wings where the line susceptibility is decreased by orders of magnitude.

F. Arams
Airborne Instruments Lab.
Melville, N. Y.
M. Birnbaum
Polytechnic Institute of Brooklyn
Brooklyn, N. Y.

[10] K. Bowers and W. Mims, "Paramagnetic relaxation in nickel fluosilicate," *Phys. Rev.*, vol. 115, pp. 285–295; July, 1959.
[11] W. Mims and J. McGee, "Cross relaxation in ruby," *Phys. Rev.*, vol. 119, pp. 1233–1237; August, 1960.

Reverse Characteristics of Low-Lifetime Germanium Diodes*

The nonsaturable reverse characteristics of p-n junctions in silicon, or in such other wide-energy-gap semiconductor materials as gallium arsenide, can be explained in terms of carrier generation in the junction depletion region.[1] In this note, the validity of this theory is confirmed for germanium devices having very low minority-carrier lifetimes.

The simple theory of depletion-region carrier generation[1] assumes that the lifetimes, mobilities, and densities of the minority carriers on both sides of the junction are equal. It is also assumed that there are single-level, uniformly distributed recombination-generation centers located at the intrinsic Fermi level. Under these conditions, the ratio of the current generated in the space-charge region (J_{r0}) to the current generated in the n and p regions (J_d) has been shown to be[1]

$$\frac{J_{r0}}{J_d} = \frac{N_n}{4N_i}\frac{t}{L_0},$$

where N_n is the electron in the n material, N_i is the intrinsic carrier concentration, t is the depletion-layer thickness, and L_0 is the minority-carrier diffusion length.

By means of diffusion techniques, low-lifetime germanium diodes have been made having depletion-layer thicknesses of the order of one micron and diffusion lengths of two microns. N_n for the material used is 10^{16} carriers per cubic centimeter. Thus, the ratio J_{r0}/J_d is of the order of 50, and it may be expected that generation in the space-charge region will be the mechanism responsible for the reverse current. Furthermore, because the depletion-region thickness increases with applied voltage, the reverse current of a low-lifetime diode should not saturate, but should increase with applied voltage.

Fig. 1 compares the reverse characteristics of a low-lifetime diode with those of a diode having one-sixth the junction area and using higher-lifetime material. As can be seen, the low-lifetime diode exhibits the voltage dependence expected of saturation current generated in the depletion region. Fig. 2 shows a similar comparison at a temperature of 80° C.

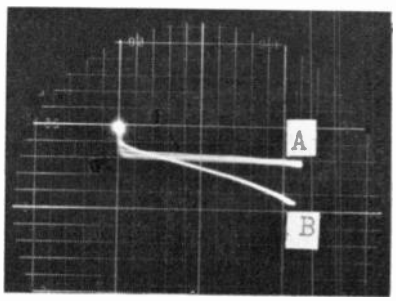

Fig. 1—Diode reverse characteristic at 25°C. (A) Conventional diode. (B) Low-lifetime diode. (Scale: vertical, 0.5 μa div.; horizontal, 1 v div.)

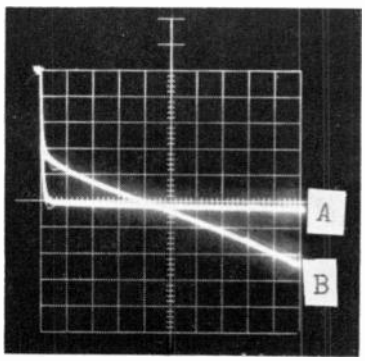

Fig. 2—Diode reverse characteristics at 80°C. (A) Conventional diode. (B) Low-lifetime diode. (Scale: vertical, 10 μa div.; horizontal, 1 v/div.)

A. Blicher
I. H. Kalish
Semiconductor and Material Div.
RCA
Somerville, N. J.

* Received by the IRE, June 8, 1961.
C. T. Sah, R. N. Noyce, and W. Shockley, "Carrier generation and recombination in p-n junctions and p-n junction characteristics," Proc. IRE, vol 45, pp. 1228–1243; September, 1957.

The Negative Resistances in Junction Diodes*

Anomalous behavior in the V-I characteristic of variable-capacitance diodes when used in parametric devices has been reported by several workers.[1,2,3] Over part of the irregular response, the V-I curve has a negative slope, and the diode behaves like a negative resistance (Fig. 1). This negative resistance is often related to the equivalent negative resistance produced by the variable capacitance of the diode. The purpose of this letter is to point out the difference between the two negative resistances, which could explain the discrepancy between the results of some of the experiments on parametric devices, and the energy equations of the nonlinear-reactance theorem as applied to the parametric phenomenon.

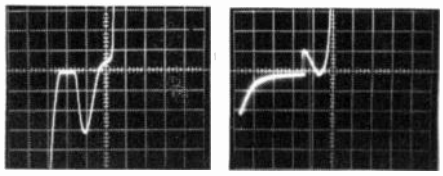

Fig. 1 Typical anomalous behavior in theV-I characteristics of junction diodes, when RF potential is applied across the diodes. (a) For p-n junction diode (MA460C varactor), the trace shows a negative-resistance behavior at the reverse current. (b) For gold-bounded welded-contact diode (Mullard OA47), the negative resistance appears at the forward current.
Vertical scale = 0.05 mA/div
Horizontal = 2 V div.

As is well known, the effect of a voltage-dependent reactance in an electric structure supporting more than one mode of oscillation is to produce a transfer of energy between the frequencies supported by the structure. In certain structural configurations, where regeneration can take place, the energy transfer mechanism is equivalent to that of inserting a negative resistance in a circuit resonant at the frequency which has a net energy gain. This equivalent negative resistance is therefore a wave property that can appear only at a prescribed frequency which is directly related to the other self and forced modes of oscillations of the structure and the energy carried at each frequency. Because this negative resistance is the result of the displacement current in the variable junction capacitance, it may be called "displacement-negative resistance."

On the other hand, the negative resistance which appears in the V-I characteristic in the bias circuit when the diode is driven hard, or when self-bias is applied, is believed to be due in part to the combined effect of the charged particles crossing the depletion-layer capacitance and being stored in the other region,[3] and not due to the displacement current that flows in the variable capacitance.

* Received by the IRE, June 14, 1961.
[1] J. C. McDade, "RF-induced negative resistance in junction diodes," Proc. IRE (Correspondence), vol. 49, p. 957; May, 1961.
[2] K. Siegel, "Anomalous reverse current in varactor diodes," Proc. IRE (Correspondence), vol. 48, pp. 1159–1160; June, 1960.
[3] I. Hefni, "Effect of minority carriers on the dynamic characteristic of parametric diodes," *Electronic Engrg.*, vol. 32, pp. 226–227; April, 1960.

This theory of current conduction through the junction capacitance is supported by the fact that such a negative resistance, which may be called "conduction-negative resistance" is not frequency dependent and can appear at any frequency with no correlation to the other modes of oscillation of the structure. Furthermore, it was found that this conduction-negative resistance was mainly dependent on the amplitude of the driving voltages, as well as the doping and construction of the junction,[3] and that any change in the modes of oscillation such as by the tuning or loading of the structure will affect the negative resistance only inasmuch as they affect the voltages across the junction. For example, it has been reported by McDade[1] that, in a parametric-harmonic generator circuit, "the negative resistance disappeared when harmonic power was drawn from the diode." This could be due to the fact that by loading the output-resonant circuit the voltages across the diode decreased, which resulted in the decrease or the disappearance of the negative resistance and not, as reported, due to "adding positive resistance to the diode." This is because by loading the output, positive resistance would be added to the harmonic and fundamental circuits and would not be added to the low-frequency bias sweeping circuit, where the negative resistance is being observed.

The conduction-negative resistance may also explain the good performance of high-order parametric subharmonic generators when self-bias is used, and the existence of frequency dividers operating at frequencies approaching the cutoff frequency of the diodes.[4]

IBRAHIM HEFNI
Lincoln Lab.†
Mass. Inst. Tech.
Cambridge, Mass.

[4] A. H. Soloman and F. Sterzer, "A parametric subharmonic oscillator pumped at 34.3 KMC," PROC. IRE, vol. 48, pp. 1322–1323; July, 1960.

† Operated with support from the U. S. Army, Navy, and Air Force.

Pattern Recognition by Moment Invariants*

A set of two-dimensional *moment invariants* has been found. Based upon these moment invariants, a pattern-recognition theory has been formulated. In this theory, geometrical patterns and alphabetical characters can be identified independently of their position, size and orientation. The two-dimensional moments of order $(i+j)$ of a pattern, described by a density distribution function $\rho(x, y)$ over a finite region D, are defined as

$$\iint_D x^i y^j \rho(x, y)\,dx\,dy, \quad i, j = 0, 1, 2, \cdots. \tag{1}$$

For simplicity, we assume D is composed of small squares, $\rho(x, y)$ is constant over each small square, and (1) will be denoted *symbolically* as

$$\sum m_0 x^i y^j, \qquad i, j = 0, 1, 2, \cdots. \tag{2}$$

It can be shown that there is one and only one $\rho(x, y)$ which can produce the same moments of all orders under the above conditions.

Let

$$x_0 = x - \sum m_0 x / \sum m_0, \qquad y_0 = y - \sum m_0 y / \sum m_0 \tag{3}$$

then we may define the central moments (moments about centroid) as

$$\sum m_0 x_0^i y_0^j, \qquad i, j = 0, 1, 2, \cdots. \tag{4}$$

It is well known that the central moments are invariant under translation. Under the similitude transformation,

$$x_1 = A x_0, \quad y_1 = A y_0, \quad A = \text{constant}; \tag{5}$$

we have $m = A^2 m_0$, and, therefore, also the moment invariant relation

$$\sum m x_1^i y_1^j / (\sum m)^{1/2(i+j)+1} = \sum m_0 x_0^i y_0^j / (\sum m_0)^{1/2(i+j)+1}. \tag{6}$$

Using similitude invariants of central moments, pattern identification can easily be accomplished independently of translation and size. The orientation independence is made possible by the following orthogonal invariants discovered in this study.

Under the orthogonal transformation or rotation,

$$x_2 = x_1 \cos\theta - y_1 \sin\theta, \qquad y_2 = x_1 \sin\theta + y_1 \cos\theta; \tag{7}$$

with the moments represented by

$$\mu_{ij}' = \sum m x_2^i y_2^j, \quad \mu_{ij} = \sum m x_1^i y_1^j, \qquad i, j = 0, 1, 2, \cdots, \tag{8}$$

it can be shown that the three second order moments satisfy the following relations:

$$\begin{aligned} &2\mu_{11}' = (\mu_{20} - \mu_{02}) \sin 2\theta + 2\mu_{11} \cos 2\theta, \\ &\mu_{20}' + \mu_{02}' = \mu_{20} + \mu_{02}, \\ &(\mu_{20}' - \mu_{02}')^2 + 4(\mu_{11}')^2 = (\mu_{20} - \mu_{02})^2 + 4\mu_{11}^2. \end{aligned} \tag{9}$$

There are two ways of using (9) to accomplish pattern identification independently of orientation: 1) The method of principal axes. If the angle θ is determined from the first equation in (9) to make $\mu_{11}' = 0$, then we have

$$\tan 2\theta = -2\mu_{11}/(\mu_{20} - \mu_{02}). \tag{10}$$

The x_2, y_2 axes determined by any particular value of θ satisfying (10) are called the principal axes of the pattern. With added restrictions, such as $\mu_{20}' > \mu_{02}'$ and $\mu_{30}' > 0$, θ can be determined uniquely. Moments determined with respect to such a pair of principal axes are independent of orientation. Discussion of certain exceptional cases in which (10) is indeterminate is omitted here. 2) The method of orthogonal moment invariants. The last two relations in (9) are invariants under rotation, and they can be used directly for orientation-independent pattern identification.

By combining (4), (6) and the two invariants in (9), two moment relations which are invariant under translation, similitude and rotation, can be derived. A simulation program using only these two invariants has been written for an LGP-30 computer. The program works satisfactorily and can identify and differentiate many different patterns under the stated conditions. In comparison, much larger and higher-speed computers are required in simulation for other pattern recognition approaches.

The alphabets "*b*" "*d*" "*p*" "*q*" cannot be distinguished by the above simple program. However, they can be distinguished by using higher-order moments in method 1 above. The value of θ is still determined by (10) but also satisfies the condition $|\theta| < 45$ degrees.

In using method 2, the discrimination property can also be increased by including higher-order moment invariants. For third-order moments, we can show that the following four expressions,

$$\begin{aligned} &(\mu_{30} - 3\mu_{12})^2 + (3\mu_{21} - \mu_{03})^2, \\ &(\mu_{30} + \mu_{12})^2 + (\mu_{21} + \mu_{03})^2, \\ &(\mu_{30} - 3\mu_{12})(\mu_{30} + \mu_{12})\left[(\mu_{30} + \mu_{12})^2 - 3(\mu_{21} + \mu_{03})^2\right] \\ &\quad + (3\mu_{21} - \mu_{03})(\mu_{21} + \mu_{03})\left[3(\mu_{30} + \mu_{12})^2 - (\mu_{21} + \mu_{03})^2\right], \\ &(\mu_{20} - \mu_{02})\left[(\mu_{30} + \mu_{12})^2 - (\mu_{21} + \mu_{03})^2\right] \\ &\quad + 4\mu_{11}(\mu_{30} + \mu_{12})(\mu_{21} + \mu_{03}), \end{aligned} \tag{11}$$

are invariants under orthogonal transformation.

Similarly, higher-order orthogonal moment invariants can be derived. In fact, it has been found that there exists a complete system of infinitely many such invariants. This complete system and some other properties of these invariants, and also the simulation program, will be published in the near future.

MING-KUEI HU
Elec. Engrg. Dept.
Syracuse University
Syracuse, N. Y.

* Received by the IRE, June 28, 1961; revised manuscript received, July 6, 1961.

Temperature Dependence of the Peak Current of Germanium Tunnel Diodes*

Esaki [1], [2] and Lesk, *et al.* [3] have presented data on the variation of the tunnel-diode current-voltage characteristic as a function of temperature. In general, it was found that the tunneling region of the characteristic is relatively independent of temperature, and that the important temperature variations occur in the injection region. Longo [4] has observed negative and positive temperature dependences which he attributes to the following: 1) the temperature effect on the energy distribution of free carriers about the Fermi level, and 2) the temperature dependence of the energy gap and its effect on the tunneling probability.

In the present work, the temperature dependence of germanium tunnel diodes was

* Received by the IRE, June 26, 1961. This work was supported by the Bureau of Ships.

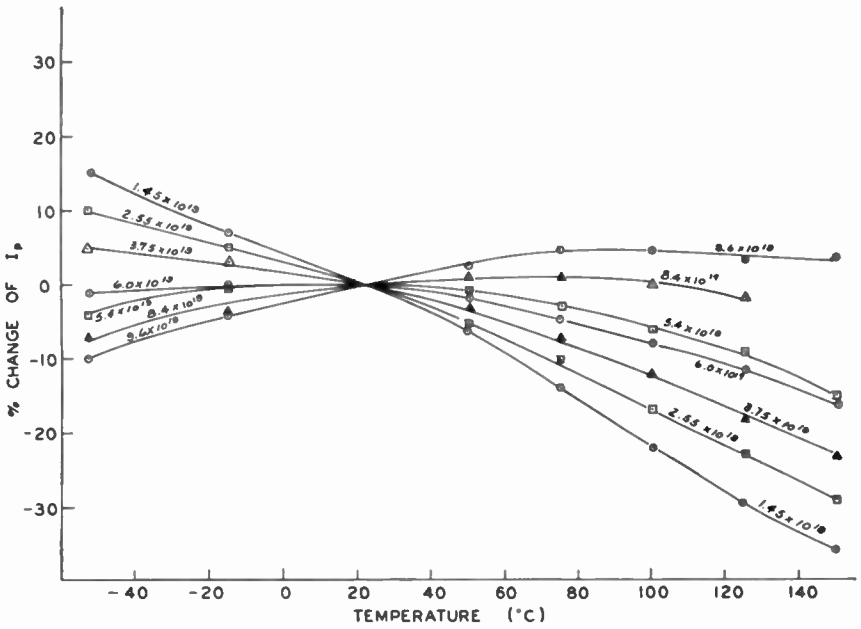

Fig. 1—Temperature dependence of peak current for germanium tunnel diodes having p-region carrier concentrations of 1.45×10^{19} to 9.6×10^{19} atoms/cc.

investigated as a function of carrier concentration. The diodes were prepared by a solution-growth technique in which epitaxial arsenic-doped n-type germanium layers are grown on gallium-doped p-type substrate. The diodes were electrolytically etched to produce peak currents of 50 ma and junction diameters ranging from 0.7 to 3.2 mils. The carrier concentration of the germanium substrate was varied from 1.45×10^{19} to 9.6×10^{19} acceptors per cm³. The n-region doping density was unknown, but was assumed to be constant because all junctions were grown under identical conditions.

Fig. 1 shows the percentage change of the peak current I_p as a function of temperature with the p-region carrier concentration as a parameter. At the lowest concentration used (1.45×10^{19} atoms per cm³), the percentage change in I_p with temperature is considerable, and the temperature coefficient is negative in the temperature range from −55°C to +150°C. Below room temperature, the temperature coefficient changes from negative to positive with increasing doping density, and is zero at approximately 6.0×10^{19} atoms per cm³. Above room temperature, the temperature coefficient is negative at low doping densities, increases to approximately zero at 8.0×10^{19}, and is slightly positive at 9.6×10^{19} atoms per cm³.

The net electron current flowing across the junction is the difference between the Esaki and Zener currents and is given by Esaki and others [1] and [5].

$$I = A\int_{E_c}^{E_v} Z[f_c(E) - f_v(E)]_c dE, \qquad (1)$$

where Z is the tunneling probability per second described by the following approximate formula [3]

$$Z = \frac{aeE}{\hbar}\exp\left[\frac{-A'm^{*1/2}E_g^{3/2}}{\hbar eE}\right] \qquad (2)$$

As all of the parameters or functions involved in the above expressions are affected by temperature and concentration to varying degrees [6–11], a very complex temperature dependence of the tunneling is indicated. In some cases, it will be necessary to take into account phonon assisted transitions as well [12–14].

The above considerations indicate tunneling current is a very complex function of temperature and carrier concentration; at this time no attempt has been made to develop an analytical expression for peak current as a function of temperature with carrier concentration as a parameter.

However, according to experimental data it is possible to design tunnel diodes having negative or positive peak current temperature coefficients. By judicious choice of carrier concentration it is possible also to minimize the temperature effects on peak current.

A. Blicher
R. M. Mixton
R. Glicksman
Semiconductor and Materials Div.
RCA
Somerville, N. J.

References

[1] L. Esaki, "New phenomenon in narrow Ge p-n junctions," *Phys. Rev.*, vol. 109, pp. 603–604; January, 1958.
[2] L. Esaki and Y. Miyahara, "A new device using the tunneling process in narrow p-n junctions," *Solid-State Electronics*, vol. 1, pp. 13–21; January, 1960.
[3] I. A. Lesk, *et al.*, "Germanium and silicon tunnel diodes—design, operation and application," 1959 IRE WESCON Convention Record, pt. 3, pp. 9–31.
[4] T. A. Longo, "On the nature of the maximum and minimum currents in germanium tunnel diodes," *Bull. Am. Phys. Soc.*, vol. 5, p. 160; March, 1960.
[5] J. J. Tiemann, "Shot noise in tunnel diode amplifiers," Proc. IRE, vol. 48, pp.1418–1423; August, 1960.
[6] M. Cardona, "Dielectric constant of germanium and silicon as a function of volume," Div. of Eng. and Applied Res., Harvard Univ., Cambridge, Mass., Contract Nonr-1866 (10), NR-017-308; July, 1959.
[7] G. G. MacFarlane, *et al.*, "Fine structure in the absorption—edge spectrum of Ge," *Phys. Rev.*, vol. 108, pp. 1377–1383; December, 1957.
[8] J. I. Pankove, "Influence of degeneracy on recombination radiation in germanium," *Phys. Rev. (Letters)*, vol. 4, pp. 20–21; January, 1960.
[9] J. I. Pankove, "Optical absorption by degenerate germanium," *Phys. Rev. (Letters)*, vol. 4, pp. 454–455; May, 1960.
[10] J. S. Blakemore, "Carrier concentrations and Fermi levels in semiconductors," *Elec. Commun.*, vol. 29, pp. 131–153; June, 1952.
[11] R. A. Smith, "Semiconductors," Cambridge University Press, London, Eng., ch. 4, p. 77; 1959.
[12] L. V. Keldysh, *Soviet Phys. JETP*, vol. 34, p. 665; October, 1958.
[13] N. Holonyak, *et al.*, "Direct observation of phonons during tunneling on narrow junction diodes," *Phys. Rev.* (Letters), vol. 3, pp. 167–168; August, 1959.
[14] P. J. Price and J. M. Radcliffe, "Esaki tunneling," *IBM J.*, vol. 3, p. 364; October, 1959.

On the Possibility of Rejecting Certain Modes in VLF Propagation*

Long-distance propagation of VLF radio waves is characterized by only a few low-order waveguide modes. This results from the excessive attenuation of the higher-order modes. In navigational systems, this is a desirable characteristic since the phase velocity approaches a constant at very great ranges when only one mode is predominant. Unfortunately, the second-order mode still exerts its influence for ranges as great as 4000 km. The possibility that this second-order mode could be discriminated against at the transmitting antenna is an intriguing one. We will discuss this problem from an analytical viewpoint. At the same time it is hoped that this might shed some light on the behavior of antenna arrays at VLF.

The field at height z of a vertical antenna at height z_0 at (great-circle) distance d on a smooth spherical earth of radius a can be written as a sum of modes in the form[1]

$$E = \frac{1}{\sqrt{\sin\,(d/a)}}\sum_n A_n e^{-ikS_n} f_n(z_0) f_n(z), \quad (1)$$

where $k = 2\pi/\text{wavelength}$.

A_n is a coefficient which does not depend on the coordinates; $f_n(z_0)$ and $f_n(z)$ are height-gain functions which approach unity for z_0 and $z=0$, respectively; and S_n is a dimensionless complex number which determines the attenuation and phase characteristics of the individual modes.

We now consider an array of P identical vertical antennas arranged in a straight line with equal spacing Δ. The current at each antenna is taken to be $I_0 \exp(-ip\psi\Delta M)$ where p ranges from 0 to $P-1$. Thus, we have a traveling wave of velocity c/M propagating down the array. The total field at the observer, who is a distance d_0 from the antenna at $p=0$, is

$$E = \sum_{p=0}^{P-1} \frac{1}{\sqrt{\sin\,(d_p/a)}}\sum_n A_n e^{-ikd_p S_n} e^{-ip\psi\Delta M} \times f_n(z_0) f_n(z), \quad (2)$$

where d_p is the great-circle distance from antenna p to the observer.

Now in most practical situations envisaged by this writer, the length of the array $P\Delta$ is small compared to both the

* Received by the IRE, July 5, 1961.
[1] J. R. Wait, "Terrestrial propagation of very-low-frequency radio waves," *J. Res. NBS*, vol. 64D (Radio Propagation), pp. 153–204; March/April, 1960.

radius of the earth and the distance d_0. Thus

$$d_p = d_0 - p\Delta \cos \beta,$$

where β is the angle subtended by the great-circle distance d_0 and the line of the array. The situation is illustrated in Fig. 1. Consequently, (2) may be approximated by

$$E = \frac{1}{\sqrt{\sin (d_0/a)}} \sum_n A_n f_n(z_0) f_n(z) e^{-ikd_0 S_n} G_n, \quad (3)$$

where

$$G_n = \sum_{p=0}^{P-1} \exp \left[ipk\Delta(S_n \cos \beta - M) \right]. \quad (4)$$

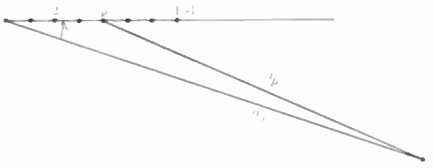

Fig. 1—Plan view of the array.

The gain function G_n can be written in closed form as follows:

$$G_n = e^{i(P-1)Z_n/2} \frac{\sin (PZ_n/2)}{\sin (Z_n/2)}, \quad (5)$$

where $Z_n = k\Delta(S_n \cos \beta - M)$.

To maximize the power going into the first mode (for $\beta = 0$), Z_1 is set equal to zero. Consequently, $M = S_1$. Now S_1 has a real part near unity and a small negative imaginary part. For practical purposes, M can be taken equal to the real part of S_1, so that all elements in the array may have currents of the same amplitude.

In order that the excitation of the second mode vanishes for $\beta = 0$, it is necessary to choose

$$PZ_2 = 2(2q - 1)\pi, \qquad q = 1, 2, 3 \cdots,$$

in order that $G_2 = 0$. The condition may be written

$$Pk\Delta(S_1 - S_2) = 2(2q - 1)\pi.$$

To illustrate the absurdity of this situation, a concrete case is taken. At 16 kc for an ionospheric reflecting height of 70 km, mode theory[2] gives

$$\frac{1}{S_1} - 1 \cong -0.0014$$

and

$$\frac{1}{S_2} - 1 \cong 0.0155$$

or $S_1 - S_2 \cong 0.0169$. (The S values are real here since all losses are neglected.) The minimum length of the array then turns out to be

$$P\Delta = \frac{2\pi}{k(S_1 - S_2)} = \frac{18.7}{0.0169} = 1100 \text{ km}.$$

Clearly this does not represent a very practical situation. If the elements were spaced one-quarter wavelength apart, some 236 elements would be required!

[2] J. R. Wait and K. Spies, "Influence of earth curvature and the terrestrial magnetic field on VLF propagation," *J. Geophys. Res.*, vol. 65, pp. 2325–2331; August, 1960.

The situation existing when a somewhat shorter array is employed is of some interest. Actually, for a fixed length of the array it is always possible to choose Z_2 so that $G_2 = 0$. Unfortunately, such an excitation is quite unfavorable to the dominant mode, and most of the power goes into the higher-order modes.

In the conventional operation of the end-fire array, M would be taken equal to Re S_1 or just unity. Then for any reasonable length of the array (*i.e.*, <100 km), G_n does not vary appreciably for low-order modes. Consequently, the gain function of any practical end-fire array for VLF is simply given by

$$|G| \cong \frac{\sin (PZ/2)}{\sin (Z/2)},$$

where $P = k\Delta(\cos \beta - 1)$. Convenient tables of the function $|G|$ are given by King[3] for $P = 2, 3, 4$ and 5.

James R. Wait
Natl. Bur. of Standards
Boulder, Colo.

[3] R. W. P. King, "Theory of Linear Antennas," Harvard University Press, Cambridge, Mass., Table 3.2, p. 604; 1956.

A Neuristor Prototype*

The neuristor is a distributed active element proposed by Crane[1,2] for eventual use in microelectronic systems. The device is essentially an active wire on which a pulse is propagated without attenuation in the same way that the axon of a neuron propagates pulses. Neuristors can be coupled together using two types of junctions: trigger (T) or refractory (R). A T junction is shown in Fig. 1(a) and the R-junction symbol is shown in Fig. 1(b). The properties of the junctions are explained in the caption.

No distributed model of the neuristor has been fabricated to date; however, Crane has reported an electromechanical lumped-element model[3] fabricated with relays to demonstrate the principles and junction properties. This note describes an electronic lumped-element model which should be suitable for extrapolation to microelectronics form.

The lumped-element model is essentially a cascade of identical active networks. Each network contains three ingredients: an energy source, an energy-storage mechanism, and a negative immittance. In principle, the negative immittance can be either open- or short-circuit stable, and the type selected will then dictate the type of source and

* Received by the IRE, May 11, 1961. This work was supported by The Bureau of Weapons, Dept. of the Navy, under Contract NOrd 7386.

[1] H. D. Crane, "Neuristor Studies," Solid State Electronic Lab., Stanford Univ., Stanford, Calif., Tech. Rept. 1506–2; 1960.

[2] H. D. Crane, "The Neuristor," IRE TRANS. ON ELECTRONIC COMPUTERS, vol. EC-9, pp. 370–371; September, 1960.

[3] H. D. Crane, "The Neuristor," presented at International Solid-State Circuits Conf., University of Pennsylvania, Philadelphia, Pa.; February 15–17, 1961.

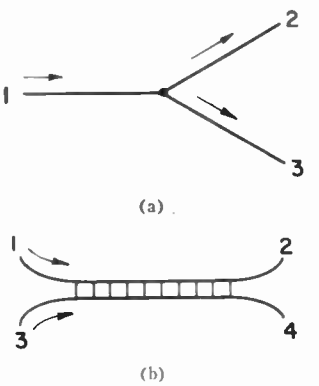

Fig. 1—(a) Trigger junction. A pulse entering at 1 moves to the right and triggers pulses at the junction which propagate toward 2 and 3. (b) Refractory junction. A pulse entering at 1 propagates to the right and leaves at 2 without energizing the line between 3 and 4. Similarly, a pulse entering at 3 leaves via 4 without triggering a pulse on 1–2. *However*, when a pulse passes the junction on either line it temporarily alters the conditions on the other line so that a pulse entering the second line (during this refractory period) cannot be propagated past the junction, and hence "dies out."

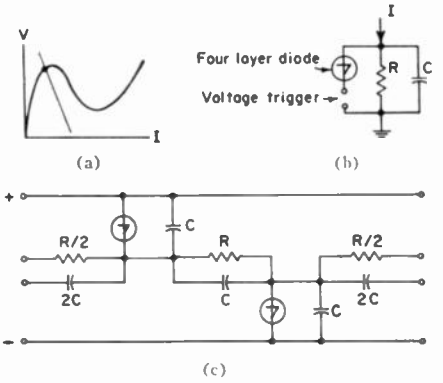

Fig. 2—Neuristor configuration (short-circuit stable active element). (a) Static characteristic. (b) Basic circuit. (c) Basic section.

storage element required. This note describes a neuristor employing a short-circuit stable active element, capacitive storage, and a current supply. Two configurations employing open-circuit stable elements have also been breadboarded; however, satisfactory T- and R-junction coupling techniques have not yet been demonstrated although the circuits do propagate pulses.

Returning to the SCS neuristor model, the active elements are appropriately biased to obtain monostable operation using a biasing network which has a bilaterally symmetrical structure as shown in Fig. 2. Although the basic section shown in Fig. 2(c) is not drawn symmetrically, by employing three diodes in the basic section and appropriately altering the properties of the outside diodes, it could be viewed as a symmetrical circuit. Note that the diodes in this model must be alternately connected to the plus and minus sides of the supply. This is necessary in order to obtain the polarities required for propagation of the pulse from diode to diode.

The sequence of operations when a diode is triggered can be explained with the aid of Fig. 3. The operating point of all diodes is initially at A. Assume a particular diode in

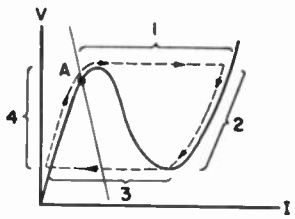

(a)

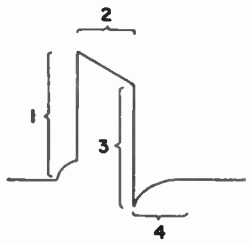

(b)

Fig. 3—Operating sequence. (a) Static characteristic. (b) Diode-current waveform.

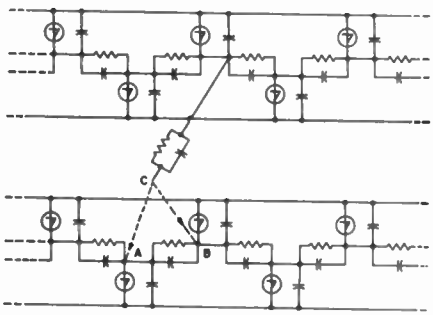

Fig. 4—Component connections for: (a) trigger junction—C is connected to A; (b) refractory junction—C is connected to B.

the line is energized. Triggering takes place during phase ①. During phase ②, the bias on the diodes on each side of that diode being triggered is being altered in the direction required to cause triggering. (Line parameters must be selected to insure that a sufficient triggering level at the adjacent diodes is achieved during this phase.) Phase ③ represents the termination of the original diode's active operation, and during the refractory period of phase ④ the diode is more difficult to trigger.

Fig. 4 illustrates the method of interconnecting two of the neuristors to obtain either the T or R junction.

A. J. Cote, Jr.
Applied Physics Lab.
The Johns Hopkins University
Silver Spring, Md.

A Two-Step Algorism for the Reduction of Signal Flow Graphs*

A very simple algorism for the complete reduction of S.F.G.s (signal flow graphs) will be described. It consists of the repeated successive application of two steps and is shown to converge.

Let N_n be an S.F.G. having n nodes. We then define a principal set of nodes p_N as a subset of nodes of N_n so chosen as to break all loops. Let P_N consist of $p_N < n$ nodes; the trivial case in which $p_N = n$ will not be regarded as defining a P_N.

The procedure is as follows:

1) In the given S.F.G., N, reduce all self loops; obtain N'.
2) In N' choose a principal set of nodes $P_{N'}$ and reduce N' to an S.F.G. drawn on $P_{N'}$.

Repeat steps one and two obtaining successively S.F.G.s N_{n_1}, N_{n_2}, N_{n_3}, $\cdots$, until all loops are eliminated. If $P_{N'}$ is properly chosen, each of its nodes which is neither a source nor a sink must have a self loop.

Proof

a) Reduction of self loops in an S.F.G. does not increase the number of nodes.

b) $p < n$ for $n \geqq 2$, provided N contains no self loops; *i.e.*, step 2 reduces the number of nodes. Now, if this theorem holds for N_n it must also hold for N_{n+1}, since P_N and node $n+1$ together constitute a principal node set of N_{n+1}. But the theorem evidently holds for $n=2$. It therefore holds for all integer $n \geqq 2$.

The repeated use of the algorism thus yields for a finite S.F.G. a sequence of decreasing integers $n_1 > n_2 > n_3 > \cdots$ which breaks off after a finite number of steps.

The reduction of a self loop of transmittance t multiplies all incoming transmittances by $1/(1-t)$. Provided the associated node is not one from or to which the through-transmittance is to be calculated, this is equivalent to multiplication of all outgoing transmittances by this factor.

The procedure commends itself in particular in complicated cases, when the exhaustion of nontouching loop sets, required in the application of topological reduction methods, becomes unwieldy.

As an example we shall find the source to sink transmittance T_{14} in the following S.F.G.[1] (principal nodes are encircled):

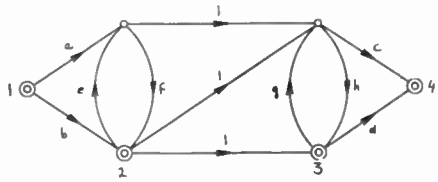

Step 2:

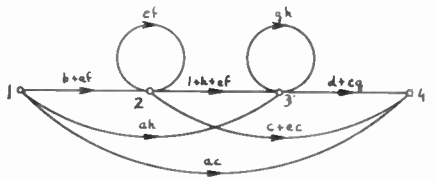

[1] S. J. Mason and H. J. Zimmermann, "Electronic Circuits, Signals, and Systems," John Wiley and Sons, Inc. New York, N. Y.; 1960.

Step 1:

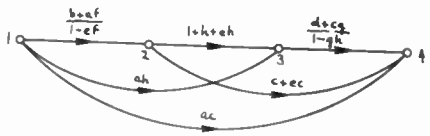

Thus

$$T_{14} = ac + ah\,\frac{d+cg}{1-gh} + \frac{b+af}{1-ef}\left[c + ce + (1+h+eh)\,\frac{d+cg}{1-gh}\right].$$

Amos Nathan
Faculty of Elec. Engrg.
Technion, Israel Inst. Tech.
Haifa, Israel

A Synthesis Procedure for an n-Port Network*

The problems of the synthesis of n-port networks have been considered by a number of investigators although the success to date has been relatively limited. We have devised a synthesis procedure, which is patterned after the Bott-Duffin synthesis procedure for two-port networks, and which seems to possess the generality and capabilities of realization to allow a solution to this problem.

The essentials of the procedure can be given in terms of three theorems, which are given below without proof. An outline of the procedure for subsequent realization is also given. Proofs of these basic theorems, together with details of the procedure for realization, will be given in a subsequent paper.

Theorem I

If $[Z(s)]$ is a "realizable" impedance matrix (immitance in the general case) of an n-port network, then it can be expanded in terms of $[Z_1(s)]$ and $[Z_2(s)]$, which are also "realizable" n-port immitance matrices for any arbitrary positive constant k,

where

$$[Z(s)] = [Z_1(s)] + [Z_2(s)]$$

$$= k\,\frac{k[Z(s)] - s[Z(k)]}{k^2 - s^2} + s\,\frac{k[Z(k)] - s[Z(s)]}{k^2 - s^2}$$

$$= \left[\frac{s}{k}\,[Z(k)]^{-1} + [\zeta_1]\right]^{-1} + \left[\frac{k}{s}\,[Z(k)]^{-1} + [\zeta_2]\right]^{-1}$$

where

$$[\zeta_1] = [Z_1(s)]^{-1} - \frac{s}{k}\,[Z(k)]^{-1}$$

* Received by the IRE, May 19, 1961.

* Received by the IRE, June 30, 1961. This paper is based on work sponsored by the U. S. Air Force, Cambridge Res. Ctr., Bedford, Mass., under contract No. AF 19(604)3887.

and

$$[\zeta_2] = |Z_2(s)|^{-1} - \frac{k}{s}\,|Z(k)|^{-1}. \qquad (1)$$

By "realizability" the following constraints on the n-port network function are implied:

1) $z_{ij} = p_{ij}f$ for $i=j$
2) z_{ij} has no rhp poles
3) all j-axes poles are simple with real residues such that $k_{ij} \geq 0$
4) Re $|Z(s)| \geq 0$ for Re $s=0$ (the matrix Re $|Z(s)|$ is of the positive definite form).

THEOREM II

$[\zeta_1]$ and $[\zeta_2]$, as defined by (1), satisfy the constraint

$$|Z(k)|^2 \times |\zeta_1| \times |\zeta_2| = 1.$$

THEOREM III

If $Z(s)$ is a "realizable" n-port immittance matrix, then it is possible to find a positive constant $k(k>0)$ such that $[\zeta_1]$ and $[\zeta_2]^{-1}$ have either the same j-axis zeros or j-axis poles simultaneously. This k is obtained by solving either $|Z_1(j\omega_0)|=0$ or $|Z_2(j\omega_0)|=0$ in (1). ω_0 is the angular frequency that makes Re$|Z(j\omega_0)|=0$.

These theorems lead to a synthesis cycle which comprises the following three operations.

1) Removal of all the j-axis zeros and poles and minimum resistance of $[Z(s)]$.
2) Selection of the constant $k(k>0)$ such that one of the terms has a j-axis pole and the other a j-axis zero, simultaneously.
3) Removal of the poles and zeros mentioned in 2).

With this synthesis cycle, the n port can be completely synthesized using known procedures.

D. HAZONY
H. J. NAIS
Case Institute of Technology
Engineering Division
Cleveland, Ohio

An Interpretation of "Paired Echo Theory" for Time-Domain Distortion in Pulsed Systems and an Extension to the Radar "Uncertainty Function"*

"Paired Echo Theory" is an elegant application of Fourier analysis to approximate the effects of distortion in pulsed systems. This method was independently developed by Wheeler[1] and MacColl[2] and recently has been used extensively to analyze the effects of frequency-domain distortion in radar systems.[3-5] For the case in which both frequency-domain, amplitude and phase distortions are small, the previously derived results can be simply stated. An analogous result for time domain distortion can also be derived, as shown below.

If both types of distortion occur in a "matched filter radar," their effects may be derived in terms of the conventional radar "uncertainty function," defined by Siebert.[6] This formulation permits a quantitative evaluation of the loss in radar performance with respect to target-parameter accuracy, ambiguity and resolution resulting from each type of distortion.

Treating frequency-domain distortion first, the input signal may be expressed as a Fourier integral:

$$g(t) = \int_{-\infty}^{\infty} G(\omega) \exp [j\omega t]df. \qquad (1)$$

If the desired transmission characteristic is given by

$$F(\omega) = A(\omega) \exp [jB(\omega)], \qquad (2)$$

the filter output will be

$$e(t) = \int_{-\infty}^{\infty} G(\omega)A(\omega) \exp [j\{\omega t + B(\omega)\}]df.$$

A distorted transmission characteristic can be defined as

$$A(\omega)[1 + D(\omega)] \exp [j\{B(\omega) + \Delta(\omega)\}], \quad (3)$$

where $D(\omega)$ is an even function and $\Delta(\omega)$ is an odd function. Hence the distorted output signal becomes

$$e_D(t) = \int_{-\infty}^{\infty} G(\omega)A(\omega)[1 + D(\omega)] \cdot \exp [j\{\omega t + B(\omega) + \Delta(\omega)\}]df. \quad (4)$$

For small phase distortion, $\exp[j\Delta(\omega)]$ can be approximated by $[1+j\Delta(\omega)]$. Substituting into (4) and neglecting second-order distortion terms, (4) becomes

$$e_D(t) = \int_{-\infty}^{\infty} G(\omega)A(\omega) \exp [j\{\omega t + B(\omega)\}] \times \{1 + D(\omega) + j\Delta(\omega)\}df. \qquad (5)$$

If the output spectral energy is confined to radian bandwidth W, the distortion terms in the bracket can be replaced by complex Fourier series

$$1 + D(\omega) + j\Delta(\omega) = 1 + \sum_{n=-\infty}^{\infty} C_n \exp\left[j\frac{2\pi n\omega}{W}\right], \qquad (6)$$

where C_0 is equal to zero. $e_D(t)$ can now be concisely written as

$$e_D(t) = e(t) + \sum_{n=-\infty}^{\infty} C_n e\left(t + \frac{2\pi n}{W}\right) \qquad (7)$$

Eq. (7) is a simplified restatement of previously obtained results for small distortions.

In a "matched filter" radar, frequency-domain distortion can be simply interpreted as creating pairs of false targets, reduced in amplitude by the Fourier distortion coefficients C_n and shifted in time by $\pm 2\pi n/W$ about each true radar echo.

For time-domain distortion, a narrow-band pulse signal $g(t)$ may be written in complex notation as

$$g(t) = a(t) \exp [j\{\omega_0 t + b(t)\}], \quad |t| \leq T/2, \quad (8)$$

and its Fourier transform is given by

$$G(\omega) = \int_{-\infty}^{\infty} g(t) \exp [-j\omega t]dt. \qquad (9)$$

Multiplicative amplitude and phase distortion produce an output signal

$$e_D(t) = a(t)[1 + d(t)] \cdot \exp [j\{\omega_0 t + b(t) + \delta(t)\}]. \quad (10)$$

where $d(t)$ is amplitude distortion and $\delta(t)$ is phase distortion. If the phase distortion is small, $\exp[j\delta(t)]$ can be approximated by $[1+j\delta(t)]$. Substituting into (10) and neglecting second-order distortion terms, (10) becomes

$$e_D(t) = a(t) \exp [j\{\omega_0 t + b(t)\}] \cdot \{1 + d(t) + j\delta(t)\}. \qquad (11)$$

Since $g(t)$ is confined to a time interval T, the distortion terms in the bracket can be replaced, as before, by a complex Fourier series

$$1 + d(t) + j\delta(t) = 1 + \sum_{m=-\infty}^{\infty} C_m \exp\left[j\frac{2\pi mt}{T}\right], \qquad (12)$$

where C_0 is again equal to zero. The spectrum of the distorted signal may now be written in the following simple form:

$$E_D(\omega) = G(\omega) + \sum_{m=-\infty}^{\infty} C_m G\left(\omega + \frac{2\pi m}{T}\right). \quad (13)$$

As might be expected, (13) indicates that undesirable time modulation produces distortion sidebands in the frequency domain. For a matched-filter radar, it is convenient to interpret time-domain distortion as creating pairs of false targets, reduced in amplitude by the Fourier distortion coefficients C_m and symmetrically displaced in Doppler frequency by $\pm 2\pi m/T$ about each true radar echo.

The radar "uncertainty function" $\psi(\tau, \omega_d)$, as defined by Siebert, expresses the interdependence between time delay and Doppler shift of a radar waveform processed by a matched filter. A perturbed uncertainty function resulting from distortion can be derived in terms of the unperturbed uncertainty function and the previously derived expansions. It can be shown that, for frequency-domain distortion, the perturbed uncertainty function $\psi_D(\tau, \omega_d)$ may be written as

$$\psi_D(\tau, \omega_d) \leq \psi(\tau, \omega_d) + \sum_n C_n \psi\left(\tau + \frac{2\pi n}{W} \cdot \omega_d\right). \quad (14)$$

For time-domain distortion, $\psi_D(\tau, \omega_d)$ becomes

* Received by the IRE, May 10, 1961.

[1] H. A. Wheeler, "The interpretation of amplitude and phase distortion in terms of paired echoes," PROC. IRE, vol. 27, pp. 359–385; June, 1939.
[2] *Ibid.*, p. 359.
[3] J. R. Klauder, *et al.*, "The theory and design of chirp radars," *Bell. Sys. Tech. J.*, vol. 39, pp. 745–808; July, 1960.
[4] J. DiFranco and W. Rubin, "Distortion analysis of radar systems," *Proc. Seventh Annual East Coast Conf. PGANE*, Baltimore, Md., pp. 2.1.3–(1–5); October, 24–26, 1960.
[5] W. Rubin and J. DiFranco, "Limitations on dynamic range and multi-target resolution for a search or track radar," *Proc. Fifth National* MIL-E-CON, Washington, D. C.; June 26–28, 1961.
[6] W. M. Siebert, "A radar detection philosophy," IRE TRANS. ON INFORMATION THEORY, vol. IT-2, pp. 204–221; September, 1956.

$$\psi_D(\tau,\omega_d) \le \psi(\tau,\omega_d) + \sum_m C_m \psi\left(\tau,\omega_d+\frac{2\pi m}{T}\right). \quad (15)$$

The results in (14) and (15) have been used to derive upper bounds on permissible distortion in terms of radar performance degradation.[5]

J. V. DiFranco
W. L. Rubin
Surface Armament Div.
Sperry Gyroscope Co.
Sperry Rand Corp.
Great Neck, N. Y.

Radar Scattering Cross Section—Applied to Moon Return*

The early work on calculation of the radar scattering cross section was based on an assumed expression for the normalized autocovariance ρ of the variation of terrain elevation from mean ground level of the form [1]

$$\rho(r) = e^{-Cr}, \quad (1)$$

where r is the distance between points on the ground and C is a characteristic constant of a certain terrain. This arbitrarily chosen expression has been used [2] in the derivation of the radar scattering cross section for randomly-rough terrain. The author questioned the validity of this assumption and attempted to determine an expression based on experimental terrain-roughness data. Various contour maps with one- to twenty-five-foot contour separations were used to obtain data on terrain elevation along randomly selected paths. Seven different types of terrain with standard deviations ranging from 5 to 1076 feet were selected from across the continental U.S.A. Twenty-three samples of such data from the maps, consisting of 58 to 612 points taken at intervals of 5 to 62.5 feet, were processed, using a CRC computer at the University of New Mexico, to calculate the normalized autocovariance $\rho(r)$. A fairly simple but reasonably accurate approximation for the experimental autocovariance curves is given by [7]

$$\rho(r) = \exp\ (-|r|/B), \quad (2)$$

where B is a constant and r is the distance between points.

Other authors [3], [6] have used expressions of the form (2) in other such similar random cases. Further work on this subject is currently in progress at the University of New Mexico.

The normalized autocovariance ρ may be used to calculate the radar scattering cross section σ_0 for any such terrain. Following Davies' [1] approach, the Kirchhoff-Huygens principle was applied to scalar waves. Certain simplifying assumptions, including those used by Davies, were made. These assumptions are that:

1) the ground is considered to be a perfect conductor and no portion of it is shielded from incident radiation;
2) the antenna gain is a constant up to an angle θ and is zero outside of this range;
3) the reradiation from small excited ground sources is isotropic; and
4) the ground surface currents are of the same order as those of a plane reflector, but their phase varies in a random manner dependent on the height of a particular point.

These assumptions were used [7] to calculate the average power received at the transmitting-receiving antenna and compared with the radar equation [8] as applied to pulse radar. Such calculations resulted in the following expression for the scattering cross section:

$$\sigma_0 = \frac{4\sqrt{2}\pi B^2}{(\lambda)^2}\left(\frac{\theta}{\sin\theta}\right)\exp\ (-4k^2\sigma^2\cos^2\theta) \cdot \sum_{n=1}^{\infty}\frac{(4k^2\sigma^2)^n(\cos^2\theta)^{n+1}}{(n-1)!\left[B^2k^2\sin^2\theta+n^2\right]^{3/2}}, \quad (3)$$

where

λ = wavelength (feet);
k = wave number;
σ = standard deviation of the terrain (feet); and
θ = angle of incidence with the vertical.

This expression checks out well against published experimental results [2], [4].

Eq. (3) reduces to

$$\sigma_0 \cong \frac{4\sigma^2}{\lambda B}(\theta\cot^4\theta) \qquad \text{for } (\theta \neq 0°), \quad (4)$$

when $1/B$ is very small as compared to k, which is very often the case, for almost flat surfaces.

Hughes [5] states that the expression for scattering from the moon

$$\sigma_0 = \sigma_1 \exp\ (-10\theta), \quad (5)$$

is a "very close fit" to the experimental data, over the range of angles from 3° to at least 14°. Eq. (3) describes a family of curves, one of which fits the Hughes' heuristic approximate expression (5) for $\sigma/\lambda = 0.10$ and $\lambda/B = 1.0$ within a very reasonable degree of accuracy. This seems to suggest that (3) may well be general, while (5) seems like a special case of the former. It is also possible that other values of B and σ may be appropriate, but only a limited set was tried. Such other possible values of B and σ can be calculated either from (3) or found by comparison of the experimental results with a large family of σ_0 vs θ curves for a wide range of B and σ given by the general expression of (3).

The fact that the scattering coefficient per unit area for rough surface, as listed in (3), fits reasonably well, while the one for a nearly smooth surface, (4), definitely does not fit the experimental results [5], seems strongly to indicate that the effective moon surface as seen by radar is rough indeed, and not quasi-smooth as indicated or assumed by some previous authors [9], [10].

H. S. Hayre
Elec. Engrg. Dept.
University of New Mexico
Albuquerque, N. Mex.

* Received by the IRE, May 1, 1961. This work is sponsored by a National Aeronautics and Space Administration Grant No. NsG 129-61.

Bibliography

[1] H. Davies, "The reflection of electromagnetic waves from a rough surface," IEE Monograph No. 90, vol. 40, pt. 4; January, 1954.
[2] A. R. Edison, *et al.*, "Radar terrain return measured at near-vertical incidence," IRE Trans. on Antennas and Propagation, vol. AP-8, pp. 246–254; May, 1960.
[3] M. A. Isakovich, "The scattering and radiation of waves by statistically inhomogenous and statistically oscillating surfaces," *J. Exper. Theoretical Phys.* (USSR) vol. 23, p. 305; 1952.
[4] D. Neilson, *et al.*, Stanford Res. Inst., Stanford, Calif., Res. Project No. 29909; May, 1960.
[5] V. A. Hughes, "Roughness of the moon as a radar reflector," *Nature*, vol. 186, pp. 873–874; June 11, 1960.
[6] See for example W. S. Ament, "Toward a Theory of reflection by a rough surface," Proc. IRE, vol. 41, pp. 142–146; January, 1953.
[7] H. S. Hayre and R. K. Moore, "Theoretical scattering coefficient for near vertical incidence from contour maps," *J. Res. NBS*, vol. 65, pt. D; to be published in September/October, 1961.
[8] R. K. Moore and C. S. Williams, "Radar terrain return at near-vertical incidence," Proc. IRE, vol. 45, pp. 228–238; February, 1957.
[9] T. B. A. Senior and K. M. Siegel, "Radar reflection characteristics of the moon," Paris Symp. on Radio Astronomy, Paris, France, August, 1958, Stanford Univ. Press, Stanford, Calif., pp. 29–46; 1959.
[10] T. B. A. Senior and K. M. Siegel, "A theory of radar scattering by the moon," *J. Res. NBS*, vol. 64D, pp. 217–230; May–June, 1960.

Gain Saturation in a Traveling-Wave Parametric Amplifier*

In two previous papers[1,2] it was shown theoretically, for a traveling-wave parametric amplifier with nonlinear shunt capacitance, that a periodic transfer of power with distance between the three frequencies, signal, idler and pump was to be expected. The periodic nature of the power transfer would only be observable in a line of considerable length, but for any given line a reduction of gain should be observable as the input signal level approaches the pump amplitude.

When the signal amplitude is very much less than the pump, the voltage gain is given by

$$\text{Gain} = \cosh \alpha_0 x \quad (1)$$

where x is the length of line and α_0, the gain coefficient, is equal to

$$\frac{\Delta C}{8C}(\beta_s\beta_i)^{1/2}.$$

Here $\Delta C/C$ is the fractional change in the shunt capacitance produced by the pump.

* Received by the IRE, May 18, 1961.

[1] A. L. Cullen, "Theory of the traveling wave parametric amplifier," *Proc. IEE*, vol. 107, pp. 101–107; March, 1960.
[2] A. Jurkus and P. N. Robson, "Saturation effects in a traveling-wave parametric amplifier," *Proc. IEE*, vol. 107, pt. B., pp. 119–122; March, 1960.

and β_s and β_i are the signal and idler phase constants, respectively.

A more correct expression for the gain is:[2]

$$\text{Gain} = \text{nd}\left(\frac{\alpha_0 x}{k}\right) \qquad (2)$$

where k is the modulus of the above elliptic function, and is equal to

$$\left(1+\frac{\beta_p}{\beta_i}\frac{V_{s0}^2}{V_{p0}^2}\right)^{-1/2}.$$

V_{s0} is the signal voltage at $x=0$ and V_{p0}, the pump voltage at $x=0$; β_p is the pump propagation constant. In the limit $V_{p0} \gg V_{s0}$, k tends to unity and the elliptic function (2) reduces to the hyperbolic cosine (1). Eq. (2) then predicts a gain that will decrease as the input signal level increases.

In order to test (2), an experimental line was constructed in the form of a low-pass, constant k filter, using fourteen GE Company EW 76 diodes as the nonlinear shunt capacitors. In the example quoted below, the pump frequency was 60 Mc and the signal frequency 26 Mc. The input pump signal was kept constant at one volt, thereby keeping α_0 constant, and the input signal level was varied. Fig. 1 shows the gain plotted as a function of the input-signal level (experimental points shown as circles). From the experimental small signal gain, the coefficient α_0 may be calculated using (1). This value was then substituted into (2) to obtain the continuous curve, the value of k being known from the measured values of V_{s0} and V_{p0}. Agreement between theory and experiment is seen to be good.

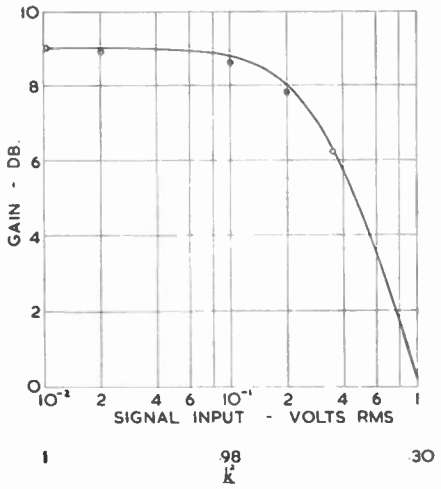

Fig. 1—Graph showing reduction in gain as signal level increases; experimental points shown as circles; theoretical curve as a solid line.

It would appear therefore that once the small signal gain is known experimentally, the gain reduction as signal level increases is readily predictable.

A. Jurkus
Radio and Elec. Engrg. Div.
National Res. Council
Ottawa, Ont., Can.
P. N. Robson
Dept. of Elec. Engrg.
The University of Sheffield,
Sheffield, England

WWV and WWVH Standard Frequency and Time Transmissions*

The frequencies of the National Bureau of Standards radio stations WWV and WWVH are kept in agreement with respect to each other and have been maintained as constant as possible with respect to an improved United States Frequency Standard (USFS) since December 1, 1957.

The nominal broadcast frequencies should for the purpose of highly accurate scientific measurements, or of establishing high uniformity among frequencies, or for removing unavoidable variations in the broadcast frequencies, be corrected to the value of the USFS, as indicated in the table below. The

WWV Frequency with Respect to U. S. Frequency Standard

1961 June	Parts in 10^{10}†
1	−150.4
2	−150.1
3	−150.3
4	−150.5
5	−150.8
6	−150.9
7	−150.9
8	−150.6
9	−150.3
10	−150.0
11	−149.7
12	−149.7
13	−149.9
14	−149.8
15	−149.9
16	−150.0
17	−150.7
18	−150.8
19	−150.6
20	−150.4
21	−150.5
22	−150.0
23	−150.0
24	−150.4
25	−150.3
26	−149.9
27	−149.5
28	−149.3
29	−149.1
30	−149.3

† A minus sign indicates that the broadcast frequency was low. The uncertainty associated with these values is $\pm 5\times10^{-11}$.

corrections reported have been arrived at by means of improved measurement methods based on LF and VLF transmissions.

The characteristics of the USFS, and its relation to time scales such as ET and UT2, have been described in a previous issue,** to which the reader is referred for a complete discussion.

The WWV and WWVH time signals are also kept in agreement with each other. Also they are locked to the nominal frequency of the transmissions and consequently may depart continuously from UT2. Corrections are determined and published by the U. S. Naval Observatory. The broadcast signals are maintained in close agreement with UT2 by properly offsetting the broadcast frequency from the USFS at the beginning of each year when necessary. This new system was commenced on January 1, 1960. A retardation time adjustment of 20 milliseconds was made on December 16, 1959; another retardation adjustment of 5 milliseconds was made at 0000 UT on January 1, 1961.

National Bureau of Standards
Boulder, Colo.

* Received by the IRE, July 20, 1961.
** "National Standards of Time and Frequency in the United States," Proc. IRE, vol. 48, pp. 105–106; January, 1960.

Correction to "Measurements on Resonators Formed from Circular Plane and Confocal Paraboloidal Mirrors"*

In the above paper,[1] the author would like to make the following correction.

The error appears in the second sentence of the last paragraph. The word "diameters" should be "radii." The corrected sentence should read: "A resonator with mirror radii of 31.5 cm and an $a^2/b\lambda$ ratio of 0.905 had a measured Q of 260,000."

Elmer H. Scheibe
Dept. of Elec. Engrg.
University of Wisconsin
Madison, Wis.

* Received by the IRE, June 21, 1961.
[1] E. H. Scheibe, Proc. IRE (Correspondence), vol. 49, p. 1079; June, 1961.

On the Cascaded Tunnel-Diode Amplifier*

In a previous work,[1] a technique for using tunnel diodes in cascaded amplifiers was presented. The procedure described was to obtain an artificial transmission line of characteristic impedance R that provided a gain instead of a loss. A "midband" equivalent circuit of a single section of such a transmission line and its terminating resistance R is shown in Fig. 1. The pertinent equations of the above-mentioned work are repeated below for convenience.

$$K = \frac{E_2}{E_1} = R/(R-r), \qquad (1)$$

$$R_{in} = R, \qquad (2)$$

$$-r_1 = R(R-r)/-r. \qquad (3)$$

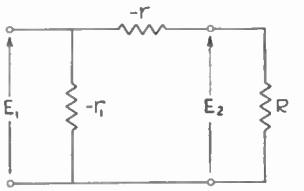

Fig. 1—An equivalent circuit of a single section of a tunnel-diode amplifier. The resistor R is the load resistance.

It was assumed in the previous work that the line was completely lossless (*i.e.*, there would be no signal power absorbed by any of its elements). If this is to be so, then both the series and shunt resistors must be negative. This requires that the series resistor $-r$ be such that $R>r$. An examination

* Received by the IRE, May 1, 1961.
[1] P. M. Chirlian, "A technique for cascading tunnel-diode amplifiers," Proc. IRE (Correspondence), vol. 48, p. 1156; June, 1960.

of (1) and (3) shows that if $R<r$ and $R>r-R$, then a voltage gain whose magnitude is greater than unity can be obtained with a positive shunt resistor. The problems of biasing and stability are considerably lessened by this procedure. In addition, only one tunnel diode is needed per stage since now the shunt resistor can be an ordinary passive resistor.

ACKNOWLEDGMENT

The author is indebted to L. Saporta of New York University, who suggested the use of such positive shunt resistors. The author also wishes to express his appreciation to L. Nardizzi, who built a two-stage cascaded tunnel-diode amplifier, with positive shunt resistors, at New York University during the summer of 1960.

P. M. CHIRLIAN
Dept. Elec. Ergrg.
Stevens Inst. Tech.
Hoboken, N. J.

The Determination of the Image Response in a Superheterodyne With Regard to Noise-Factor Measurement*

Correct noise-factor measurements of a superheterodyne receiver, using a broadband noise source, generally require that the receiver response at the image frequency be known. This is especially the case for receivers using direct input end conversion, as in radar receivers. In receivers of this kind, the noise factor for the signal frequency differs from the measured one by a factor of 3 db, less the attenuation in the response at the image frequency due to any filter preceding the mixer. Normally, the difference between the signal- and the image-frequency responses can be measured by means of a carefully calibrated RF signal generator, but at very high frequencies such as X band and above, and/or narrow receiver bandwidths, it is often quite difficult to set the normally available signal generators exactly at the maximum of the signal pass band. In cases where small changes in SWR have a negligible effect on the noise performance of the system, the method shown in Fig. 1 can be used to overcome this difficulty. This is a conventional noise-factor measurement system, with the exception that an absorption wavemeter has been added to the noise-lamp generator.

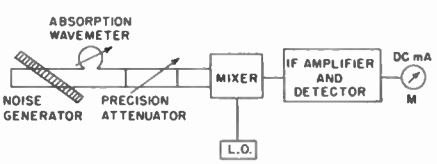

Fig. 1—Set-up for the measurement.

When the noise lamp is fired and the absorption wavemeter is set far from both pass bands of the receiver, the response of the latter to the noise input can be pictured as in Fig. 2. The output meter will give a deflection proportional to

$$P_T = KT_LB(1+\alpha) = P_S + P_I,$$

where K is the Boltzmann constant, B the bandwidth of the IF amplifier, α the ratio of the response of the image frequency to the response of the signal frequency, T_L the equivalent temperature of the noise lamp, P_S the power in the signal-frequency band, and P_I is the power in the band around the image frequency. It is evident that the bandwidth is the same for both components.

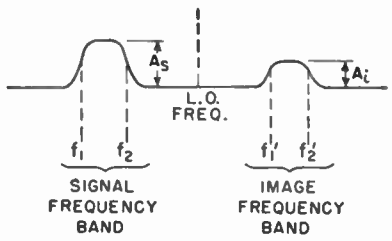

Fig. 2—Relative frequency responses of the signal and its respective image.

If the wavemeter now is tuned in the signal, band, it will absorb a portion δ of the power generated by the noise lamp. Therefore, the deflection of the output meter will become

$$P_T' = (P_S - \delta) + P_I.$$

But as $P_I = P_S\alpha$, we have

$$P_T' = (P_S - \delta) + P_S\alpha.$$

When the wavemeter is tuned in the image band, the deflection on the meter is equal to

$$P_T'' = P_S + (P_I - \delta\alpha) = P_S + (P_S - \delta)\alpha.$$

The difference between P_T and P_T' is

$$P_T - P_T' = \delta.$$

The value of δ is obtained directly by adjusting the precision attenuator to return the output to the original value, P_T. The difference between P_T and P_T'' is

$$P_T - P_T'' = \delta\alpha,$$

where $\delta\alpha$ is obtained in the same manner as used to obtain δ above. Therefore, the value of α is

$$\alpha = \frac{(\delta\alpha)}{(\delta)}.$$

It may be noted that the only requirement on the absorption wavemeter is that its absorption be constant over the range of frequencies between the two receiver responses; *i.e.*, over a range equal to twice the IF frequency. For an adequate indication on the output meter, its bandwidth should be about $\frac{1}{5}$ or $\frac{1}{4}$ the IF bandwidth, and its selectivity should be such that there will be practically no absorption at the image frequency. With the normal IF encountered in radar work (*i.e.*, 30 to 60 Mc) and for bandwidths between 5 and 15 Mc, very reliable readings were obtained with a cavity wavemeter of 2-Mc bandwidth at X band. This wavemeter was of very simple and inexpensive construction and was therefore directly incorporated in the noise-generator mount.

The author wishes to thank Maj. Mezzina and Lieut. Bianchi of the Italian Navy for their criticisms during the development of the technique.

M. PIATTELLI
S.M.A. Radar
Firenze, Italy

* Received by the IRE, May 23, 1961; revised manuscript received, June 5, 1961.

The Effect of Nonsymmetrical Doping on Tunnel Diodes*

The changes in the I-V characteristic of the tunnel diode with the relative doping of the p- and n-type regions will be discussed. Esaki's model, which neglects phonon interaction effects and assumes parabolic band edges and a constant tunneling probability, will be used.[1] We shall not, however, restrict the model to equal degeneracy energies on each side of the junction. The model is calculated for 0°K. Comparison with graphical solutions at 300°K indicates that the resulting voltages derived do not change by more than a few per cent.

At any given voltage, the tunnel current I_t may be found by evaluating the following integral given by Esaki:

$$I_t = A\int_{E_c}^{E_v}\{f_c(E) - f_v(E)\}_\varepsilon\,\rho_c(E)\rho_v(E)dE \quad (1)$$

where the various terms are defined by Esaki. At 0°K the above integral may be expressed exactly by equations containing transcendental and quadratic terms. Two degeneracy voltages, V_{dv} and V_{dc}, are defined as

$$V_{dv} = \frac{E_v - E_f}{e}, \quad (2)$$

and

$$V_{dc} = \frac{E_f - E_c}{e}, \quad (3)$$

where E_f is the fermi energy and E_v and E_c are the band edges of the p-type and n-type sides of the junction, respectively. It has been shown that a forward bias equal to $V_{dv}+V_{dc}$ causes tunnel current to cut off.[2] We shall then define the tunnel cutoff voltage as

$$V_{co} = V_{dv} + V_{dc}. \quad (4)$$

A degeneracy ratio α is defined as

$$\alpha = \begin{cases} \dfrac{V_{dc}}{V_{dv}} & \text{for } V_{dv} > V_{dc} \\ \dfrac{V_{dv}}{V_{dc}} & \text{for } V_{dc} > V_{dv}. \end{cases}$$

* Received by the IRE, May 8, 1961; revised manuscript received, May 22, 1961.

[1] L. Esaki, "New phenomenon in narrow Ge p-n junctions," *Phys. Rev.*, vol. 109, pp. 603–604; January, 1958.
[2] I. A. Lesk, *et al.*, "Germanium and silicon tunnel diodes—design, operation and application," 1959 IRE WESCON CONVENTION RECORD, pt. 3, pp. 9–31.

The general properties of the tunnel diode characteristic can be shown to be functions of the V_{co} and α.

The Peak Voltage: The position of peak voltage is determined by

$$\left.\frac{dI_t}{dv}\right|_{V_p} = 0, \tag{5}$$

letting

$$V_p = \beta V_d. \tag{6}$$

Where V_d is the smaller of the two degeneracy voltages, solutions of (5) give the following relation:

$$\sin^{-1}\left[\frac{\beta-(\alpha-1)}{(1+\alpha)-\beta}\right]+\sin^{-1}\left[\frac{\beta+(\alpha-1)}{(1+\alpha)-\beta}\right] = \frac{\pi}{(1+\alpha)-\beta}\{[\alpha-\beta]^{1/2}+[\alpha(1-\beta)]^{1/2}\}. \tag{7}$$

Resulting solutions of $\beta(\alpha)$ are given in Fig. 1. It can be seen that in the limit of large α

$$V_p \to \frac{1}{1+\alpha} V_{co}. \tag{8}$$

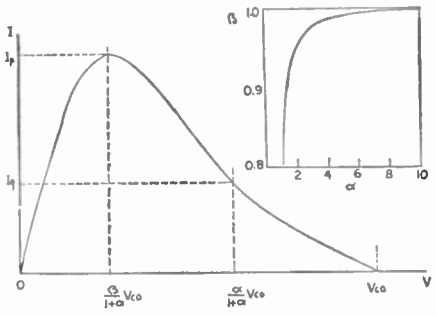

Fig. 1—Variation of V_p and V_v with α and V_{co} including $\beta=\beta(\alpha)$.

The Maximum Negative Conductance G_m: The condition of maximum negative conductance

$$\left.\frac{d^2I_t}{dv^2}\right|_{V_v} = 0 \tag{9}$$

was shown to occur at

$$V_v = \frac{\alpha}{1+\alpha} V_{co}. \tag{10}$$

The current at the peak negative conductance was

$$I_v = \frac{AZ\pi V_{co}^2}{8}\left(\frac{1}{1+\alpha}\right)^2 \tag{11}$$

with a resulting peak negative conductance

$$G_m = \frac{AZ\pi V_{co}}{4}\left(\frac{1}{1+\alpha}\right) \tag{12}$$

where A and Z are given in (1). The peak current was found to be related to I_v as follows:

$$\frac{I_p}{I_v} = \frac{4}{\pi}\left(\sqrt{\alpha-\beta}+\alpha\sqrt{\alpha(1-\beta)}\right). \tag{13}$$

It should be noted that, although the voltages derived remain nearly constant with temperature, the currents can vary by as much as 2 to 1 between 0°K and room temperature.

Conclusions

It has been shown that the properties of the tunnel diode are quite dependent upon the parameters α and V_{co}.

Given a constant peak voltage, the increase of V_{co} with increasing α allows tunnel currents beyond the cutoff voltage predicted by a symmetrical model. Such a mechanism may account for part of the excess current observed in most diodes.

From the circuit point of view, it should be noted that, given a constant V_{co}, the impedance level would rise and the current level fall at G_m with increasing α. Both of the above results indicate that diodes with a large α would be more suitable for use in amplifiers and, conversely, diodes with $\alpha \simeq 1$ would be more suitable for oscillators and switches.

F. D. Shepherd
A. C. Yang
Air Force Cambridge Res. Labs.
Laurence G. Hanscom Field
Bedford, Mass.

Reconstruction Error and Delay for Amplitude-Sampled White Noise*

It is well known that a signal, band-limited to the frequencies 0 to W cps, is completely specified by its amplitudes at a discrete set of time instants spaced $1/2W$ seconds apart. Such a signal has the following representation:[1]

$$s(t) = \sum_{n=-\infty}^{+\infty} s(nT)\,\frac{\sin(2\pi Wt-n\pi)}{2\pi Wt-n\pi}, \qquad T \equiv 1/2W. \tag{1}$$

Assume that such a signal is further restricted to be wide-sense stationary white noise, *i.e.*, its spectrum is constant over the band 0 to W. Let the signal be sampled at a rate of $2W$ times per second, so that its amplitude is known at only the discrete time instants nT, n being an integer. An interesting problem is to specify a best mean-square reconstruction scheme and the associated mean-square reconstruction error over an interval $mT<t<(m+1)T$, if only the samples with indexes $(m-L)\leq n\leq(m+K)$ may be used. This means that the reconstruction scheme is being constrained to a delay time of KT seconds and a memory time of $(L+1)T$ seconds.

Since the signal is stationary, it will be sufficient to solve the problem for the interval $0<t<T$. The results will apply to all intervals.

Ensemble averages are denoted by $E[\ ]$. Without loss of generality, it is assumed that

$$E[s^2(t)] = 1 \quad \text{and} \quad E[s(t)] = 0.$$

Using well-known techniques,[2] the best mean-square linear reconstruction function is readily found to be

$$\hat{s}(t) = \sum_{n=-L}^{K} s(nT)\,\frac{\sin(2\pi Wt-n\pi)}{2\pi Wt-n\pi}. \tag{2}$$

If the signal is a Gaussian process, then (2) is the conditional mean of $s(t)$ upon the hypothesis $s(nT)$, $-L\leq n\leq K$. Hence, (2) specifies the absolute best mean-square reconstruction process for Gaussian white noise.

Although $s(t)$ is assumed to be drawn from a wide-sense stationary process, the sampling mechanism introduces a fluctuation in the error statistics over the interval 0 to T. Thus, the mean-square reconstruction error will be defined as an average over both the ensemble and time

$$MSE = \frac{1}{T}\int_0^T dt E[\{s(t)-\hat{s}(t)\}^2]. \tag{3}$$

Noting that $E[s(nT)s(mT)]=0$ when $n\neq m$,

$$MSE = 1-\sum_{n=-L}^{K}\frac{1}{T}\int_0^T dt\,\frac{\sin^2(2\pi Wt-n\pi)}{(2\pi Wt-n\pi)^2}. \tag{4}$$

It can readily be shown that

$$\frac{1}{T}\int_0^T dt\,\frac{\sin^2(2\pi Wt-n\pi)}{(2\pi Wt-n\pi)^2} = \frac{Si(2\pi n)-Si(2\pi[n-1])}{\pi} \tag{5}$$

where

$$Si(x) = \int_0^x dt\,\frac{\sin t}{t}$$

is a well-known and tabulated function.[3] Hence (4) becomes

$$MSE = 1-\frac{Si(2\pi K)}{\pi}-\frac{Si(2\pi[L+1])}{\pi}. \tag{6}$$

The following approximation is very good for $n\geq 1$:[3]

$$Si(2\pi n) \cong \frac{\pi}{2}-\frac{1}{2\pi n}.$$

Thus, for $L\geq 0$ and $K\geq 1$,

$$MSE \cong \frac{1}{2\pi^2}\left(\frac{1}{K}+\frac{1}{L+1}\right). \tag{7}$$

As an example of the delay and memory required for a low reconstruction error, consider the infinite memory case where $L\to\infty$. For an rms error of about ten per cent, K must equal 5. For an rms error of one per cent, K must equal 506.

The author wishes to thank Prof. P. M. Schulthesiss for his helpful comments and suggestions.

D. S. Ruchkin
Dept. of Elec. Engrg.
University of Rochester
Rochester, N. Y.
Formerly of Dunham Lab. of Elec. Engrg.
Yale University,
New Haven, Conn.

* Received by the IRE, May 3, 1961. The work reported in this note was supported by the Bell Telephone Labs., Murray Hill, N. J.

[1] C. E. Shannon and W. Weaver, "The Mathematical Theory of Communication," The University of Illinois Press, Urbana, p. 53; 1949.

[2] S. Goldman, "Information Theory," Prentice Hall, Inc., New York, N. Y., Appendix XI; 1953.

[3] E. Jahnke and F. Emde, "Tables of Functions," Dover Publications, Inc., New York, N. Y., Sect. I; 1945.

Relativity and the Clock Paradox*

This note is an attempt to show that the so-called "clock" and other "paradoxes" of the special relativity theory are not really paradoxes, and they cannot be used as arguments against the theory. To prove the point, a "mechanical" model of the constant velocity relativistic situation is presented. Observers are placed on the moving and stationary axes. The model demonstrates that although each observer sees a quantitatively different effect, each viewpoint is in harmony with the accepted laws of transformation.

The paradox, as usually given, notes that relativity predicts that a traveler will age less than a stay-at-home. Since we cannot, according to the same theory, define who is traveling and who is stationary and, because of an apparent symmetry, a paradox exists. Our model will demonstrate, however, by viewing the situation through the eyes of observers in each frame in turn, that even they do not disagree as to who ages less, dispelling the paradox.

For a pair of relatively moving reference frames, moving in x only, with clocks synchronized in each (also corrected for propagation delay) so that the clocks at the origins read zero only when they cross, ($t'_{x'=0}=0 = t_{x=0}$, $x'=x=0$) the following well-known transformations result:

$$x' = \beta(x - vt),\ x = \beta(x' + vt') \qquad (1)$$

where

$$\beta = \left(1 - \frac{v^2}{c^2}\right)^{-1/2}.$$

Next,

$$\epsilon = t_{x_1}' - t_{x_1} = \frac{x_1/\beta - x_1'}{v} + \frac{x_1'/\beta - x_1}{v}$$

$$= -\frac{\beta-1}{\beta v}(x_1 + x_1') \qquad (2)$$

where ϵ is the error between clock pairs, in both frames, which are for the moment opposite each other and x_1 and x_1' are the momentary coordinates of the above clocks, ($x_1' \neq x_1$).

Observers are defined as being infinitely distant on the y and y' axes. The stationary observer on the y axis would see what is represented in Fig. 1. (For clarity, these figures are drawn with an incorrect perspective.)

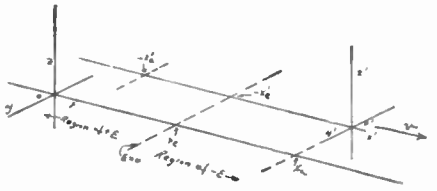

Fig. 1.

The moving origin is momentarily opposite x_a, but the stationary observer notes, of course, that $\overline{0' \to -x_a'}$ (where $|x_a'| = |x_a|$) is less than $\overline{0 \to x_a}$. He also notices a single "opposite-point-pair" which momentarily has the same numerical value, $|-x_\epsilon'| = |x_\epsilon|$. A line connecting these points defines $\epsilon = 0$ in (2), and separates regions of $+$ and $-\epsilon$.

The instantaneous value of x_ϵ is:

$$x_\epsilon = -x_\epsilon' = \frac{vt\beta}{1+\beta} \qquad (3)$$

since the distance traveled by 0', vt, is $x_\epsilon + x_\epsilon/\beta$. With clock error defined by (2), we can now represent a possible "photograph" of the clocks, by the y observer (Fig. 2).

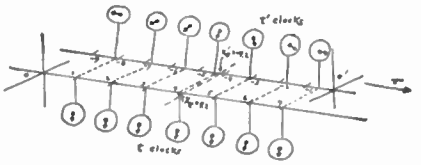

Fig. 2.

The "Clock Paradox" will be explained by permitting a traveler to jump from the fixed frame at x_1, to the moving frame, then back to the fixed frame at x_2, then to a frame moving in the opposite direction, then back to the fixed frame to the same point, x_1, where he started. Since his clock does not instantly change during his jumps, the time gain or loss (Δt) as he observes on his clock is obviously the difference between the errors at the 2 jumping points:

$$\Delta t = \epsilon_2 - \epsilon_1. \qquad (4)$$

To simplify the expressions, we permit the traveler to jump onto the moving frames at their origins so that in (2) $x'=0$.

Then,

$$\Delta t_a = \epsilon_2 - \epsilon_1 = -\frac{\beta-1}{\beta v}(x_2 + 0) - (-)\frac{\beta-1}{\beta v}(x_1 + 0)$$

and

$$\Delta t_a = -\frac{\beta-1}{\beta v}(\Delta x). \qquad (5)$$

Now, let the traveler return to earth via the same process using a frame of velocity $-v$.

$$\Delta t_b = +\frac{\beta-1}{\beta v}(x_1 + 0) - (+)\frac{\beta-1}{\beta v}(x_2 + 0)$$

$$\Delta t_b = -\frac{\beta-1}{\beta v}(\Delta x). \qquad (6)$$

$$\Delta t_{tot} = \Delta t_a + \Delta t_b = -2\frac{\beta-1}{\beta v}\Delta x. \qquad (7)$$

Thus, the accumulation of errors during this trip gives his clock a smaller reading than one he comes back to by $-2(\beta - 1/\beta v)\Delta x$.

As mentioned, let us examine the same problem through the eyes of an observer on the moving frames. (It is well known that both observers agree, and verify by measurements, that the relative velocity is v as observed from either frame.)

Suddenly a traveler leaps to our (the 0') frame, from x_1, and lands on our origin, $x'=0$. He waits a while and jumps off when point x_2 goes by. If we consistently apply (2), (note velocity is $-v$), we get:

$$\Delta t_a = \epsilon_2 - \epsilon_1 = +\frac{\beta-1}{\beta v}(x_2 + 0) - (+)\frac{\beta-1}{\beta v}(x_1 + 0) = \frac{\beta-1}{\beta v}\Delta x$$

and for similar analysis for the return trip:

$$\Delta t_b = \frac{\beta-1}{\beta v}\Delta x.$$

$$\therefore\ t_{tot} = \Delta t_a + \Delta t_b = 2\frac{\beta-1}{\beta v}(\Delta x).$$

Thus, the magnitude of the error is the same as computed before. The oppositeness of the sign from the point of view of the "other" frame indicates the sense of the error is also the same.

The paradox originally arose because of a belief that a "symmetry" exists in this situation. The simple fact is that there is no symmetry. The stay-at-home does not change frames, while the traveler makes at least 3 changes. The traveler says that he traveled x light years and the other says he traveled x/β light years.

Some skeptics of the effects of relativity maintain that the biological process of living is not tied up with mechanical clocks. Thus, the traveler would have as many heartbeats, eat as many meals, think as many thoughts, etc., as the people who remained at home regardless of his slower running clock. This is a rather dangerous proposal because:

1) The observant traveler will then notice that his clock seems to be running slowly with respect to his metabolism.
2) It will seem to run slowly regardless of his direction or speed.
3) Therefore, it will always appear to run fastest only when he is stationary with the earth.
4) Therefore, there is something special about the velocity of the earth.

An obvious fallacy.

A. Roth
Canoga Electronics Corp.
Fort Walton Beach, Fla.

* Received by the IRE, May 8, 1961; revised manuscript received, May 19, 1961.

Electron Radiation Damage in Unipolar Transistor Devices*

Unipolar transistor devices were proposed by Shockley[1] in 1951. Dacey and Ross[2] constructed such a device and observed the predicted effects. More recently

* Received by the IRE, July 5, 1961.

[1] W. Shockley, "A unipolar field-effect transistor," Proc. IRE, vol. 40, pp. 1365–1377; November, 1952.
[2] G. C. Dacey and I. M. Ross, "Unipolar 'field-effect' transistor," Proc. IRE, vol. 41, pp. 970–979; August, 1953.

RCA[3] produced several elementary units of gallium arsenide and Westinghouse[4] has produced silicon unipolars that exhibit usable characteristics and appear very promising. Three silicon and one gallium arsenide experimental unipolar transistors have been investigated for radiation damage sustained when bombarded by 1 Mev electrons.

The three silicon unipolar devices of quite similar properties behaved similarly throughout the bombardment experiments. Fig. 1 shows the source-to-drain current-voltage characteristic of one silicon unit after various levels of irradiation. Fig. 2 shows the transconductance as a function of total electron bombardment for the three units. A 50 per cent decrease in transconductance after 1.2 to 1.5×10^{16} electrons/cm² is observed.

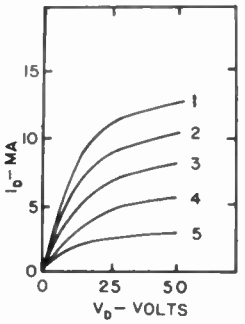

Fig. 1—V-I characteristics for $V_g=6$ volts as a function of irradiation: 1) original; 2) after 5×10^{15} electrons/cm²; 3) after 1×10^{16}; 4) after 2×10^{16}; 5) after 3×10^{16} electrons cm² at 1 Mev.

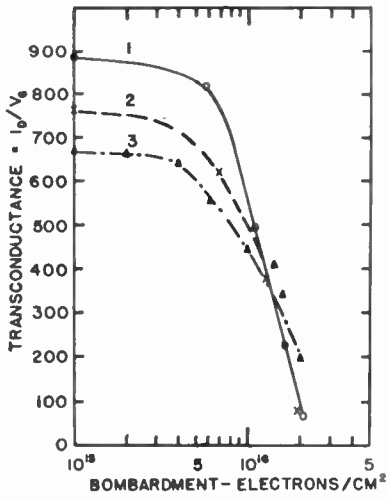

Fig. 2—Transconductance as a function of bombardment; $V_{s-d}=40$ volts, $V_g=-9$ volts for units 1 and 2, $V_g=20$ volts for unit 3.

Even after the other characteristics of the device were destroyed, the silicon units would still perform a rectifying function in the gate-to-source junction. No attempt was made to obtain detailed data of this phenomenon.

The experimental Gallium Arsenide device irradiated was not as good as the silicon units but a drain characteristic curve was obtainable. A 35 per cent change in the drain characteristics was observed after 5×10^{17} electrons/cm² at 1 Mev struck the device.

After the operational characteristics of unit no. 1 were destroyed by bombardment with 6×10^{16} electrons/cm², the transistor was annealed at 300°C for two 30-minute periods. The device recovered 40 per cent of its initial characteristics on the first annealing period. The second annealing period of 30 minutes at 300°C resulted in a recovery of 55 per cent. An attempt was made to anneal at 350°C but the soft solder mounting melted, thus destroying the unit.

Unit no. 2 was annealed at 200°C for 30 minutes resulting in a recovery of 75 per cent of the initial characteristics. An additional 30 minutes of 250°C increased the recovery to 85 per cent.

Unit no. 3 was allowed to remain at room temperature for five days after irradiation and a definite recovery trend was observed. The device recovered to 12 per cent of its initial characteristics after five days. Heat treating for 30 minutes at 100°C produced a 14 per cent recovery.

The annealing of the samples reported here appears somewhat erratic, however, it is probable that the 300°C heat treatment used for device no. 1 was too high and the heating itself contributed to a degradation of the device.

ACKNOWLEDGMENT

The authors wish to thank R. Conklin of Wright Air Development Division, USAF, the Westinghouse Electric Corp., and RCA for supplying the transistors used in this work.

B. A. KULP
Aeronautical Research Lab.
Wright-Patterson AFB
Dayton, Ohio
J. P. JONES
A. F. VETTER
USAF Institute of Technology
Wright-Patterson AFB
Dayton, Ohio

Negentropy Revisited*

Information content, when defined in terms of the *a priori* probability of a choice, is equivalent to negentropy only through an analogy. The analogy stems from the computation of the entropy in a world defined by complexions (in the manner of Planck). Because quantum states are complexions, Planck's prescription for the computation of the entropy is quasi-universal. Thus, the classical definition of the entropy

$$\Delta S = \frac{\Delta Q}{T}, \tag{1}$$

does not yield results other than does the statistical definition

$$S = k \ln P, \tag{2}$$

where P is the number of complexions, Q the heat, T the temperature, k Boltzmann's constant, and S the entropy.

The classical definition of negentropy is

$$\Delta N = \frac{\Delta W}{T}, \tag{3}$$

where W is the nondegraded or available energy. Brillouin,[1] after introducing the negentropy by its statistical form, switched to the classical form in the discussion of numerous examples. In practice, he assumed that the information gained is given by

$$\Delta I = \frac{\Delta W}{T}. \tag{4}$$

The two definitions of information form a dichotomy.

Suppose one reads a page of a book. The information gained, as far as the usual definition of information is concerned, is independent of the reader. With the classical definition of negentropy, the information gained and the entropy generated to gain the information depend on the reader's possible previous knowledge of the written page. Thus, a page known by heart can be read in the dark without increase of either entropy or negentropy. A page previously known and partially forgotten will necessitate some generation of entropy to regain the level of negentropy obtained after the first reading.

The flexibility of the classical thermodynamic definition (4), and the rigidity of the usual definition of information content based on probabilities known *a priori*, may well be a sufficient reason for preferring the thermodynamic definition.

Note that the meaning of the text in the example above is not important. Only the reader's previous knowledge of the text concerns us. With the classical thermodynamic definition of negentropy, the amount of information gained by reading a page cannot exceed the probabilistic information content of that page, but may be quite less.

P. A. CLAVIER
Aeronutronic
Div. of Ford Motor Co.
Newport Beach, Calif.

Optical Erasure of EL-PC and Neon-PC Storage Elements*

Desirable characteristics for opto-electronic storage elements[1] include the ability to store and erase information selectively.

Voltage control [1]–[5] and infrared quenching [2] have been previously de-

[3] Radio Corporation of America, Contract No. USAF 33(600)-3726.
[4] Westinghouse Electric Corporation, Contract No. USAF 33(616)-6278.

* Received by the IRE, June 13, 1961.
[1] L. Brillouin, "Science and Information Theory," Academic Press, Inc., New York, N. Y.; 1956.

* Received by the IRE, May 1, 1961; revised manuscript received, May 16, 1961.
[1] Opto-electronic storage elements will hereinafter be referred to as optrons (after Loebner [2]).

scribed as methods of erasure. A new method of selective optical storage and erasure is reported here. Neon-PC and EL-PC bistable elements employing CdS or CdSe photoconductors can be latched and erased by serial irradiation from a single light source of constant intensity, when its emission lies within the sensitivity region of the photoconductor. Short (less than 30 msec.) light pulses of sufficient intensity latch optrons; longer (greater than 200 msec.) pulses effect erasure. Complete optical control of optoelectronic storage elements is therefore provided.

The basic optron circuit consists of series-connected light-emitting (neon or EL) and light-sensitive components arranged so that a positive light feedback path exists [Fig. 1(a)].

The optron operates as follows: In the dark, the photoconductor is in its high-resistance state and the lamp is dark. If the photoconductor is briefly illuminated, its resistance drops and the lamp lights. The positive optical feedback continues to keep the lamp on [Fig. 1(b)].

The latched optron can be erased if the PC is re-illuminated by the same external source for a period greater than the triggering pulse. The application of the extended erase light pulse to the latched optron drives the photoresistivity to a lower level. Upon extinction of the light pulse, the optron does not return to the latch level, but rather undershoots it and turns off [Fig. 1(c)].

Optrons were constructed from various EL, neon, CdS and CdSe elements. Each optron was pulse-irradiated at room temperature by various light sources emitting from the near-infrared to the green region of the spectrum. Light pulses of varying duration were obtained with a variable-speed camera shutter. Optron current was continuously monitored with an oscilloscope. EL-PC and neon-PC combinations were ac-operated at frequencies from 60 to 1000 cps. Neon-PC elements were also operated under dc voltages. Measurements of dc power dissipation in the PCs were made by observing PC current and voltage values under latch and erase conditions.

Optrons made with either CdS or CdSe photoconductors could be optically erased. In all cases, behavior of the type shown in Fig. 1(c) was obtained. The effect was found to be quite sensitive to applied voltage. It is most easily and reproducibly observed at or near the minimum voltage necessary to maintain the latch.

Photocurrent undershoot is observed in CdSe photoconductors [6] (Fig. 2). A reference-current level in a dc-biased CdSe PC is established by a small light bias. When the light-biased PC is irradiated with an additional pulse, at the termination of the pulse the PC current undershoots the reference level, then slowly recovers toward it. Longer light pulses tend to increase the extent of the undershoot. While CdSe shows undershoot readily at room temperature, CdS shows undershoot only above 100°C [6].

While optrons made with CdSe photoconductors reacted rapidly to external irradiation and erased under widely varied levels of illumination and power dissipation, those made with CdS tended to be much

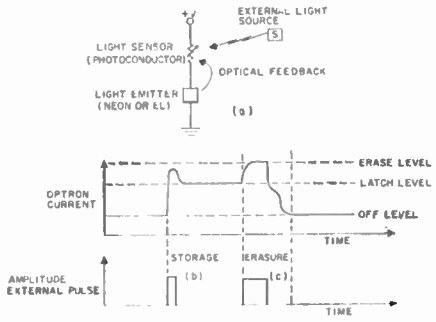

Fig. 1.

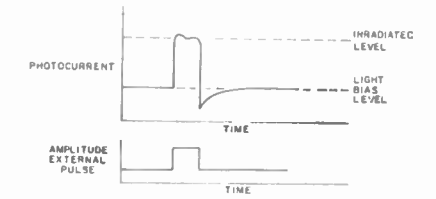

Fig. 2.

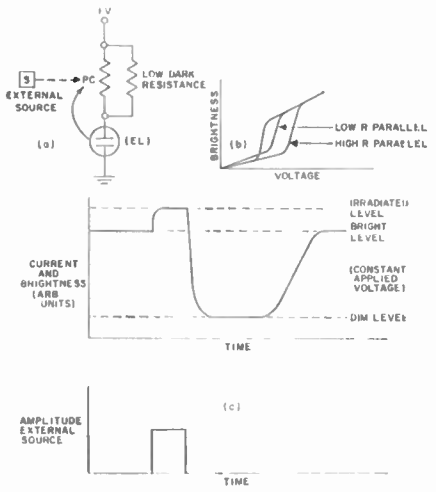

Fig. 3.

more sluggish and less sensitive to external irradiation. Observations of the dc power dissipation in latch and erase states indicated that CdS devices are erased only under conditions that would tend to produce an increase in temperature of the photoconductor.

Under most cases examined, photocurrent undershoot seems to best explain erasure with CdSe. In those cases where the power dissipation in the CdSe is increased during the erase pulse, undershoot and thermal effects probably act together to effect erasure.

As an additional application of undershoot in CdSe, we have constructed another series EL-PC device called a Persistroff.[2] The Persistroff circuit is shown in Fig. 3(a). By shunting the photoconductor in an optron circuit (or by using PCs with low dark resistance) a device with the nonlinear brightness-voltage characteristics shown in Fig. 3(b) may be obtained. The Persistroff is a voltage-controlled device in which the width of the hysteresis loop can be varied by varying the shunt (dark) resistance [7]. The behavior of the device is shown in Fig. 3(c). The applied voltage is set above the self-turn-on voltage. Circuit parameters are arranged so that an hysteresis loop of about 5–6 volts is obtained. Undershoot resulting from a pulse of radiation from an external source, incident on the CdSe PC, will force the cell into a low brightness condition.

After a short time, 10–30 seconds, during which recovery from the undershoot occurs, the device will again return to its full brightness condition.

J. A. O'Connell
General Telephone and Electronics Labs.
Bayside, N. Y.
Formerly at IBM Prod. Dev. Lab.
Poughkeepsie, N. Y.
B. Narken
IBM Prod. Dev. Lab.
Poughkeepsie, N. Y.

[2] This device is the opto-electronic complement of the Persistron described by MIT Lincoln Labs. [1].

References

[1] W. Gardner, D. E. Barker and M. Zimmerman, "Optical memory panels," Mass. Inst. Tech., Cambridge, Mass., Group Rpt. 2G-2480; July, 1957.
[2] E. E. Loebner, "Opto-electronic devices and networks," Proc. IRE, vol. 43, pp. 1897–1906; December, 1955.
[3] J. E. Rosenthal, "Theory and experiments on a basic element of a storage light amplifier," Proc. IRE, vol. 43, pp. 1882–1888; December, 1955.
[4] B. Kazan and F. H. Nicoll, "An electroluminescent light-amplifying picture panel," Proc. IRE, vol. 43, pp. 1888–1897; December, 1955.
[5] G. Diemer, H. A. Klasens and J. G. van Santen, "Solid state image intensifiers," *Phillips Res. Repts.*, vol. 10, pp. 401–424; December, 1955.
[6] R. H. Bube, "Analysis of photoconductivity applied to cadmium-sulfide-type photoconductors," *J. Phys. Chem. Solids*, vol. 1, pp. 234–248; October, 1957.
[7] R. Halstead, U. S. Patent No. 2,836,766; May, 1958.

A Magnetically Tunable Microwave-Frequency Meter*

The availability of single-crystal YIG (yttrium iron garnet) with narrow-resonance line widths (< 1 oe) makes it possible to construct a magnetically tunable frequency meter with useful accuracy over a broad bandwidth.

The application of YIG spheres to microwave band-reject filters has been suggested,[1] and a magnetically tunable frequency meter has been constructed using a paramagnetic material.[2] The advantages of using a YIG sphere loosely coupled to a strip transmission line are: no auxiliary equipment other than a detector is required, and useful accuracy can be obtained with a minimum of precision parts in a compact structure.

Fig. 1 gives some essential characteristics of an *S*-band YIG frequency meter con-

* Received by the IRE, May 26, 1961.
[1] P. S. Carter, G. L. Matthaii, and W. J. Getsinger, "Design Criteria for Microwave Filters and Coupling Structure," Stanford Res. Inst., Stanford, Calif. Tech. Rept. No. 8; October, 1959.
[2] P. H. Vartanian and J. L. Melchor, "Broadband microwave frequency meter," Proc. IRE, vol. 44, pp. 175–178; February, 1956.

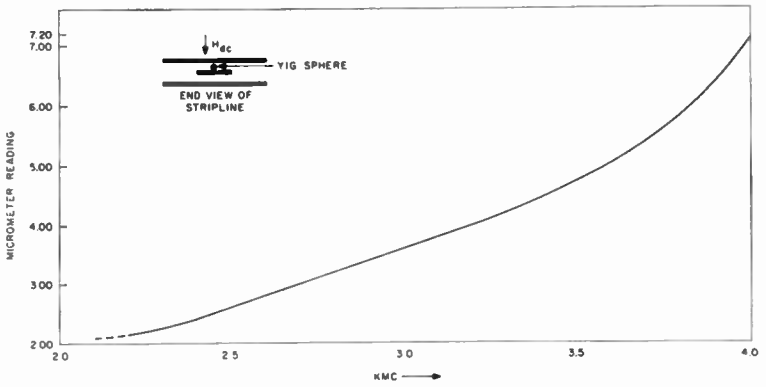

Fig. 1.

structed at these laboratories. A micrometer screw advances or retracts a magnetic shunt to change the magnetic field required for resonance. A calibration chart is used to convert micrometer readings to frequency.

At ferromagnetic resonance there is a 10 per cent dip in the microwave energy transmitted through the wavemeter which is readily detectable with a crystal or bolometer. VSWR and insertion loss are negligible and are almost entirely due to the stripline structure when the frequency meter is tuned "off resonance." The magnetic field required for resonance should not change with temperature due to the spherical geometry of the YIG. Well-known techniques may be used to stabilize the magnetic circuit; this work is in progress now.

A simple direct method of measuring frequency with an accuracy of 0.3 per cent or better has been devised using single-crystal spheres of YIG; further improvement may be expected using 0.5 oe material and a better magnetic circuit. Accuracies of 0.1 per cent should be easily attainable from *S* through *X* bands in a single unit.

GEORGE H. THIESS
Apparatus Division
Texas Instruments Inc.
Dallas, Tex.

A Bistable Flip-Flop Circuit Using Tunnel Diode*

A recent paper[1] gives a good survey of the circuits developed in the last two years; there are very useful and interesting circuits. Voltage stable negative-resistance devices have been known for over thirty years during which time certain circuits realizing negative resistance have been developed. With the invention of tunnel diodes, we have to look forward to much simpler and reliable circuit realizations. Keeping these facts in mind, we have developed in this laboratory quite a few circuits using tunnel diodes. One of them is the bistable flip-flop circuit shown in Fig. 1, using one tunnel diode and one ordinary diode. Using the *I-V* characteristic of the tunnel diode, the circuit works as follows (See Fig. 2).

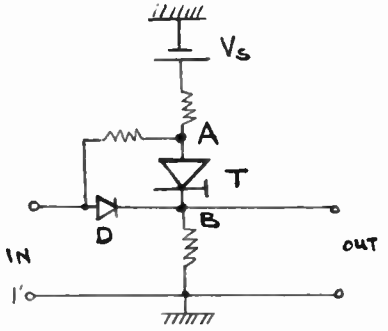

Fig. 1.

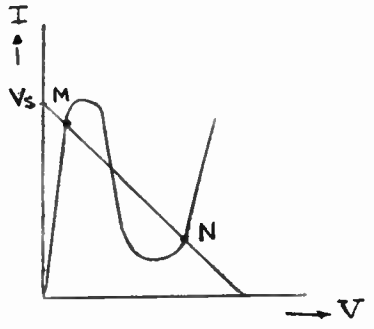

Fig. 2.

Suppose that the device is in its high operating point *M*. The potential drop across the diode *D* is low. A positive pulse applied at 1-1' will not have any access to point *B*, as the forward bias on diode *D* is not enough to make it conduct, but will have an access to point *A*, of course, and shift the operating point to *N*. Now we need a negative pulse at *A* or a positive pulse at *B* to shift the operating point back to *M*. As tunnel diode *T* is now in its high-voltage state, the drop across *D* is high. A positive pulse applied at 1-1' will appear at *A* as well as at *B*, because diode *D* is conducting now due to the higher voltage across it. Pulse appearing at *A* cannot affect the device as the tunnel diode is already in its high-voltage state. The same pulse appears slightly later at *B*, depending on the transit time of the carriers through the diode *D*. Thus, the pulse appearing at *B* will shift the operating point back to *M*.

The values of resistances can easily be adjusted, and R_1 has to be large enough not to disturb the impedance level of the device. Diode *D* can be germanium or silicon. Silicon will necessitate higher driving pulses.

Several of these circuits have been successfully coupled using properly biased diodes. The speed of operation of a single stage, neglecting stray inductive and capacitive effects, is limited merely by the speed of the diode *D*. Single stages have been operated successfully at around 30 Mc, which does not show, of course, the highest speed of operation. The circuit would easily operate in the range of several hundred Mc within reasonable stability.

Sensitivity of the circuit depends on the location of the load line and its effective value. Increasing the load resistance will increase stability and make operation less effective on the parameter variations, but on the other hand will also necessitate higher driving signals. Therefore, a compromise has to be made between the sensitivity and the amplitude of the driving signal.

V. UZUNOGLU
Solid State Advanced Dev. Lab.
Westinghouse Elec. Corp.
Baltimore, Md.

Microwave Determination of Semiconductor-Carrier Lifetimes*

Recent publications have proposed the use of a transverse post or rod of semiconducting material in a waveguide, as a means of obtaining the lifetime of injected carriers in the semiconductor by an observation of the decay curve of the transient of transmitted microwave power, after the injection of carriers.[1-3] It is the purpose of this note to show that, if the semiconductor carrier density decays exponentially in a typical configuration of this kind, the transient of transmitted microwave power is also exponential only under special circumstances, and in general may have a decay curve of complex form.

The problem of waveguide transmission in a semiconductor medium has been treated,[4] but the impedance character of a semiconductor post was not discussed. The transmission characteristics of a centered cylindrical post in a waveguide are given by the *T* network configuration shown in Fig.

* Received by the IRE, January 26, 1961; revised manuscript received, May 17, 1961.
[1] Sims, *et al.*, "A survey of tunnel-diode digital techniques," PROC. IRE, vol. 49, pp. 136–146; January, 1961.

* Received by the IRE, April 20, 1961.
[1] A. P. Ramsa, H. Jacobs, and F. A. Brand, "Microwave techniques in measurement of lifetime in Germanium," *J. Appl. Phys.*, vol. 30, pp. 1054–1060; July, 1959.
[2] H. Jacobs, A. P. Ramsa, F. A. Brand, "Further consideration of bulk lifetime measurement with a microwave electrode-less technique," PROC. IRE, vol. 48, pp. 229–233; February, 1960.
[3] R. D. Larrabee, "Measurement of semiconductor properties through microwave absorption," *RCA Rev.*, vol. 21, pp. 124–129; March, 1960.
[4] H. A. Atwater, "Microwave measurement of semiconductor carrier lifetimes," *J. Appl. Phys.*, vol. 31, pp. 938–939; May, 1960.

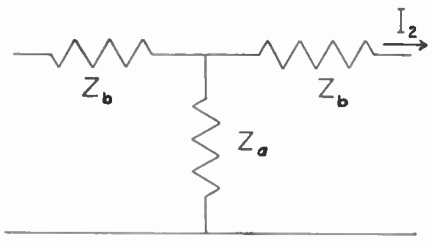

Fig. 1

1.[5] The impedance elements in Fig. 1, for a post centered in the waveguide and having its axis parallel to the dominant-mode E field, are given by

$$\frac{2Z_a}{Z_0}+\frac{Z_b}{Z_0}\approx -j\frac{a}{\lambda_g}\csc^2\frac{\pi}{2}\cdot\left[\frac{2\lambda^2}{\pi^2d^2(\epsilon_r-1)}-S_0-\frac{1}{4}\frac{\epsilon_r-3}{\epsilon_r-1}\right] \quad (1)$$

$$\frac{Z_b}{Z_0}\approx j\frac{a}{8\lambda_g}\left(\frac{a}{\lambda}\right)^2(\epsilon_r-1)\left(\frac{\pi d}{a}\right)^4\sin^2\frac{\pi}{2}\cdot\left[1+\frac{\epsilon_r-2}{6}\frac{\pi^2d^2}{\lambda^2}\right], \quad (2)$$

where, for X-band waveguide operating at 10 kMc,

$$S_0\approx \ln\left(\frac{4a}{\pi d}\right)-0.686. \quad (3)$$

In (1) to (3) a is the waveguide width, d is the diameter of the post, λ_g the guide wavelength, λ the free-space wavelength, and Z_0 is the characteristic impedance of the waveguide. The quantity ϵ_r is the complex relative dielectric constant of the semiconducting post: $\epsilon_r=\epsilon/\epsilon_0$. If the T network is terminated in a matched load equal to Z_0, the current in the load per input volt is

$$I_2=\frac{Z_a}{Z_b(2Z_a+Z_b)+Z_0(Z_a+Z_b)}. \quad (4)$$

The power in a matched detector terminating the waveguide beyond the semiconducting sample will be proportional to the square of I_2 in (4). The semiconductor sample diameter d is usually made small in order to avoid skin-effect difficulties, and $(d/a)^2$ and $(d/\lambda)^2$ are small compared to unity. The quantity ϵ_r, with zero injected carrier density, is equal to 16.5 for germanium and 12 for silicon. Thus, using the typical value[1] $d=3$ mm, with the conditions cited above, (1) and (2) may be written approximately

$$\frac{2Z_a+Z_b}{Z_0}\approx -j0.67\csc^2\left[\frac{31.8}{\epsilon_r-1}-\frac{5\pi}{4}\right] \quad (5)$$

$$\frac{Z_b}{Z_0}\approx j0.0012(\epsilon_r-1). \quad (6)$$

Consequently, in (4),

$$I_2=\frac{1}{Z_0}\cdot\frac{-j0.33\csc^2\left[\frac{31.8}{\epsilon_r-1}-\frac{5\pi}{4}\right]-j0.0006(\epsilon_r-1)}{0.0008(\epsilon_r-1)\csc^2\left[\frac{31.8}{\epsilon_r-1}-\frac{5\pi}{4}\right]+j0.0006(\epsilon_r-1)-j0.33\csc^2\left[\frac{31.8}{\epsilon_r-1}-\frac{5\pi}{4}\right]}. \quad (7)$$

The complex dielectric constant for germanium is[6]

$$\epsilon_r=16.5-\frac{Ne^2\tau_s^2}{m^*\epsilon_0(1+\omega^2\tau_s^2)}+j\frac{Ne^2\tau_s}{m^*(1+\omega^2\tau_s^2)}. \quad (8)$$

where N is the carrier density, and τ_s is the lattice scattering relaxation time for conduction. For 9.34-ohm cm germanium at room temperature and 10^{10} cps, data given by Benedict yields approximately

$$\epsilon_r\approx 16.5-5\left(1+\frac{\Delta N}{N}\right)(1+j20)$$

$$\epsilon_r\approx\left(11.5-5\frac{\Delta N}{N}\right)-j100\left(1+\frac{\Delta N}{N}\right), \quad (9)$$

where ΔN is the injected surplus carrier density.

The fundamental assumption of the microwave measurement of carrier lifetime[1] is that the surplus carrier density in the semiconducting material decays exponentially with a time constant equal to the carrier lifetime, and that the power transmitted beyond the semiconducting post also decays exponentially with this same time constant. From (9) it may be seen that if

$$\Delta N=\Delta N_0e^{-t/\tau} \quad (10)$$

is the decay curve of the surplus carrier density, where τ is the carrier lifetime, the complex dielectric constant ϵ_r also decays with this time constant. It is apparent that the use of an exponential ϵ_r in the expression for detector current (7) will not lead to an expression with exponential time dependence.

An exception to the above circumstance will occur when the argument of the cosecant term in (5) approaches $n\pi$, where n is an integer. Then, the value of the parallel impedance Z_a approaches infinity, and the detector current is governed solely by the series impedance $2Z_b$, which decays exponentially with ϵ_r, as shown by (6).

Returning to (1), the condition for infinite shunt impedance is thus

$$\frac{\lambda^2}{\pi^2d^2(\epsilon_r-1)}-\frac{1}{2}\ln\left(\frac{4a}{\pi d}\right)-0.343-\frac{1}{8}\frac{\epsilon_r-3}{\epsilon_r-1}=n, \quad (11)$$

where n is an integer. This condition can be satisfied only in keeping with the time dependence of ϵ_r. It may be seen from the foregoing, however, that if the choice of operating conditions leads to a very large effective shunt impedance in Fig. 1, the detector current transient decays in the same manner as does the surplus carrier density. If the detector is a square law detector, its indication will be proportional to $(I_2)^2$. In any event, of course, the total duration of the transient will be a measure of the carrier lifetime, although, as shown above, it is not a direct indication of the latter.

H. A. Atwater
The Pennsylvania State Univ.
University Park, Pa.

Author's Comment[7]

In the note by Mr. Atwater, the following statement is made:

> Recent publications have proposed the use of a transverse post or rod of semiconducting material in a waveguide as a means of obtaining the lifetime of injected carriers in the semiconductor by an observation of the decay curve of the transient of transmitted microwave power, after the injection of carriers. It is the purpose of this note to show that if the semiconductor carrier density decays exponentially in a typical configuration of this kind, the transient of transmitted microwave power is also exponential only under special circumstances, and in general may have a decay curve of complex form.

The question raised at the close of the note is whether or not a direct measurement of lifetime can be obtained by observing changes in microwave absorption as excess minority carriers decay in a semiconductor.

In the early work,[8] where rectangular rods were inserted in the waveguide and light pulses flashed onto the semiconductor, correlation was established between the conventional dc current measuring techniques and the microwave absorption technique. When the two methods gave the same experimental value of lifetime for samples in the resistivity range studied, the method was assumed to provide an electrodeless measurement of lifetime. Furthermore, it was pointed out that for smaller changes in carrier concentration due to the incident light, the correlation was improved. In fact, with low level light pulses, the agreement between the conventional conductivity test and the microwave absorption technique was as good as obtained by testing various samples using the conductivity test alone. We can conclude from the above that there are general circumstances for a decay curve of exponential form. It turns out in the analysis that if the resistivity of the material is high and the change from equilibrium small, consistent with conventional small signal semiconductor device theory, a direct microwave measurement of lifetime can be obtained.

Parenthetically, upon checking the original article by Benedict,[9] it appears there is a mistake in (8) in the note by Mr. Atwater. Eq. 8 should read as follows:

$$\epsilon_R'=\epsilon_R-\frac{Ne^2\tau^2}{m^*\epsilon_0(1+\omega^2\tau^2)}-\frac{j}{\omega\epsilon_0m^*}\frac{Ne^2\tau}{(1+\omega^2\tau^2)}. \quad (1)$$

[7] Received by the IRE, May 26, 1961.

[5] N. Marcuvitz, "Waveguide Handbook," McGraw-Hill Book Co., Inc., New York, N. Y., p. 266; 1951.

[6] T. S. Benedict, "Microwave observation of the collision frequency of holes in germanium," *Phys. Rev.*, vol. 91, pp. 1565–1566; September 15, 1953.

[8] A. P. Ramsa, H. Jacobs and F. A. Brand, "Microwave techniques in measurement of lifetime in germanium," *J. Appl. Phys.*, vol. 30, pp. 1054–1060; July, 1959.

[9] T. S. Benedict, "Microwave observation of the collision frequency of holes in germanium," *Phys. Rev.*, vol. 91, p. 1563; September, 1953.

This, together with any inaccuracy in the value of τ, may have caused an error in (9).

In any case, the note does point out a basic difficulty in using approximations when the detailed analysis of the use of rods is complicated at the outset. This brings us to a suggestion which is currently being studied and which has been reported in relation to resistivity measurements,[10] but has not yet been reported on in detail with respect to lifetime. Here we suggest the use of a distributed line rather than a lumped parameter approach. The distributed line together with the change in geometry of the sample can make the analysis completely accurate with no approximations needed. If one then desires to make subsequent approximations the per cent error can be exactly determined.

In this approach a germanium plug is inserted, completely filling the waveguide. The equations for calculation of the transmitted field is then given as follows,

$$\frac{E_0}{E_{in}} = r_t\left(\cosh \Gamma_2 l_2 - \frac{Z_{02}}{Z_{ab}}\sinh \Gamma_2 l_2\right), \quad (2)$$

$$r_t = \frac{2Z_{ab}}{Z_{ab} + Z_{01}} \quad (3)$$

and

$$Z_{ab} = Z_{02}\left(\frac{Z_{03} + Z_{02}\tanh \Gamma_2 l_2}{Z_{02} + Z_{03}\tanh \Gamma_2 l_2}\right), \quad (4)$$

where

Z_{01} is the impedance of the waveguide in air,
Z_{02} is the impedance of the waveguide filled with germanium and is a function of conductivity and wavelength,
Z_{ab} is the impedance of the germanium at the front surface,
Γ_1 is the propagation constant in air in the waveguide,
Γ_2 is the propagation constant in germanium in the waveguide,
l_2 is the thickness of the slab of semiconductor.

Using (2), (3) and (4), the transmitted field to incident field ratio was calculated. Data obtained this way were experimentally checked and found to be accurate.

Now a small slit can be made in the side of the waveguide allowing low level light pulses to fall upon the germanium. Under these conditions the decay in excess minority concentration has been found to be linearly related to the increase in current from the detector diode located so as to detect changes in power transmitted. As a result, exponential changes (in agreement with earlier findings)[8] have been detected. Further experiments on this work are now in progress.

HAROLD JACOBS
U. S. Army Signal Res.
and Dev. Lab.
Ft. Monmouth, N. J.

[10] H. Jacobs, *et al.*, "Electrodeless measurement of semiconductor resistivity at microwave frequencies," PROC. IRE, vol. 49, pp. 928–932; May, 1961.

Antigravity*

Although many people do not realize it, antigravity has been with us since 1918 when Thirring investigated the coriolis type effects of moving masses which arise from Einstein's Principle of General Relativity.[1–4] This form of antigravity consists of the generation of non-Newtonian gravitational forces by moving masses. These forces, in a local region, will act on a body in exactly the same way as gravity. Thus, by generating these fields in an upward direction at some spot on the earth, we could theoretically counteract the earth's gravitational field.

An example of such a generator is a system of accelerated masses whose mass flow can be approximated by the current flow in a wire-wound torus.

In the electromagnetic case, the current I through the wire causes a magnetic field in the torus. If the current is constantly increasing, then the magnetic field also increases with time. This time-varying magnetic field then creates a dipole electric field. The value of this field at the center of the torus is

$$E = -\frac{\mu N \dot{I} r^2}{4\pi R^2},$$

where R is the radius of the torus, r is the radius of one of the loops of wire wound around it, and N is the total number of turns.

We can now use the analogies between the electromagnetic and gravitational fields that were developed by Forward.[2] We transform all the electromagnetic quantities to the gravitational quantities to get

$$G = \frac{\eta N \dot{T} r^2}{4\pi R^2}.$$

where G is the gravitational field generated by the total accelerated mass current $N\dot{T}$.

Unfortunately, since the "gravitational permeability of space" has the very small value of $\eta = 3.73 \times 10^{-26}$ m/kg, it would require very large systems to obtain even a measurable amount of acceleration, much less practical antigravity. For example, if we could accelerate matter with the density of a dwarf star through pipes wide as a football field wound around a torus with kilometer dimensions, then we could create a gravitational field at the center of the torus of about

$$G \approx 10^{-10}\, a,$$

where a is the amount of acceleration we can give the dwarf star material. With an acceleration of $a = 10^{11}$ msec^2, we could counteract the earth's gravitational field for a few milliseconds.

It is obvious that these minimum requirements are so far from present capabilities, that practical antigravity will unfortunately be unattainable for centuries.

ROBERT L. FORWARD
Physics Department
University of Maryland
College Park, Md.

* Received by the IRE, June 2, 1961.

[1] A. Einstein, "The Principle of Relativity," Dover Publications, Inc., New York, N. Y.; 1923.
[2] R. L. Forward, "General relativity for the experimentalist," PROC. IRE, vol. 49, pp. 892–904; May, 1961.
[3] C. Møller, "The Theory of Relativity," Oxford University Press, London, Eng.; 1952.
[4] J. Weber, "General Relativity and Gravitational Waves," Interscience Publishers, Inc., New York, N. Y.; 1961.

On the Nomenclature of TE_{0l} Modes in a Cylindrical Waveguide*

The indices n and l which have been used to identify the species of different modes in a circular-cylindrical waveguide seem to have been firmly established. In practically all the textbooks n is used to denote the order of the Bessel functions, and l (or m) the ordinal numeral for the roots of the Bessel functions or its derivatives. In the case of circularly symmetrical modes of the TE type, where $n=0$, one normally assigns $l=1$ to denote the first nontrivial root of the equation $J_n'(x)=0$. Thus, if one denotes these roots by p_{nl}', then the conventional designations are $p_{01}'=3.832$, $p_{02}'=7.016$, etc., and these modes are called TE_{01}, TE_{02}, etc. This nomenclature has been adopted by the authors of many well-known textbooks on electromagnetics or waveguide theory, such as the ones by Kraus, Marcuvitz, Ramo-Whinnery, Stratton and the new book by Collin. However, if one displays the roots of

$$J_n(x) = 0$$

and

$$J_n'(x) = 0,$$

denoted, respectively, by p_{nl} and p_{nl}', in a figure such as the one shown here (Fig. 1),

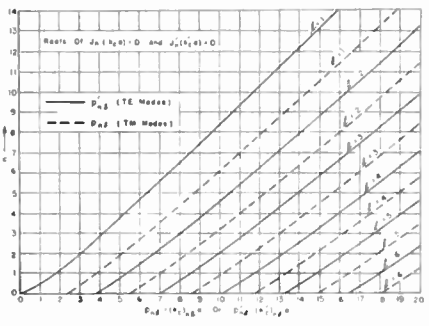

Fig. 1.

* Received by the IRE, April 13, 1961.

then one would naturally label $l=1, 2, \cdots$, as the ordinal numerals for these roots. In such a designation the root p_{01}' is numerically equal to zero, corresponding to a trivial mode. The first nontrivial mode of the TE_{0l} set would be TE_{02}. In tabulated form the roots p_{nl}' would appear as the one shown in Table I for $n, l \leq 3$.

TABLE I
ROOTS OF $J_n'(x)=0$

n \ l	1	2	3
0	0	3.832	7.016
1	1.841	5.331	8.535
2	3.054	6.706	9.969
3	4.201	8.015	11.346

The orderly appearance of such a table as compared with the old arrangement is obvious. One may remember that in the old notation the TE_{01} is not the dominant mode, in spite of the fact that the indexes are of lower order than TE_{11}. In the present notation TE_{01} would be the dominant mode if it were not trivial. The inclusion of this trivial mode does bring into order a more logical nomenclature for all the modes in a cylindrical waveguide. A similar nomenclature was used for rectangular waveguides, whereas the trivial modes TM_{0n} and TM_{m0} never bothered us.

The graph presented here is useful to determine the number of propagation modes for a given waveguide. When one elects a vertical line on the abscissa at a distance equal to ka, where $k=2\pi/\lambda$ denotes the free space-wave number, then all the modes at the left side of the line are propagating, while those at the right are evanescent. Incidentally, we may mention that in Ramo-Whinnery's work[1] the mode TE_{12} is missing in the display of the first few spectral lines. This mode should lie beyween TE_{41} and TM_{02}, as can be checked from the present graph. The graph can also be used to interpolate the characteristic values of wedge-shaped circular waveguides corresponding to fractional values for n.

This note is prompted by a conversation with Prof. R. Collin of the Case Institute of Technology. The author acknowledges with thanks his interest in this topic. For teachers and engineers who have become accustomed to the old designation for the TE_{0l} modes, it is hoped that the suggested change will not cause any inconvenience. For new teachers, the author encourages them to consider this more logical presentation. A limited supply of the copies of the figure presented in this correspondence can be obtained by writing to the Department of Electrical Engineering, The Ohio State University, Columbus 10, Ohio.

C. T. TAI
Dept. of Elec. Engrg.
The Ohio State University
Columbus, Ohio

[1] S. Ramon and J. R. Whinnery, "Fields and Waves in Modern Radio," John Wiley and Sons, Inc., New York, N. Y., 2nd ed., p. 377.

On Minimum Reading Times for Simple Current-Measuring Instruments*

In their paper,[1] Praglin and Nichols thoroughly analyze some relationships between electrometer noise, bandwidth and sensitivity. By making the assumption that signal and white-noise currents flow into a current node A (see Fig. 1) through an equivalent parallel RC circuit and are read

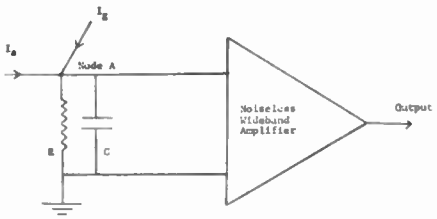

Fig. 1—Typical current and voltage-measuring device showing principal rolloff RC.

out by a low-noise wide-band voltage amplifier, we wish to determine the minimum time necessary to detect the smallest expected dc signal current I_s. Signal-current noise I_s^2 due to I_s flowing through the RC impedance generates a mean-square voltage per unit angular frequency ω of

$$\frac{\Delta E_s^2}{\Delta\omega} = \frac{eI_s}{\pi}\cdot\frac{R^2}{1+(RC\omega)^2}.$$

Proceeding to differentials and integrating over all frequencies,

$$E_s^2 = \frac{eI_sR}{\omega C}\cdot\int_0^\infty \frac{d(RC\omega)}{1+(RC\omega)^2} = \frac{eR}{2C}\cdot I_s.$$

Similar treatment applied to grid current I_g (or other "pure" leakage currents) and resistor thermal noise yields the wide-band mean-square noise voltages, respectively,

$$E_g^2 = \frac{eR}{2C}\cdot I_g,$$

$$E_T^2 = \frac{kT}{C}.$$

As noise power (or noise-square voltages) add linearly, therefore the total mean-square noise voltage

$$E_n^2 = \frac{eR}{2C}\left[I_s + I_g + \frac{2kT}{eR}\right] = \frac{eR}{2C}\cdot I_n$$

where I_n represents the sum of the modulus of diode-like currents flowing into point A. It may be shown that even tube shot noise, provided it is limited in frequency by a similar RC time constant, is included in I_n by the addition of one more term. To arrive at a signal-to-noise ratio, consider

$$S^2 = \frac{I_s^2R^2}{E_n^2} = \frac{2RC}{e}\cdot\frac{I_s^2}{I_n}.$$

S will always be >1 for sufficient RC constant.

In practice, of course, this result is not completely realistic, since non-Gaussian noise sources such as tube drifts, power supply and component changes swamp these finer effects. Approximately, however, values of S uniquely determine RC. Further, if the minimum signal voltage must exceed amplifier drifts, then R is also explicit.

To evaluate noise reading times, it is necessary to investigate the Poisson distribution of random particle currents associated with I_n. After an observing time I_n, I_nT_n/e particles arrive at the node with an rms counting error of $[I_nT_n/e]^{1/2}$, and a large sample most-probable relative error in the measurement of signal I_s in the presence of noise equal to

$$(0.6745)\left[\frac{I_nT_n}{e}\right]^{1/2}\Big/\frac{I_sT_n}{e} = \left[\frac{I_ne}{T_n}\right]^{1/2}\cdot\frac{(0.6745)}{I_s}.$$

Thus, the current mean-square signal-to-noise ratio is simply

$$\frac{I_s^2T_n}{eI_n(0.6745)^2}.$$

Identifying this with the similar expression S^2 yields a minimum time T_n in terms of RC necessary to read the signal to within the mean-square signal-to-noise ratio (typically between 1 and 10, depending on peak-to-peak confidence limits).

$$T_n = 2RC(0.6745)^2 = 0.91RC.$$

Finally, the minimum total reading time T will consist of two parts, a period T_n to read noise and a dynamic range (D) rise time.

$$T = RC\,[0.91 + \log D].$$

True, there are other feedback and rolloff effects that must be enumerated before T may be evaluated. However, low-level electrometers and vacuum tube voltmeters that were developed are relatively easy to analyze in this manner and have yielded consistently accurate observation time requirements.

P. F. HOWDEN
Information Systems, Inc.
Los Angeles, Calif.

* Received by the IRE, May 19, 1961; revised manuscript received, June 5, 1961.

[1] J. Praglin and W. Nichols, "High speed electrometers for rockets and satellite experiments," PROC. IRE, vol. 48, pp. 771–779; April, 1960.

Gyromagnetic Resonance of Ferrites and Garnets at UHF*

For the development of reciprocal and nonreciprocal devices with ferrites for UHF, it is necessary to know materials whose resonance frequency is sufficiently low. Therefore we have explored the nonreciprocal attenuation at ferromagnetic resonance of magnesium-manganese ferrites whose sat-

* Received by the IRE, May 25, 1961.

uration magnetization was lowered by addition of aluminum, yttrium-garnet, and yttrium-gadolinium-garnets down to 300 Mc. Fig. 1 shows the arrangement of the probes in the waveguide. The experiments have shown that a clean resonance exists only if the material is saturated. This condition is fulfilled if the dc field H_a is larger than the perturbation field H^*, plus the demagnetizing field $N_z M$ in the direction of the dc field:

$$H_a > H^* + N_z M. \quad (1)$$

H^* is a perturbation field which describes the action of internal stresses, anisotropy forces, inpurities, etc.

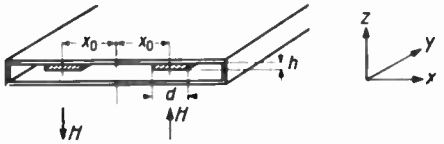

Fig. 1—Arrangement of probes within the waveguide.

In connection with Kittel's equation,[1] it follows that

$$\omega_r > \gamma \sqrt{(H^* + N_x M)(H^* + N_y M)}. \quad (2)$$

This equation shows how the resonance frequency can be lowered:

1) By means of a suitable compound, the gyromagnetic ratio of some materials can be lowered below its theoretical value.

2) Nothing can be said today about the reduction of the perturbation field strength H^* because the research in this field is not far enough advanced.

3) The reduction of the saturation magnetization M can be achieved by an admixture of Al_2O_3, but one would have to put up with a simultaneous reduction of the Curie-temperature.

4) A useful, and for a given material the only possible way is the reduction of the demagnetizing factors N_x and N_y (or the increase of N_z, as the sum $N_x+N_y+N_z=1$).

Fig. 2 shows the influence of the demagnetizing factors. It shows the nonreciprocal attenuation per unit length of a magnesium-manganese ferrite with a content of aluminum in the range of 490 to 590 Mc. The thickness of the probes decreases from left to right, corresponding with the increase of the demagnetizing factor N_z. At the left, the lowest resonance frequency is higher than the highest frequency of the band. A nonreciprocal attenuation does exist here too, but the attainable ratio of attenuations is significantly lower than in the case of resonance (right curve). The dc field strength is chosen for maximum isolation at the midband frequency of 540 Mc. With decreasing thickness the resonance moves to lower frequencies. At the right, the resonance lies

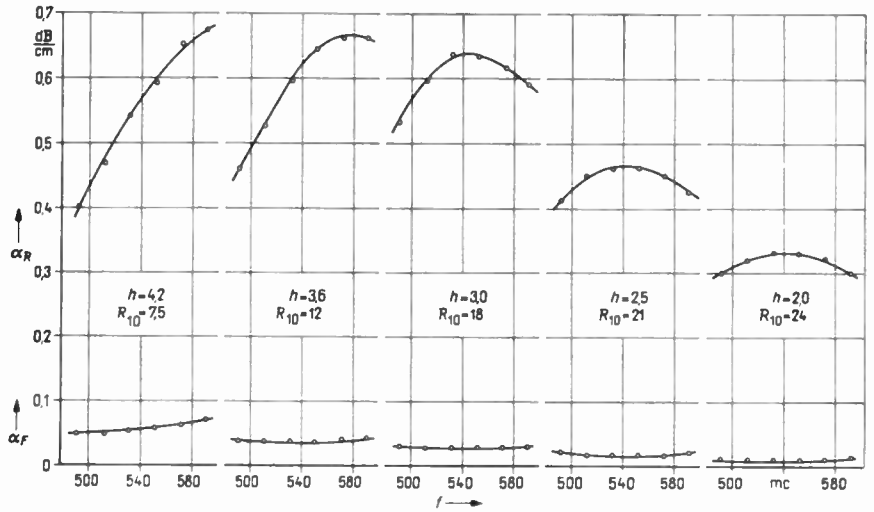

Fig. 2—Nonreciprocal attenuation of a ferrite for various heights h

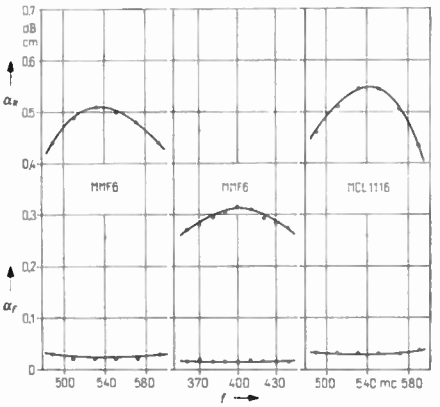

Fig. 3—Nonreciprocal attenuation of several materials.

near the midband frequency of 540 Mc. Here the isolation decreases symmetrically from the midband frequency to the ends of the band, and the attainable ratio of the attenuations is largest. Fig. 3 shows the attenuations per unit length of a magnesium-manganese-ferrite with a content of aluminum in the ranges 490 to 590 Mc and 360 to 440 Mc. This ferrite had a linewidth of magnetic resonance ΔH of about 130 Oe (at 4 kMc).

In addition, the attenuations of the yttrium-gadolinium-garnet MCL 1116 of Microwave Chemical Labs., New York, N. Y., are shown in the range of 490 to 590 Mc. The linewidth ΔH of this garnet is about 50 oe. In spite of the very different linewidths,[2,3] the attenuations of the ferrite and of the garnet are nearly the same in this band. The ratio of the smallest reverse attenuation to the largest forward attenuation

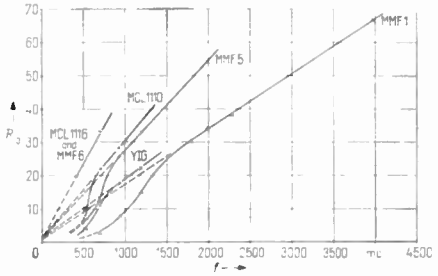

Fig. 4—Ratio of attenuations R_{10} as function of frequency.

TABLE 1

Material	Saturation Magnetization M Gauss	Linewidth ΔH (at 4 kMc) Oe	Curie-temperature Tc °C
MM F1	2000	≈160	255
MM F5	930	≈160	190
MM F6	730	≈150	150
YIG	1750	≈ 35	275
MCL 1110	1200	≈ 80	250
MCL 1116	600	≈ 50	170

in a band of 10 per cent bandwidth (R_{10}) for these two materials is about 25 for the best arrangement at 540 Mc. At about 400 Mc the ferrite has a ratio of about 18 for 10 per cent bandwidth, and at about 300 Mc the ratio is 12.

Fig. 4 shows the ratio R_{10} defined above for several materials as function of the frequency. Table 1 gives the values of the saturation magnetization M, of the linewidth ΔH (at 4 kMc), and of the Curie-temperature Tc of the materials. One can see from Fig. 4 that above a certain frequency, which is characteristic for the material and which depends moreover on the geometry of the probes, one obtains straight lines, which all go through the point 1 for the frequency 0. The slope of these straight lines seems to be a property of the material, it is nearly inversely proportional to the saturation magnetization. One can see that materials with

[1] C. Kittel, "Interpretation of anomalous larmor frequencies in ferromagnetic resonance experiment," *Phys. Rev.*, vol. 71, pp. 270–271; February, 1957.

[2] B. Lax, "Frequency and loss characteristics of microwave ferrite devices, PROC. IRE, vol. 44, pp. 1368–1386; October, 1956.

[3] C. L. Hogan, The low-frequency problem in the design of microwave gyrators and associated elements," IRE TRANS. ON ANTENNAS AND PROPAGATION, vol. 4, pp. 495–501; July, 1956.

low saturation magnetization give at low frequencies the same ratio of attenuations as materials with greater saturation magnetization at higher frequencies. Below a certain frequency (which agrees approximately with the lowest resonance frequency according to (2)), the ratio of attenuation R_{10} decreases rapidly and approaches the value 1. In this range the dc field strength necessary for resonance is lower than the field necessary for saturation according to (1).

We could not find a direct influence of the linewidth ΔH on the lowest resonance frequency or the ratio of the attenuations. But it seems that ΔH influences indirectly the lowest resonance frequency because the linewidth ΔH and the perturbation field strength H^* are probably connected.

Detailed results of our experiments (at other frequencies and with various materials) will be published in the near future in the *Nachrichtentechnische Zeitschrift*.

J. Deutsch
H. G. Maier
Zentrallaboratorium
der Siemens & Halske AG
Muenchen, Germany

One-Tunnel-Diode Binary*

A recent letter by Kaenel[1] described a one-tunnel-diode flip-flop which, for its explanation, required a complex shape for the driving pulse. The purpose of this note is to show that a simple pulse is sufficient and that, therefore, the "armchair analysis" is not adequate.

The pair of simultaneous differential equations which describe this circuit can be examined by any of several means described in standard textbooks on nonlinear analysis.[2] The significant result for the purpose of explaining the flip-flop action is that a positive driving pulse can drive the tunnel diode from its high-voltage state to its low-voltage state as well as vice versa. Also a negative driving pulse can produce either transition. Fig. 1 shows the two paths along which the switching can take place in response to positive driving pulses.

Fig. 2 is a schematic of the flip-flop from which the traces in Fig. 3 were taken. The driving pulse was from a well-terminated mercury switch pulse with no evidence of overshoot. The width of the driving pulse was about 3 nsec. The photograph shows transition times to be on the order of 10 to 15 nsec. The pulse height of the input is somewhat critical, about 10 per cent, at these speeds, and the position of the load line must be chosen by varying the dc voltage or the potentiometer. Slower flip-flops with larger inductances are very easy to set up. The binary stage shown in Fig. 1 has also been driven by a tunnel-diode univibrator. Two univibrators and two binary stages have been cascaded to produce a scale of four, and there appears to be no problem in ganging more together, provided diode coupling is used.

A. L. Whetstone
S. Kounosu
University of Pennsylvania
Philadelphia, Pa.

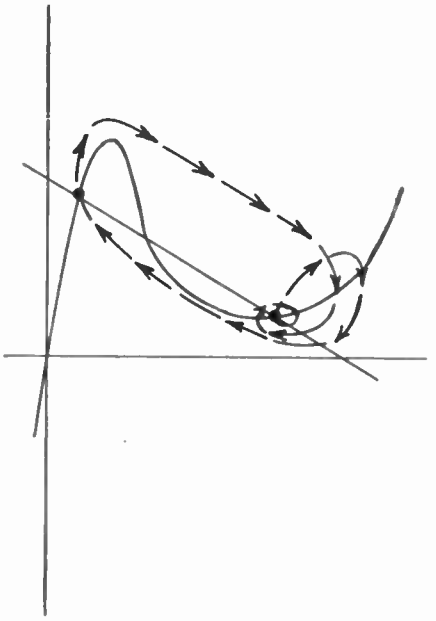

Fig. 1—Switching paths.

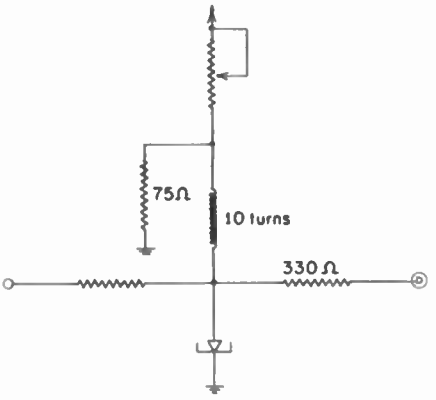

Fig. 2—Tunnel-diode binary stage using a 10-ma Ga As diode.

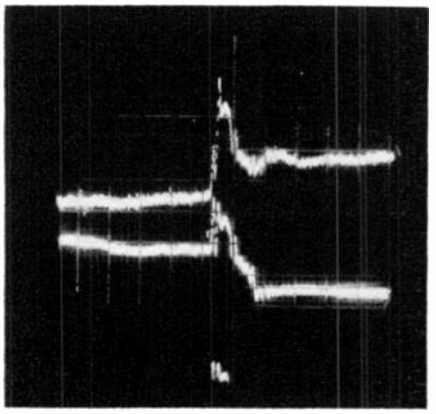

Fig. 3—Flip-flop transitions. Horizontal scale is 5 nsec per division.

Author's Comment[3]

The comment by Whetstone and Kounosu relating to my recent IRE letter[1] is of course correct. In fact, they should be congratulated for their success in cascading together several of these stages, forming a scale of four. Their observation that there seem to be "no problems in ganging more stages together" is a good argument for the high reliability of the one-tunnel-diode binary driven by a bipolar pulse. After all, the margin requirements for this type of trigger pulse are significantly less stringent than those encountered when using the nonlinear transient response of the binary stage configuration. The high operational reliability suggests that some gating functions can successfully be incorporated in the circuit as, for example, by controlling the power supply voltage. Forward and backward counters utilizing one-diode binary stages seem, therefore, feasible.

It is undoubtedly of value to briefly point out the mathematical reason for the circuit to operate as a binary when driven by a unipolar pulse. When the binary has switched to the high state, the relaxation transient that brings the circuit to its high-voltage stable state initiates at a point in the (i_{inductor}, $e_{\text{tunnel diode}}$) phase plane, whose coordinates will be designated (i_{iL}, e_{iL}). In contrast, when the binary is in the high-voltage state and is triggered, the ensuing transient initiates at point (i_{ih}, e_{ih}). Because of the nonlinearity of the tunnel-diode characteristic, the initial voltage across the diode e_{ih} is close to e_{iL}, whereas the initial current through the inductor i_{iL} is very much larger than i_{ih}. The nonlinearity causes the transient that initiates with a small inductor current to oscillate more vigorously than that beginning with a large current. This property is principally responsible for the binary operating as described by the authors.

R. A. Kaenel
Bell Telephone Labs
Murray Hill, N. J.

* Received by the IRE, March 20, 1961.

[1] R. A. Kaenel, "One-tunnel-diode flip-flop," Proc. IRE (Correspondence), vol. 49, p. 622; March, 1961.

[2] W. J. Cunningham, "Nonlinear Analysis," McGraw-Hill Book Co., Inc., New York, N. Y., p. 106; 1958.

[3] Received by the IRE, April 18, 1961.

Notes on "Fourier Series Derivation"*

In connection with Gadsden's letter,[1] I believe it is worthwhile mentioning that the derivation of the Fourier series from the Laplace transform is not only of mathematical interest but also has great practical importance. Provided that the waveforms considered satisfy Dirichlet's condition (*e.g.*, those occurring in engineering practice), this method can be used, and has been used for some years.[2]

From a practical point of view the most important group of the waveforms is the one built up of lines, of which the Laplace transforms can be determined as the sum of transforms of linear functions such as

$$\pm P_1(s) = \pm \frac{1}{s}, \qquad \pm P_2(s) = \pm \frac{1}{s^2},$$

$$\pm P_3(s) = \pm \epsilon^{-s\tau} \frac{1}{s}, \qquad \pm P_4(s) = \pm \epsilon^{-s\tau} \frac{1}{s^2}.$$

Forming $P(s)$, the transformed function of the waveform from the functions above, we obtain the Fourier series in exponential form:

$$p(t) = \frac{1}{T} C_0 + \frac{2}{T} \sum_{-\infty}^{+\infty} C_n \epsilon^{j2\pi nt/T-1},$$

where

$$C_0 = \lim_{s \to 0} P(s)$$

$$C_n = \lim_{s \to s_n} P(s)$$

and

$$s_n = j2\pi nT^{-1} \quad n = \pm 1, \pm 2, \pm 3, \cdots.$$

JENÖ TAKÁCS
R. B. Pullin and Co., Ltd.
Brentford, England

* Received by the IRE, June 19, 1961.

[1] C. P. Gadsden, "Fourier series derivation," PROC. IRE (Correspondence), vol. 48, p. 1652; September, 1960.

[2] J. Takacs "Determination of Fourier amplitudes by means of Laplace transform," *Magyar Hiradästechnika*, vol. 4, pts. 7–8, pp. 93–96; July–August, 1953.

Theoretical Techniques for Handling Partially Polarized Radio Waves with Special Reference to Antennas*

I. Introduction

In the analysis of radio antennas, one normally assumes that the incident radio wave is completely polarized. The response of a receiving antenna to a completely polarized radio wave incident upon the antenna has been thoroughly discussed in the literature.[1,2] A completely polarized wave is a limiting case of a more general type of wave, that is, a partially polarized wave. The purpose of this communication is to point out some theoretical techniques for handling partially polarized radio waves with special reference to antennas.

The main properties of partially polarized waves were thoroughly investigated by Stokes.[3] A partially polarized electromagnetic wave may be considered as the sum of a randomly polarized wave and a completely polarized wave independent of the former. This representation is unique. A partially polarized radio wave may be characterized completely either by the Stokes parameters or by a density matrix (*i.e.*, statistical matrix).[4]

II. The Stokes Parameters

Let $\boldsymbol{E}_i$ represent the electric field incident upon a receiving antenna. We shall define a unit polarization vector $\boldsymbol{n}_i$ for the incident wave by

$$\boldsymbol{E}_i = |\boldsymbol{E}_i| \boldsymbol{n}_i = |\boldsymbol{E}_i| (i_\theta n_\theta + i_\Phi n_\Phi), \quad (1)$$

where $n_\theta = a_1(t) \exp j[\omega t + kr - \alpha_1(t)]$ and $n_\Phi = a_2(t) \exp j[\omega t + kr - \alpha_2(t)]$. a_1, a_2, α_1 and α_2 vary with time, since the incident wave is assumed to be a partially polarized wave. $|\boldsymbol{E}_i|$ represents $\sqrt{\langle \boldsymbol{E}_i \cdot \boldsymbol{E}_i^* \rangle}$.

The property of the receiving antenna may be represented by the distant electric field intensity $\boldsymbol{E}_t$, which is produced by the antenna when used for transmitting. We define a unit polarization vector $\boldsymbol{m}_t$ for the antenna by

$$\boldsymbol{E}_t = |\boldsymbol{E}_t| \boldsymbol{m}_t = |\boldsymbol{E}_t| (i_\theta m_\theta + i_\Phi m_\Phi), \quad (2)$$

where $m_\theta = b_1 \exp j(\omega t - kr - \beta_1)$ and $m_\Phi = b_2 \exp j(\omega t - kr - \beta_2)$.

Let A_e represent the effective aperture of the antenna. Then $A_e = \lambda^2 G/4\pi$, where G is the power gain of the antenna, and λ is the wavelength. Let P represent the total power flux of the incident wave, and p represent the degree of polarization which is the ratio of the power flux of the polarized part of the incident wave to the total power flux P.

We shall define the Stokes parameters for the partially polarized incident wave $P[s_i]$ and for the receiving antenna $A_e[s_i']$ in the form of a four-vector as follows:

$$P[s_i] = P \begin{bmatrix} s_0 \\ s_1 \\ s_2 \\ s_3 \end{bmatrix} \quad (3)$$

$$A_e[s_i'] = A_e \begin{bmatrix} s_0' \\ s_1' \\ s_2' \\ s_3' \end{bmatrix}, \quad (4)$$

where $s_0 = 1$, $s_1 = |\langle a_1^2 \rangle - \langle a_2^2 \rangle|$, $s_2 = \langle 2a_1 a_2 \cos(\alpha_2 - \alpha_1) \rangle$, $s_3 = \langle 2a_1 a_2 \sin(\alpha_2 - \alpha_1) \rangle$; $s_0' = 1$, $s_1' = b_1^2 - b_2^2$, $s_2' = 2b_1 b_2 \cos(\beta_1 - \beta_2)$, $s_3' = 2b_1 b_2 \sin(\beta_1 - \beta_2)$. The angular brackets $\langle \ldots \rangle$ represent the time averages.

The power available from the antenna due to the partially polarized wave incident upon it may be written in a concise form as

$$W = \tfrac{1}{2} P A_e [\tilde{s}_i'][s_i] = \tfrac{1}{2} P A_e \sum_{i=0}^{3} s_i' s_i, \quad (5)$$

where $[\tilde{s}_i']$ is the transpose of $[s_i]$. Eq. (5) may be written as[5]

$$W = \tfrac{1}{2} A_e P(1 + p \cos \delta)$$
$$= \tfrac{1}{2} A_e P(1 - p) + p A_e P \cos^2(\delta/2), \quad (6)$$

where δ is the angle between the two four vectors on the Poincaré sphere representing the state of polarization of the incident wave and the antenna. The first term of (6) represents the power due to the randomly polarized part of the incident wave, while the second term is due to the polarized part. When $p = 1$, the wave becomes completely polarized, and (5) and (6) reduce to a similar form discussed by Deschamps for elliptically polarized waves.[6]

III. The Density Matrix

Let us represent the incident wave by a 2×2 density matrix

$$P[\rho_{ij}] = P \begin{bmatrix} \rho_{11} & \rho_{12} \\ \rho_{21} & \rho_{22} \end{bmatrix}, \quad (7)$$

where

$$\rho_{11} = \langle n_\theta n_\theta^* \rangle = \langle a_1^2 \rangle,$$
$$\rho_{12} = \langle n_\theta n_\Phi^* \rangle = \langle a_1 a_2 \exp[-j(\alpha_1 - \alpha_2)] \rangle,$$
$$\rho_{21} = \langle n_\theta^* n_\Phi \rangle = \langle a_1 a_2 \exp[j(\alpha_1 - \alpha_2)] \rangle,$$

and

$$\rho_{22} = \langle n_\Phi n_\Phi^* \rangle = \langle a_2^2 \rangle.$$

The density matrix is Hermitian since $\rho_{ij} = \rho_{ji}^*$. The elements of the density matrix are related to the Stokes parameters by the following relations:[4,7]

$$\rho_{11} = \tfrac{1}{2}(s_0 + s_1) \quad \rho_{12} = \tfrac{1}{2}(s_2 + j s_3),$$
$$\rho_{21} = \tfrac{1}{2}(s_2 - j s_3) \quad \text{and} \quad \rho_{22} = \tfrac{1}{2}(s_0 - s_1).$$

We shall define a similar matrix for the antenna

$$A_e[\rho_{ij}'] = A_e \begin{bmatrix} \rho_{11} & \rho_{12} \\ \rho_{21}' & \rho_{22}' \end{bmatrix}, \quad (8)$$

where $\rho_{11}' = b_1^2$, $\rho_{12}' = b_1 b_2 \exp[j(\beta_1 - \beta_2)]$, $\rho_{21}' = b_1 b_2 \exp[-j(\beta_1 - \beta_2)]$ and $\rho_{22}' = b_2^2$.

It can be readily shown that the available power from the antenna due to the partially polarized radio wave may be given by a concise form

$$W = \text{Trace}\{A_e[\rho_{ij}'] \times P[\rho_{ij}]\}. \quad (9)$$

Eqs. (9) and (5) are equivalent since

$$\text{Trace}\{A_e[\rho_{ij}'] \times P[\rho_{ij}]\}$$
$$= A_e P(\rho_{11}'\rho_{11} + \rho_{12}'\rho_{21} + \rho_{21}'\rho_{12} + \rho_{22}'\rho_{22})$$
$$= \tfrac{1}{2} A_e P(s_0' s_0 + s_1' s_1 + s_2' s_2 + s_3' s_3).$$

* Received by the IRE, June 14, 1961. Supported in part by AF Cambridge Res. Labs. under Contract No. AF 19(604)-4079 through the Ohio State Univ. Res. Foundation.

[1] V. C. Yeh, "The received power of a receiving antenna and the criteria for its design," PROC. IRE, vol. 37, pp. 155–158; February, 1949.

[2] H. G. Booker, *et al.*, "Techniques for handling elliptically polarized waves with special reference to antennas," PROC. IRE, vol. 39, pp. 533–552; May, 1951.

[3] G. Stokes, "On the composition and resolution of streams of polarized light from different sources," *Trans. Cambridge Philosophical Soc.*, vol. 9, pt. 3, pp. 399–416; 1856.

[4] M. Born and E. Wolf, "Principles of Optics," Pergamon Press, New York, N. Y.; 1959.

[5] H. C. Ko, "On the Analysis of Radio Astronomical Observations Made with High Resolution Radio Telescope Antennas," Ohio State Univ., Columbus, Ohio, Radio Observatory Rept. No. 21; February, 1961.

[6] G. A. Deschamps, "Geometrical representation of the polarization of a plane electromagnetic wave," PROC. IRE, vol. 39, pp. 540–544; May, 1951.

[7] D. L. Falkoff and J. E. MacDonald, "On the Stokes parameters for polarized radiation," *J. Opt. Soc. Am.*, vol. 41, pp. 851–862; November, 1951.

The Stokes parameters and the density matrix are both used in the quantum mechanical treatment of the polarization of photons and elementary particles.[8,9] The representation of receiving antennas by (4) and (8) fits in very well with the formalism of the quantum theoretical treatment of the polarization of photons. This is to be expected since the receiving antenna may be considered as a polarization analyzer for incident radio photons.

H. C. Ko
Radio Observatory
Dept. Elec. Engrg.
Ohio State University
Columbus, Ohio

[8] U. Fano, "Remarks on the classical and quantum-mechanical treatment of partial polarization," *J. Opt. Soc. Am.*, vol. 39, pp. 859–863; October, 1949.
[9] J. M. Jauch and F. Rohlich, "Theory of Photons and Electrons," Addison Wesley Publishing Co., Inc., Cambridge, Mass.; 1955.

Laurent-Cauchy Transforms*

During the study of the very interesting paper by Ku and Wolf,[1] I looked in detail at (39), $(n+1)\dot{y}_{n+1}(t)+ay_n(t)=0$, and found a very simple general solution. The method can be employed on all equations of the type

$$(n+k+q)(n+k-1+q)\cdots(n+1+q)y_{n+k}^{(k)}$$
$$+a_{k-1}(n+k-1+q)\cdots(n+1+q)y_{n+k-1}^{(k-1)}+\cdots$$
$$+a_1(n+1+q)\dot{y}_{n+1}+a_0y_n=f_n(t),$$

which can be reduced by the substitution $y_n=x_n:\Gamma(1+q+n)$ to the simpler form

$$x_{n+k}^{(k)}+a_{k-1}x_{n+k-1}^{(k-1)}+\cdots+a_1\dot{x}_{n+1}+a_0x_n$$
$$=\Gamma(1+q+n)f_n=g_n(t).$$

I want to demonstrate my method by means of (39). With $y_n=x_n:n!$ the simpler equation

$$\dot{x}_{n+1}+ax_n=0 \tag{1}$$

results. From it, by means of Laplace transformation with $X_n(s)=\int_0^\infty x_n(t)e^{-st}dt$, we get a difference equation for $X_n(s)$

$$sX_{n+1}(s)+aX_n(s)=x_{n+1}(0), \tag{2}$$

whereby initial values $x_{n+1}(0)$ appear which can be chosen in any way. Applying to (2) a Taylor transformation[2] by multiplying with r^n, and summing over all n, we obtain with

$$V(r,s)=\sum_{n=0}^{\infty}X_n(s)\cdot r^n \text{ and } v(r)=\sum_{n=0}^{\infty}x_n(0)\cdot r^n$$

the purely algebraic connection

$$\frac{s}{r}[V(r,s)-X_0(s)]+a\cdot V(r,s)=\frac{1}{r}[v(r)-x_0(0)]$$

from which the generating function

$$V(r,s)=\frac{sX_0(s)-x_0(0)+v(r)}{s\left(1+\frac{a}{s}r\right)} \tag{3}$$

results. In inverse transformation, this equation is to be presented as a power series. Since

$$1:\left(1+\frac{a}{s}r\right)$$

is the sum of the alternating geometric series, we obtain

$$\sum_{n=0}^{\infty}X_n(s)\cdot r^n=\frac{sX_0(s)-x_0(0)}{s}\sum_{n=0}^{\infty}\left(-\frac{a}{s}\right)^n r^n$$
$$+\frac{1}{s}\sum_{n=0}^{\infty}x_n(0)\cdot r^n\cdot\sum_{n=0}^{\infty}\left(-\frac{a}{s}\right)^n r^n.$$

From it, the Laplace transform of the solution

$$X_n(s)=\frac{sX_0(s)-x_0(0)}{s}\left(-\frac{a}{s}\right)^n$$
$$+\frac{1}{s}\sum_{m=0}^{n}x_{n-m}(0)\left(-\frac{a}{s}\right)^m$$

results, or with $sX_0(s)-x_0(0)=L[\dot{x}_0(t)]$

$$X_n(s)=\frac{(-a)^n}{n!}\frac{n!}{s^{n+1}}L[\dot{x}_0(t)]$$
$$+\sum_{m=0}^{n}\frac{(-a)^m}{m!}\frac{m!}{s^{m+1}}x_{n-m}(0). \tag{4}$$

This relation can very simply be transformed back. One obtains the general solution of (1)

$$x_n(t)=\frac{(-a)^n}{n!}\int_0^t\dot{x}_0(\tau)(t-\tau)^n d\tau$$
$$+\sum_{m=0}^{n}\frac{(-at)^m}{m!}x_{n-m}(0). \tag{5}$$

This solution is apparently completely determined when in addition to $x_n(0)$ also $x_0(t)$ or $\dot{x}_0(t)$ are given. If $x_n(0)=1$ and $x_0(t)=e^{-at}$, as Wolf has shown, the solution $x_n(t)=e^{-at}$ results. But any number of other solutions are possible. With $x_n(0)=0$ $(n>0)$, $x_0(0)=1$, $x_0(t)=0$ (unit impulse) one obtains $x_n(t)=(-at)^n:n!$; or with $x_n(0)=(-1)^n$ and $x_0(t)=at+1$

$$x_n(t)=(-1)^n\sum_{m=0}^{n+1}\frac{(at)^m}{m!}.$$

Naturally one can find the solution solely by looking at (39); however, in this case the solution of a differential equation for the generating function

$$W(r,s)=\sum_{n=0}^{\infty}Y_n(s)\cdot r^n$$

has to be found, which is certainly more difficult.

I read with interest Wolf's discussion with Bohn.[3] I am of the opinion that all these sum transformations which relate to the discrete quantities $X_n(s)$ or $x_n(0)$ are not really identical, but completely of equal value. It is only a question of utility as to which of them should be used in a concrete case. In the case at hand, it is apparent that the Taylor transformation is more useful than the Laurent-Cauchy transform or the z transform used by Wolf.

Johann Tschauner
DVL Oberpfaffenhofen
Post Wessling, Obb.
Germany

* Received by the IRE, June 19, 1961.
[1] Y. H. Ku and A. A. Wolf, "Laurent-Cauchy transforms for analysis of linear systems described by differential-difference and sum equations," Proc. IRE, vol. 48, pp. 923–931; May, 1960.
[2] J. Tschauner, "Einführung in die Theorie der Abtastsysteme," Verlag R. Oldenbourg, Munich, Germany, p. 168; 1960.
[3] E. V. Bohn and A. A. Wolf, "The equivalence of the Taylor-Cauchy and Laurent-Cauchy transform analysis with conventional methods," Proc. IRE (Correspondence), vol. 49, pp. 358–361; January, 1961.

Pickard's Regenerative Detector*

Professor G. W. Pickard reported the observation of an oscillating cat's whisker crystal detector in 1920.[1] Pickard's original note is not too well documented. He was obviously unaware of the concept of negative resistance or the tunnel effect at that time. We have observed that a commercial tunnel diode can be substituted directly in Pickard's original circuit resulting in an oscillating detector. Fig. 1 is Pickard's circuit with a tunnel diode in place of the cat's whisker detector. The original circuit called for a 9-v battery. We would expect that Pickard's crystal detector had a fairly high-spreading resistance, high-negative resistance, and a somewhat higher potentiometer resistance. This could account for the higher-bias voltage required. It is also possible that Pickard observed oscillations due to avalanche-injection effects, as well as tunnel effects. We have observed avalanche-injection phenomena in old time cat's whisker detectors using naturally occurring iron-pyrite crystals.

Improved operation of this detector can be achieved by the circuit of Fig. 2. This

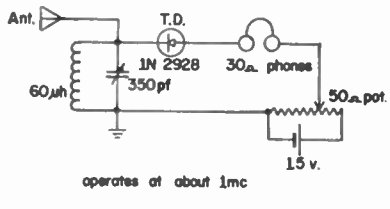

Fig. 1—Pickard's regenerative detector with T.D.

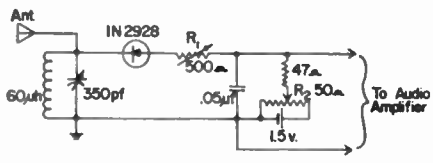

Fig. 2—Improved regenerative detector.

* Received by the IRE, June 12, 1961.
[1] G. W. Pickard, "Oscillating detector," *QST*, vol. 4, pp. 44; March, 1920.

uses somewhat more modern electronic art, and isolates the audio circuit from the RF circuit. The regeneration control R_1 is made independent of the bias-supply potentiometer R_2. This has the approximate effect of varying R_s/R_n in Anderson's diagram.[2] The circuit parameters are chosen from Anderson's criteria with a value of $Qn \geq 1$ at RF frequencies and $Qn \gg 1$ at audio frequencies. Similar regenerative detector circuits have been suggested for tunnel diodes.[3] Detectors of this type have the typical squeals and heterodynes common to other regenerative circuits and have rather poor selectivity because of the single-tuned circuit.

RALPH W. BURHANS
Res. Dept.
The Standard Oil Co.
Cleveland, Ohio

[2] M. E. Hines, "High-frequency negative-resistance circuit principles for Esaki diode applications," *Bell Sys. Tech. J.*, vol. 39, pp. 447–513; May, 1960.
[3] W. F. Chow, *et al.*, "Tunnel Diode Circuit Aspects and Applications," AIEE Conf. Paper No. CP 60-297, N. Y.; January, 1960.

Temperature Effects on GaAs Switching Transistors*

High-frequenty *n-p-n* gallium arsenide mesa-type transistors were fabricated, and the current transfer ratio at temperatures from −100 to 350 degrees Centigrade was measured. It was found that the current transfer ratio increases slightly at high temperatures and up to tenfold at low temperatures.

The transistors were prepared from vertically pulled and from horizontally grown GaAs *n*-type material with an average electron concentration of 3×10^{16}/cm^3 and an electron mobility of 4500 volt^{-1}-sec^{-1} at room temperature. The corresponding values at liquid nitrogen temperatures were 2×10^{16}/cm^3 and 6000 volt^{-1}-sec^{-1}, respectively.

The transistors were prepared by diffusion of manganese into etched *n*-type GaAs wafers. After ohmic contacts were made to the base region, mesas were produced by etching, and a high temperature emitter dot was alloyed into the emitter area. Finally a 0.5 mil nickel wire was used for the emitter connection in order to withstand high temperature operation. Fig. 1 shows a cross section of the finished device prior to mounting.

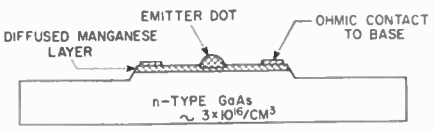

Fig. 1.

* Received by the IRE, June 21, 1961; revised manuscript received June 23, 1961. This work was performed under the sponsorship of the Electronic Tech. Lab., Aeronautical Systems Div., Air Force Systems Command, U. S. Air Force.

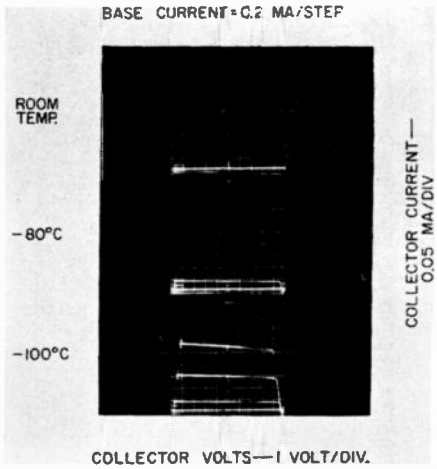

Fig. 2.

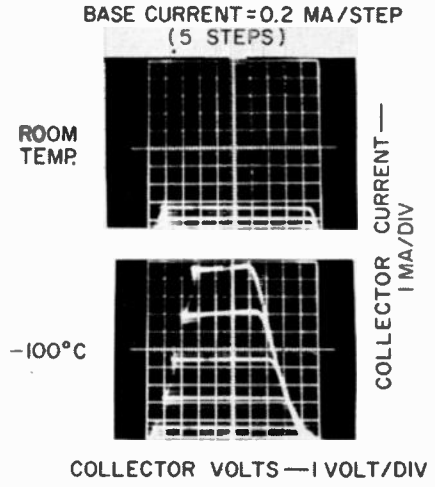

Fig. 3.

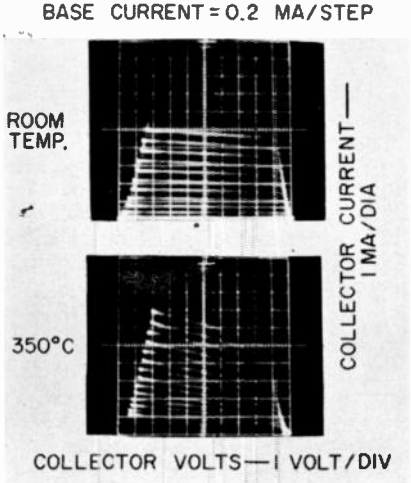

Fig. 4.

These units exhibited typical collector and emitter breakdown voltages of 35 and 5 volts respectively at 100 μa, collector reverse leakage currents less than 1×10^{-8} amperes, and a base series resistance of 45 ohms. Collector-to-base capacitances of 5 $\mu\mu$f were measured, as well as "on" and "off" switching times of 20 nsec each, with no storage time observed.

For low-temperature measurements, the transistor was slowly lowered into a dewar containing liquid nitrogen and the temperature was read directly on an attached low-temperature thermometer. For the high-temperature measurements, a thermocouple wire was connected directly to the transistor header, which was heated to the desired temperature in a furnace.

Fig. 2 shows the common emitter current transfer ratio for low collector currents at three different temperatures as measured on a curve tracer (Tektronix Type 575 or equivalent). The level of base current was chosen so that the curve would start at −80 degrees Centigrade. At higher current levels an increase in the saturation resistance is observed as the temperature is reduced as shown in Fig. 3. One can also observe here a slope indicating a negative-resistance region, commonly found at lower temperatures. The increase in current transfer ratio at the above temperatures was found to be independent of emitter material, etching, and gas ambients.

Fig. 4 shows the characteristic of the first transistor at room temperature and at 350 degrees Centigrade. The leakage current is about one milliampere at 10 volts. These transistors were found to be mechanically stable at temperatures exceeding 400 degrees centigrade, in spite of the fact that the leakage current had increased considerably at these temperatures (10 ma at 10 volts and 400 degrees Centigrade). When the transistors are cooled down from these high temperatures, they return to their original electrical state.

Comparable germanium and silicon switching transistors measured at −60 degrees Centigrade show a substantial decrease in the current transfer ratio from their room temperature value, and especially silicon, as is already well known.

An attempt is under way to explain this increase in the current transfer ratio for GaAs transistors, taking into consideration recombination rates, trapping effects and changes in mobility at low temperatures.

ACKNOWLEDGMENT

The authors would like to express their appreciation to Dr. D. J. Donahue, Dr. J. Hilibrand, and N. Ditrick for their cooperation.

E. D. HAIDEMENAKIS
J. A. MYDOSH
N. ALMELEH
R. BHARAT
E. L. SCHORK
Semiconductor and Materials Div.
RCA
Somerville, N. J.

Comments on "Operation of Radio Altimeters Over Snow-Covered Ground or Ice"*

It is interesting that the findings of our British associates, Piggott and Barclay,[1,2] in the Antarctic agree so thoroughly with the 440-Mc measurements made by the Signal Corps Antarctic Research Team in 1957 and 1958 through the 800-foot-thick seaborne ice at Little America V and in the 500-foot-thick landborne ice, ten miles inland from Wilkes Base, south of Australia.

It is also of interest that altimeter readings of 2000 feet have been obtained at several locations by the Signal Corps over 1200-foot-thick ice in the Arctic when UHF signals were transmitted downwards from a height of only four feet above the surface.

First radio ice-sounding data were released to British, Australian, New Zealand, French, American, and Russian scientists in the International Geophysical Year Symposium in Wellington, New Zealand, in February, 1958, and published in the March and June 1960 issues of *Antarctic*, the quarterly news bulletin of the New Zealand Antarctic Society.[3,4] Unclassified Signal Corps notes on depth measurements were presented to Sir Vivian Fuchs' expedition, together with full verbal altimeter warnings on board the Danish ship *Kista Dan* when it was extricated from heavy ice in Marguerite Bay in January, 1960, by the USS *Glacier*. This information included the findings of five years' research on the thick ice of Greenland and the Antarctic, with additional details of the excavation of deep ice pits that permitted 40–400-Mc horizontal communications studies at distances up to a mile which had originally outlined the limitations of through-ice communication.

A detailed mathematical analysis was first reported to and published by the Ordnance Corps Symposium on Environmental Factors Influencing Optimum Operation of Ordnance Material, September, 1960, at San Antonio, Texas.[5]

A more comprehensive paper, which examines all phases of radio wave propagation through and over thick ice and snow, with special emphasis on the fact that high latitude users of pulsed 440 Mc altimeters can be dangerously misled, was presented at the IRE International Convention on March 20, 1961. This paper is currently being published in the IRE Convention Record and has been submitted for subsequent publication in the Proceedings.[6] It contains 26 references pertinent to the subject of radio wave propagation through ice.

Amory H. Waite, Jr.
Exploratory Research
Division C
USASRDL
Fort Monmouth, N. J.

* Received by the IRE, June 19, 1961.

[1] W. R. Piggott, "The operation of ratio altimeters over snow-covered ground or ice," Proc. IRE, vol. 49 (Correspondence), p. 965; May, 1961.

[2] W. R. Piggott and L. W. Barclay, "The reflection of radio waves from an ice cap," *J. Atmospheric and Terrest. Phys.*, vol. 20, pp. 298–299; April, 1961.

[3] "Antarctic ice depth measured by radio altimeters," an interview with Amory H. Waite, *Antarctic*, a news bulletin of the New Zealand Antarctic Society, vol. 2, no. 5; March, 1960.

[4] "Height over ice, altimeter may mislead," *Antarctic*, news bulletin of the New Zealand Antarctic Society, vol. 2, p. 205; June, 1960.

[5] A. H. Waite, "Ice depth soundings with ultra high frequency radio waves in the Arctic and Antarctic and some observed over-ice altimeter errors," *Proc. Symp. on Environmental Factors Influencing Optimum Operation of Ordnance Material*, San Antonio, Tex., pp. 292–308; March, 1961.

[6] A. H. Waite and S. J. Schmidt, "Gross Errors in Height Indication from pulsed Radio Altimeters Operating Over Thick Ice or Snow," presented at the IRE International Convention, Session on Advances in Navigation and Flight Safety Systems, March 20, 1961. To be published in the Convention Record.

A Simple Calibration Technique for Vibrating Sample and Coil Magnetometers*

The vibrating sample magnetometer is rapidly being accepted as one of the more convenient means for determining the saturation magnetization of a ferromagnetic material.[1] Heretofore, calibration of these instruments has been accomplished by using a "standard sample" such as nickel. The following discussion suggests a very simple technique for calibrating these magnetometers in which the permeability and the magnetization characteristics of the calibrating specimen need not be accurately known.

The equations describing the magnetization of a paramagnetic sphere also describe the magnetization of a homogeneous and isotropic ferromagnetic sphere. The voltage induced in the magnetometer pick-up coils is given in all cases as $E = KVI$, where K is a constant, V is the volume of the spherical sample, and I is the magnetization per unit volume. The magnetization of a magnetic sphere of permeability μ in a uniform magnetizing field H_0 is:[2]

$$I = \frac{3}{4\pi}\left(\frac{\mu - 1}{\mu + 2}\right) H_0.$$

If the permeability of the sphere is constant for the initial region of magnetization then,

$$\frac{dI}{dH_0} = \frac{3}{4\pi}\left(\frac{\mu - 1}{\mu + 2}\right) = \frac{1}{KV}\frac{dE}{dH_0}$$

or

$$KV = \frac{4\pi}{3}\left(\frac{\mu + 2}{\mu - 1}\right)\frac{dE}{dH_0}.$$

* Received by the IRE, June 5, 1961. This work was partially supported by the Dept. of the Navy under a Bureau of Ships contract.

[1] N. V. Frederick, "A vibrating sample magnetometer," IRE Trans. on Instrumentation, vol. I-9, pp. 194–196; September, 1960.

[2] L. Page and N. I. Adams, Jr., "Principles of Electricity," D. Van Nostrand Co., Inc., New York, N. Y., p. 141, 2nd ed.; 1949.

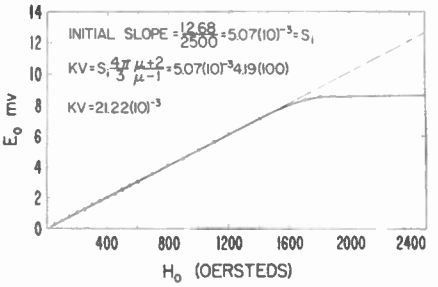

Fig. 1—Magnetometer output vs magnetizing field for a high-permeability sample ($\mu \simeq 3000$).

Hence, the instrument can be calibrated by using the initial slope of the output voltage vs the external magnetizing field, and the initial permeability of the sample. If $\mu > 100$, then

$$\left(\frac{\mu + 2}{\mu - 1}\right) \simeq 1$$

and does not vary rapidly with μ; hence μ need not be known to high accuracy. The equations above also show that the volume of the sphere need not be known and that for any high permeability sample the instruments are self-calibrating. Typical results for the magnetization obtained on the NBS magnetometer using a high-permeability ($\mu = 3000$) ferrite sphere are given in Fig. 1.

N. V. Frederick
National Bureau of Standards
Boulder, Colo.

Frequency Modulation of a Reflex Klystron with Minimum Incidental Amplitude Modulation*

It can be shown that the output power modes of a reflex klystron may be represented as a family of constant power curves as shown in Fig. 1.[1] In order to obtain frequency modulation with low incidental amplitude modulation, the output power of the klystron must remain essentially constant as the reflector voltage is modulated. This may be accomplished by simultaneously modulating the beam and reflector voltages over a linear portion of a selected mode curve.

The linearity of the constant power curves will vary with different reflex klystron-tube types. For a given tube type, the lower-numbered modes will provide the highest output power level; however, the higher-numbered modes will provide the largest bandwidth for low incidental AM.

* Received by the IRE, May 29, 1961.

[1] D. R. Hamilton, J. K. Knipp, and J. B. H. Kuper, "Klystrons and Microwave Triodes," McGraw-Hill Book Company, Inc., p. 360; 1948.

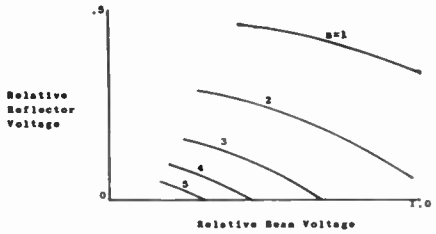

Fig. 1—Plot of beam voltage vs reflector voltage for maximum output power for each mode of a reflex klystron.

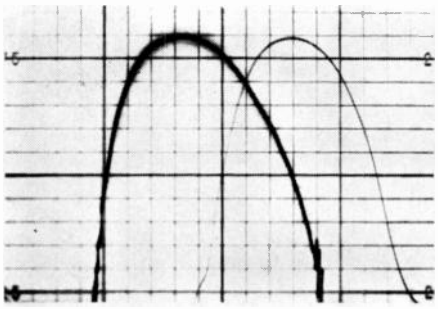

Fig. 2—Mode shape with reflector voltage modulation.

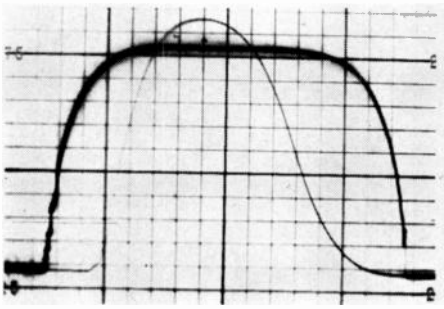

Fig. 3—Mode shape with simultaneous reflector-voltage and beam-voltage modulation.

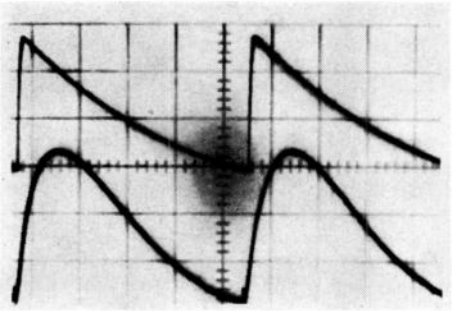

Fig. 4—Modulating voltage waveforms: upper trace—reflector; lower trace—beam.

A Sperry SRU-226, K_u-band, reflex klystron was operated with simultaneous modulation of the beam and reflector voltages. Fig. 2 shows the output power mode shape with reflector voltage modulation only. The half-power bandwidth is 40 megacycles. Simultaneous reflector and beam voltage modulation produced the mode shape shown in Fig. 3. The half-power bandwidth is 70 Mc and the "flat-top" bandwidth is 32 Mc. Fig. 4 shows the modulating voltage waveforms applied to the reflector and beam respectively.

A reflex klystron which can be frequency modulated with minimum incidental AM provides an economical swept frequency source for microwave component testing. Additional applications may be found in communications systems and FM Doppler radars.

WALTER R. DAY, JR.
Sperry Electronic Tube Div.
Gainesville, Fla.

Analog Study of Posicast Control by Relay Systems*

The Posicast control has been developed to improve the operation of a linearly-damped oscillatory system and to remove completely the oscillatory component in the output response to a step input.[1,2] Different techniques have been produced to realize such controls for various situations. The following discussion serves to introduce a method of realization which is convenient for studying the Posicast control on an analog computer.

The block representation of the Posicast control is shown in Fig. 1(a), in which $G(s)$ represents the transfer function of any damped oscillatory system. The preceding block, with the transfer function of $r+(1-r)e^{-t_0 s}$, is able to switch a partial step input $r\theta_i(t)$ to the total step input at the proper time t_0 when the oscillatory output reaches its first maximum. r is the ratio of the steady-state step response of $G(s)$ to the maximum value of the step response, or in Fig. 1(b), $r=\theta_{0s}/\theta_{0m}$. The system output due to a step-input, and its derivative $\theta_0'(t)$ from $t=0$ to $t=t_0$, are shown in solid lines in Fig. 1(b). The fact that $\theta_0'(t_0)=0$ is the basis of operation of the relay circuit to be discussed.

The magnetic field required to make a relay contact close is greater then the field necessary to hold the contact closed. In Fig. 2, E_1+E_2 and E_1 are the make-and-break potentials, respectively, of relay R_1. For automatic switching, the output $\theta_0(t)$ is the command signal for the Posicast control. At time zero, relay R_2 is not energized, and it allows a potential of $-(E_1+E_2)$ to energize relay R_1. Relay contact R_{1a} closes to apply a step input $rU(t)$ from point a of the potentiometer to the system. From $t=0$ to $t=t_0$, the first derivative of the output function is positive. The output from

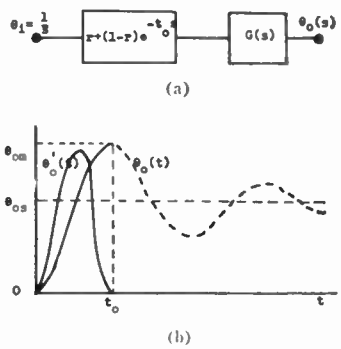

Fig. 1—(a) Block representation of the Posicast control. (b) System output and its derivative.

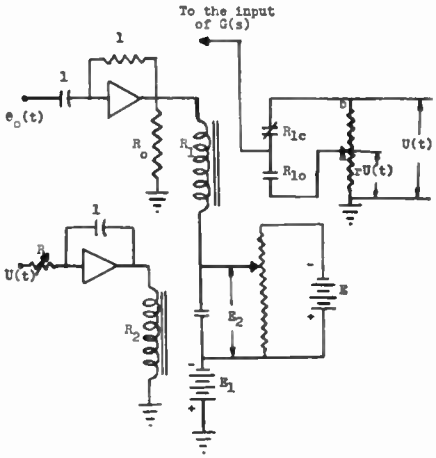

Fig. 2—Relay arrangement for analog study of Posicast control. R_0 is the equivalent output resistance of the amplifier stage associated with computer.

the differentiator of the analog computer $-d\theta_0(t)/dt$ is then additive to $-(E_1+E_2)$. The total voltage across the relay R_1 is

$$-\left(E_1+E_2+\frac{d\theta_0(t)}{dt}\right)$$

with R_2 not energized. Relay R_2 can be energized, as shown in the figure, by a simple integrator operating on the applied step voltage with its gain adjusted such that relay R_2 is energized at any instant between $t=0$ and $t=t_0$. The closing of contact R_{2a} reduces the voltage across relay R_1 to

$$-\left(E_1+\frac{d\theta_0(t)}{dt}\right)$$

which forces the magnetic field of the relay R_1 to follow the variation of $d\theta_0(t)/dt$. At $t=t_0$, the system output reaches the first maximum value and its derivative, which is the negative of the differentiator output, becomes zero automatically, and relay R_1 opens since the remaining voltage E_1 is equal to the break potential of relay R_1. Contact R_{1c} then applies the total step input from point b on the potentiometer at the moment of maximum response, to the system. If the potentiometer, which is connected directly to the input step is preadjusted to meet the requirement on the

* Received by the IRE, May 29, 1961. This letter is a portion of the author's Master thesis at the North Dakota State University, Fargo, N. D.

[1] O. J. M. Smith, "Posicast control of damped oscillatory systems," PROC. IRE, vol. 45, pp. 1249–1255; September, 1957.

[2] H. C. So and G. J. Thaler, "A modified posicast method of control with applications to higher-order systems," *Trans. AIEE*, vol. 79 (Applications and Industry, no. 51), pp. 320–326; November, 1960.

voltage ratio r, the arrangement will perform the Posicast control properly.

The writer is indebted to R. Longhenry of the North Dakota State University, for his helpful advice and encouragement.

CHIAO-YAO SHE
Elec. Engrg. Dept.
North Dakota State University
Fargo, N. D.

Elimination of Ionospheric Refraction Effects*

This communication will describe a method of eliminating ionospheric refraction effects on the frequency of signals received from a mobile radio transmitter at high altitude. It will be particularly useful in locating the vehicle transporting the transmitter, by the direct analysis of the Doppler effect on its radio signals.

The elimination of the ionospheric refraction can be attained by the simultaneous reception of several signals of different frequencies, which will enable us to cancel the refraction part of the received frequencies. Though this is not a novel idea, as can be seen in Guier and Weiffenbach,[1] an attempt will be made to present a general analytical procedure for using this principle in a practical form.

The frequency of the signals received from a mobile radio transmitter is

$$f_r(t,f) = f\left[1 - \frac{\dot{R}(t)}{c}\right] + \frac{\alpha_1(t)}{f} + \frac{\alpha_2(t)}{f^2} + \cdots, \tag{1}$$

where

t = Time.
f = Frequency of the emitted signals.
f_r = Frequency of the received signals.
$\dot{R}(t)$ = Rate of change of distance between the receiving antenna and the transmitter.
$\alpha(t)$ = Time dependent coefficients that characterize the ionospheric properties along the transmission path.
c = Electromagnetic propagation speed in vacuum.

The demonstration of (1) has been outlined by Guier and Weiffenbach.[1] The first term represents the frequency received in absence of refraction (usually referred to as vacuum frequency) and only includes the Doppler shift $f\dot{R}(t)/c$. The following terms represent the frequency shift produced by the ionospheric refraction. These terms form an infinite series in powers of $1/f$, with time dependent coefficients. The number of terms taken in account in this series depends on the accuracy required for the determination of the vacuum frequency. If we need to consider the first $(n-1)$ terms, in order to eliminate them we will require the reception of n simultaneous frequencies.

The frequencies considered here for the transmitter are the first n harmonics of a fundamental frequency f. If $f_{r1}, f_{r2}, f_{r3}, \cdots, f_{rn}$, are the frequencies of the n corresponding received signals, we have from (1)

$$f_{r1}(t,f) = f\left[1 - \frac{\dot{R}(t)}{c}\right] + \frac{\alpha_1(t)}{f} + \frac{\alpha_2(t)}{f^2} + \cdots + \frac{\alpha_{n-1}(t)}{f^{n-1}}, \tag{2a}$$

$$f_{r2}(t,f) = 2f\left[1 - \frac{\dot{R}(t)}{c}\right] + \frac{\alpha_1(t)}{2f} + \frac{\alpha_2(t)}{2^2f^2} + \cdots + \frac{\alpha_{n-1}(t)}{2^{n-1}f^{n-1}}, \tag{2b}$$

$$\cdots\cdots\cdots\cdots\cdots\cdots$$

$$f_{rk}(t,f) = kf\left[1 - \frac{\dot{R}(t)}{c}\right] + \frac{\alpha_1(t)}{kf} + \frac{\alpha_2(t)}{k^2f^2} + \cdots + \frac{\alpha_{n-1}(t)}{k^{n-1}f^{n-1}}, \tag{2c}$$

$$\cdots\cdots\cdots\cdots\cdots\cdots$$

$$f_{rn}(t,f) = nf\left[1 - \frac{\dot{R}(t)}{c}\right] + \frac{\alpha_1(t)}{nf} + \frac{\alpha_2(t)}{n^2f^2} + \cdots + \frac{\alpha_{n-1}(t)}{n^{n-1}f^{n-1}}. \tag{2d}$$

Such a system of equations corresponds to an instant t represented by the parameters $\dot{R}(t)$, $\alpha_1(t)$, $\alpha_2(t)$, $\cdots$, $\alpha_n(t)$. Thus, we will tacitly assume that all the following analysis is valid for a particular instant t of the observation, and the variable t will be omitted from the symbols.

If we multiply (2b) by a factor F_2, (2c) by a factor F_k, and so forth until the nth equation, and add all the resulting equations to (2a), we can eliminate all the terms of the power series provided the following matrix equation holds:

$$\begin{bmatrix} \frac{1}{2} & \frac{1}{3} & \frac{1}{4} & \frac{1}{5} & \cdots & \frac{1}{k} & \cdots & \frac{1}{n} \\ \frac{1}{4} & \frac{1}{9} & \frac{1}{16} & \frac{1}{25} & \cdots & \frac{1}{k^2} & \cdots & \frac{1}{n^2} \\ \frac{1}{8} & \frac{1}{27} & \frac{1}{64} & \frac{1}{125} & \cdots & \frac{1}{k^3} & \cdots & \frac{1}{n^3} \\ \cdots & \cdots & \cdots & \cdots & \cdots & \cdots & \cdots & \cdots \\ \frac{1}{2^{n-1}} & \frac{1}{3^{n-1}} & \frac{1}{4^{n-1}} & \frac{1}{5^{n-1}} & \cdots & \frac{1}{k^{n-1}} & \cdots & \frac{1}{n^{n-1}} \end{bmatrix} \times \begin{bmatrix} F_2 \\ F_3 \\ F_4 \\ \vdots \\ F_k \\ \vdots \\ F_n \end{bmatrix} = \begin{bmatrix} -1 \\ -1 \\ -1 \\ \vdots \\ -1 \\ \vdots \\ -1 \end{bmatrix}. \tag{3}$$

By reducing this matrix equation, we can obtain the general factor F_k.

$$F_k = (-1)^{k-1}\frac{(n-1)!\,k^{n-1}}{(k-1)!(n-k)!} \qquad k = 2, 3, 4, \cdots, n. \tag{4}$$

According to the properties of the factors F_k, we can obtain from (2)

$$f_{r1} + \sum_{k=2}^{n}(F_k f_{rk}) = f\left[1 - \frac{\dot{R}(t)}{c}\right]\left[1 + \sum_{k=2}^{n}(kF_k)\right].$$

Thus, the fundamental vacuum frequency is

$$f_r = \frac{f_{r1} + \sum_{k=2}^{n}(F_k f_{rk})}{1 + \sum_{k=2}^{n}(kF_k)}. \tag{5}$$

It is a frequent practice in the observation of satellites and other vehicles by the Doppler effect to measure the difference frequency obtained from the beating between the received signal and the output signal of a stable oscillator tuned to a frequency near the former.

For the channels $f_{r1}, f_{r2}, f_{r3}, \cdots, f_{rn}$, we will consider n harmonically-related local oscillators of known frequencies ϕ, 2ϕ, 3ϕ, $\cdots$, $n\phi$, respectively. So the difference frequencies resulting from the beating in each channel are:[2]

$$f_{r1}' = f_{r1} - \phi, \tag{6a}$$

$$f_{r2}' = f_{r2} - 2\phi, \tag{6b}$$

$$f_{r3}' = f_{r3} - 3\phi, \tag{6c}$$

$$\cdots\cdots\cdots$$

$$f_{rn}' = f_{rn} - n\phi. \tag{6d}$$

By combining (6) and (5), we obtain

$$f_r = \frac{f_{r1}' + \sum_{k=2}^{n}(F_k f_{rk}')}{1 + \sum_{k=2}^{n}(kF_k)} + \phi. \tag{5a}$$

Table I gives us the values of F_k computed from (4) for $n = 2$, 3 and 4.

TABLE I

	$n=2$	$n=3$	$n=4$
F_2	-2	-8	-24
F_3	—	9	81
F_4	—	—	-64

* Received by the IRE, June 20, 1961.

[1] W. H. Guier and G. C. Weiffenbach, "A satellite Doppler navigation system," PROC. IRE, vol. 48, pp. 507–516; April, 1960.

[2] It will be assumed that ϕ, 2ϕ, 3ϕ, etc. are always smaller than f_{r1}, f_{r2}, f_{r3}, etc., respectively.

By replacing these numerical values in (5a), we can compute the vacuum frequencies for observations made with two, three and four harmonically-related frequencies.

$$f_r = \frac{2f_{r2}' - f_{r1}'}{3} + \phi, \qquad \text{for } n = 2.$$

$$f_r = \frac{9f_{r3}' - 8f_{r2}' + f_{r1}'}{12} + \phi, \quad \text{for } n = 3.$$

$$f_r = \frac{64f_{r4}' - 81f_{r3}' + 24f_{r2}' - f_{r1}'}{60} + \phi, \quad \text{for } n = 4.$$

The procedure for observations with various frequencies, by instance three, is to measure in several instants the difference frequencies f_{r1}', f_{r2}' and f_{r3}', and then to compute for the same instants the fundamental vacuum frequencies f_r [(5a)]. The frequencies f_r, which will depart a little from f_{r1}, are ready to be used in the analysis of the Doppler effect in vacuum.

Lt. José M. Brito-Infante
Escuela de Electronica
Armada de Chile
Viña del Mar, Chile

Antenna-Beam Configurations in Scatter Communications*

In a recent presentation[1] on the possible application, for communications purposes, of incoherent scattering by free electrons in the upper atmosphere,[2] Eshleman and Peterson have pointed out that the preferred antenna-beam shape is narrow in azimuth and relatively wide in elevation. They also expressed some surprise over the failure on the part of tropospheric-scatter systems designers to note and take advantage of this preferred beam configuration.

The purpose of this note is to clarify a distinction between the two types of scattering involved. The distinction arises because of the difference in directivity of the scattering process in the incoherent-electron case and in the tropospheric case. Free electrons having sufficient mean-free-path length scatter with a dipole pattern (nondirective except for a polarization factor). Tropospheric scattering occurs predominantly in the forward direction. An antenna pattern optimized for application to one situation is generally not optimum for the other (even aside from differences arising from choice of frequency, path length, etc.).

The preferred beam configuration advocated for the incoherent-electron case is based on geometrical considerations. Received power is directly proportional to transmitting and receiving antenna apertures and to the volume of ionosphere common to both antenna beams. The size of this volume is inversely proportional to the product of the two antenna-aperture heights (H_1 and H_2) and to the wider of the two widths (say, W_1) so that the received power is

$$P_R \propto \frac{(H_1W_1)(H_2W_2)}{H_1H_2W_1} \propto W_2. \qquad (1)$$

It varies directly with the width of the smaller of the two antennas (which consequently might as well be as large as the other). On the basis of this argument there is little merit in building antennas of extreme height for this application.

Because of the relative nondirectivity of this scattering, each portion of the illuminated volume contributes equally, or nearly so, on the average, to the total received signal. It is in this regard that the tropospheric case is markedly different. Since the scattering coefficient there is strongly dependent on scatter angle, contributions from the portion of the volume having the smallest scatter angle may be many times the contributions from other portions.

A quantitative determination of optimum beamwidth and shape would depend on the detailed model of tropospheric structure chosen to account for the propagation mechanism. Here theoretical opinions differ and experimental evidence is not yet conclusive. Nevertheless, the general nature of the contrast with the incoherent-electron case can be illustrated by starting from one of the simpler scattering models, one whose statistical characteristics are homogeneous and isotropic, and whose scattering pattern is described (approximately) by an inverse power dependence on scatter angle. For practical geometries and modest antenna sizes, the pertinent portion of the troposphere contributing to the received signal is delineated by the scatter-angle dependency; any incremental increase in antenna gain is reflected in a corresponding increase in average received signal, and details of antenna-beam shapes are immaterial. As the antenna beams are narrowed, a point is reached at which the scattering volume is limited by beamwidth. This limit occurs first for azimuthal beamwidth and second for elevation beamwidth. Consequently, in this transition region, optimum beam shapes are the reverse of those in the incoherent-electron case. They call for tall, narrow antennas. With a further narrowing of the beams, the volume is completely delineated by them, and is so restricted that the scattering coefficient is nearly constant; the fractional change in scatter angle within the volume is small. In this extreme case, then, the arguments used for the incoherent-electron case apply to the tropospheric case. Optimum antenna apertures are wide and relatively low, and have fan-shaped beams.

This relationship was at least partly implicit in the work of Booker and de Bettencourt[3] when they showed the received power to be inversely proportional to beamwidth (for the symmetrical narrow-beam case). It was also referred to by Staras[4] in his statement that aperture-to-medium coupling loss was not shared equally among the antenna beams. In addition, a paper of the author's[5] pointed out that there was no aperture-to-medium coupling loss associated with the broader of the two azimuthal beamwidths. [This statement is tantamount to setting received power proportional to width of the (smaller) antenna, as in (1) above.]

The situation is further complicated if the troposphere is considered to be inhomogeneous—for example, if its scattering ability decreases with height. This circumstance restricts the pertinent scattering volume in elevation, so that the transition region referred to two paragraphs above, in which the volume begins to be limited by beamwidth, is confined to narrower elevation angles than otherwise. Consequently, the contrast between this transition region and the extreme narrow-beam case is exaggerated.

If the atmospheric structure is anisotropic (which seems likely), so that scattering within a vertical plane has a different angle dependency from scattering in an oblique plane, then the situation is complicated in yet another manner. If the atmosphere has systematic components to its structure and variations, then other antenna-coupling problems can be visualized that involve more than just optimum aperture size and shape.

It is easy to see how the complications multiply once the scattering becomes angle-dependent. It is this angle dependence that makes the difference, and it has been the intent of this note to point out some consequences of that difference.

Alan T. Waterman, Jr.
Stanford Electronic Labs.
Stanford University
Stanford, Calif.

* Received by the IRE, June 26, 1961.

[1] V. R. Eshleman and A. M. Peterson, "On Radio Communication by Means of Scattering from Density Fluctuations in the Ionospheric and Exospheric Plasma," presented at URSI, Washington, D. C.; May 1–4, 1961.

[2] W. E. Gordon, "Incoherent scattering of radio waves by free electrons with applications to space exploration by radar," Proc. IRE, vol. 46, pp. 1824–1829; November, 1958.

[3] H. G. Booker and J. T. de Bettencourt, "Theory of radio transmission by tropospheric scattering using very narrow beams," Proc. IRE, vol. 43, pp. 281–290; March, 1955.

[4] H. Staras, "Antenna-to-medium coupling loss," IRE Trans. on Antennas and Propagation, vol. AP-5, pp. 228–231; April, 1957.

[5] A. T. Waterman, Jr., "Some generalized scattering relationships in transhorizon propagation," Proc. IRE, vol. 46, pp. 1842–1848; November, 1958.

An Extended Definition of Linearity*

There are not many notions in mathematics, science and engineering that are as basic and as well-established as that of linearity. Nevertheless, the definitions of

* Received by the IRE, June 23, 1961. This work was supported in part by the National Science Foundation.

of linearity which are commonly in use suffer from a serious limitation—they are predicated on the assumption that the system is initially at rest. The purpose of this note is to suggest a more general definition which does not have this limitation, and to sketch some of its implications.

Notation and preliminary definitions: The symbol $u(t)$ will stand for the value of a time-function u at time t. The symbol $u_{t_0\leq t\leq t_1}$ will stand for the segment of u lying between, and including, the points t_0 and t_1.

Definition 1: We shall say that a system (black box) B with input u and output y is *completely characterized* if there exists a function F and a variable $\mathbf{s}(t_0)$ such that for all t_0, t_1 and $u_{t_0\leq t\leq t_1}$, $y(t_1)$ is expressible as a function of $\mathbf{s}(t_0)$, $u_{t_0\leq t\leq t_1}$, t_0 and t_1, *i.e.*,

$$y(t_1) = F[\mathbf{s}(t_0); u_{t_0\leq t\leq t_1}; t_0, t_1]. \quad (1)$$

Furthermore, this relation should yield all possible outputs which B is capable of producing in response to $u_{t_0\leq t\leq t_1}$ when $\mathbf{s}(t_0)$ runs through all of its possible values. The variable $\mathbf{s}(t)$ is called the *state* of B at time t, with the range of $\mathbf{s}(t)$ being the *state space* of B. Roughly, $\mathbf{s}(t)$ constitutes a description of the internal conditions in B at time t. Generally, $\mathbf{s}(t)$ can be represented as a vector in a finite—or infinite—dimensional space. A particular state, that is, a value of $\mathbf{s}(t)$, will be denoted by $\boldsymbol{q}$. The output time-function (over the interval $[t_0, t_1]$) resulting from the application to B of an input $u_{t_0\leq t\leq t_1}$, with B initially in state $\mathbf{s}(t_0)$, $\mathbf{s}(t_0)=\boldsymbol{q}$, will be denoted by $B[\mathbf{s}(t_0); u_{t_0\leq t\leq t_1}]$ or, more simply $B(\boldsymbol{q}; u_{t_0\leq t\leq t_1})$ or, still more simply, $B(\boldsymbol{q}; u)$.

Definition 2: Suppose that B is initially (at time t_0) in state $\boldsymbol{q}$ and a zero input, $u(t)=0$, $t_0\leq t\leq t_1$, is applied. Let $\mathbf{s}(t_1)$ denote the state of B at t_1. Now, as $t_1\rightarrow\infty$, $\mathbf{s}(t_1)$ may or may not converge to a fixed state in the state space of B. If $\mathbf{s}(t_1)$ does converge to a fixed state $\mathbf{s}(\infty)$, and if $\mathbf{s}(\infty)$ is independent of the initial state $\boldsymbol{q}$, then $\mathbf{s}(\infty)$ will be called the *ground state* of B and will be denoted by O.

Definition 3: B will be said to be *linear with respect to initial state* $\boldsymbol{q}$ if and only if for all pairs of input time-functions u and v, all values of t_0 and t_1 and all real constants k the following relation holds:

$$k[B(\boldsymbol{q}; u_{t_0\leq t\leq t_1}) - B(\boldsymbol{q}; v_{t_0\leq t\leq t_1})] = B[O; k(u_{t_0\leq t\leq t_1} - v_{t_0\leq t\leq t_1})]. \quad (2)$$

That is, k times the difference of the responses of B to u and v, with B initially in state $\boldsymbol{q}$, is identical with the response of B to $k(u-v)$, with B initially in the ground state.

We are now ready to formulate an extended definition of linearity which, unlike the conventional definition, takes into account the initial state of the system.

Definition 4: B is *linear* if and only if it is linear with respect to all possible initial states, that is, if the relation

$$k[B(\boldsymbol{q}; u_{t_0\leq t\leq t_1}) - B(\boldsymbol{q}; v_{t_0\leq t\leq t_1}) = B[O; k(u_{t_0\leq t\leq t_1} - v_{t_0\leq t\leq t_1})] \quad (3)$$

holds for all t_0, t_1, $u_{t_0\leq t\leq t_1}$, $v_{t_0\leq t\leq t_1}$, k, and all $\boldsymbol{q}$ in the state space of B.

Comments: The conventional definition of linearity is formulated in terms of additivity and homogeneity, which in turn are defined for systems which are initially in the ground state. On setting $\boldsymbol{q}=O$, $v=0$ in (3), we obtain $kB(O; u)=B(O; ku)$, which implies that B is homogeneous. On setting $\boldsymbol{q}=O$, $k=1$, $w=-v$, we have $B(O; u)+B(O; w)=B(O; u+w)$, which implies that B is additive. Thus, a system which is linear in the general sense defined above is linear also in the conventional sense. However, the converse is not true for all systems, as is demonstrated by the network shown in Fig. 1.[1] The system in question comprises a capacitor, resistors and ideal diodes, and is in its ground state when C has zero charge. If the system is initially in ground state, then, by inspection, it behaves like a unit resistor and hence is linear in the conventional sense. On the other hand, if C is initially charged, then the system will behave like a nonlinear system.

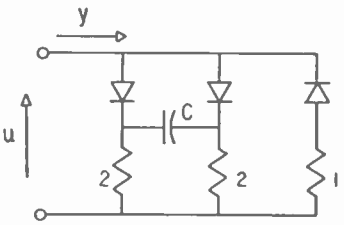

Fig. 1—An example of a nonlinear network which is ground-state linear.

A link between the conventional definition of linearity (which is, essentially, linearity with respect to the ground state) and the more general definition given here is provided by the following theorem: *If B is linear with respect to the ground state then it is also linear with respect to all states which are reachable[2] from the ground state.*

Proof: By hypothesis,

$$k[B(O; u) - B(O; v)] = B[O; k(u - v)] \quad (4)$$

for all k, u, v. We wish to prove that if $\boldsymbol{q}$ is reachable from O, then

$$k[B(\boldsymbol{q}; u) - B(\boldsymbol{q}; v)] = B[O; k(u - v)] \quad (5)$$

for all k, u, v.

Let $w_{0\leq t\leq t_0}$ be an input which takes the system from O (at $t=0$) to $\boldsymbol{q}$ (at $t=t_0$). Let r be a time-function which coincides with w over the interval $[0, t_0]$ and with u over the interval $(t_0, t_1]$. Similarly, let $r''=w$ for t in $[0, t_0]$ and $r''=v$ for t in $(t_0, t_1]$. Then,

$$B(O; r') = B(O; w_{0\leq t\leq t_0}) + B(\boldsymbol{q}; u_{t_0<t\leq t_1}) \quad (6)$$

$$B(O; r'') = B(O; w_{0\leq t\leq t_1}) + B(\boldsymbol{q}; v_{t_0<t\leq t_1}). \quad (7)$$

On substracting (7) from (6), we have

$$B(\boldsymbol{q}; u) - B(\boldsymbol{q}; v) = B(O; r') - B(O; r'') \quad (8)$$

and since by (4)

$$B(O; r') - B(O; r'') = B(O; r' - r'') = B(O; u - v) \quad (9)$$

we can write

$$k[B(\boldsymbol{q}; u) - B(\boldsymbol{q}; v)] = kB(O; u - v) = B(O; k(u - v)) \quad (10)$$

which is what we set out to prove.

It follows from this theorem that if all the states of a system are reachable from the ground state, then the conventional and the general definitions of linearity become equivalent. Thus, the conventional definition of linearity is adequate for all systems which have this property (*i.e.*, reachability of all states in the state space from the ground state) but not for those systems which contain states which are not reachable from the ground state.

It is also of interest to note that by setting $v=0$ and $k=1$ in (3), we obtain the relation

$$B(\boldsymbol{q}; u_{t_0\leq t\leq t_1}) = B(\boldsymbol{q}; 0) + B(O; u_{t_0\leq t\leq t_1}), \quad (11)$$

which means that the response of B to $u_{t_0\leq t\leq t_1}$ with B initially in state $\boldsymbol{q}$, is the sum of the response of B to zero input, with B initially in state $\boldsymbol{q}$, plus the response of B to $u_{t_0\leq t\leq t_1}$, with B initially in the ground state. Thus, with the general definition of linearity as the starting point, the basic relation (11) becomes one of its immediate consequences.

As a final remark, we note that the approach used in this note can be applied to the notion of time-invariance. The basic fact—well known in the theory of sequential machines—is that if $\boldsymbol{q}_1$ and $\boldsymbol{q}_2$ are two equivalent states (in the sense that, for any input, the response starting in $\boldsymbol{q}_1$ is the same as the response starting in $\boldsymbol{q}_2$) then any two states which are reachable from $\boldsymbol{q}_1$ and $\boldsymbol{q}_2$ by the same input are also equivalent. Thus, the time-varying network shown in Fig. 2 is a constant-resistance network if $L(t)\equiv C(t)$.

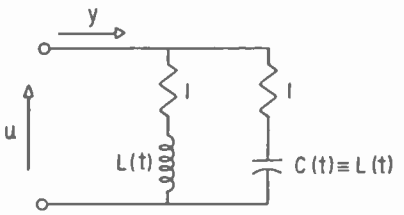

Fig. 2—An example of a time-varying network which is ground-state time-invariant.

In effect, the network in question is ground-state-equivalent to a unit resistor, and it behaves like a unit resistor for any initial state [*i.e.*, current in $L(t)$ and voltage across $C(t)$] which is reachable from the ground state. For other initial states it does not behave like a unit resistor.

L. A. Zadeh
Dept. of Elec. Engrg.
Univ. of Calif.
Berkeley, Calif.

[1] This counterexample was suggested by Donald Cargille, a student at the University of California.

[2] A state $\boldsymbol{q}'$ is reachable from $\boldsymbol{q}$ if there exists an input u which takes the system from $\boldsymbol{q}$ to $\boldsymbol{q}'$.

Thickness-Shear Mode Quartz Cut with Small Second- and Third-Order Temperature Coefficients of Frequency (RT-Cut)*

The theory of plane waves in anisotropic media was first given by Green[1] and later by Christoffel,[2] stating that for any direction of propagation, there are in general three plane waves, each with a different velocity, the three directions of vibrations being mutually perpendicular. Accordingly, three different types of thickness vibrations exist in crystal plates; one extensional mode and two shear modes and their overtones. The resonance frequencies of thickness modes of an infinite crystal plate can be solved in closed form, while correspondingly simple solutions for the thickness modes are not obtainable for a bounded plate. The equations for thickness-shear and flexural modes of finite crystal plates are solved in a series of papers by Mindlin.[3]

Curves for the three Christoffel moduli c_m, their temperature coefficients first order, $Tc_m^{(1)}$, and the effective piezoelectric constants e_m for quartz as a function of the polar angle θ in the range $\theta=0°$ to 180°, for the azimuth $\Phi=0°$, 10°, 20°, 30°, were first calculated in 1935.[4] These curves are reproduced in Cady's "Piezoelectricity."[5] In another paper,[6] the values for the frequency constants N_m, and the temperature coefficients of frequency first order $Tf_m^{(1)}$, at the same intervals, are given. The notation used for these three modes is such that the frequency constants $N_i=f_i\cdot t$ $(i=1, 2, 3)$, where f_i is the frequency of one of the three fundamental modes and t the thickness of the plate, follow the order of magnitude $N_A>N_B>N_C$, where A designates the extensional mode and B and C the two shear modes. These values have been recalculated in steps of 6° for the angle Φ using the values for the elastic and piezoelectric constants recently given by the author.[7] The temperature coefficients first order of the elastic moduli for quartz, originally determined by Bechmann[8] and Mason,[9] further the temperature coefficients of the elastic moduli second and third order, are being computed. The IRE rotational symbol[10] is now used to define the orientation of a crystal plate, for quartz plates with trigonal symmetry the azimuth angle Φ is used in the range 0° to 30° and the polar angle θ in the range 0° to ±90°. As orientations for the C mode exist in the full range of Φ and for the B mode in part of the range on the negative side of the angle θ, where a change of sign for the first-order temperature coefficient of frequency occurs, cuts in the vicinity of these orientations, particularly at negative θ angles, have been selected for this investigation serving a two-fold purpose: 1) the determination of the higher order temperature coefficients of the elastic moduli related to the coordinate axes, and 2) the investigation of quartz cuts whose frequency-temperature coefficients are smaller than those of the AT-cut. The temperature dependence of these cuts has been measured in the range −196°C to +170°C and developed in a power series up to the third order. The frequency-temperature coefficients a, b, and c of the first, second, and third order, respectively, have been determined for both shear modes B and C of these cuts.

Temperature Coefficients at 25°C

$$a=0 \qquad \frac{\partial a}{\partial\theta}=1.7\cdot10^{-6}/°C$$

$$b=-6.5\cdot10^{-9}/(°C)^2 \qquad \frac{\partial a}{\partial\Phi}=1.7\cdot10^{-6}/°C$$

$$c=-2\cdot10^{-12}/(°C)^3 \qquad \frac{\partial b}{\partial\theta}\approx0\cdot10^{-9}/(°C)^2$$

$$\frac{\partial T_m}{\partial\theta}\cong110°C$$

where T_m is the temperature maximum of the parabola.

In Fig. 1, a comparison is made of the following cuts: 1) AT-cut C mode $(y\times l)$ 35°15′,[11] inflection temperature 25°C; 2) AT-cut with a so-called optimum orientation dependent on the temperature range used, e.g., $(y\times l)$ 35°21′; 3) BT-cut with values shown in Bechmann,[11] B mode, $(y\times l)$ −49°12′; 4) RT-cut, C mode, $(y\times wl)$ 15°, −34°30′. In double-rotated plates, all three modes are usually excitable. The separation between the B and C modes of the RT-cut is about 7 per cent. By use of a circuit, the B mode can be sufficiently suppressed.

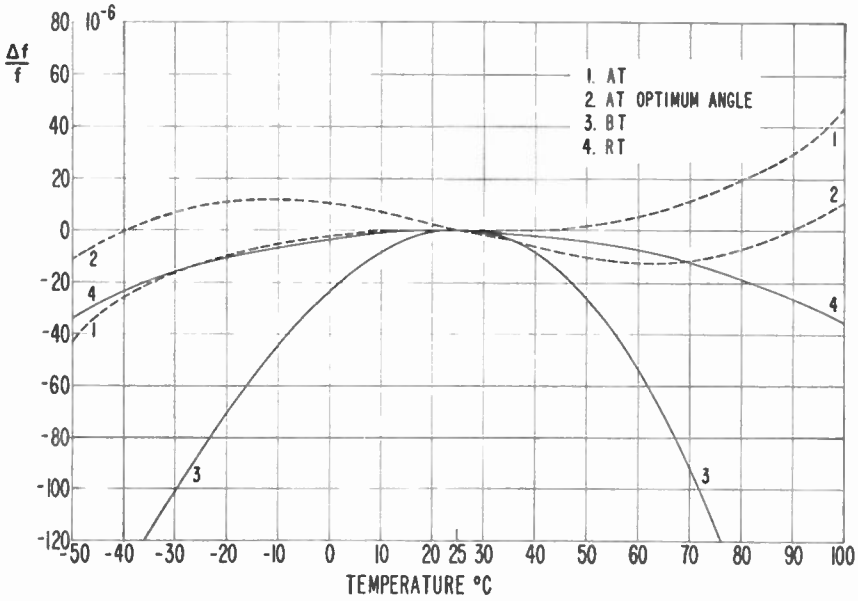

Fig. 1.

In the vicinity of $\Phi=15°$, the second-order temperature coefficient reaches a minimum for the C mode. In particular, a cut designated as the RT-cut, has a small second- and third-order temperature coefficient of frequency and may be used for frequency control purposes. The data for this cut are:

Orientation

$\Phi=15°$, $\theta=-34°30'$

Frequency Constant

$N=2040$ kc·mm

C Mode

Considering the B mode, the second-order temperature coefficient, b, is rather large, being in the order of $-40\cdot10^{-9}/(°C)^2$ for all angles which have a zero temperature coefficient of frequency first order. The third-order temperature coefficient, c, is also large so that the B mode has no practical advantage.

Results regarding the properties of double-rotated quartz crystals will be discussed at a later date.

R. Bechmann
U. S. Army Signal Res. and Dev. Lab.
Fort Monmouth, N. J.

* Received by the IRE, June 23, 1961.

[1] G. Green, *Trans. Cambridge Phil. Soc.*, vol. 7; 1839.

[2] E. B. Christoffel, "Ueber die Fortpflanzung von Stössen durch elastische feste Körper," *Ann. di Matematica Milano (II)*, vol. 8, pp. 193–243, 1877.

[3] R. D. Mindlin, "Thickness-shear and flexural vibrations of crystal plates," *J. Appl. Phys.*, vol. 22, pp. 316–323; March, 1951.

[4] R. Bechmann, "Untersuchungen über die elastischen Eigenschwingungen piezoelektrisch angeregter Quarzplatten," *Z. tech. Physik*, vol. 16, pp. 525–528; December, 1935.

[5] W. G. Cady, "Piezoelectricity," McGraw-Hill Book Co., Inc., New York, N. Y., pp. 144–145; 1946.

[6] R. Bechmann, "Quarzoszillatoren," *Telefunken Ztg.*, vol. 16, pp. 36–47; March, 1936.

[7] R. Bechmann, "Elastic and piezoelectric constants of alpha-quartz," *Phys. Rev.*, vol. 110, pp. 1060–1061; June, 1958.

[8] R. Bechmann, "Über die Temperatur-Koeffizienten der Eigenschwingungen Piezo-Elektrischer Quarz platten und Stäbe," *Hochfrequenztech. u. Elektakust* vol. 44, pp. 145–160; 1934.

[9] W. P. Mason, "Piezoelectric Crystals and Their Application to Ultrasonics," D. Van Nostrand Co., Inc., New York, N. Y., p. 103; 1950.

[10] "Standards on Piezoelectric Crystals, 1949," PROC. IRE, vol. 37, pp. 1378–1395; December, 1949.

[11] R. Bechmann, "Frequency-temperature-angle characteristics of AT- and BT-type quartz oscillators in an extended temperature range," PROC. IRE (Correspondence), vol. 48, p. 1494; August, 1960.

Restrictions in Synthesis of a Network with Majority Elements*

Recently, significant progress has been made in the new field of majority logic. Synthesis of a general network with more than a single majority element is a challenging problem [1] though difficult if optimization is aimed for. It may be interesting and important to consider requirements of a network in making a theoretical model from a viewpoint of engineering feasibility and to accordingly classify the synthesis problem. Though some requirements were mentioned in the author's paper [3], these are discussed more explicitly here.

1) The sum of input weights $\Sigma\omega_i$ which can be coupled to a single element is limited in order to give sufficient threshold discrimination. Parametron circuitry with $\Sigma\omega_i = 3$ has been very extensively investigated by many workers in Japan [4]–[6], including some work on the median ternary operation. Parametrons with $\Sigma\omega_i = 5$ have also been used in some computers and it seems feasible to construct parametrons with a greater $\Sigma\omega_i$.

2) The number of elements in the next stage which can be coupled from the output of a single element is limited. Otherwise, input control of the element may be disturbed by signals coupled backward from elements in the later stages which is called "back coupling" [7].

3) In some type of circuitry, interconnection among elements is restricted. In a circuit where all elements are phase-clocked, such as parametron circuitry, the output of an element can be coupled only to elements which are clocked by a pulse with the next time phase (see the details in the author's paper [3]).

4) Whether input variables are available at elements of any stage or only at first stage elements is an important starting point for the synthesis. If we are concerned about parallel transmission of information as in a parallel-type computer, we may generally encounter the case where the input variables are available only at the first-stage elements. When the repetition rate of input variables is considerably slower than switching time of elements (even though elements are phase-clocked or not), the input variables can be provided at elements through a range of stages, although there is still limitation on the depth of this range. Therefore, there are at least two essentially different types of synthesis problems.

In a criterion for goodness of a synthesized network, the number of required elements in terms of over-all cost and the number of required stages in terms of speed may have primary importance unless other conditions are considered.

Restriction 4 may be more important than it seems. While designing computers and telephone exchanges with parametrons in Japan, we learned that fewer elements are generally required if input variables are allowed to be available at elements at any stages.

Minnick [2] devised an ingenious algorithm for synthesizing a network with linear programming (independently of Muroga, *et al.*'s linear programming approach to structure determination of a single majority element [8]). However, it is important to note the difference in the input requirements between Minnick's result and the author's [3]. The author provides input variables only for the first stage elements; Minnick assumes input variables available to elements of other stages, too. If his network is applied to the case where input variables are available only for first stage elements, the delay elements are necessary and the total number of required elements will exceed that of the author's network. In this sense, Minnick's comparison of the two cases [2] is improper.

Sasaki[1] observed a further simplification in the case of a modulo two adder when a zero input of weight one is coupled to each element in the first stage and a one input of weight one is coupled to the second stage element with half of the number of inputs to each of the first stage elements being complemented. (This is the case of an even number of variables. In the case of an odd number of variables, the above zero input should be replaced by the additional variable, and the one input by negation of the additional variable. This requires an additional element in the first stage for delay.)

Possibly, synthesis of a majority element for a given Boolean function, if it is realizable with a single element, is simpler than that of a general network with more than one element. Such an algorithm is known [9], particularly by using linear programming [2], [8]. Though Paull and McCluskey [10], Winder [9], and Muroga, *et al.* [8] independently obtained a necessary condition for realizability by a single majority element, counter examples of Moore [10] and Winder [9] showed that it cannot be a sufficient condition. The second stagement of Muroga, *et al.*'s [8] necessary condition rejected Moore's counter example [12], but later Winder [11] showed that this condition also cannot be sufficient. A necessary and sufficient condition in a language of input values was first obtained by Elgot [12] and Chow [13], independently, Elgot [12] showed its interesting relation to the above stated necessary conditions. Later the author stated its realizability condition in majority function form [11].

Acknowledgment

The author wishes to thank C. C. Elgot and H. Fleisher for their illuminating comments.

Saburo Muroga
IBM Research Center
Yorktown Heights, N. Y.

* Received by the IRE, June 23, 1961.

[1] Communicated through E. Goto.

References

[1] See references in R. O. Winder, "Some recent papers in threshold logic," Proc. IRE (Correspondence), vol. 49, p. 1100; June, 1961. The author would like to add to his note the fact that our work on majority logic was motivated by the parametrons, being independent of activities in other places.
[2] R. C. Minnick, "Linear-input logic," IRE Trans. on Electronic Computers, vol. EC-10, pp. 6–16; March, 1961. Portions of this paper were delivered at the 6th Annual Symp. on Computers and Data Processing of the Denver Res. Inst., Denver, Colo.; July, 1959.
[3] S. Muroga, "Logical Elements on Majority Decision Principle and Complexity of their Circuits," presented at the Internatl. Conf. on Information Processing, Paris, France, UNESCO NS/ICIP/G. 2. 10; June, 1959.
[4] H. Tahahashi and Z. Kiyasu, Eds., "Parametron," Parametron Institute, Tokyo, Japan; 1960.
[5] "Parametron and Its Application," Institute of Electrical Communication Engineers of Japan, Tokyo, Japan, 1960. (In Japanese.)
[6] "Studies on Parametron I," Parametron Institute, Tokyo, Japan; 1959. (In Japanese.)
[7] S. Muroga and K. Takashima, "The parametron," digital computer MUSASINO-1," IRE Trans. on Electronic Computers, vol. EC-8, pp. 308–316; September, 1959. See especially p. 311.
[8] S. Muroga, I. Toda and S. Takasu, "Theory of majority decision elements," *J. Franklin Inst.*, vol. 271, pp. 376–418; May, 1961.
[9] R. O. Winder, "Single-Stage Threshold Logic," AIEE, Conf. Paper No. 60-1261; October, 1960.
[10] M. C. Paull and E. J. McCluskey, Jr., "Boolean functions realizable with single threshold devices," Proc. IRE, vol. 48, pp. 1335–1337; July, 1960.
[11] To be delivered at General Fall Meeting of AIEE, Detroit, Mich.; October, 1961.
[12] C. C. Elgot, "Truth Functions Realizable by Single Threshold Organs," AIEE, Conf. Paper No. 60-1311; October, 1960.
[13] C. K. Chow, "Boolean functions realizable with single threshold device," Proc. IRE, vol. 49, pp. 370–371; January, 1961.

Satellite Supported Communication at 21 Megacycles*

Kraus and others[1] have reported WWV signal enhancements occurring at times related to the orbits of artificial earth satellites. He looked ahead to the time when satellites would be sufficiently numerous to permit long-distance communication by means of this enhancement phenomenon.

After a year of preliminary observations using WWV, the author organized a group of advanced radio amateurs to test Kraus' prediction. Tests began in November, 1959, between New York, N. Y., and Bethesda, Md., with each station transmitting for 20-second tandem periods from ten minutes before each scheduled near-satellite approach to ten minutes after. K2QBW, New York, and K3JTE each used 300 watts CW on a frequency of 21.011 Mc, with a receiver pass band of 500 cycles, and center-fed nonrotatable long-wire antennas. In addition,

* Received by the IRE, June 26, 1961.

[1] J. D. Kraus, R. C. Higgy, and W. R. Crone, "The satellite ionization phenomenon," Proc. IRE, vol. 48, pp. 672–678; April, 1960.
J. D. Kraus, "Evidence of satellite-induced ionization effects between hemispheres," Proc. IRE, (Correspondence) vol. 48, p. 1913; November, 1961.
J. D. Kraus and R. C. Higgy, "The relation of the satellite ionization phenomenon to the radiation belts," Proc. IRE (Correspondence), vol. 48, p. 2027; December, 1960.

TABLE 1
SUPERIMPOSED OCCURRENCE CHARTS OF BOTH PRIMARY STATIONS

Object	Height Statute Miles	Burst Occurrence			Magnetic A Index		University of Colorado Solar Flare Index
		Early	Center	Late	(1)	(2)	
58042	230	0	1	0	-	9	140
59012	350	0	0	0	-	9	140
58042	460	0	1	0	4	5	80
58042	460	0	3	1	14	15	0
58042	460	0	1	0	10	10	0
58042	140	0	0	1	3	4	120
59091	430	0	1	0	3	4	120
59091	420	0	0	0	3	4	400
59012	500	0	0	1	3	4	400
58042	140	0	2	2	3	4	400
59091	410	0	2	0	6	7	200
58042	140	0	3	0	6	7	200
*58042	140	0	1	0	11	11	1600
*59012	410						
59091	380	0	3	0	12	15	1000
58042	140	0	2	0	12	15	1000
*58042	130	0	3	0	18	20	140
*59091	370						
59091	370	0	0	0	6	6	100
58042	130	0	0	0	6	6	100
59091	670	1	2	0	5	5	400
59091	660	0	0	0	8	9	1000
59091	660	0	0	0	16	16	1100
59091	650	0	0	0	16	18	5500
59091	650	0	0	0	158	158	260
59011	490	0	0	0	158	158	260
59011	570	0	4	1	30	30	1100
Aggregate Observed Bursts: Each Period		1	29	6			
Aggregate Actual Listening Time: Each Period in Minutes		165	156	165			

* Overlapping center periods. See text.
(1) Fort Belvoir Magnetic A Index.
(2) University of Colorado Preliminary A Index.
The solar flare index cited above is an index of integrated flare energy from the sun's visible disk per unit of observing time. An index of zero indicates that the sun was visible, but that no flares were observed.

monitors were listening from Chevy Chase, Md. (W3EQB/EQD), and Sackets Harbor, N. Y. (K2QHR). A three-letter code, based on received signal strength, was employed as the information to be exchanged.

Tests were conducted at times when the ionosphere would not support normal communication over the path in question, so no background levels were audible. Table I shows the occurrence frequency of received signal bursts at both stations in terms of the following class intervals. The time of nearest approach plus/minus three minutes is called the center period. This normally lasted six minutes, except when two suitable near approaches occurred within six minutes of each other. In these cases the center period was extended to three minutes beyond the *second* near approach time. The early and late periods, each normally lasting seven minutes, bracket the center period. In addition to the test-by-test results, the aggregate number of received bursts observed in each of the three periods and the actual aggregate listening time spent in each period are also shown.

In our analysis of these results, let us assume that the received signals did *not* result from a satellite pass relation. We would then expect each of the 36 received bursts to be positioned in a purely random distribution along the time axis. Making use of the Monte Carlo method, we position each burst according to a table of random digits, then apply the familiar chi-square test to the hypothesis that this random distribution fits. Repeating this procedure five times, we obtain successive chi-square values of 38.14, 32.08, 27.18, 46.88, and 61.50. If one repeats the random positioning many times, and sums the resulting distributions, it would be found that the limit of the sum is a distribution in which the expected frequency for each interval is proportional to the length of the interval. Comparing the expected with the observed values for this limiting case yields a chi-square of 39.94, sufficient to *reject* our hypothesis at the 99.99999979th percentile of the chi-square distribution. This corresponds to nearly absolute certainty that our hypothesis is wrong, and that the burst distribution obtained experimentally was indeed a function of $(t-t_0)$, where t_0 is the time of nearest satellite approach. This result is by no means an exclusive property of the three-interval scheme of presentation employed in Table I. The author has similarly employed a wide variety of other class-interval breakdowns, all yielding rejections of our now defunct random hypothesis at comparably high levels of significance. Our results tell us nothing about the nature of the time-difference function, nor about the physical mechanism which produces it. In view of the physical situation, however, it is difficult to comprehend how this function can result except by some form of satellite causation.

As an additional experimental check, ten tests were conducted at times when no satellites were expected. Those falling during known meteor showers—none of the satellite-pass tests did—produced numerous bursts throughout the test period; those falling during times of known sporadic-E ionization produced steady signals; and those falling into neither category produced no received signals at all. Some of these were "blind tests," conducted in the belief that a satellite was in proximity.

The typical satellite-pass burst appeared a bit weaker than its meteor-shower counterpart; both were of the order of one microvolt in strength, suggesting the possibility of an ionization phenomenon. Also, it was apparent from the sound of the received bursts that they were incoherent; rather, they returned as smears. This would tend to support this possibility. On the other hand, the activity data in Table I are inconclusive, and it is apparent that more work needs to be done before we can consider the problem of causation mechanisms solved.

Physics notwithstanding, the experiments achieved success in their basic objective—the establishment of two-way communication. During the early morning of February 6, 1960, the author's signal was received in Bethesda, acknowledging successful receipt of the Maryland transmission one minute earlier. This completed the two-way contact, during the ten-minute center period formed by the overlapping near approaches of Explorer VII and Sputnik III. Under the auspices of the Office for Satellite Scatter Coordination, many radio amateurs are working today to improve communication range and effectiveness possible with these techniques, and to learn more about the physical mechanism involved.

ACKNOWLEDGMENT

The author is indebted to J. D. Kraus of The Ohio State University and M. Balser of Lincoln Laboratory for their constructive reviews and suggestions, and to P. I. Klein of the University of Pennsylvania for his assistance during the experimental phase of the project.

RAPHAEL SOIFER
Mass. Inst. Tech.
Cambridge, Mass.

Contributors

Aaron A. Galvin (S'53–M'56) was born in New York, N. Y., on April 13, 1932. He received the B.S. and M.S. degrees in electrical engineering from the Massachusetts Institute of Technology, Cambridge, Mass., in 1955. While attending M.I.T., he was employed at the Bell Telephone Laboratories under the M.I.T. Electrical Engineering Cooperative Program.

A. A. GALVIN

In 1955 he joined the staff of the M.I.T. Lincoln Laboratory, Lexington, Mass., where he specialized in the development of techniques and equipment for the processing of radar data.

In 1960 he became Leader of the Special Radars Group of the Lincoln Laboratory.

Mr. Galvin is a member of Eta Kappa Nu and Sigma Xi.

❖

James F. Gibbons was born in Leavenworth, Kan., on September 19, 1931. He received the B.S.E.E. degree from Northwestern University, Evanston, Ill., in 1953, where he was a co-winner of the Eshback Award for the outstanding engineering graduate, and the M.S.E.E. and Ph.D. degrees from Stanford University, Stanford, Calif., in 1954 and 1956, respectively. He was a National Science Foundation Fellow from 1953 to 1955, and a National Academy of Sciences Fellow in 1956. After completion of his graduate studies, he was awarded a Fulbright Fellowship to Cambridge University, England, for the year 1956–1957, where he studied nuclear magnetic resonance.

J. F. GIBBONS

Since 1957 he has been a member of the Solid State Electronics Faculty at Stanford University, where he is an Associate Professor. During 1957–1958 he also worked half-time with the Shockley Transistor Corporation, a Unit of Clevite Transistor, Palo Alto, Calif., where he is a Consultant.

Dr. Gibbons is a member of Phi Eta Sigma, Pi Mu Epsilon, Eta Kappa Nu, Tau Beta Pi, Sigma Xi, and an honorary member of the Western Society of Professional Engineers.

Marcel J. E. Golay (SM'51–F'60) was born in Neuchatel, Switzerland, on May 3, 1902. He attended the Gymnase Scientifique of Neuchatel, where he received the B.S. degree in 1920, and the Federal Institute of Technology in Zurich, where he received the Licentiate in Electrical Engineering in 1924. He attended the University of Chicago, Ill., where he obtained the Ph.D. degree in physics in 1931.

M. J. E. GOLAY

From 1924 until 1928, he was with the Bell Telephone Laboratories. After a short association with the Automatic Electric Company, Chicago, Ill., he entered the civil service in 1931, and was a member of the Signal Corps Engineering Laboratories at Fort Monmouth, N. J., until 1955. He is now serving as consultant to the Philco Corporation, Philadelphia, Pa. and The Perkin-Elmer Corporation, Norwalk, Conn.

Dr. Golay is a member of the American Physical Society, the Optical Society of America, the American Rocket Society, and the Society for Applied Spectroscopy. He is the recipient of the 1951 IRE Harry Diamond Award, the 1961 ACS Sargent Award, and the 1961 Distinguished Achievement Award of the Instrument Society of America.

❖

Kaneyuki Kurokawa (M'60) was born in Tokyo, Japan, on August 14, 1928. He received the B.S.E.E. and Doctor of Engineering degrees in 1951 and 1958, respectively, from the University of Tokyo.

K. KUROKAWA

He was a participant of the Foreign Student Summer Project held at the Massachusetts Institute of Technology, Cambridge, in 1954. In 1957, he became Assistant Professor at the University of Tokyo after having worked one year as an Assistant. There, he spent most of his time on the development of sounding rocket electronics. For this work, he shared the Progress Prize of 1959 from the IEE of Japan. In 1959, on a leave of absence from the University, he came to Bell Telephone Laboratories, Murray Hill, N. J., where he has been engaged in research on low-noise amplifiers.

Dr. Kurokawa is a member of the IEE of Japan and the Institute of Electrical Communication Engineers of Japan.

D. Thomas Magill (S'56–M'58) was born in Evanston, Ill., on May 14, 1935. In 1957 he received the B.S.E.E. degree from Princeton University, Princeton, N. J. He received the M.S. degree in 1960, from Stanford University, Stanford, Calif., where he is presently studying for the Ph.D. degree in electrical engineering.

D. T. MAGILL

From 1958 to 1960 he worked in the field of ionospheric research as a Research Assistant at the Radioscience Laboratory, Stanford Electronics Laboratories, Stanford University. Since 1960 he has been employed in the Communications and Controls Research Department, Missiles and Space Division, Lockheed Aircraft Corporation, Palo Alto, Calif.

❖

R. L. McFarlan (SM'51), for a photograph and biography, please see page 2 of the January, 1960, issue of PROCEEDINGS.

❖

James J. Spilker, Jr. (S'55–M'59), was born in Philadelphia, Pa., on August 4, 1933. He attended the College of Marin, Kentfield, Calif., where he received the A.A. degree in 1953. He specialized in electrical engineering, receiving the B.S. degree in 1955, the M.S. degree in 1956, and the Ph.D. degree in 1958, all from Stanford University, Stanford, Calif.

J. J. SPILKER

From 1956 to 1958 he held the positions of Research Assistant at the Stanford Electronics Laboratories, and Teaching Assistant in the Electrical Engineering Department at Stanford University where he did work on transistor circuits and network theory. Since 1958, he has been with the Communications and Controls Research Department, Lockheed Missiles and Space Division, Palo Alto, Calif., where he has been engaged in research in the areas of statistical theory of communications and network theory.

Dr. Spilker is a member of Sigma Xi.

Books

Sequential Decoding, by John M. Wozencraft and Barney Reiffen

Published (1961) by the Technology Press, Mass. Inst. Tech., Cambridge 39, and John Wiley and Sons, Inc., 440 Park Avenue South, New York 16, N. Y. 67 pages+v pages+6 appendix pages+1 reference page. Illus. 6×9¼. $3.75.

"Recognition of the fact that communication can be made as reliable as desired, provided that the transmission rate R_T is less than the channel capacity C, entices the communication engineer to attempt the design of systems that perform this way." This seemingly harmless statement, proved by C. E. Shannon (and quoted from page 25 of this tidy little volume), contains the impetus behind much of the coding-theory literature that has developed in the last decade, much of it exceedingly interesting and pertinent. "Sequential Decoding" falls into this category and can be recommended to anyone interested in one of the current frontiers of coding theory. Wozencraft and Reiffen have prepared a concise and well-written exposition of their topic.

Let the reader beware, however, if he is seeking a general exposition of coding theory, either for an introduction to the subject or for a comparative discussion of various techniques. This book is obviously not intended for these purposes. The term "sequential decoding" refers to a particular decoding scheme developed by the authors, and not to the general use of sequential techniques in coding systems. In this reader's opinion, no little sophistication is needed in following the path laid out; in the author's own words: "It requires . . . an elementary knowledge of the calculus and probability theory. Background experience in communication engineering will be generally helpful." But for the specialist or fledgling specialist in communication and coding theory, these comments do not apply, and the volume will be a welcome and essential discussion of a uniquely different and interesting decoding technique that is not elsewhere readily available in the published literature.

The book, which is really a research monograph, is well organized into six chapters plus an appendix. The first chapter is brief and expository; it identifies redundant transmission as an essential ingredient of communication and defines the binary symmetric channel as the model with which the sequel is concerned. The second chapter treats block codes in general and presents the necessary theoretical foundations, particularly regarding expected error probabilities.

The following two chapters on sequential decoding and convolutional encoding contain the heart of the matter. Sequential decoding is based upon a particular recurrent coding scheme wherein each symbol is decoded, one at a time, by comparing the received sequence sequentially with each possible sequence that could succeed the last decoded symbol, and discarding one of the two possible subsets corresponding to the two possible symbol values. Rejection of a subset is tantamount to decoding the symbol, and the process is recommenced with the next symbol to be decoded. It is shown that the average probability of error for a given symbol has the same exponent as for the case of random block codes, although once an error is made, the succeeding results are apparently catastrophic.

The encoding process is carried out by convolving the information sequence with a randomly constructed generator sequence, and a canonic shift register form of such an encoder is presented.

The fifth chapter presents brief confirmatory results of a digital computer simulation, while the last chapter indicates possible generalizations, principally of the channel model.

In summary, "Sequential Decoding" is a concise, well-done presentation of a research effort, and a welcome addition to the literature of coding theory.

ROBERT A. SHORT
Stanford Research Inst.
Menlo Park, Calif.

Fundamentals of Modern Physics, by Robert Martin Eisberg

Published (1961) by John Wiley and Sons, Inc., 440 Park Avenue South, New York 16, N. Y. 705 pages+23 index pages+xiii pages+bibliography by chapter. Illus. 6¼×9¼. $10.50.

The average radio engineer who is concerned with the development and application of today's exotic devices such as masers and lasers must frequently feel the limitations imposed by his lack of familiarity with the basic principles of quantum physics. There is really no way to remedy this situation other than to take some time off and to study systematically a few good books on the subject.

For those who have this urge, and decide to act on it, this book will make an excellent and relatively painless introduction. The style is excellent; each subject is introduced with a summary of experimental evidence, and then the theory is built up in a logical fashion, using arguments that can be appreciated by a reader well trained in elementary physics, and in mathematics through intermediate calculus.

The first chapter is a short presentation of the theory of relativity, a fairly novel approach, but a logical one, considering the frequency with which relativity gets cranked into later quantum mechanical problems. The next three chapters discuss the historical transition from classical to modern physics. The more advanced treatment starts with Chapter 5, and among the subjects discussed are Bohr's theory of atomic structure, particles and waves, Schroedinger's theory, perturbation theory, one- and multi-electron atoms, magnetic moments, spin, and related relativistic effects, identical particles, collision theory, X rays, and the nucleus.

Mention should be made of an error in the chapter on relativity. On page 10 the author states that "there exists a theorem due to Fresnel and Lorentz which says that it is impossible to devise an optical experiment where the velocity of the apparatus with respect to the ether can produce a first order effect." Now stellar aberration, and the Sagnac and Michelson-Gale experiments are first order effects, and clearly what should be said is that it is difficult to devise an optical experiment where a first order effect can be employed to distinguish between the ether theory and the relativity theory. The author, like so many other textbook writers, considers the relation $E=mc^2$ as establishing the validity of relativity theory beyond reasonable doubt, despite the fact that this result may be obtained without the help of relativity.

On page 171, in discussing the physical unreality of quantum mechanical wave functions, the author makes the statement that "we should not try to answer, or even pose, the question: Exactly what is waving, and what is it waving in? The reader will recall that consideration of just such questions concerning the nature of electromagnetic waves led nineteenth century physicists to the fallacious concept of the ether." The engineer developing or using an optical laser must quite often put this question to himself, despite the interdiction by the author. His device starts with the stimulated emission of photons, according to strictly quantum mechanical rules, but somehow these individual photons get together and produce a beam of radiation that displays all of the properties of coherence prescribed by the classical wave theory!

Criticisms of this sort can be directed to almost any text on modern physics. They should in no way detract from the enjoyment of this book by a reader who is interested in learning the fundamentals of quantum mechanics.

C. W. CARNAHAN
Varian Associates
Palo Alto, Calif.

Mechanical Waveguides, by Martin R. Redwood

Published (1961) by Pergamon Press, Inc., 122 E. 55 St., New York 22, N. Y., 273 pages+4 index pages+ix pages+21 appendix pages. Illus. 5¾×8¾. $9.00.

In the brief title "Mechanical Waveguides," the author describes a book on the theory of sound wave propagation in bounded fluid and solid media. The content of this book is most directly applicable to the field of ultrasonic engineering, particularly to the development of ultrasonic delay lines and to material studies by ultrasonic techniques. The choice of a term not in common usage to describe the subject is perhaps unfortunate in that it may fail to attract the attention of many prospective

readers in the ultrasonics field. This book presents a unified analysis of a number of topics heretofore covered in scattered journal articles and texts. After a brief review of propagation phenomena in unbounded media and at a reflecting interface, the author launches into a quite thorough treatment of topics in the propagation of elastic waves in fluid-filled waveguides with either free or rigid boundaries. The author has treated at great length and in an excellent manner the subject of wave propagation in solid waveguides such as cylinders, plates and multilayered waveguides. Two chapters are devoted to pulse propagation in elastic waveguides. Treated in abbreviated form are topics in solid resonators and wave propagation in anisotropic media. An appendix contains useful mathematical reference material on special techniques and functions used in the text. An outstanding feature of this book is the very complete bibliography of over 700 items covering publications in this field as late as 1959.

The book fills a great need for a textbook in this field. It should serve the advanced undergraduate well, since the mathematics is kept relatively unsophisticated, yet it possesses sufficient rigor and depth of treatment to constitute a basis for a short graduate course. Probably the greatest community of readers, however, will be found among those practicing scientists just entering the ultrasonic waveguide field either to pursue a new interest or to take advantage of many of the ultrasonic techniques for measuring the properties of solids and liquids. For these readers the book presents an excellent introduction complete with bibliography and pertinent mathematical background.

If a criticism of the book is to be raised, it may be concerned with the brevity of treatment of many topics. In many cases the author has given enough introduction to a topic to stimulate the reader's interest in the finer points of the matter only to leave him to consult the periodicals for further details. On the whole, however, the book is a very worthwhile and much needed addition to the literature of ultrasonics.

John E. May, Jr.
Bell Telephone Labs.
Whippany, N. J.

Error Correcting Codes, by W. W. Peterson

Published (1961) by The Technology Press, Mass. Inst. Tech., Cambridge 39, and John Wiley and Sons, Inc., 440 Park Avenue South, New York 16, N. Y. 244 pages+5 index pages+x pages+8 reference pages+28 appendix pages. Illus. 6×9¼.

"Error Correcting Codes," by Wesley Peterson is a specialist's book on a very special topic. It is unusual in books of this nature, in that portions may be read profitably by the nonspecialist as well as the specialist.

The theory of error correcting codes is an area where a morass of mathematics often obscures the goal of the theory. It is to Peterson's credit that he has been able to write a lucid yet nonelementary treatment covering almost all of the significant topics in the theory of error correcting codes.

The first five chapters of the book treat the conventional Hamming-Slepian coding theory. Particularly noteworthy in this first part of the book are Chapters 2 and 4. Chapter 2 presents a compact and readable introduction to the theory of groups, rings, fields, vector spaces and matrices. Chapter 4 presents a sorting out of some of the most important coding bounds. To this reviewer's knowledge, this is the only available organized presentation of these bounds.

Chapters 6–10 treat algebraic coding theory. Much of the material in this part of the book is due to Peterson and some of it is presented here for the first time. Chapter 6 introduces the algebraic ideas of ideals, residue classes and Galois fields in just the dosage necessary for the rest of the book. Chapter 7 deals with linear switching circuits and their use. The reviewer felt that this chapter was somewhat lacking in the clairty of presentation of the rest of the book. It would have made more sense to start Chapter 7 with the Huffman material presented at the end of this chapter. Chapter 8 treats cyclic codes in general; Chapter 9 treats the Bose-Chaudhuri codes; and Chapter 10 covers the Fire burst-error-correcting codes.

The rest of the book treats a collection of miscellaneous coding subjects—several decoding methods, Hagelbarger codes, and codes for checking arithmetic operations. Wozenkraft's sequential codes are mentioned only briefly. Five appendixes are included with the book. The most useful of these is a table of irreducible polynomials over GF(2). Excerpts from Shannon's ubiquitous unpublished notes on error bounds—unpublished apparently only by Shannon—comprise another appendix.

All in all, this a fine book worth reading—cover to cover for the coding specialist; perhaps just the first five chapters for the mildly interested.

Norman Abramson
Stanford University
Stanford, Calif.

Magnetic Tape Instrumentation, by Gomer L. Davies

Published (1961) by the McGraw-Hill Book Co., Inc., 330 W. 42 St., New York 36, N. Y. 241 pages+9 index pages+vii pages+12 appendix pages. Illus. 6×9¼. $8.50.

Mr. Gomer L. Davies' book, "Magnetic Tape Instrumentation," is another contribution to the literature on magnetic recording techniques and their many applications. The author covers, by necessity, much of the same material as authors have done in previous publications. The value of this book lies in the fact that Mr. Davies has correlated modulation and digital techniques to the specific problems of recording signals on and reproducing them from moving magnetic recording media.

The author's preference for circuitry becomes apparent from the illustrations. There are hardly any sketches showing solutions, in principle, to design requirements of components for magnetic recording systems used in instrumentation applications.

Among the eleven chapters, the one entitled "Techniques Used in Data Recording," might well be considered the heart of the book. Unfortunately, the treatment lacks detail in some instances. Such subject matters as video recording occupy hardly more than one page of descriptive information notwithstanding the fact that video recording plays an increasingly important position in the instrumentation field. In the same chapter, information handling capacity is reviewed, but the treatment does not seem to do justice to the many pivotal and rather complex problems.

The references at the end of each chapter are very helpful, particularly since they call attention to many recent publications. If a suggestion could be made, it is that works of foreign authors might have been given a little more space.

All in all, the book will make a worthwhile addition to the libraries of those who are interested in data storage and evaluation.

S. J. Begun
Clevite Corp.
Cleveland, Ohio

Circuit Analysis, by Elias M. Sabbach

Published (1961) by The Ronald Press Co., 15 E. 26 St., New York 10, N. Y. 446 pages+9 index pages +viii pages. Illus. 6¼×9¼. $8.75.

This book has been designed for a first course in circuit analysis, and was developed and tested over several years with Purdue University sophomores. An understanding of college algebra and calculus is assumed, but no prior electrical engineering courses are necessary.

In early chapters, a discussion of the electrical structure of matter, electric current, conduction, and electrostatic and magnetic fields gives a valuable introduction to circuit analysis but will not supplant later physics and electro-magnetic fields courses.

The twenty-five chapters progress logically and cover the expected subjects of circuit elements, network equations, dc and sinusoidal ac analysis, complex algebra, resonance, and general methods of network solution. Intermeshed with the above in appropriate places, the author discusses phasors, effective values and power, complex frequency plane analysis, network graphs, signal flow diagrams, special techniques for network solution, three-phase circuits, coupled circuits, and Fourier series. This material forms an extremely good base for more advanced work on network analysis and synthesis. A deficiency readily noted is the lack of references to other published material.

The text material is clearly presented and amply illustrated with many line drawings and problems; add to this the easily-read typography and the well-executed illustrations and you have a book from which studying and teaching will be a pleasure.

Ian O. Ebert
Michigan State University
East Lansing

Advances in Electron Tube Techniques, David Slater, Ed.

Published (1961) by Pergamon Press, 122 E. 55 St., New York 22, N. Y. 231 pages+3 index pages +viii pages. Illus. 8½×11¼. $15.00.

This book reports on the Proceedings of the Fifth National Conference on Tube Techniques which was held in September, 1960, and was sponsored by the Working Group on Tube Techniques, Advisory Group on Electron Tubes, Office of the Director of Defense, Research and Engineering. This Conference is held every two years, and the selection of papers presented is decided upon by the Program Committee.

For this Conference the Program Committee, consisting of J. H. Bloom, Chairman, R. E. Palmateer, L. N. Heynick, M. F. Axler and D. Slater, selected 46 papers from a total of 90 submitted, of which 44 papers are included in these Proceedings.

We quote from the opening speech of Dr. W. H. Kohl, who defines the philosophy of the conference as follows:

> The subjects treated at these conferences were always either of a theoretical or a practical nature, both approaches being equally represented at a given symposium so that both the technician and the researcher could derive benefit from their respective attendance. One might say, then, that Tube Techniques is a generic term for knowledge of the properties of materials and experience in the use of processes, both being applied to the construction of electron tubes.

The papers included in this volume cover recent activity in such fields as electron tube materials and techniques, thermionic emitters, internal and external factors affecting electron tubes, ruggedization and life of electron tubes. Within these fields techniques involving ceramics, emitters, gases, getters, glasses, metals and vacuums are covered in addition to environment and life testing, nuclear radiation effects and electron tube performance studies.

Generally speaking, the papers covered in this volume are of excellent quality and reflect a considerable effort both on the part of the members of the Program Committee and the contributors. The great amount of detail included in describing a number of techniques is indeed commendable and should be appreciated by both the initiated as well as the uninitiated regarding the art of electron tube techniques.

This volume, together with Volumes 3 and 4, should be included in the library of all researchers and technicians working in the fields of electron tube technology.

GEORGE A. ESPERSEN
Philips Labs.
Irvington-on-Hudson, N. Y.

Information Retrieval and Machine Translation, Part II, Allen Kent, Ed.; Advances in Documentation and Library Science Series, Vol. 3, Jesse H. Shera, General Editor

Published (1961) by Interscience Publishers, Inc., 250 Fifth Ave., New York 1, N. Y. 652 pages+17 index pages+v pages+17 appendix pages. Illus. 6¼×9¼. $25.00.

This volume contains a set of thirty-eight papers originally presented in Cleveland in September, 1959, at the International Conference for Standards on a Common Language for Machine Searching and Translation. Another set of twenty-one papers from the same Conference was published in a companion volume which was reviewed earlier (PROC. IRE, vol. 49, p. 853; April, 1961).

The criticism previously voiced concerning the presentation of these Conference Proceedings is equally applicable to the present volume. Each paper is labelled as a separate "chapter," and no visible attempt is made to bring together related material. As a result the book should be difficult to use by all but the most expert readers. The lack of organization is particularly serious because of the many different topics covered, and the peculiar points of view expressed. Moreover, the title of the book is not indicative of the contents; many aspects of information retrieval are completely ignored, and contributions in machine translation are included from only a very few of the groups active in the field. To compensate for this lack of concentration in information retrieval and machine translation, some papers deal with the construction of various artificial universal languages, including one on "minigraphy," a new shorthand system; papers are also included on the simulation of behavioral systems, learning theory, and the operation of various Standard Associations. All but two of the contributions are in English; Chapters 51 and 57 are printed in French.

A number of papers deal with various aspects of linguistic analysis. In Chapter 24, Albani, *et al.*, present an impressive system for analyzing the content of utterances and relations between words; since each word in the language requires individual analysis, it is not clear, however, whether the ideas can ever be incorporated in a practical automatic process. Some aspects of syntactic analysis for machine translation are covered by Hiz, Gleitman, Joshi, and Micklesen, *et al.*, in Chapters 30, 31, 32, and 34, respectively. Lexicographic problems are discussed by Reifler in Chapter 33 and Pacak in Chapter 36. Some of these papers bear evidence of serious work, and should represent the most valuable part for the reader interested in machine translation.

A second group of papers deals with the over-all structure of documentation and language systems. Fairthorne in Chapter 44 exhibits relations between texts in a bibliographic space-time structure, and displays interconnections between various problems in the field of documentation. This work is difficult to evaluate in the absence of further details. Andreyev in Chapter 49 establishes various hierarchies of languages, and looks toward the creation of a universal code of science. Cordonnier in Chapter 51 expresses many diverse and original ideas in the field of human communication, among which is the construction of a universal language each word of which is pronounceable and transformable into a numeric code; many of the included ideas do not, unfortunately, seem to be too practical. Another universal language is proposed by Bölting in Chapter 52. De Grolier may have had some of the preceding papers in mind when he warns in Chapter 55 of the dangers of designing admirable plans for all encompassing systems which are generally doomed to failure.

The old controversy concerning the use of a common intermediate language for mechanical translation is taken up by Andreyev, Melton, Kulagina, *et al.*, and Parker-Rhodes in Chapters 23, 28, 35, and 39, respectively. Andreyev and Kulagina, *et al.*, sketch some of the work in mechanical translation going on in their respective laboratories in the USSR. There is unfortunately a complete lack of detail. Melton in his well-written article makes a plea for the use of the "semantic code" developed at Western Reserve University as an intermediate language, and Parker-Rhodes outlines a program of translation by means of an interlingua; in the latter case, the mechanization of many parts of the proposed program is not made clear.

The case for working with the natural language directly, instead of with an intermediate artificial language, is made by Yngve and Luhn in Chapters 40 and 45, respectively.

Problems in the indexing of information for information retrieval are treated by Ranganathan in Chapters 46 and 47, and in the interesting articles by Vickery in Chapter 54. The latter includes comparisons showing the type of indexing obtained respectively in a faceted classification, the universal decimal classification, and the Western Reserve University system.

A number of miscellaneous problems are also included in the volume. Some equipment considerations are treated by Booth in Chapter 37, and Cordonnier in Chapter 57. Standardization activities are treated by Offenhauser and Kingery in Chapters 59 and 60, respectively. An interesting simulation procedure for behavioral systems is described in Chapter 56 by B. K. Rome and S. C. Rome. Various learning procedures in applied linguistics are treated by Solomonoff in Chapter 41, and the use of logic for the detection of syntactic ambiguity in documents is discussed by L. Allen in Chapter 42. Finally, A. Kent, who is also the Editor of the volume, makes a plea in Chapter 61 for coordination and for the standardization of nomenclature and the exchange of personnel and materials.

Some of the discussions by Conference participants are included in the book as Chapters 38, 62 and 63. Much of the discussion deals with the conference aims of establishing standards on a common language for machine searching and translation. Running through the transcript is a general feeling of frustration because of disagreement on what to standardize, and how to standardize it. An "International Continuing Committee on Information Retrieval and Machine Translation," as well as several subcommittees were formed as a result of the Conference. Any activities of these committees during the past year and a half have not come to the reviewer's attention.

To summarize, this volume contains a few interesting contributions. However, because of the attempts to satisfy the aims of the Conference in creating "standards for a common language," and in establishing permanent international organizations, the material is often slanted in such a way that it becomes valuable neither in the field of information retrieval, nor in machine trans-

lation. As such the book can be recommended only to institutional libraries. The presentation is again marred by many typographical errors. The price of $25.00 seems to this reviewer to be inexcusably high.

GERARD SALTON
Harvard University
Cambridge, Mass.

Management Control Systems, Donald G. Malcolm and Alan J. Rowe, Eds.; Lorimer F. McConnell, General Editor

Published (1960) by John Wiley and Sons, Inc., 440 Fourth Ave., New York 16, N. Y., 357 pages+15 pages+xvii pages. Illus. 6×9¼. $7.25.

This book constitutes the *Proceedings* of a symposium on Management Information Control Systems held at the System Development Corporation in Santa Monica, Calif., in July, 1959, which had as its purpose the exploration of the present state-of-the-art, the likely future developments, and the need for research in the field. The book includes not only the papers which were presented at the meeting but also a summary of the discussions that followed in which about thirty experts participated.

The book is organized in six thematic sections followed by a summary and a fifteen-page index. The six themes are: The Opportunity for Innovation in Management Controls, The Concepts of Management Control—Present Practices, The Impact of Computers on the Design of Management Controls, Examples of Automated Management Controls, New Approaches—Future Possibilities in Management Control and Information Systems, and Research in Management Control System Design.

Concepts of management control in military as well as business and industry areas are treated, the military systems treatment being in some respects more impressive than some of the business-origin presentations.

While much of the substance is speculative and bordering on the abstract, albeit altogether competent, several of the papers are based on hard-core automation in being. One of these is "Integrated Systems Planning at G.E.," by H. Ford Dickie. Some of the implications of this paper are momentous, especially since it indicates the long-range and large-scale policies of one of our greatest corporations:

> Now that indirect labor exceeds direct labor in many cases, now that major improvement opportunities are available in data processing, why should not the economic availability of electronic data processing be an essential consideration in plant site selection? . . . The complexity of conceiving and installing a system grows with something like the square of the number of functions involved. . . . We have to stop applying broad overhead factors because the base of our overhead —direct labor—is fast disappearing.

But in this paper, as in the others, although by title the systems concept is intended, the contingent factors in the over-all economy that are involved—affecting the community as well as the enterprise and the industry—seem to be negligibly considered. Perhaps there ought to be another symposium such as the EIA Automation Systems Conference at Arizona State University in 1958, or one along the lines of that held at Margate, England, in 1955 on "The Automatic Factory—Dream or Nightmare," the *Proceedings* of which were published by the British Institution of Production Engineers. Something more substantially beneficial to the over-all system might result.

JAMES J. LAMB
Ramo-Woodridge
Div. of Thompson Ramo Wooldridge, Inc.
Sierra Vista, Ariz.

Scanning the Transactions

All-magnetic computing systems are receiving a growing amount of attention in the computer literature. Whether this trend continues remains to be seen. However, it is significant that the last issue of PGEC TRANSACTIONS devoted some 40 pages to four papers on the topic. Magnetics have, of course, already played an important part in the rapid development of large-scale digital computers during the past decade. Magnetic cores, tapes and drums are almost universally used today for memory functions. Serious efforts are now being made to extend the use of magnetic elements to logic systems as well. The motivation for this work lies in the high reliability and low cost of the magnetic devices themselves. Considerable work has been done recently in developing circuits which employ magnetic devices in conjunction with diodes. There is particular interest, however, in all-magnetic circuits, which avoid the use of diodes. For the most part, only very small pieces of all-magnetic logic systems have actually been constructed to date. Whether such systems can be effectively assembled on a large scale is an important and unanswered question. A 650-component all-magnetic arithmetic unit was recently built to provide a partial answer to this question, and on the basis of the results it would appear that all-magnetic logic holds considerable promise for the future. (J. L. Haynes, "Logic circuits using square-loop magnetic devices: A survey"; D. R. Bennion, *et al.*, "A bibliographical sketch of all-magnetic logic schemes"; H. D. Crane, *et al.*, "Design of an all-magnetic computing system," (Parts I and II); IRE TRANS. ON ELECTRONIC COMPUTERS, June, 1961.)

The vibrations of the heart have been found to provide a great deal of information about the state of this vital organ and other body conditions. The heart produces vibrations and sounds of widely varying intensity over a frequency range from below 2 cps to above 1000 cps. Less than one per cent of this vibrational energy, however, is audible. These audible sounds are the ones in common use today for clinical diagnosis. Information in this audible region is principally concerned with the operation of the heart valves, whereas the inaudible 99 per cent is largely associated with the muscular contraction and the general performance of the heart. A technique has recently been developed for detecting and analyzing inaudible, as well as audible, heart vibrations in which a simple capacitance microphone coupled to the chest by a short column of surgical jelly serves as a vibration transducer, producing what is known as a vibrocardiogram. The vibrocardiogram reveals changes in timing and relative strength of major cardiac events with an accuracy and resolution far exceeding that of an electrocardiogram. In addition to its value as a diagnostic tool, this technique is especially attractive for telemetering applications because of its simplicity and because a great deal of cardiac information is obtained from a narrow bandwidth channel. Vibrocardiography may therefore find its greatest value as a bio-astronautical instrumentation technique. (C. M. Agress and L. G. Fields, "The analysis and interpretation of the vibrations of the heart, as a diagnostic tool and physiological monitor," IRE TRANS. ON BIO-MEDICAL ELECTRONICS, July, 1961.)

Much is heard of magnetohydrodynamics these days, but how many are acquainted with the field of electrohydrodynamics? The latter term refers to the conduction of unipolar ions in insulating liquids, which provides a useful mechanism

for exchanging electrical and hydrodynamic energy. When an ionizer, in the form of several corona points, and an ion collector are immersed in a suitable insulating liquid, and a high voltage is applied between them, a small ion current will flow which, by frictional momentum transfer from moving ions to the liquid, will generate a reasonably effective pressure in the liquid. This makes it possible to pump liquids directly with electrical power or, conversely, to build up electrical energy from liquid motion. An ion drag pump has recently been developed, using this principle. Moreover, it is possible to build quite a variety of high-impedance electrohydrodynamic components, including switches, relays, voltage regulators, voltage generators, small motors, and dc transformers. The art is still in the research stage, but because the theoretical conversion efficiency is reasonably high it is likely that electrohydrodynamics will find important applications in the future. (O. M. Stuetzer, "Electrohydrodynamic components," IRE TRANS. ON COMPONENT PARTS, June, 1961.)

High-speed spectrum analysis is being considered with increasing interest for inclusion in a variety of instrumentation systems, as the essential link which transfers spoken commands into intelligence recognizable by the more classical data-handling devices. Usually the need is for real-time analysis, so design information regarding sweep-frequency methods of analysis is becoming of keener interest to more engineers. Moreover, new systems of spectrum analysis are being studied. In one new system incoming signals are stored and simultaneously processed during a *processing period*, at the end of which the spectrum is read out in a much shorter *readout period*. Thus spectrum samples are available at intervals only slightly longer than the processing period, which is related to the resolution required in the output spectrum. (L. G. Zukerman, "Applications of a spectrum analyzer for use with random functions" and J. Capon, "High-speed Fourier analysis with recirculating delay-line heterodyner feedback loops," IRE TRANS. ON INSTRUMENTATION, June, 1961.)

Abstracts of IRE Transactions

The following issues of TRANSACTIONS have recently been published, and are now available from the Institute of Radio Engineers, Inc., 1 East 79th Street, New York 21, N. Y., at the following prices. The contents of each issue and, where available, abstracts of technical papers are given below.

Sponsoring Group	Publication	IRE Members	Libraries and Colleges	Non Members
Antennas and Propagation	AP-9, No. 4	$2.25	$3.25	$4.50
Audio	AU-9, No. 3	2.25	3.25	4.50
Bio-Medical Electronics	BME-8, No. 3	2.25	3.25	4.50
Education	E-4, No. 2	2.25	3.25	4.50
Electronic Computers	EC-10, No. 2	2.25	3.25	4.50
Engineering Management	EM-8, No. 2	2.25	3.25	4.50
Information Theory	IT-7, No. 3	2.25	3.25	4.50
Instrumentation	I-10, No. 1	2.25	3.25	4.50
Space Electronics and Telemetry	SET-7, No. 2	2.25	3.25	4.50

Antennas and Propagation

VOL. AP-9, NO. 4, JULY, 1961

The Traveling-Wave Linear Antenna—E. E. Altshuler (p. 324)

It is shown experimentally that an essentially travelling-wave distribution of current can be produced on a linear antenna by inserting a resistance of suitable magnitude one-quarter wavelength from the end of the antenna. A theory for the resistively-loaded dipole antenna is formulated on the basis that the inserted resistors (one in each arm) can be replaced by equivalent generators and that the resulting triply-driven antenna can be solved by the superposition of singly- and doubly-driven dipoles. Approximately 50 per cent of the power is dissipated in these resistors.

With a traveling-wave distribution of current on an antenna available, the properties of this antenna are then investigated and compared with those of the conventional linear antenna. It is found that the input impedance of the traveling-wave antenna remains essentially constant as a function of antenna length, whereas that of the conventional linear antenna varies considerably. It is also shown that the input impedance of the traveling-wave antenna varies only slightly over a 2 to 1 frequency band. The directional properties of the traveling-wave and conventional dipole are compared, and it is shown that a minor lobe does not appear in the radiation pattern of the traveling-wave dipole until it is much longer than the conventional dipole. Also, it is shown that where the directional properties of the conventional dipole are quite sensitive to a change in frequency, those of the traveling-wave dipole are not.

Resonance Characteristics of a Corrugated Cylinder Excited by a Magnetic Dipole—J. R. Wait and A. M. Conda (p. 330)

Radiation from an axial magnetic-current element in the presence of a corrugated cylinder is considered. It is indicated that the power radiated in a given mode depends on the surface reactance, the circumference of the cylinder and the elevation angle. For certain values of the parameters, particular modes are strongly excited in a manner corresponding to the resonance condition of the circumferential (or spiral) surface waves.

New Circularly-Polarized Frequency-Independent Antennas with Conical Beam or Omnidirectional Patterns—J. D. Dyson and P. E. Mayes (p. 334)

A conical beam may be obtained from balanced equiangular spiral antennas by constructing an antenna with more than two spiral arms and symmetrically connecting these arms to provide a suppression of the radiated fields on the axis of the antenna. The angle of this conical beam can be controlled and, with proper choice of parameters, confined to the immediate vicinity of the azimuthal ($\theta = 90°$) plane.

An antenna with four symmetrically spaced arms can provide a radiation pattern that is within 3 db of omnidirectional circularly polarized coverage in the azimuthal plane. The standing-wave ratio of this antenna referred to a 50-ohm coaxial cable is less than 2-to-1 over the pattern bandwidth.

This four-arm version retains the wide frequency bandwidths of the basic conical log-spiral antenna, and it provides a coverage which heretofore has been difficult to obtain even with narrow-band antennas.

Arbitrary Polarization from Annular Slot Planar Antennas—F. J. Goebels and K. C. Kelly (p. 342)

This paper describes the analysis and design of a class of antennas which can radiate and receive constant-shape pencil beams with either circular sense, any linear or elliptical polarization by a simple adjustment in the feed circuit. Such radiators are called arbitrarily polarized antennas. The apertures described are located on upper plates of radial waveguides and are composed of annular slots, with each annulus consisting of a discrete number of crossed slots.

The annular slots are positioned so that each arm of the crossed slots can couple by a constant factor with the radial or circumferential currents flowing over the aperture plate to produce a common instantaneous direction for the electric field in each slot pair. Both standing-wave and traveling-wave array types are employed. The standing-wave array requires only one radial waveguide mode for its operation. The traveling-wave array requires two modes and results in greater bandwidth and greater freedom in arraying many annuli. The methods used to excite the various radial waveguide modes are discussed; theoretical and experimental radiation patterns at *X* band are compared.

A Theoretical Limitation on the Formation of Lossless Multiple Beams in Linear Arrays—J. L. Allen (p. 350)

It is well known that through the use of lenses, several independent beams can be formed from a single antenna, with each beam having essentially the gain corresponding to the aperture of the lens. Recently, feed systems have been developed for linear arrays which achieve similar performance through the use of directional couplers.

In this paper it is shown that the shape of the beams which can be formed from an equispaced array by such a feed matrix is not arbitrary, unless one is willing to accept losses in addition to normal plumbing losses. It is shown that the array space factors associated with the individual beams must be such that they are mutually orthogonal over a period of the space-factor pattern.

A General Analysis of Nonplanar, Two-Dimensional Luneberg Lenses—S. Adachi, R. C. Rudduck, and C. H. Walter (p. 353)

A class of two-dimensional, nonplanar, modified Luneberg lenses is developed which generalizes the properties of many of the previously developed lenses. By this development the radiated beam can have an arbitrary direction relative to the plane of the lens as compared to previously developed designs in which the beam must lie in the plane of the lens. The lenses are of arbitrary contour; however, only the spherical and the planar contours are considered in detail.

The Numerical Evaluation of Radiation Integrals—J. H. Richmond (p. 358)

In the numerical evaluation of radiation integrals, the number of terms required depends on the accuracy desired, the method of integration, the current distribution on the antenna, the length of the antenna, and the observation angle. Simpson's rule and the trapezoidal rule appear to be used almost exclusively at present. A "piecewise linear rule" introduced here is shown to yield greater accuracy for a given calculation time.

An Iris-Excited Slot Radiator in the Narrow Wall of Rectangular Waveguide—D. G. Dudley (p. 361)

The inclined, narrow-wall slot radiator has been used extensively in antenna arrays. The slot is easily machined and handles high power. The inclination of the slot, however, produces an undesirable cross-polarized radiation component. This cross polarization, coupled with the variation of the slot admittance with frequency, causes pattern deterioration and loss in array efficiency. A noninclined, narrow-wall slot radiator has been developed. This slot is excited by two compound irises which produce an inclination of the electric field as it passes the slot. The field inclination replaces the slot inclination, thereby eliminating the cross-polarized component. Although the power handling capability of the slot is limited by the iris structure, the slot has improved conductance characteristics. Variation of slot excitation in both amplitude and phase has been produced by varying the iris dimensions. The iris-excited, narrow-wall slot radiator has application to receiving and to low-power transmitting arrays.

Reflection of Electromagnetic Waves from a Stratified Inhomogeneity—R. Yamada (p. 364)

This paper deals with the partial reflection of electromagnetic waves from a stratified inhomogeneity. When the refractive index profile is an analytic function and the wave number is large, the reflection coefficient is calculated by the use of the Volterra integral equation and the relation between the WKB approximation and the internal reflection is examined. The reflection coefficient in this case is calculated also by the WKB method using the connection formula around the turning point which lies in the complex plane. When the index profile is discontinuous, the reflection coefficients are calculated for simple models. The reflection coefficients of the above two cases are compared. The reflected field from randomly distributed multi-layers is discussed using the above results.

On Propagating Discontinuities in an Electromagnetic Field—K. R. Johnson (p. 370)

The propagation of discontinuities of an electromagnetic field is considered for the case of a conducting medium. Conditions relating the values of the discontinuities in the electric and magnetic fields are obtained, and equations governing the transport of the discontinuities through space are derived. Such discontinuity conditions and transport equations are obtained both for the fields and for the nth order partial time derivatives of the fields. Previous derivations have treated the case of a nonconducting medium and have used distribution theory. The present treatment does not use distribution theory.

Elevated Duct Propagation in the Tradewinds—D. L. Ringwalt and F. C. MacDonald (p. 377)

All of the maximum propagation (220 Mc) ranges observed in an elevated duct regime varied from 500 to 1200 miles compared to less than 400 miles observed with the same equipment elsewhere. The measurements were made at the optimum season (November) in a tradewind regime between Brazil and Ascension Island (8° S. latitude). The field strengths above 4000 feet altitude are as much as 40 db larger than those at lower altitudes. From the level at average duct height (6000 feet) the field decreases slowly to 10,000 feet, the maximum altitude investigated. The slow fading rate usually associated with duct propagation is not always observed even on the very long range runs.

An extrapolation to propagation conditions in the month of March via refractive index measurements indicates quite minimal ducting conditions 10 per cent to 20 per cent of the time.

Frequency Variations Due to Over-the-Horizon Tropospheric Propagation—J. H. Chisholm, S. J. Goodman, J. M. Kennedy, L. B. Lambert, L. P. Rainville, and J. F. Roche (p. 384)

An experiment was performed over a 161-mile path between Alpine, N. J., and Round Hill, Mass., to determine the frequency fluctuations produced by the propagation mechanism on a highly stable signal in an over-the-horizon tropospheric circuit. A signal at 388.0 Mc was transmitted from Alpine using a 10-kw transmitter and a 12° beamwidth antenna. These transmissions were received at Round Hill with a 5° beamwdith antenna and heterodyned to 416.7 Mc using a highly stable local oscillator and retransmitted to Alpine. Using coherent reception techniques, the retransmitted signal was received at Alpine and heterodyned with the signal originally transmitted. The difference frequency was fed to a bank of narrow-bandwidth crystal filters. An analysis of the data obtained from these filters indicated that the standard deviation of the frequency fluctuations of the signal was approximately 0.6 cps when CW transmission was employed.

An additional feature of the experiment was an attempt to measure the variations of the propagation path length as a function of time. It appears that the standard deviation of the path length variations was less than 55 meters when the average path length in $\frac{1}{6}$-second intervals was measured.

Simultaneous Scintillation Observations on 1300-Mc and 3000-Mc Signals Received During the Solar Eclipse of October 2, 1959—J. Aarons and J. P. Castelli (p. 390)

During the total solar eclipse of October 2, 1959, and during a 10-day control period bracketing this date, measurements were made of radio signals received at frequencies of 224 Mc, 1300 Mc, and 3000 Mc. These measurements indicated that point sources on the sun rather than the total disk, were the constant-energy sources responsible for the scintillations of the received signals. This conclusion is in agreement with the work of Kazes and Steinberg. The fact that, during the period of totality, scintillations were observed at the two higher frequencies indicated that limb sources produced the scintillations.

Inteferometric maps of the sun taken during this period showed plage areas at frequencies of 1420 Mc and 3300 Mc; however, at a frequency of 169 Mc, these maps showed only a relatively uniformly bright sun. In line with these findings, the recorded radio data did not show scintillations at the 224-Mc frequency but did show scintillations at the 1300-Mc and 3000-Mc frequencies.

During the control period, the scintillations at 1300 Mc were well correlated in detail with those at 3000 Mc. For this frequency range, it therefore appears that the scintillation oscillations are not frequency dependent. The two sets of data were taken at different antenna apertures. The 1300 Mc data were taken on an 84-foot parabolic antenna, whereas the 3000 Mc readings were made on an 8-foot parabolic antenna, 80 feet distant from the larger unit. Thus, it appears that, for this frequency range, the mechanism is not only independent of frequency but, within the experimental limits, is also not greatly affected by the size of the antenna.

The periods of the scintillations (30 seconds to 2 minutes) show that the shadow pattern is large in extent. Almost all scintillations took place when the sun was below 4° of altitude.

A hypothesis is advanced that the blob structure of the troposphere, possibly at the height of the tropopause, is formed into a curved lens. The focusing of the energy through this concave lens produces the scintillations observed.

Studies of Meteor Propagation at 49 and 74 Mc—J. B. Berry, Jr., J. C. James, and M. L. Meeks (p. 395)

The characteristics of meteor propagation were investigated over two nearly parallel paths from Walpole, Mass., to Congaree, S. C. (1250 km) and from Walpole, Mass., to Smyrna, Ga. (1480 km). Simultaneous measurements were made at 49 Mc and 74 Mc. The duty cycle for meteor propagation was measured at both frequencies with separate determination of the contributions from underdense trails, specular overdense trails, and nonspecular trails. As a function of signal amplitude A, the data could be fitted by assuming the duty cycle to be proportional to A^{-k}, where k lies between 0.9 and 1.8 depending on the time of day and types of trail contributing. Roughly half of the duty cycle came from nonspecular overdense trails and only 10 to 20 per cent from underdense trails. Simultaneous measurements with two separate receiving systems were made at both 49 Mc and 74 Mc in order to determine the effects of antenna height-difference and

various lateral antenna-separations. The meteor signals were strongly decorrelated by certain antenna height-differences. Overdense trails produced some decorrelation with lateral antenna-separation, but underdense trails gave well-correlated echoes. No significant differences in meteor echo rate were found between receiving systems in very flat terrain at Congaree, S. C., and hilly terrain at Smyrna, Ga. For the hilly terrain, best signal correlation was found for nearby antennas which were at the same height above sea level.

A Method for Computing Ionospheric Focusing of Radio Waves, Using Vertical Incidence Ionograms—E. Warren and D. Muldrew (p. 403)

The dependence of the signal strength of radio waves upon ionospheric focusing and spatial attenuation is calculated for a spherical ionosphere in terms of parameters obtainable from the appropriate vertical incidence ionogram. The signal strength at any given distance can be presented as a function of these ionospheric parameters in the form of a contour chart from which the unabsorbed field strength can be obtained easily as a function of frequency. The geometrical optics approximation is used. The limits of the region at the skip distance for which this method fails are estimated by comparing the results of a ray- and a wave-type calculation.

Audio

VOL. AU-9, NO. 3, MAY-JUNE, 1961

Enhanced Stereo—R. W. Benson (p. 63)

Practices utilized in producing a stereo recording are discussed relative to the performance of stereo-sound reinforcement systems. The reproduction of these recordings results in an enhanced stereo effect.

A New Stereophonic Amplifier—N. H. Crowhurst (p. 66)

A central feature of the new design of a stereo amplifier is an output transformer with original features that makes possible reduced cost and improved performance at the same time.

This paper discusses a varied possibility of design objectives for a stereo system, and explains the way in which the new output transformer functions. By variation in its method of use, or in choice of parameters, a whole range of amplifiers can apply advantages in different proportions or degrees.

The basic design of an output transformer, which is essentially inexpensive to make, provides for separation between "left" and "right" as well as crossover, and combining networks for mixed lows, if desired, without additional external circuits. It makes possible a new type of tone control, achieving high performance economically, using feedback, and/or improved matching between amplifier and loudspeakers over the entire frequency range as well as better separation and efficiency than the single-ended and push-pull transformer matrix can give.

One particular amplifier is discussed in detail, while a more general discussion shows possible application to more diverse design objectives.

An Improvement in Simulated Three-Channel Stereo—P. W. Tappan (p. 72)

Some two-channel stereo systems have employed a third full-range speaker system in the center, reproducing an equal in-phase mixture of the signals in the two channels. Advantages of this arrangement over the usual two-speaker array are better reproduction of the location and size of central sound sources. A disadvantage is the sizeable reduction in the apparent spread, or distance between flanking sources.

The reasons for these effects are discussed, and it is indicated that this disadvantage can be largely overcome by electrically reducing the ratio of sum to difference of the two channels, which ratio was effectively increased by the addition of the center speaker. It is shown that the signals to the three speakers may be regarded as three independent channels with certain signal-to-crosstalk ratios, which are derived as a function of the level of the center speaker and the amount of electrical reduction of the sum-to-difference ratio. The choice of optimum parameter values and appropriate circuits is discussed.

Transient Distortion in Loudspeakers—R. J. Larson and A. J. Adducci (p. 79)

The response of a loudspeaker to sudden starts and stops of its input signal is analyzed both theoretically and experimentally. Transient distortion occurs when the acoustic output level does not change as suddenly as the input signal. Waveforms of loudspeaker response to various input signals are shown, and a method for plotting a continuous transient response curve is described. The curves indicate a correlation exists between a speaker's steady-state frequency response and its transient performance.

It was found that little correlation exists between the transient performance of a loudspeaker and musical listening tests. Two explanations are given. One discusses how the psychoacoustic performance of the ear tends to make it insensitive to the shape of the wave envelope of a tone burst. Another relates how echoes in the usual listening room tend to mask the hangover transient of the loudspeaker.

A Low-Noise Microphone Preamplifier—A. B. Bereskin (p. 86)

This paper describes a low-noise two-transistor preamplifier which has been developed for use with microphones. For a source resistance of 1000 Ω, a noise figure of 1.3 db has been achieved. A corresponding middle-frequency gain of 40 db, bandwidth of 30 kc and output impedance of 175 Ω resulted.

Cathode Followers and Feedback Amplifiers with High-Capacitance Loads—T. L. Greenwood (p. 89)

Investigation, both theoretically and experimentally, was made into the mode of operation of cathode followers and feedback amplifiers with high-capacitance loads. The capacitance loaded cathode follower compares unfavorably with the resistance loaded cathode follower, particularly regarding operation with fluctuating input signals. Input overdrive of a capacitance loaded cathode follower causes production of transient voltages in the output circuit. Threshold of input overdrive is considerably lower than in resistance loaded cathode followers, especially at high audio frequencies. Also, harmonic distortion is increased at high frequencies and high-frequency response drops off. Experimental analysis of the voltage relations between the input and output circuits was made, and guides for design were developed. It was found that a symmetrical E_g-I_p curve is the most important factor in development of a cathode follower for driving high-capacitance loads where transient distortion is to be avoided.

Bio-Medical Electronics

VOL. BME-8, NO. 3, JULY, 1961

Thirteenth Annual Conference on Electrical Techniques in Medicine and Biology, Washington, D.C., October 31–November 2, 1960

Techniques for Obtaining Absorption Spectra on Intact Biological Samples—K. H. Norris and W. L. Butler (p. 153)

Absorption spectra can be obtained on a wide range of biological samples with little or no sample preparation by using a high sensitivity, low-noise spectrophotometer with the sample in close juxtaposition with the photocathode. An instrument designed for such measurements is described, and possible applications are discussed.

The spectrophotometer is a single-beam recording unit using a double-prism monochromator, 100-watt tungsten source, end-window multiplier-type phototube and an X-Y recorder. The phototube is operated at a constant anode current and a logarithmic voltmeter measures the dynode voltage, providing a photometer which is linear with density change over an optical-density range of 8. The noise level for samples of low density is equivalent to an optical-density change of 0.002 with a response time of 1 second for full scale pen travel. Any part or all of the wavelength region from 200 to 1200 mμ may be scanned with a wide choice of scanning speeds. Provision is included for electrical correction of system response to give a flat baseline characteristic for a selected region of the spectrum. This permits measurements at high sensitivity on samples with high scatter loss.

Versatile sample mounting arrangements permit measurement of a wide range of materials. Liquids, powders, and homogenates are measured in sample cells of appropriate size. Tissue slices and solid samples are mounted on a metal plate with an aperture in the center for the transmitted light to reach the phototube. All samples are mounted with one surface as close to the photocathode as possible, while the opposite surface is illuminated with monochromatic light. A dewar-type cell is described for measurements at liquid nitrogen temperature. Typical spectra are given for a number of biological samples.

Introduction to Digital Computers and Automatic Programming—R. S. Ledley (p. 158)

The vastly increased capabilities that computers offer the bio-medical research worker are primarily due to the utilization of high-speed digital computers. The techniques of automatic programming are attempts to lighten the load of the programmer and coder, by making the computer itself help prepare the program or code, minimizing the amount of writing a programmer need do. From a functional point of view, three types of automatic programs can be distinguished: the algebraic automatic program that can "understand" a code written almost directly in the usual algebraic symbols; the data-manipulation automatic program that greatly facilitates the handling of large masses of data; and the simulation automatic program, which greatly facilitates model building on the computer. The role of the automatic program is to translate "pseudoinstructions," that nearly resemble ordinary language, into direct computer or "machine language" instructions. In this tutorial paper, the basic concepts of the "machine language" are described, first, and then a sketch of some of the techniques for composing and utilizing automatic programming "languages" is given.

Short Distance Broadcasting of Physiological Data—L. A. Geddes, H.H.E. Hoff, and W. A. Spencer (p. 168)

For the transmission of physiological data not requiring complete freedom for the subject, a direct wire system offers many practical advantages including low cost and high reliability.

Such a system is particularly well adapted for bedside monitoring and for the usual studies in the clinical laboratory where the patient is required by his illness to be in a fixed position.

For general purpose physiological telemetry it is necessary to transmit a bandwidth extending to zero cycles per second. Experience has demonstrated that such transmission is possible over a direct wire circuit for a distance of at least half a mile. An over-all response time of 100 μsec provides an adequate bandwidth for the most rapidly changing physiological events.

Measurement of Cerebral Blood Flow by External Collimation Following Intravenous Injection of Radioisotope—W. H. Oldendorf (p. 173)

A technique is described which studies cerebral circulation by monitoring with external collimated scintillation detectors the passage through each cerebral hemisphere of a bolus of radioisotope injected intravenously. The test is simple, harmless, almost painless, and repeatable at frequent intervals. Radiation of the patient is minimized by use of a rapidly excreted isotope. Theoretical considerations of the test are presented. The clinical applications carried out to date are described. The test appears to give a quick relative determination of the total blood flow of each cerebral hemisphere. The possibilities of obtaining an absolute determination are considered.

The Analysis and Interpretation of the Vibrations of the Heart, as a Diagnostic Tool and Physiological Monitor—C. M. Agress and L. G. Fields (p. 178)

This work has been concerned with the development of a presymptomatic diagnostic tool and with the determination of cardiac function by analysis and interpretation of the vibrations of the heart. The data processing associated with the study includes the use of time-frequency analysis and display equipment, power area measurement circuitry, and also automatic digital interval measurements. With this technique, a single channel of data can provide information concerning the heart rate, relative cardiac output, blood-pressure changes, breathing rate, and the effect of changed blood oxygen saturation. The value and application of this technique to bio-astronautical instrumentation can be great.

EEG Records from Cortical and Deep Brain Structures During Centrifugal and Vibrational Accelerations in Cats and Monkeys—W. R. Adey, J. D. French, R. T. Kado, D. F. Lindsley, D. O. Walter, R. Wendt, and W. D. Winters (p. 182)

Electroencephalographic records have been taken from deep regions of the brains of cats and monkeys with chronically implanted electrodes during centrifugal and shaking accelerations comparable to booster forces. Histological and X-ray controls have indicated that displacement of the electrodes does not occur, and that damage to brain tissue is comparable with nonaccelerated animals. A transistorized EEG amplifier suitable for recording in satellite biopack environments has been developed.

In centrifuge tests, transverse accelerations up to 8 G were associated with rhythmic "arousal" patterns of slow waves in hippocampal regions of the temporal lobe during increasing or decreasing acceleration. Longitudinal accelerations between 5 and 6 G produced blackouts after 30 to 40 seconds, with flattening of EEG records, and frequently with induction of epileptic seizure activity in temporal-lobe leads. Shaking tests suggested that vibrational acceleration may be associated with the intermittent "driving" of the cerebral rhythms, in a fashion resembling photic driving, at shaking rates from 11 to 15 cps, and from 22 to 30 cps.

The Electrocardiogram as an Indicator of Acceleration Stress—W. C. Sipple and B. D. Polis (p. 189)

By means of a transistor amplifier mounted before the slip rings of an animal centrifuge it was possible to obtain recordings of the EKG of rats under acceleration stress. With this information, a physiological end point for the tolerance of the rat to 20 G (positive acceleration) was defined as the time to reduce the heart rate of the animal from an initial state ranging from seven to nine beats per second to a final moribund state of 2 beats per second. The instrumentation and techniques employed permit the option of recovering the animal alive after approaching the limit of tolerance to acceleration.

Endoradiosondes for Pressure Telemetering—B. Jacobson and L. Nordberg (p. 192)

Two miniature radio transmitters have been developed for telemetering pressure values from internal body cavities. The large sonde has a volume of 4.1 cc and has a life-time of up to three months when a mercury battery is used. It is employed for physiological studies on animals, and is attached to the wall of the gastrointestinal canal or other body cavities by sutures at operation. The small sonde has a volume of 1.0 cc and a lifetime of three weeks. It is used for gastrointestinal investigations on humans. The transducer in both sondes responds to a pressure variation of 300 cm H_2O which gives a 30-Kc deviation of the 300 to 400 Kc carrier frequency.

A Miniaturized Pneumograph Monitor—P. Stoner and D. A. Holaday (p. 197)

This pneumograph, by virtue of its small size and simplicity, has found application as a physiological monitor during anesthesia. The instrument measures chest and abdominal expansion and does not impede respiration or impose on the upper airway.

Construction of a Neuron Model—R. J. Scott (p. 198)

An application of a linear programming technique to the economical construction of the neuron model introduced by McCulloch is described. Given a set of functional requirements for a neuron, a model satisfying these requirements is efficiently constructed.

Letters to the Editor (p. 203)

Notices (p. 205)

Education

Vol. E-4, No. 2, June, 1961

Editorial—W. R. LePage (p. 47)

Today's Dilemma in Engineering Education—G. S. Brown (p. 48)

The present wide-scale activity to increase the science content of engineering curricula can, if not skillfully accomplished, result in the teaching of science, and not the engineering of science, to engineers. The changes experienced in the substance of the curricula are sometimes so great that faculties encounter great difficulty in providing worthwhile engineering examples to support their presentations of engineering science.

Programmed Learning in Engineering Education—A Preliminary Study—E. M. Williams (p. 51)

A recent study of programmed learning, including experimental use in an electrical engineering department, indicated that the most fruitful application of teaching machine methods is in the presently nonprogrammed or loosely programmed hours spent by students outside classroom or laboratory periods. Programs already developed for use in this study have been concerned with analytical skills; further programs under development are concerned with concepts. Larger scale experiments are planned in which additional questions can be answered, particularly as to whether exposure to programmed instruction adversely affects the capacity of the student to learn independently.

TV Production Techniques and Teaching Efficiency—J. B. Ellery (p. 59)

Educators who venture into the realm of television immediately encounter this question: What equipment is required, and what can be done with it? This paper attempts to provide some basis for an intelligent answer.

In designing the research from which this report derived, attention was focused upon basic television production techniques. A series of instructional segments were produced utilizing these techniques; a second series was subsequently produced with the same instructors and subject matter, but with more elaborate techniques. The two series were then presented for viewing by various student audiences. A control group viewed the first series; an experimental group was shown the second series. Preliminary knowledge of subject matter was determined by a pre-test; degree of learning and retention were measured by an immediate post-test, and a delayed post-test. Those data were then analyzed by means of standard statistical instruments.

In collating and appraising the obtained results it was apparent that a one camera production, with true flat lighting, utilizing close-up camera coverage and a modicum of technical skill and imagination, was as effective as the more elaborate production in ordinary lecture-teaching situations.

An Experiment in Laboratory Education—G. Kent and W. H. Card (p. 63)

A departure from traditional forms of under graduate laboratory education has been incorporated into the electrical engineering curriculum at Syracuse University. In this paper is presented a summary of the reasons for this innovation, a description of the course, and an evaluation of our experiences with it.

As curricula in electrical engineering become more science centered, it is essential that the undergraduate engineering laboratory take as its prime objective the development of skills requisite to the planning and execution of meaningful experiments and the promotion of an understanding of the relationships between theory and experiment. Briefly, the objective is an education in the experimental aspects of scientific method.

This objective has not been well served in the past by the traditional laboratories. Too frequently, student motivation has been poor enough to limit substantially the learning process, and the typical experiment was not likely to afford an opportunity for education in science.

To attempt to fulfill the objectives stated, a separate course in laboratory was initiated. The separation of the laboratory from its traditionally dependent role was expected to permit greater freedom in the technical content of the course and to emphasize the importance of the laboratory to science. The plan of the course was inspired by the belief that motivation, the prime force in the learning process, is determined in part by the significance of the experiments the student is asked to perform, and that an education in science can be obtained only by the exercise of its method. Accordingly, the experiments were conceived as nontrivial real engineering problems whose solutions demand independent study and planning on the part of the student. The technical content of the experiments was arranged to constitute an organized development of scientific knowledge.

Consistent with this general conception, the course is built around a sequence of problems which the student is expected to solve. These assignments state the problem and discuss its

origin and significance. A list of apparatus, references to the literature, and occasionally some experimental hint in the form of a provocative statement are given. The students plan their experiments and proceed with them at their own pace. The only time limitations are that a reasonable number of projects must be completed during the course. In addition to keeping laboratory notebooks, the students are required to prepare several specific kinds of reports. In contrast to the common practice of marking solely on the report, grades are determined by total laboratory performance.

The evaluation of this program is a continuous process. Although at this date no conclusive judgments can be made, early indications of student response have stimulated great enthusiasm among the teaching staff. We are confident that progress toward our objectives is substantial.

The Computer Revolution in Engineering Education—R. E. Machol (p. 67)

The ready availability of high-speed digital computers has wrought a fundamental and unprecedented change in engineering education. Described herein are one university's experiences with a small digital computer, on which thousands of undergraduates have been taught to program within the past year. A new approach to the teaching and administration of computers is required, as is a new approach to almost every aspect of the engineering curriculum. The shape of things to come is briefly examined.

Engineering Education in Canada and the Cooperative Electrical Engineering Program at the University of Waterloo—B. R. Myers and J. S. Keeler (p. 71)

Although cooperative engineering is practiced at several universities in the United States, that at the University of Waterloo is unique in Canada. The baccalaureate program requires five years of continual attendance, during which the student spends alternate three-month periods in school and in industry.

A distinctive feature of the plan is the maintenance of a Coordination Department within the University organization. Staffed by senior professional engineers, this department acts as liaison between industry and the students.

Two programs of study are offered in the undergraduate electrical engineering curriculum. One of these is designed for the heavy electromechanical and power systems engineer. The other embraces electronics, communication and computery disciplines, with a greater concentration of theoretical studies.

Although the University is still in its infancy, both industrial and student acceptance of the cooperative plan has exceeded initial expectations. There is every indication that co-operative engineering education will rapidly assume a dominant role in the Canadian academic scene.

Electronic Computers

VOL. EC-10, NO. 2, JUNE, 1961

A Straightforward Way of Generating All Boolean Functions of N Variables Using a Single Magnetic Circuit—K. V. Mina and E. E. Newhall (p. 151)

A correspondence has been established between the topology of relay contact networks and the topology of magnetic circuits, which may be applied to a relay tree to produce a magnetic structure capable of generating, in a simple manner, all Boolean functions of N variables. Once the basic magnetic topology is established, it may be distorted to achieve winding simplicity at the expense of magnetic circuit complexity. In the resulting arrangement, the drive, hold (variable) and reset windings are always in the same position, regardless of the function to be generated. Any one of the 2^{2^N} functions of N variables is generated by linking a selected group of the output legs.

The structure is such that all switching paths are of equal length, causing all outputs to be equal in amplitude. This balanced arrangement also permits the holding MMF to be significantly smaller than the drive MMF. The holding scheme is a symmetrical one, specifically arranged to overcome shuttle flux problems and reduce noise.

An 8-leg manganese magnesium zinc ferrite structure is operated easily at a 4-μsec cycle time with an output of 500 mv into 5 ohms. The peak-signal-to-peak noise ratio was at worst 8:1. A 1-in-256 selector, using seventeen 16-leg structures, is under construction.

The structure described here is in a sense the complement of the laddic, in that the drive and hold windings are always applied in fixed positions and different functions are generated by linking different sets of output legs.

On the State Assignment Problem for Sequential Machines—I. J. Hartmanis (p. 157)

In this paper, the problem of determining economical state assignments for finite-state sequential machines is studied. The fundamental idea in this study is to find methods for selection of these assignments in which each binary variable describing the new state depends on as few variables of the old state as possible. In general, these variable assignments in which the dependence is reduced yield more economical implementation for the sequential machine than the assignments in which the dependence is not reduced. The main tool used in this study is the partition with the substitution property on the set of states of a sequential machine. It is shown that for a sequential machine the existence of assignments with reduced dependence is very closely connected with the existence of partitions with the substitution property on the set of states of the machine. It is shown how to determine these partitions for a given sequential machine and how they can be used to obtain assignments with reduced dependence.

A Generalization of a Theorem of Quine for Simplifying Truth Functions—J. T. Chu (p. 165)

A method of Quine for identifying the core prime implicants of a given truth function, without obtaining all its prime implicants, is generalized under the so-called "don't care" conditions. It is shown that our method is equivalent to, and sometimes an improvement of, a result of Roth. When all the prime implicants (under the don't care conditions) of a truth function are given, our method becomes a generalization of a result of Ghazala and is equivalent to another result of Roth. It is also pointed out that our method may be used, in a way similar to using Roth's, for simplifying truth functions.

Reducing Computing Time for Synchronous Binary Division—R. G. Saltman (p. 169)

The computing time for binary division is shortened by performing division, radix 2^p on the binary operands, where p is a positive integer. Each quotient digit radix 2^p is computed in almost the same time required to determine a binary quotient digit. Therefore, computing time is reduced by approximately the factor p over conventional binary division. The method is most useful for synchronous machines but can be applied to either serial or parallel operation.

The theory of nonrestoring division in any integral radix r is discussed. Each quotient digit is considered as the sum of two recursive variables a_k and b_k, whose values depend on the divisor multiplier and relative signs of the partial remainders. The divisor multiplier is limited to odd integers in order to determine the quotient digit unambiguously. Using a_k and b_k, a single recursive equation combining all sign conditions is derived. This permits the derivation of the correct round-off procedure and shows that binary nonrestoring division is a particular case of nonrestoring division, radix r.

An arrangement of components for a serial computer and a sample division for radix four are given.

The Philips Computer Pascal—H. J. Heijn and J. C. Selman (p. 175)

PASCAL is a binary parallel computer with a word length of 42 bits, a clock-pulse repetition time of $1\frac{1}{2}$ μsec, performing, on the average, 60,000 operations per second. Wired-in floating-point facilities are provided. Core storage is backed by a drum and by magnetic tape. There are modification versions for indexing as well as for stepping-up purposes. Special instructions include count and repeat instructions, jumps on the result of an earlier comparison, and two kinds of link instructions for facilitating the use of subroutines and interpretative programs. Transfer instructions enable a simultaneous bi-directional data flow between drum and cores or between tape and cores while computations are going on.

Esaki Diode NOT-OR Logic Circuits—H. S. Yourke, S. A. Butler, and W. G. Strohm (p. 183)

A basic technique is presented which enables the development of Esaki diode NOT-OR logic circuits. Two embodiments of the basic scheme are discussed, which, when combined with an OR-DELAY circuit, provide a logically complete system. Emphasis is placed on the more economical of the two embodiments. A tolerance analysis is included, which demonstrates that the technique enables the practical design of logic circuits. The requirements placed on Esaki diode characteristics, and the speed limitations of the circuits, are discussed. Examples of working circuits are shown, including photographs of voltage wave shapes.

Logic Circuits Using Square-Loop Magnetic Devices: A Survey—J. L. Haynes (p. 191)

The past decade has been a productive period for development in the field of large-scale digital computers. Magnetics has played an increasingly important part in these developments. Magnetic cores, tapes, and drums have found almost universal acceptance for memory functions. Some future computers will undoubtedly use magnetic logic and control circuits. This survey is a capsule view of twenty-four square-loop magnetic logic circuits which have been proposed or developed so far, with a brief description of the way each circuit or circuit family meets the requirements of logic circuitry. All circuits are treated with a consistent terminology, and the generic relationships among circuits are stressed. Included in this survey are parallel and series transfer core-diode schemes, core-transistor schemes, and all-magnetic schemes of various topologies.

A Bibliographical Sketch of All Magnetic Logic Schemes—D. R. Bennion, H. D. Crane, and D. C. Engelbart (p. 203)

An all-magnetic logic scheme is one with which a workable digital system could be constructed involving only magnetic elements, current-carrying conductors, and sources of clock pulses. Historical developments of both resistance schemes (dependent upon coupling-loop resistance) and nonresistance schemes (possessing at least first-order independence of coupling loop resistance) are described, with reference to all relevant published work known to the authors. Included are: 1) schemes using electric-circuit transfer linkage with simple cores,

multipath cores, and thin-film elements, and 2) schemes using continuous magnetic structures where transfer linkage is purely magnetic.

Design of an All-Magnetic Computing System: Part I—Circuit Design—H. D. Crane and E. K. Van de Riet (p. 207)

This paper describes the circuits used in a decimal arithmetic unit which utilizes ferrite magnetic elements and copper conductors only. The arithmetic operations of addition, subtraction, and multiplication are performed with a product and sum capacity of three decimal digits. The sole logical building block of this system is a two-input inclusive-OR module with a fan-out capability of three with any desired logical positive and negative combination. The system involves the use of some 325 modules, each of which contains two magnetic multiaperture devices (MAD's). This paper gives a complete description of the circuit and physical arrangement of the machine. The system is controlled from a manual keyboard, and readout from the machine is via incandescent lamps controlled directly from the MAD elements, no intermediate elements being required.

The "worst case" drive-pulse amplitude range for the completed machine, varying all clock pulses simultaneously, is ±10 per cent.

Design of an All-Magnetic Computing System: Part II—Logical Design—H. D. Crane (p. 221)

A logical design technique is developed for use with the particular module developed for this system. The detailed properties of this module, as well as the philosophy that led to its particular form, were covered in Part I of the paper. Briefly, the module forms the (inclusive) OR function of two input variables. This function can subsequently be transmitted to three receivers, each transfer being independently logically positive or negative. The read-outs are non-destructive and the transmitter module must be explicitly cleared before read-in is again possible. In view of the relatively small fan-in and fan-out for this module, and since only the OR function can be directly formed during any single transfer, complex logic functions must be formed slowly, a step at a time. This step-by-step generation of functions results in the need for more modules than might otherwise be required, but aside from that, the synthesis techniques are not particularly different from those of customary logical design. In particular, the design of an arithmetic unit designed for decimal addition, subtraction and multiplication is outlined. Some comparisons are noted between this particular all-magnetic logic scheme and conventional core-diode schemes. Comparisons are also made between magnetic logic schemes in general and some other realization schemes, such as ac-operated parametrons and conventional transistor systems.

A 2.18 Microsecond Megabit Core Storage Unit—C. A. Allen, G. D. Bruce, and E. D. Council (p. 233)

A magnetic core memory is described which has a read-write-cycle time of 2.18 μsec, an access time of 1 μsec, and a storage capacity of 1,179,648 bits. The array configuration and the design of the driving system are shown. The core and transistor requirements are discussed, and a description is given of the sensing and the driving circuitry. Design factors which governed the choice of the 3-dimensional system organization are presented.

Matrix Switch and Drive System for a Low-Cost Magnetic-Core Memory—W. A. Christopherson (p. 238)

A unique system of ferrite-core matrix switches and drivers has been developed for a low-cost magnetic-core memory. The memory uses coincident-current techniques and has a capacity of 10,000 characters with seven bits per character. A 20-μsec read-compute-write cycle features serial-by-character processing. Approximately 7 μsec is computing time, and 13 μsec is read-write time.

The matrix switch requires only two sets of five drivers to select one out of 100 individual outputs. The drivers operate in an unusual three-out-of-five coding arrangement. A Set and Reset a driver, each using four transistors in parallel, are also required for the matrix switch. Two matrix switches provide the 200 *X-Y* half-select drives for a 100×100 seven-plane core array. At read time, two half-select current pulses of 250 ma to 300 ma are emitted with an effective 10 per cent to 90 per cent rise time of 0.3 μsec. At write time, half-select current pulses with 1.2-μsec rise time are emitted on the same selected lines, but in the opposite direction.

A new method of timing the drive current allows the read pulse to rise in 0.3 μsec, even with a low-voltage power supply and an inductive load that would otherwise limit the rise time to 0.8 μsec.

All current-driving circuits use alloy junction transistors. The drive current is furnished from a 10 to 12 volt power supply, and temperature compensation of the drive currents is accomplished through control of power-supply voltage. Operating temperatures range from 10°C to 40°C.

Serial Matrix Storage Systems—M. Lehman (p. 247)

Coincident-current techniques, usually associated with parallel ferrite-core stores, may also be used for the operation of serio-parallel or purely serial memories. After outlining, in block diagram form, one possible physical realization of a serial system, the paper examines the conditions under which such a store is economically justified. The distinguishing feature of the system discussed is that coincidence is established in the memory matrix between two currents representing an address signal and a time signal, respectively. Studies of the characteristics and economics of serio-parallel devices are, however, not reported in detail.

It is shown how the properties of the time-controlled serial store may lead to the adoption of a word-asynchronous design for serial digital computers. In such a machine, timing is not controlled or determined by limited store access. As examples, the paper indicates how the serial techniques facilitate the incorporation into small serial computers, of autonomous transfers, automatic floating point operations, high speed multiplication, division and shift orders and asynchronous transfers between, say, a high speed store and a magnetic drum

A Flexible and Inexpensive Method of Monitoring Program Execution in a Digital Computer—F. F. Tsui (p. 253)

A method of monitoring the program execution in a digital computer on the basis of the flow diagram of the computing program has been devised. A comparatively low-cost equipment for monitoring a maximum of 64 boxes in a flow diagram has been constructed.

The monitoring method is flexible and convenient in its application. It can be used in connection with relative or symbolic addresses, compilers, etc. The user must provide only a flow diagram drawn on translucent paper in a certain form and the information to correlate this diagram with the computing program. A subroutine modifies the computing program as needed for the monitoring purpose and restores it to its original form when the user so desires. The monitoring introduces only a very small increase in computing time, requiring for each call-up of a box in the flow diagram only a time amounting to that needed for two simple unconditional jumps. The monitor can be used to present during the computation a visual dynamic picture of the progress of the program and to register, on occurrence, the whereabouts of an interruption, thus facilitating the tracing of the error.

The principle of the monitoring method and the subroutine program, and the essentials of the constructed monitor equipment, are described in detail.

On the Encoding of Arbitrary Geometric Configurations—H. Freeman (p. 260)

A method is described which permits the encoding of arbitrary geometric configurations so as to facilitate their analysis and manipulation by means of a digital computer. It is shown that one can determine through the use of relatively simple numerical techniques whether a given arbitrary plane curve is open or closed, whether it is singly or multiply connected, and what area it encloses. Further, one can cause a given figure to be expanded, contracted, elongated, or rotated by an arbitrary amount. It is shown that there are a number of ways of encoding arbitrary geometric curves to facilitate such manipulations, each having its own particular advantages and disadvantages. One method, the so-called rectangular-array type of encoding, is discussed in detail. In this method the slope function is quantized into a set of eight standard slopes. This particular representation is one of the simplest and one that is most readily utilized with present-day computing and display equipment.

An Accurate Analog Multiplier and Divider—E. Kettel and W. Schneider (p. 269)

In the time-division multiplier the product $x_1 \cdot x_2$ is formed by pulse-duration modulation with x_1 and amplitude modulation with x_2. The circuit can be arranged in such a manner that division by means of a quantity x_3 can be carried out simultaneously, the output being $x_1 \cdot x_2/x_3$. When transistor switches are employed the error is $1 \cdot 10^{-4}$ machine units only. The zero error for x_2, used for amplitude modulation, can be reduced to $2 \cdot 10^{-5}$ machine units.

High-Speed Analog-to-Digital Converters Utilizing Tunnel Diodes—R. A. Kaenel (p. 273)

Two analog-to-digital sequential converters have been devised which combine in one tunnel-diode pair per bit the functions of an amplitude discriminator and memory. In addition, one of the two schemes utilizes each tunnel-diode pair as a delay network. The conversion duration of one of these six-bit converters, which employs germanium 2N559 transistors and gallium arsenide 1N651 tunnel diodes, has been set to 1 μsec. Shorter conversion times are possible, but are not required in the present application of that converter as an integral part of an electronic high-speed signal processing system. The use of tunnel diodes presents a significant improvement in the art of converter design by virtue of circuit simplicity and performance.

The paper describes the principle and operation of the converters and discusses pertinent considerations for their design. Particular emphasis is given to the discriminator property of a series-aiding tunnel-diode pair.

A comprehensive bibliography relating to tunnel-diode switching circuits is attached.

Engineering Management

VOL. EM-8, NO. 2, JUNE, 1961

Two examples of plant design are described and an abstract model of the process of design is suggested. The model is used to discuss the search for possible solutions, the strategies for their examination and the rules for choosing between them. It seems likely that the model applies only to problems requiring novel solutions and not to those for which the form of solution is known, but the choice of parameters to meet conflicting objectives is difficult.

Analysis of Engineering Performance—H. Versteege (p. 71)

An analytical scheme is presented for measuring the physical completion of engineering effort and relating this to the appropriate segment of a budget curve, representing planned expenditure of effort. The method was developed in connection with weapons systems projects. A measure (the delta factor) is devised of the variation of actual physical engineering completion from the standard or expected value. A computational algorithm for the delta formula is given. Illustrations are given of its use as a diagnostic tool.

A Systematic Procedure for System Development—R. C. Hopkins (p. 77)

A technique is described for the development of system objectives, requirements, specifications, and conceptual design. It is derived from experience with a number of actual systems in the fields of air defense and airborne fire control. The need for precise knowledge of system functional objectives is stressed. A checklist relating to environmental requirements is presented. A seven-step process is described from functional objectives to model and test.

Engineering Organization for a Large Air Force Communication System—R. D. Chipp (p. 86)

This paper describes the engineering organization which was set up by a contractors' team to design a major Air Force Communication System. It discusses some aspects of the first year's operation.

The Core Concept of System Management—J. D. McLean (p. 92)

Some deficiencies in the practice of systems management, and the need for an "architect" in addition to the contractor are presented. The "core concept" is described. Several advantages of this approach are indicated and its separation from hardware design and fabrication are stressed.

Pitfalls and Safeguards in Real-Time Digital Systems with Emphasis on Programming—W. A. Hosier (p. 99)

Real-time digital systems are largely a technical innovation of the past decade, but they appear destined to become more widespread in the future. They monitor or control a real physical environment, such as an air-traffic situation, as distinguished from simulating that environment on an arbitrary time scale. The complexity and rapid variation of such an environment necessitates use of a fast and versatile central-control device, a role well suited to digital computers. The usual system will include some combination of sensors, communication, control, display, and effectors. Although many parts of such a system pose no novel management problems, their distinguishing feature, the central digital device, frequently presents unusually strict requirements for speed, capacity, reliability and compatibility, together with the need for a carefully designed stored program. These features, particularly the last, have implications that are not always foreseen by management. An attempt is made to point out specific hazards common to most real-time digital systems and to show a few ways of minimizing the risks associated with them.

Information Theory

VOL. IT-7, NO. 3, JULY, 1961

This is the first in a series of invited tutorial, status and survey papers that will be provided from time to time by the PGIT Committee on Special Papers, whose Chairman is currently L. A. Zadeh. Hopefully these papers will fill a gap that we have long felt existed in our publication program. In the past, there has been no formal method, short of entire Special or Monograph Issues, of providing basic introductory material or surveys of portions of the information theory field.—*The Administrative Committee*

A narrow-band process is conveniently characterized in terms of a complex envelope whose magnitude is the envelope, and whose angle is the phase variation of the actual narrow-band process. When the narrow-band process is normally distributed, the complex envelope has the properties of a complex normally distributed process. This paper investigates the approach to the complex normally distributed form of the complex envelope of the output of a narrow-band filter when the input is wide-band non-Gaussian noise of a certain class, and the bandwidth of the narrow-band filter approaches zero. The non-Gaussian input consists of a train of pulses having identical waveshapes, but random amplitudes and phases. While the derivations assume statistical independence between pulses, it is shown that the results are valid for a certain interesting class of dependent pulses. The Central Limit Theorem is proved in the multidimensional case for the output process.

In a stationary Gaussian Markov process (or Ornstein-Uhlenbeck process) the expected number of axis crossings per unit time, the probability density of the lengths of axis-crossing intervals, and the probability of recurrence at zero level do not exist as ordinarily defined. In this paper new definitions are presented and some asymptotic formulas are derived. Certain renewal equations are approximately satisfied, thereby suggesting an asymptotic approach to independence of the lengths of successive axis-crossing intervals. Mention is made of an application to the filter-clip-filter problem.

The ideal probability-compounding M-ary receiver is derived for a fading, noisy, multi-diversity channel, in whose the link fadings may be mutually correlated, as may the link noises. The results are interpreted in terms of block diagrams involving various filtering operations. Two special cases, those of very fast and very slow fading, are considered in detail.

In the discrete case, the Shannon expression for entropy is obtained as a line integral in probability space. The integrand is the "information density vector" $(\log p_1, \log p_2, \cdots, \log p_n)$. In the continuous case, the continuous analog of information density is integrated to obtain the entropy expression for continuous probability distributions.

The paper considers group codes whose function is split between error correction and error detection with retransmission. For a given code, the minimum error probability is obtained when retransmission occurs whenever an error is detected. An estimate of the redundancy added by retransmission is given and the behavior of retransmission channels as the length of the code words increases is studied. Most of the analysis is for the binary symmetric channel, although some of the results apply to more general channels.

Many problems in electrical engineering, such as the synthesis of linear n ports and the detection and filtration of multivariable systems corrupted by stationary additive noise, depend for their successful solution upon the factorization of a matrix-valued function of a complex variable p.

This paper presents several algorithms for affecting such decompositions for the class of rational matrices $G(p)$, *i.e.*, matrices whose entries are ratios of polynomials in p. The methods employed are elementary in nature and center around the Smith canonic form of a polynomial matrix. Several nontrivial examples are worked out in detail to illustrate the theory.

Instrumentation

VOL. I-10, NO. 1, JUNE, 1961

A High-Resolution Ammonia-Maser-Spectrum Analyzer—J. A. Barnes and L. E. Heim (p. 4)

A quartz crystal oscillator was phase locked to an ammonia beam maser to give a sufficiently monochromatic signal to enable the measurement of power spectra of other crystal oscillators multiplied from 1458 to 145,800 times in frequency. The perturbing effects of amplifiers introduced in the early stages of multiplication were observed. It was found that, for maximum purity, dc filaments on the oscillator and early stages of multiplication were essential. With this system it was possible to investigate sidebands and noise on various oscillators and determine which oscillators were most suited for precise frequency measurements with the National Bureau of Standards atomic frequency standards.

An RF Voltage Standard for Receiver Calibration—G. U. Sorger, B. O. Weinschel, and A. L. Hedrick (p. 9)

Accurate sources of low-level RF voltage are very useful for calibrating receivers and for other laboratory purposes, but they are difficult to achieve. The main errors in standardizing such sources are in knowledge of RF impedance. This is a critical factor because, although we can measure power accurately at RF, we must derive voltage from power and impedance. The use of bolometer bridge thrumounts and micropotentiometers as voltage standards is discussed, and a series combination of these two types of elements is analyzed in some detail. An arrangement is described which can provide output voltages from 1 volt to 10 μv in decade steps over the frequency range of 2 to 1000 Mc with an absolute accuracy (traceable to the National Bureau of Standards) of the order of 3 per cent.

Data Transmission for the NRL Space Surveillance System—M. G. Kaufman and F. X. Downey (p. 18)

A data-transmission system has been developed which links four distant receiving sites

of the U. S. Navy Space Surveillance system to a data-reduction center located at Dahlgren, Va. The receiving sites form a fence located on a great circle route across the southern U. S. from Georgia to California. Each receiver site is coupled to the data center by a commercial voice-quality, duplex (two-way) telephone line. Standard FM telemetry techniques are used to transmit eight channels of analog data on each telephone line. These data are transmitted on eight discrete frequency-modulated carriers in a frequency band from 270–2455 cps. In addition to these FM data carriers, unmodulated tones are used for monitoring, compensation, and command functions.

The data from each receiver site are permanently stored on paper recordings at the data-reduction center, so that this information can be assimilated at one location on a real-time basis. These data are used to compute the orbital parameters of satellites detected by the Space Surveillance system.

The data-transmission system has been in operation for a year on a 24-hour basis with negligible down time. Off-line calibration techniques have been employed, so that errors introduced into the data by the transmission system can be held to 2 per cent without interfering with the detection capabilities of the surveillance system. Tests indicate that the number of channels can be increased from 8 to 24 per telephone line by the use of crystal-controlled oscillators and crystal filters.

Stable Microwave Signal Source Using a Backward-Wave Oscillator—M. M. Brady (p. 23)

A backward-wave oscillator has been combined with a waveguide frequency discriminator in a feedback loop to provide a tunable stable microwave signal source that can be readily built up from standard microwave laboratory components. The use of a backward-wave oscillator in a frequency-stabilization system results in a system that can be analytically and physically less complex than an equivalent system using a reflex klystron. The small-signal linearity inherent in the microwave portion of the system allows descriptive equations to be written concerning the system operation. The equations developed are not necessarily restricted to a system using a backward-wave oscillator; they may well apply to any system using a voltage-tuned oscillator. The degree of stabilization desired can be realized through the proper design of the feedback amplifier involved and is limited only by the frequency stability of the cavity reference. An experimental system using an X-band backward-wave oscillator and a medium-Q cavity achieved a stability of 1 to 1.5 parts in 10^7.

Automatic Digital-Data-Error Recorder—E. J. Hofmann (p. 27)

In view of the widespread interest in digital communication systems, and in order to better understand the nature of long data circuits, an automatic digital - data - error recorder (ADDER) has been developed. The ADDER is a device which automatically detects and records errors occurring during the transmission of digital information over data circuits.

Information of known structure is transmitted at one end of a data channel and compared at the output by means of the ADDER.

The ADDER is composed of analog-to-digital converters, shift registers, counters for storing information, comparator circuits for error detection, and sequencing logic to control the shifting, storing, and punching out of information. Flip-flop storage is used to store a maximum of 126 bits of information.

The following information in regard to the transmission performance of the over-all system is obtained:

1) The number of words in error and their time distribution,
2) The number of bits in error in erroneous words and their position,
3) The relative occurrence of lost or gained sync (or start) pulses.

The output of the device is punched paper tape which, through the use of a suitable program, may be analyzed by an IBM 709 or similar computer.

The ADDER has been used to obtain the error performance of several telephone circuits in the past year. Results of these tests indicate that the major limitation of the present ADDER is its inability to record clusters of errors *in toto*.

High-Speed Fourier Analysis with Recirculating Delay-Line-Heterodyner Feedback Loops—J. Capon (p. 32)

It is often desired to obtain high-speed spectrum analysis. Previously, the only feasible manner in which this could be done was by means of a bank of parallel filters.

The coherent memory filter is a device that represents a new and novel approach to the spectrum analysis problem. It is shown that the response of this device to any arbitrary input signal is a close approximation of the input spectrum. Thus, this instrument meets the requirement mentioned previously.

In addition, the coherent memory filter has the advantage, with respect to the bank of filters, of being capable of observing rapid changes in the input spectrum that occur from one processing period to the next. This is due to the fact that the device employs a delay line and heterodyner in a closely regulated unity-gain feedback loop, so that there are no problems of energy storage in resonant filter elements.

The applications of the coherent memory filter are also discussed. These include such fields as speech recognition, vibration and noise analysis, and radar-pulse compression systems.

Application of a Spectrum Analyzer for Use with Random Functions—L. G. Zukerman (p. 37)

Curves are presented relating the resolution, stability, and analysis time for sweep-type spectrum analyzers when used for spectral studies of random functions. Simple precautions are mentioned for such applications of spectrum analyzers.

Multiphase Wattmeters Based on the Magneto-Resistance Effect of Semiconductor Compounds—M. J. O. Strutt and S. F. Sun (p. 44)

Owing to the great carrier mobilities, the magneto-resistance effect of indium-antimonide and indium-arsenide is considerable. Within a certain range around a properly chosen magnetic bias flux density, the change of resistance is very nearly proportional to the change of magnetic flux density. If this change of flux density is made proportional to the alternating phase current of an electric power circuit, whereas the current through the magneto-resistance element is made proportional to the phase voltage, a dc voltage arises between the contacts of this element, which is proportional to the real power. By altering the above arrangement, the dc voltage between the contacts of the magneto-resistance element may be made proportional to the reactive power.

These circuits have been adapted to multiphase circuits.

If the temperature changes, the wattmeter indications change also, due to a change of resistance of the magneto-resistive elements. In a compensating circuit, a relatively large resistance is arranged in series with the element, both depending on temperature according to similar curves. A third resistance, of the same order of magnitude as the element, is arranged in parallel to the series connection. By proper adjustment of the two compensating resistances, satisfactory compensation of temperature effects may be obtained.

The magneto-resistive elements are preferably Corbino-disks, the ring contacts of which are broken up and properly interconnected so as to avoid short-circuit rings.

Space Electronics and Telemetry

VOL. SET-7, NO. 2, JUNE, 1961

Noise Figure Measurements Using Celestial Sources—F. G. Kelly (p. 32)

Several convenient sources of radio noise exist in the heavens. It is possible to utilize these sources for accurate measurements of receiver noise figure, provided that a suitable high-gain antenna is available. The method for making such a measurement is described herein.

Low-Speed Time-Multiplexing with Magnetic Latching Relays—J. F. Meyer (p. 34)

Many satellite and spacecraft telemetry systems require that measurements be time-shared at relatively low rates (less than one sample per second) and that several rates be available in order to minimize redundant sampling. This paper discusses a multiplexing system designed specifically for low-speed operation and multiple-rate flexibility so as to gain advantage in other critical areas of performance.

A unique synthesis of the basic circuit provides for the time-multiplexing of n measurements with $n-1$ magnetic latching relays. Assuming an external two-phase clocking source, no other components, active or passive, are required in the circuit. Other advantages of the circuit are: 1) low average power consumption, 2) no additional monitoring or reset circuitry required to insure proper operation at turn-on or after momentary power failure, and 3) the virtual impossibility of switching more than a single measurement to the common output line, even in the case of component or wiring failure.

Thermal-Noise Errors in Simultaneous-Lobing and Conical-Cs Scan Angle-Tracking Systems—J. A. Develet, Jr. (p. 42)

Relationships for rms angular errors are developed for certain common active space probe and satellite angle-tracking systems. The only source of error considered is the thermal and shot noise of the receiver, bandlimited by the tracking servo noise bandwidth. If additional smoothing after angular readout is performed, only the special case of many samples averaged over a time long compared to the reciprocal servo noise bandwidth is considered.

These thermal-noise errors are by no means the usual practical accuracy limitations of an angle-tracking system. They do, however, set bounds on minimal signal strength allowable for the desired tracking accuracy.

The received signals were assumed to be sinusoidal of constant peak amplitude with the information, if any, contained in phase or frequency modulation. This is the most common signal in space probe or satellite tracking.

Some Elementary Considerations of Satellite Earth Communication Systems—T. Teichmann (p. 51)

The relation between transmitter bandwidth, information gathering rate, and communication system cost is discussed for a simple model of a satellite-ground system, in terms of basic power, weight and cost parameters.

Abstracts and References

Compiled by the Radio Research Organization of the Department of Scientific and Industrial Research, London, England, and Published by Arrangement with that Department and *Electronic Technology*, London, England

NOTE: The Institute of Radio Engineers does not have available copies of the publications mentioned in these pages, nor does it have reprints of the articles abstracted. Correspondence regarding these articles and requests for their procurement should be addressed to the individual publications, not to the IRE.

The number in heavy type at the upper left of each Abstract is its Universal Decimal Classification number. The number in heavy type at the top right is the serial number of the Abstract. DC numbers marked with a dagger (†) must be regarded as provisional.

UDC NUMBERS

Certain changes and extensions in UDC numbers, as published in PE Notes up to and including PE 666, will be introduced in this and subsequent issues. The main changes are:

Artificial satellites:	551.507.362.2	(PE 657)
Semiconductor devices:	621.382	(PE 657)
Velocity-control tubes, klystrons, etc.:	621.385.6	(PE 634)
Quality of received signal, propagation conditions, etc.:	621.391.8	(PE 651)
Color television:	621.397.132	(PE 650)

The "Extensions and Corrections to the UDC," Ser. 3, No. 6, August, 1959, contains details of PE Notes 598–658. This and other UDC publications, including individual PE Notes, are obtainable from The International Federation for Documentation, Willem Witsenplein 6, The Hague, Netherlands, or from The British Standards Institution, 2 Park Street, London, W.1., England.

ACOUSTICS AND AUDIO FREQUENCIES

534.2:530.145 2438

Quantum-Mechanical Many-Particle Treatment of Sound Propagation—D. E. McCumber. (*Nuovo Cim.*, vol. 17, Suppl. 1, pp. 8–42; 1960. In English.)

A list of organizations which have available English translations of Russian journals in the electronics and allied fields appears each June and December at the end of the Abstracts and References' section.

The Index to the Abstracts and References published in the PROC. IRE from February, 1960 through January, 1961 is published by the PROC. IRE, May, 1961, Part II. It is also published by *Electronic Technology* and appears in the March, 1961, issue of that Journal. Included with the Index is a selected list of journals scanned for abstracting with publishers' addresses.

534.23 2439

Synthesis of Stepped Acoustic Transmission Systems—J. E. Holte and R. F. Lambert. (*J. Acoust. Soc. Am.*, vol. 33, pp. 289–301; March, 1961.) Procedures are described enabling acoustic systems supporting one-dimensional harmonic waves to be synthesized for a prescribed frequency dependence of the input reflection coefficient, the characteristic impedance of the system being allowed to vary in steps.

534.232:534.24 2440

Effect of a Reflecting Plane on an Arbitrarily Oriented Multipole—D. A. Bies. (*J. Acoust. Soc. Am.*, vol. 33, pp. 286–288; March, 1961.) General expressions are given for the acoustic power radiated by either a dipole or quadrupole oriented above an infinite rigid reflecting plane are derived.

534.232:537.228.1 2441

Transients and the Equivalent Electrical Circuit of the Piezoelectric Transducer—L. Filipczyński. (*Acustica*, vol. 10, no. 3, pp. 141–154; 1960.) A transmission-line equivalent circuit is derived from an analysis of thickness vibrations of an X-cut quartz transducer.

534.24:534.88 2442

Theoretical Development of Volume Reverberation as a First-Order Scattering Phenomenon—H. R. Carleton. (*J. Acoust. Soc. Am.*, vol. 33, pp. 317–323; March, 1961.) A statistical distribution of scatterers described by a spatial correlation function leads to a representation of the reverberation by random noise passing through a narrow filter whose properties are determined by the transmission mode.

534.283–8:537.311.31 2443

Ultrasonic Attenuation in Normal Metals at Low Temperatures—A. B. Bhatia and R. A. Moore. (*Phys. Rev.*, vol. 121, pp. 1075–1086; February, 1961.)

534.6:621.374.5 2444

Acoustic Delay Line—I. Ver. (*Frequenz*, vol. 14, pp. 317–321; September, 1960.) A system is described which has a continuously variable delay in the range 0–3 ms; it consists of pressure chambers coupled to microphones by metal tubing. The application of the delay line for the determination of noise correlation functions is illustrated.

534.6–8:621.385.83:537.228.1 2445

Ultrasonic Image Conversion with an Electron Mirror—G. Koch. (*Acustica*, vol. 10, No. 3, pp. 167–170; 1960. In German.) A development of the image converter is described [see, *e.g.*, 2084 of 1959 (Freitag and Martin)] in which slow electrons reflected from an oscillating quartz crystal in the ultrasonic field in a water tank containing the object are separated from the incident beam by means of a magnetic field. The contrast is greatest with moving objects.

534.6.087.2 2446

Automatic Evaluation Equipment for Subjective Assessments—G. Steinke, M. Wasner, and J. Seyfried. (*Tech. Mitt. BRF, Berlin*, vol. 4, pp. 85–88; September, 1960.) The apparatus described is designed for use in tests for assessing the quality of sound transmission systems.

534.75 2447

Loudness Function and Differential Sensitivity of the Intensity—I. Barducci. (*Ricerca Sci.*, vol. 30, pp. 1518–1523; October, 1960. In English.) The method proposed by Schiaffino (*Ann. Télécommun.*, vol. 12, pp. 349–358; October, 1957) for deducing the loudness function from experimental values of differential auditory sensitivity can be modified to agree with more recent data obtained *e.g.*, by Robinson and Dadson (1947 of 1958).

534.76 2448

The Transmission of 'Room Information'—K. Wendt. (*Rundfunktech. Mitt.*, vol. 4, pp. 209–212; October, 1960.) A two-channel sound transmission system, designed for the transmission of direct sound in addition to information relating to the acoustic quality of the room in which the sound originates is discussed. Measurements have been made of the optimum loudness for the information channel; this varies with the size and reverberation time of the room.

534.76:621.396.97 2449

Subjective Evaluation of Factors Affecting Two-Channel Stereophony—F. K. Harvey and M. R. Schroeder. (*J. Audio Eng. Soc.*, vol. 9, pp. 19–28; January, 1961.)

534.78:621.376.22:538.632 2450

A Correlator employing Hall Multipliers applied to the Analysis of Vocoder Control Signals—J. N. Holmes and J. N. Shearme: A. R. Billings and D. J. Lloyd. (*Proc. IEE*, pt. B, vol. 108, pp. 237–238; March, 1961.) A discussion of 4083 of 1960 is given.

534.78:621.391 2451

The Quantization of Speech in Few Stages—W. Andrich. (*Nachrtech. Z.*, vol. 13, pp. 379–

383; August, 1960.) This is an extension of earlier work [3855 of 1959 (Küpfmüller and Andrich)]. Measurements of logatom intelligibility are discussed; intelligibility can be improved for an even number of thresholds when noise is mixed with the speech before quantization.

534.833.1 2452
Measurement of the Sound Insulation by Random and by Normal Incidence of Sound—E. Brosio (*Acustica*, vol. 10, no. 3, pp. 173–175; 1960. In English.) Experimental data on transmission loss measured for random and normal incidence are compared. The results support London's theory.

534.84 2453
The Construction and Acoustic Properties of the Large Anechoic Chamber in the B.R.F.—P. Schubert and J. Scholze. (*Tech. Mitt. BRF, Berlin*, vol. 4, pp. 101–112; September, 1960.) Full details are given of the materials used and construction procedure adopted; comparisons are made with results obtained in other anechoic chambers [*e.g.*, 393 of February (Kraak *et al.*)].

534.846 2454
The Sound-Scattering Properties of Segments of Spheres and Cylinders on the Walls of Reverberation Chambers—G. Venzke. (*Acustica*, vol. 10, no. 3, pp. 170–172; 1960. In German.) Results are given of an experimental investigation based on measurements of the sound absorption coefficient of a large absorbing sheet in a reverberation chamber of 250 m³ fitted with scattering elements.

621.395.614:534.76.001.57 2455
Ultrasonic Microphones with Cardioid and Figure-of-Eight Patterns for M.S. Stereophony—J. Bolch. (*Frequenz*, vol. 14, pp. 315–317; September, 1960.) The design of condenser microphones for use on acoustic model tests is described.

ANTENNAS AND TRANSMISSION LINES

621.372.2 2456
Electromagnetic-Field-Theory Solution of the Infinite Tapered-Plane Transmission Line—N. Amitay, A. Lavi, and F. Young. (*Z. angew. Math. Phys.*, vol. 12, pp. 89–99; March, 1961. In English.) The mathematical technique used is based on the exact solution in EM field theory of the oblique-plane transmission line, in conjunction with Lagrange's method of variation of parameters.

621.372.8:537.525 2457
A Gas-Discharge Microwave Power Coupler—R. W. Otthus. (PROC. IRE, vol. 49, pt. 1, pp. 949–956; May, 1961.) A cylindrical resonator having a gas-discharge tube along its axis has power coupled into it in a mode with E transverse to the axis. A probe extracts power in a transverse mode with E normal to the first mode. Coupling takes place only when an axial magnetic field is present.

621.372.8:621.39 2458
Long-Distance Waveguide Transmission—R. Hamer. (*Electronic Engrg.*, vol. 33, pp. 218–225 and 279–283; April and May, 1961.) The feasibility of long-distance circular-waveguide (H_{01}-wave) transmission using FM is examined on the assumptions that a special waveguide structure is provided and that waveguide imperfections are random. The analysis is made with particular reference to multichannel telephony. Results are applied to a hypothetical route; the limitations examined do not preclude the use of FM in long-distance circular-waveguide transmission.

621.372.829:621.374.5 2459
The Helix as Delay Line—G. Piefke. (*Nachrtech. Z.*, vol. 13, pp. 370–374; August, 1960.) Treatment of the helix waveguide as a delay line on the basis of earlier work (*e.g.*, January 27) is discussed.

621.372.837:621.375.9:538.569.4 2460
Use of a Y-Type Circulator Switch with a 21-Centimetre Maser Radiometer—B. F. C. Cooper. (*Rev. Sci. Instr.*, vol. 32, pp. 202–203; February, 1961.) The switch eliminates baseline drifts observed with an automatic gain stabilization system (see 2521 below).

621.372.85.017.7:535.569.3 2461
The Heating Process in Circular Dielectric Disks in the High-Frequency Field of H_{0r}-Mode Waveguides—H. Buchholz. (*Arch. Elektrotech.*, vol. 45, pp. 447–465; December, 1960.) Green's function of thermal conduction is used in calculating exactly the internal heating of lossy dielectrics in a high-frequency EM field.

621.372.852.15 2462
Matched, Tunable Cavities as Circuit Elements of Waveguide Filters—H. Urbarz. (*Nachrtech. Z.*, vol. 13, pp. 383–391; August, 1960.) Design and construction problems relating to tunable cavities formed by inductive or capacitive obstacles in rectangular waveguides are investigated. Design charts are derived from equivalent circuits. Bandwidth variations during tuning are determined on the basis of the charts, and are confirmed by results of measurements.

621.372.852.323 2463
Millimetre-Wave Field-Displacement-Type Isolators with Short Ferrite Strips—K. Ishii, J. B. Y. Tsui, and F. F. Y. Wang. (PROC. IRE, vol. 49, pt. 1, pp. 975–976; May, 1961.) Attenuation of 35db (backward) and 1db (forward) is obtained with a 0.2-in single-crystal strip.

621.372.852.5 2464
Mode Conversion in the Excitation of TE_{01} Waves in a TE_{01}-Mode Transducer (Rectangular→Sector Portion→Circular)—S. Iiguchi. (*Rev. Elec. Commun. Lab., Japan*, vol. 8, pp. 324–334; July/August, 1960.) Expressions for the transverse fields in the cross sections of the transducer are expanded into a series of normal-mode functions of sector waveguides, and by substitution into Maxwell's equations expressed in oblique coordinates, the theoretical magnitudes of the unused TE_{11}, TE_{21}, TE_{31}, and TM_{11} modes are obtained. Experimental values agree to within 1 db.

621.372.853.1.002.2 2465
Dielectric-Coated Waveguide Construction Characteristics—K. Noda and K. Yamaguchi. (*Rev. Elec. Commun. Lab., Japan*, vol. 8, pp. 309–323; July/August, 1960.) Several different techniques are described and the theoretical attenuation increase due to the coating is calculated.

621.372.855.3:537.56 2466
Perturbation Method for the Propagation of Electromagnetic Waves in a Plasma Partially Filling a Circular Waveguide—L. Cairó. [*C.R. Acad. Sci., (Paris)*, vol. 250, pp. 4129–4131; June, 1960.] A relation is found between the value of the propagation constant and the diameters of the two concentric tubes of a waveguide, the plasma being contained in the inner tube.

621.396.67 2467
Development of Optimum Wide-Band Omnidirectional Aerials—H. G. Wahlsweiler. (*Z. angew. Phys.*, vol. 12, pp. 450–461; October, 1960.) A detailed treatment is given of the design of radiators of rotational symmetry, covering a range of aperture angles and including an investigation of their polar diagrams. For another treatment of a similar problem see 1418 of May (Meinke).

621.396.677:621.396.963.3 2468
A Fast Electronically Scanned Radar Receiving System—Davies. (See 2614.)

621.396.677.012.12:621.317.3 2469
Field Pattern Measurements of Various H.F. Directional Aerials using Aircraft—R. T. Rye. (*Proc. IRE (Australia)*), vol. 21, pp. 879–885; December, 1960.) Horizontally-arrayed dipoles, rhombic, sloping-V and Franklin antennas are investigated, giving the performance at the design frequencies, the off-frequency performance of a horizontally-arrayed dipole, and information on antenna interaction effects.

621.396.677.3 2470
Backward-Wave Radiation from Periodic Structures and Application to the Design of Frequency-Independent Antennas—P. E. Mayes, G. A. Deschamps, and W. T. Patton. (PROC. IRE, vol. 49, pt. 1, pp. 962–963; May, 1961.) The antenna is considered as a locally periodic structure whose period varies slowly, increasing linearly with the distance to the apex.

621.396.677.3.012.12(083.5) 2471
Tables of Horizontal Radiation Patterns of Dipoles Mounted on Cylinders—P. Knight and R. E. Davies. (*BBC Engrg. Div. Monographs*, No. 35, pp. 5–41; February, 1961.) A comprehensive range of mast sizes and dipole spacings is covered.

621.396.677.4 2472
Long-Wire Antenna for Meteor-Burst Communications—D. K. Reynolds and J. M. Bartlemay. (*Electronics*, vol. 34, pp. 40–42; March, 1961.) A simple long-wire antenna system for use in the 30–100 Mc range is described.

621.396.677.7:621.372.823 2473
Investigation of the Radiation Characteristics of Elliptical Waveguide and of the Possibility of Generating a Circularly Polarized Radiation Field—K. E. Müller. (*Hochfrequenz. und Elektroak.*, vol. 69, pp. 140–151; August, 1960.) Addition to earlier work on open waveguides (3959 of 1959) is given.

621.396.677.81.012.12 2474
Directivity Diagrams in the Horizontal Plane of a Vertical Dipole in the Presence of a Parallel Cylindrical Parasitic Element—H. Baret. (*Ann. Télécommun.*, vol. 14, pp. 220–235; September/October, 1959.) Directivity diagrams are calculated by a method due to Hallén in which a sinusoidal current distribution is not assumed *a priori*. Results are in good agreement with those calculated by other methods.

621.396.677.833:621.396.65 2475
Development of Radio-Link Aerials for the 4000-Mc/s Band—J. A. C. Jackson. (*Marconi Rev.*, vol. 24, no. 140, pp. 26–38; 1961.) Paraboloid antennas of 6-ft and 10-ft diameter are described, having efficiencies of 58 per cent and 63 per cent and gains of 35 db and 39 db, respectively. The impedance match of the complete antennas gives a voltage SWR better than 0.95 over a 400-Mc band when using a flanged waveguide feed; other types of feed are discussed.

621.396.677.85 2476
Lens-Compensated Biconical Aerial—L. Solymar. (*Electronic Tech.*, vol. 38, pp. 211–213; June, 1961.) The radiation pattern is calculated

and a practical example is worked out to show the design procedure for a lens of polystyrene or plexiglass if the half-power points are given.

621.396.679.4:621.372.43 2477
p-i-n Diodes control Shorted Stub—R. H. Mattson. (*Electronics*, vol. 34, pp. 76–77; April, 1961.) The length of a shorted stub for matching in the range 225–400 Mc can be altered electronically by opening or closing diode switches mounted at intervals along the stub.

621.396.679.4:621.372.8:621.317.333.4 2478
A Swept-Frequency Method of Locating Faults in Waveguide Aerial Feeders—J. Hooper. (*P.O. Elec. Engrg. J.*, vol. 54, pt. 1, pp. 27–30; April, 1961.) A rapid 400-Mc sweep obtained from a carcinotron in the band 2500–4500 Mc enables discontinuities having reflection coefficients exceeding 0.005 to be located to a positional accuracy within 2 per cent at distances up to 300 ft.

AUTOMATIC COMPUTERS

681.142 2479
Accuracy and Limitations of the Resistor Network used for Solving Laplace's and Poisson's Equations—J. R. Hechtel and J. A. Seeger. (PROC. IRE, vol. 49, pt. 1, pp. 933–940; May, 1961.) The accuracy of a resistor network is higher than that of the best comparable electrolyte tank. Improved methods of simulating boundary conditions are described.

681.142 2480
Storing Decimal Digits with One Clock Pulse—A. A. Jaecklin. (*Electronics*, vol. 34, pp. 50–53; March, 1961.) A method based on the magnetization time of ferrite cores is given.

681.142 2481
Transistorized Electronic Analogue Multiplier—S. Deb and J. K. Sen. (*Rev. Sci. Instr.*, vol. 32, pp. 189–192; February, 1961.) A four-quadrant circuit using the exponential I/V characteristics of the input of grounded-base junction transistors is described. The performance compares favorably with that of other types.

681.142:538.221 2482
Solving Design Problems in All-Magnetic Logic—U. F. Gianola. (*Electronics*, vol. 34, pp. 61–66; May, 1961.) A survey is made of general problems and methods of design of magnetic logic circuits, excluding parametron and ferroresonant circuits.

681.142:621–52 2483
Discrete Analogue-Computer Compensation of Sampled-Data Control Systems—T. Glucharoff. (*Proc. IEE*, pt. B, vol. 108, pp. 167–176; March, 1961. Discussion, pp. 176–179.) Operational amplifiers and Si-diode switches for performing the basic functions of sampling, holding, and time delay are described. Performance is analyzed, and an arrangement for avoiding saturation in a feedback system is also described.

CIRCUITS AND CIRCUIT ELEMENTS

621.316.86:539.23 2484
Tin Oxide Resistors—R. H. W. Burkett. (*J. Brit. IRE*, vol. 21, pp. 301–304; April, 1961.) The characteristics of thin oxide films are discussed and techniques of manufacture and performance figures of tin oxide resistors for various applications are given.

621.318.57:523.164 2485
R.F. Switching Circuits and Hybrid Ring Circuits used in Radio Astronomy—F. G. Smith. (*Proc. IEE*, pt. B, vol. 108, pp. 201–204; March, 1961.) Low-loss diode and other switching systems used in comparing small RF noise powers are described.

621.318.57:621.382.333.33 2486
Designing Avalanche Switching Circuits—Rufer. (See 2810.)

621.372.4 2487
The Equivalent Wave Source—H. J. Butterweck. (*Arch. elekt. Übertragung*, vol. 14, pp. 367–372; September, 1960.) The application of wave parameters to two-terminal sources is discussed. An equivalent wave source is derived which corresponds to the conventional equivalent voltage or current source.

621.372.4:621.3.024 2488
The Law of Small Variations in Characteristics and its Application to Nonlinear and Linear Networks—E. Schwartz. (*Arch. elekt. Übertragung*, vol. 14, pp. 405–410; September, 1960.) Current changes resulting from small variations in characteristics in nonlinear dc networks can be calculated approximately by reference to an equivalent circuit. Examples of linear networks considered are a Wheatstone bridge circuit and reactance two-poles.

621.372.41 2489
The Reliability Conditions for the Impedance Functions of Electrical Two-Pole Networks allowing for Losses in Coils and Capacitors—F. H. Effertz and W. Meuffels. (*Arch. Elektrotech.*, vol. 45, pp. 418–428; October, 1960.)

621.372.5 2490
Some Energy Relations for RC Networks—A. H. Zemanian. (*J. Franklin Inst.*, vol. 270, pp. 353–358; November, 1960.) Certain relations are established and associated with the compact RC network whose open-circuit impedance parameters have residues that possess the same ratio at corresponding poles.

621.372.5 2491
Non-ideal Gyrators—K. H. R. Weber. (*Nachrtech.*, vol. 10, pp. 334–339; August, 1960.) The analogy between non-ideal gyrators and non-ideal transformers is established. Equations are derived for the "perfect" gyrator and the gyrator with leakage; matching and directional characteristics are discussed.

621.372.54 2492
The Effect of Tolerances in the Elements of Image-Parameter Filters—J. W. Scholten. (*Philips Telecommun. Rev.*, vol. 22, pp. 63–77; January, 1961.)

621.372.54:534.143 2493
The Insertion Characteristics of Cascaded Circuits—W. Herzog. (*Nachrtech. Z.*, vol. 13, pp. 424–427; September, 1960.) A method of dealing with series-connected filter circuits, in particular those consisting of electromechanical elements, is considered. A single quadripole is derived to represent n cascade-connected equal and symmetrical quadripoles, and different types of end-section are added to this equivalent quadripole. The impedance matrix of the equivalent network is determined; the application of the principle to a combination of unequal quadripoles is outlined.

621.372.54:537.228.1 2494
Piezoelectric Ceramic Transformers and Filters—A. E. Crawford. (*J. Brit. IRE*, vol. 21, pp. 353–360; April, 1961. Discussion.) Some of the types of transformers and filters which are produced from the lead zirconate-lead titantate series are described.

621.372.54:538.652 2495
Magnetostrictive Transducers as Selective Quadripoles—C. Kurth. (*Frequenz*, vol. 14, pp. 272–288; August, 1960.) The relations between electrical and mechanical quantities in magnetostrictive energy transducers are given and equivalent circuits derived. Design formulas are obtained using image-parameter theory. (See also 4135 of 1960.)

621.372.543.2 2496
Some Comments on Narrow Band-Pass Filters—M. Rosenblatt. (*Quart. Appl. Math.*, vol. 18, pp. 387–393; January, 1961.)

621.372.543.2:534.143 2497
The Measurement of the Characteristic Values of Electromechanical Coupling Filters—E. Trzeba. (*Hochfrequenz. und Elektroak.*, vol. 69, pp. 119–123; August, 1960.) See also 2122 of July.

621.372.55:621.397 2498
Quadripole Networks for Phase Correction in Low-Pass and Band-Pass Amplifiers—G. Coldewey. (*Frequenz.*, vol. 14, pp. 299–305; September, 1960.) The design of delay equalizers for television transmission systems is described.

621.372.552 2499
Bode's Variable Equalizer—S. S. Hakin. (*Electronic Tech.*, vol. 38, pp. 224–227; June, 1961.) Design procedure for an equalizer, in which the insertion-loss characteristic can be varied by the variation of one network element (a thermistor), is developed from basic theory.

621.372.6 2500
Coupling of Multipoles represented as a Wave-Transmission Problem—G. Salzmann. (*Nachrtech.*, vol. 10, pp. 353–355; August, 1960.) The method of solving multipole coupling problems by means of a scattering matrix is described.

621.372.6 2501
Network Synthesis with Negative Resistors—H. J. Carlin and D. C. Youla. (PROC. IRE, vol. 49, pt. 1, pp. 907–920; May, 1961.) The theory of the incorporation of the negative resistor as a basic circuit element in problems of linear network analysis and synthesis is presented. Nine circuit theorems are given.

621.373.029.6 2502
Note on Coherence vs Narrowbandedness in Regenerative Oscillators, Masers, Lasers, etc—M. J. E. Golay. (PROC. IRE, vol. 49, pt. 1, pp. 958–959; May, 1961.)

621.373.42:621.317.77 2503
A Method for Generating Signals of Arbitrary yet Frequency-Independent Phase Differences—O. K. Nilssen. (PROC. IRE, vol. 49, pt. 1, pp. 964–965; May, 1961.) Two balanced-peak detectors are used. The phase difference remains constant over a range 10 cps–1 kc.

621.373.42.072.6:621.376.32 2504
Improvement of the Frequency Stability of a High-Frequency Oscillator Frequency-Modulated by means of a Condenser Microphone—H. Maier. (*Nachrtech. Z.*, vol. 12, pp. 436–440; September, 1960.) A frequency-stabilizing system is described in which the condenser microphone serves simultaneously for frequency modulation and as an electrostatic control element. The system finds application in miniature VHF transmitters and eliminates the need for crystal control.

621.373.421.11:621.374.32 2505
High-Frequency Oscillator Stabilization by Pulse Counting Techniques—R. P. Thatte. (*J. Brit. IRE*, vol. 21, pp. 361–373; April, 1961. Discussion.) A system is described for frequency stabilization to within 5 parts in 10^7 in the range 2–30 Mc, using an LC tuned oscillator locked to a standard frequency. A description of the trochotron divider used in the circuit is given.

621.373.421.13:529.786 2506
Quality Measurements on Oscillator Crystals by the Decay Method—G. Becker. (*Frequenz*, vol. 14, pp. 269–271; August, 1960.) Equipment is described for measuring the time constant of the decay of free oscillations of quartz oscillators. The method is suitable for measuring the Q factor of crystals of high resonance frequency.

621.373.43:621.374.4 2507
8- and 11- Gc/s Nanosecond Carrier Pulses Produced by Harmonic Generation—A. F. Dietrich. (PROC. IRE, vol. 49, pt. 1, pp. 972–973; May, 1961.) Pulses are generated directly from the harmonics present in the sharp step at the end of the recovery transient of a selected Type-FD-100 diode which is mounted across a waveguide used as a high-pass filter.

621.373.43:621.385.632 2508
A Simple Method of Generating Nanosecond Pulses at X Band—J. K. Pulfer and B. G. Whitford. (PROC. IRE, vol. 49, pt. 1, p. 968; May, 1961.) The technique is based on the pulse response of a traveling-wave tube.

621.374.33:621.318.57:621.372.44 2509
Magnetic Gate Circuits Controlled by High-Frequency Signals—I. Endo and K. Kusunoki. (*Rev. Elec. Commun. Lab., Japan*, vol. 8, pp. 335–342; July/August, 1960.) Principles of operation of three- and four-core gating circuits based on the nonlinear properties of parametron-type cores are described. Experimental characteristics and applications are noted.

621.374.4:621.372.44 2510
High-Efficiency Variable-Reactance Frequency Multiplier—T. Utsunomiya and S. Yuan. (PROC. IRE, vol. 49, pt. 1, p. 965; May, 1961.) A conversion efficiency of 40 per cent was obtained using variable-capacitance diodes with input frequency 0.84 Mc and output frequency 12.6 Mc.

621.374.5 2511
Stabilized Delay Circuit Provides High Accuracy—C. K. Friend and S. Udalov. (*Electronics*, vol. 34, pp. 78, 80; April, 1961.) A transistorized circuit is given providing delays up to 120 μsec with a high degree of accuracy and stability.

621.374.5:621.382.333.33 2512
Electrically Variable Time Delay using Cascaded Drift Transistors—R. W. Ahrons. (*Semiconductor Prod.*, vol. 4, pp. 37–40; March, 1961.) Eight cascaded transistors provide a variation of delay of 0.11 μs with a minimum cutoff frequency of 5 Mc.

621.375:621.372.44:621.372.632 2513
Parametric Up-Converter Tunable over an 18:1 Frequency Band—G. P. Shepherd and D. G. Kiely. (PROC. IRE, vol. 49, pt. 1, p. 966; May, 1961.) By using an adjustable X-band pump frequency, a gain of 5–12 db is obtained with signal frequencies ranging from 100 to 1800 Mc.

621.375.018.756 2514
Two Simple Estimates for Overshoot and Group Delay—H. Sulanke and H. Dobesch. (*Tech. Mitt. BRF, Berlin*, vol. 4, pp. 83–85; September, 1960.) Approximations relating to the transient response of cascade-connected quadripoles are made. See also 467 of February (Dobesch & Sulanke).

621.375.029.64/.65:621.38 2515
Low-Noise Amplifiers for Centimetre and Shorter Wavelengths—G. Wade. (PROC. IRE, vol. 49, pt. 1, pp. 880–891; May, 1961.) A summary is made of the techniques used to make low-noise amplifiers. The devices covered are traveling-wave tubes, parametric amplifiers, tunnel diodes, masers, photon counters and photosensitive detectors.

621.375.4 2516
Calculations of Distortion and Interference Effects in Transistor Amplifier Stages on the Basis of the Equivalent Circuit Diagram—J. S. Vogel and M. J. O. Strutt. (*Arch. elekt. Übertragung*, vol. 14, pp. 397–404; September, 1960.) Low-frequency conditions and input signals up to maximum permissible amplitude are considered, and the calculations are applied to two-stage circuits. The extension of the theory to high-frequency conditions is indicated.

621.375.4 2517
Improving Gain Control of Transistor Amplifiers—J. S. Brown. (*Electronics*, vol. 34, pp. 108–110; April, 1961.) Better temperature stability and a lower noise figure are obtained by using separate AGC loops for each stage.

621.375.9:538.569.4 2518
Proposal for a Pulsed Ferromagnetic Microwave Generator—M. W. Muller. (PROC. IRE, vol. 49, pt. 1, p. 957; May, 1961.) Spin precession is induced by rotating the applied field from a metastable to a stable magnetizing direction.

621.375.9:538.569.4 2519
Stimulated Emission from HCN Gas Maser Observed at 88.6 kMc/s—D. Marcuse. (*J. Appl. Phys.*, vol. 32, p. 743; April, 1961.) HCN is considered as an alternative to NH_3 for a gas maser. The relative position and strength of the absorption lines are shown, and the construction of the proposed maser is described.

621.375.9:538.569.4 2520
Beam Maser for 3 Millimetres uses Hydrogen Cyanide—F. S. Barnes and D. Maley. (*Electronics*, vol. 34, pp. 45–49; March, 1961.) A practical description of the development and construction of a maser operating at 88 Gc which may be useful as a power source, amplifier, or as a frequency standard is given.

621.375.9:538.569.4:523.164 2521
An Operational Ruby Maser for Observations at 21 Centimetres with a 60-Foot Radio Telescope—J. V. Jelley and B. F. C. Cooper. (*Rev. Sci. Instr.*, vol. 32, pp. 166–175; February, 1961.) Details are given of a preamplifier, weight 200 pounds, for mounting at the focus of a 60-ft reflector. An automatic gain stabilization system is incorporated. Total input noise temperature of the radiometer is 85°K with gain stabilization, and 148°K without.

621.375.9:621.372.44 2522
A Variable-Dual-Reactance Traveling-Wave Parametric Amplifier—R. D. Wanselow. (PROC. IRE, vol. 49, pt. 1, p. 973; May, 1961.) Two transmission lines are coupled together by inductance and capacitance which vary at a pump frequency.

621.375.9:621.372.44:538.221 2523
K_a-Band Ferrite Amplifier—R. W. Roberts. (PROC. IRE, vol. 49, pt. 1, p. 963; May, 1961.) A parametric amplifier using a sphere of Y-Fe garnet and giving 10 db gain at 20.8 G is discussed.

621.375.9:621.372.44:621.382.23 2524
Parametric Amplification by Charge Storage—D. L. Hedderly. (PROC. IRE, vol. 49, pt. 1, pp. 966–967; May, 1961.) Both parametric amplification and subharmonic oscillation can be obtained through charge storage effects, using the circuit described.

621.375.9:621.372.44:621.382.23 2525
C-Band Nondegenerate Parametric Amplifier with 500-Mc/Bandwidth—J. Kliphuis. (PROC. IRE, vol. 49, pt. 1, p. 961; May, 1961.) The amplifier uses two Si pill varactor diodes in a balanced circuit and has a gain of 10 db.

621.375.9:621.372.44:621.382.33 2526
Parametric-Excited Resonator Using Junction Transistor—Y. Cho. (PROC. IRE, vol. 49, pt. 1, p. 974; May, 1961.) Oscillations in the collector circuit are phase-locked by a signal applied to the reverse-biased emitter.

621.375.9:621.382.23 2527
A Matched Amplifier Using Two Cascaded Esaki Diodes—D. R. Hamann. (PROC. IRE, vol. 49, pt. 1, pp. 904–906; May, 1961.) A circuit consisting of a quarter-wave transmission line whose ends are terminated by negative conductances is discussed and its characteristics calculated. A 30-Mc amplifier using two Esaki diodes has been found to have a gain of 8.9 db with a noise figure of 4.3 db.

GENERAL PHYSICS

530.12 2528
General Relativity for the Experimentalist—R. L. Forward. (PROC. IRE, vol. 49, pt. 1, pp. 892–904; May, 1961.)

530.162 2529
Direct Determination of Boltzmann's Constant from Resistance Noise—L. Storm. (*Naturwiss.*, vol. 47, p. 490; November, 1960.) The value of k obtained from thermal-noise measurements in the frequency range 2–20 kc is 1.3809×10^{-23} joules/degree, to an accuracy within ±0.12 per cent is discussed.

537.311.1 2530
Friedel Sum Rule for a System of Interacting Electrons—J. S. Langer and V. Ambegaokar. (*Phys. Rev.*, vol. 121, pp. 1090–1092; February, 1961.)

537.312.8 2531
Theory of the Magnetroresistance Effect—J. Hajdu. (*Z. Phys.*, vol. 160, pp. 47–58 and 481–490, September and November, 1960; and vol. 163, pp. 108–118, May, 1961.) Magnetoresistance effects in metals are studied on the basis of a single quantum theory of electron transport in a magnetic field.

537.32 2532
Response of a Thermocouple Circuit to Nonsteady Currents—T. T. Arai and J. R. Madigan. (*J. Appl. Phys.*, vol. 32, pp. 609–616; April, 1961.) A general expression for the transient response is derived and applied to several special forms of time-dependent current.

537.533 2533
Note on the Mechanism of the Multipactor Effect—F. Paschke. (*J. Appl. Phys.*, vol. 32, pp. 747–749; April, 1961.) By modifying the theory of Krebs and Meerbach (2913 of 1955) to take into account the velocity distribution of secondary electrons and the phase-defocusing effect, excellent agreement is obtained with the experimental results of Hatch & Williams (2629 of 1954).

537.56 2534
Determining Electron Density and Distribution in Plasmas—H. L. Bunn. (*Electronics*, vol. 34, pp. 71–75; April, 1961.) A microwave interferometer technique is used for measurements on low-temperature magnetically contained plasmas.

537.56 2535
Transport Coefficients of Plasma in a Magnetic Field—S. Kaneko. (*J. Phys. Soc. Japan*, vol. 15, pp. 1685–1696; September, 1960.) The electrical and thermal conductivities, and the coefficient of thermal diffusion are calculated.

537.56:538.566 2536
Proposed Diagnostic Method for Cylindrical Plasmas—J. Shmoys. (*J. Appl. Phys.*, vol. 32, pp. 689–695; April, 1961.) Expressions are derived for two methods whereby the electron density variation across a plasma column can be obtained more easily than hitherto from an observed diffraction pattern.

537.56:538.566.029.6 2537
Microwave Attenuation by Cyclotron Resonance in a Slightly Ionized Gas—T. Dodo. (*J. Phys. Soc. Japan*, vol. 16, pp. 293–301; February, 1961.) The Boltzmann equation is solved for the distribution function of electrons in a static magnetic field B and a HF electric field. The tensor dielectric constant and propagation constant k are hence obtained. The attenuation spectrum is discussed for the two cases of k parallel and perpendicular to B.

537.56:538.566.029.6 2538
Spectrum of the Electron Synchrotron Resonance in a Plasma—T. Dodo. (*J. Phys. Soc. Japan*, vol. 16, pp. 348–349; February, 1961.) Experimental verification of a theoretical formula for cyclotron resonance frequency (see 2537 above) is given.

537.56:538.566.029.6 2539
Heating of an Ionized Gas Sheath by Microwaves—M. S. Sodha. (*Appl. Sci. Res.*, vol. B8, no. 3, pp. 208–212; 1960.) Formulas are derived from which the temperature of a plasma sheath can be found, as a function of time when it is heated by high-energy microwave radiation.

537.56:538.566.029.6 2540
Backward-Wave Microwave Oscillations in a System Composed of an Electron Beam and a Hydrogen Gas Plasma—R. Targ and L. P. Levine. (*J. Appl. Phys.*, vol. 32, pp. 731–737; April, 1961.) A traveling-wave interaction structure is used to investigate the properties of a low-density plasma. Microwave oscillations near the electron cyclotron frequency are observed as the result of growing waves in a beam/plasma interaction. Electron densities determined by observing the correlation between the measured frequencies of oscillation and the theoretical predictions of Trivelpiece and Gould (815 of 1960) are verified by observation of the shift in the resonance frequency of a microwave cavity containing the plasma.

537.56:621.372.8 2541
The Influence of the Cross-Sectional Distribution of Electron Density of a Longitudinally Magnetized Plasma in a Metal Waveguide on the Propagation of E. M. Waves—W. O. Schumann. (*Z. angew. Phys.*, vol. 12, pp. 442–446; October, 1960.)

538.122:538.221 2542
The Magnetization and Field of Rod-Shaped Objects—G. Obermair and C. Schwink. (*Z. Phys.*, vol. 160, pp. 268–276; October 1960.) The magnetization process is analyzed and general formulas are given for the demagnetizing field. An electron-optical method [3441 of 1959 (Schwink and Murrman)] for determining the magnetic distribution in and around the rod is discussed.

538.311 2543
Determination of the Energy of a Plane Magnetic Field by Representation of the Latter in an Electric Current Field—F. Stier. (*Arch. Elektrotech.*, vol. 45, pp. 343–346; August, 1960.)

538.311:621.374 2544
Equipment for Generating Strong Magnetic Fields of Short-Period Constancy—J. Durand, O. Klüber, and H. Wulff. (*Z. angew. Phys.*, vol. 12, pp. 385–393; September, 1960.) A suitably terminated low-pass filter network is used to produce flat-topped current pulses for generating strong magnetic fields which are constant for periods of the order of 2 msec.

538.566 2545
A Dipole Absorber for Centimetric Electromagnetic Waves with Reduced Reflection at Oblique Incidence—G. Kurtze and E. G. Neumann. (*Z. angew. Phys.*, vol. 12, pp. 385–393; September, 1960.) The addition to a resonance absorber of arrays of dipoles parallel and perpendicular to the absorber surface minimizes reflection at oblique incidence; experimental results and theory are given.

538.566:535.43 2546
Multiple Scattering by a Random Stack of Dielectric Slabs—I. Kay and R. A. Silverman. (*Nuovo Cim.*, vol. 9, Suppl. no. 2, pp. 626–645; 1958. In English.) When the number of slabs is large, the Neumann series for the mean-square transmission and reflection coefficients converge much more rapidly than would be inferred from the smallness of the perturbation of the incident field by the scattering medium.

538.569.4 2547
Detection of Double Resonance by Frequency Change: Application to Hg^{201}—R. H. Kohler. (*Phys. Rev.*, vol. 121, pp. 1104–1111; February, 1961.)

538.569.4:535.33:621.375.9 2548
The Three-Level Gas Maser as a Microwave Spectrometer—T. Yajima and K. Shimoda. (*J. Phys. Soc. Japan*, vol. 15, pp. 1668–1675; September, 1960.) A method of microwave spectroscopy using three-level maser action is described and results of experiments on HDCO are discussed in relation to theory. See also 1481 of May (Shimoda *et al.*).

538.569.4:538.221 2549
Distribution of Fields from Randomly Placed Dipoles: Free-Precession Signal Decay as Result of Magnetic Grains—R. J. S. Brown. (*Phys. Rev.*, vol. 121, pp. 1379–1382; March, 1961.)

538.569.4:538.221 2550
Ferromagnetic Relaxation caused by Interaction with Thermally Excited Magnons—E. Schlömann. (*Phys. Rev.*, vol. 121, pp. 1312–1319; March, 1961.)

538.569.4:538.221 2551
Note on the Back-Reaction Term in Ferromagnetic Relaxation Equations—H. Callen. (*J. Appl. Phys.*, vol. 32, p. 738; April, 1961.) A clarification is given of the status of the last term of the equation $\dot{n}_0=\lambda_{0k}n_0+\lambda_{k0}\bar{n}_k$, proposed in a paper on the analysis of ferromagnetic resonance line width in ferrites (3901 of 1958).

538.569.4:538.222 2552
On the Theory of Spin-Lattice Relaxation in Paramagnetic Salts—R. Orbach. (*Proc. Phys. Soc.*, vol. 77, pp. 821–826; April, 1961.)

538.569.4:621.375.9:535.61-2 2553
Spatial Coherence in the Output of an Optical Maser—D. F. Nelson and R. J. Collins. (*J. Appl. Phys.*, vol. 32, pp. 739–740; April, 1961.)

538.569.4:621.375.9:535.61-2 2554
Optically Efficient Ruby Laser Pump—P. A. Miles and H. E. Edgerton. (*J. Appl. Phys.*, vol. 32, pp. 740–741; April, 1961.)

GEOPHYSICAL AND EXTRATERRESTRIAL PHENOMENA

523.14:538.69 2555
Note on the Magnetic Structure of the Galaxy—F. Hoyle and J. G. Ireland. (*Monthly Notices Roy. Astron. Soc.*, vol. 122, no. 1, pp. 35–39; 1961.) Earlier theory (see 843 of March) is reassessed.

523.164 2556
A Comparison of Three Surveys of Radio Stars—A. S. Bennett and F. G. Smith. (*Monthly Notices Roy. Astron. Soc.*, vol. 122, no. 1, pp. 71–77; 1961.) A recent survey of radio stars is compared with results of earlier measurements by Mills *et al.* (423 of 1959) and Edge *et al.* (*Mem. Roy. Astron. Soc.*, vol. 68,pt. 2, pp. 37–60; 1959).

523.164 2557
First Results of Radio Star Observations using the Method of Aperture Synthesis—P. F. Scott, M. Ryle, and A. Hewish. (*Monthly Notices Roy. Astron. Soc.*, vol. 122, pp. 95–111; March, 1961.) Four surveys, centered on declinations of 52°, 50°, 42° and 05° have been made at a wavelength of 1.7 m with a large interferrometric radio telescope based on the technique of aperture synthesis [3724 of 1960 (Ryle and Hewish)]. Details of the observational method, calibration, data reduction and analysis of the computed results are given.

523.164 2558
Observations of some Radio Sources on 3.2 cm—A. M. Karachun, A. D. Kus'min, and A. E. Salomonovich. (*Astron. Zhur.*, vol. 38, pp. 83–86; January/February, 1961.) A report of observations of discrete RF sources Taurus-A, Orion, Cygnus-A and Cassiopeia-A made during June, 1960, with a 22-m radio telescope.

523.164:621.318.57 2559
R. F. Switching Circuits and Hybrid Ring Circuits used in Radio Astronomy—Smith. (See 2485.)

523.164:621.375.9:538.569.4 2560
An Operational Ruby Maser for Observations at 21 Centimetres with a 60-Foot Radio Telescope—Jelley and Cooper. (See 2521.)

523.164.32:523.75 2561
On the Relativistic Electrons in the Solar Atmosphere—K. Sakurai. (*J. Geomag. Geoelect.*, vol. 12, no. 2, pp. 70–76; 1961.) The ejection of relativistic electrons in association with flares is discussed and the loss of energy of these electrons through synchrotron radiation is related to type-IV RF bursts.

523.164.4 2562
The Surface Brightness of Radio Sources at Galactic Latitudes Greater than 20°—P. R. R. Leslie. (*Monthly Notices Roy. Astron. Soc.*, vol. 122, no. 1, pp. 51–59; 1961.)

523.164.4 2563
The Relation between the Optical and Radio Magnitudes of Galaxies—R. J. Long and D. R. Marks. (*Monthly Notices Roy. Astron. Soc.*, vol. 122, no. 1, pp. 61–70; 1961.) A statistical relation is found from observations of 200 sources.

523.165 2564
A Radio Wave Mechanism to account for the Known Distribution of Van Allen Belts about the Earth—J. M. Boyer. (*Nature*, vol. 190, pp. 597–599; May, 1961.) A mechanism based on a conducting spherical earth illuminated by EM and corpuscular radiation from the sun is given to account for the positions of the Van Allen belts. Interference between backscattered and incident radiation exhibits resonance peaks in a standing-wave pattern, in which peaks solar particles are trapped.

523.165:550.38 2565
Motion of Low-Energy Solar Cosmic-Ray Particles in the Earth's Magnetic Field—K.

Sakurai. (*J. Geomag. Geoelect.*, vol. 12, no. 2, pp. 59–69; 1961.)

523.165:551.507.362.2 2566

Cosmic Noise Measurements from 1960 η1 at 3.8 Mc/s—A. R. Molozzi, C. A. Franklin, and J. P. I. Tyas. (*Nature*, vol. 190, pp. 616–617; May, 1961.) Noise field strengths are given, as measured in the satellite, for positions in both hemispheres.

523.42:621.396.96 2567

A New Determination of the Solar Parallax by means of Radar Echoes from Venus—J. H. Thomson, G. N. Taylor, J. E. B. Ponsonby, and R. S. Roger. (*Nature*, vol. 190, pp. 519–520; May, 1961.) The value of $8.7943 \pm 0.0003''$ of arc obtained for the solar parallax is compared with values obtained by other workers. See also *ibid.*, vol. 190, p. 592; May, 1961.

523.75:523.165 2568

The Time Variations of Solar Cosmic Rays during July 1959 at Minneapolis—J. R. Winckler, P. D. Bhavsar, and L. Peterson. (*J. Geophys. Res.*, vol. 66, pp. 995–1022; April, 1961.) Balloon observations with ion chambers, Geiger counters and scintillation counters of solar cosmic rays accompanying three large solar flares are reported. Correlation with magnetic data is given and proton energy spectra calculated.

523.75:523.165 2569

The High Energy Cosmic-Ray Flare of May 4, 1960: Part 1—High-Altitutde Ionization and Counter Measurements—J. R. Winckler, A. J. Masley, and T. C. May. (*J. Geophys. Res.*, vol. 66, pp. 1023–1027; April, 1961.) Measurements of cosmic rays from a solar flare are reported. Various types of counters were used in a balloon. The rate at which the particle flux decreased with time is compared with neutron flux measurements at the ground.

523.75:523.165 2570

The High-Energy Cosmic-Ray Flare of May 4, 1960: Part 2—Emulsion Measurements—S. Biswas and P. S. Freier. (*J. Geophys. Res.*, vol. 66, pp. 1029–1033; April, 1961.) Nuclear emulsions recovered from a balloon give the energy spectrum of the cosmic rays. Excess flux was observed of protons in the energy range 200–1000 Mev. (Part 1: 2569 above.)

550.385:539.16 2571

Experimental Analysis of Magnetic and Telluric Effects of the Argus Experiment Recorded at French Stations—S. Eschenbrenner, L. Ferrieux, R. Godivier, R. Lachaux, H. Larzillière, A. Lebeau, R. Schlich, and E. Selzer. (*Ann. Géophys.*, vol. 16, pp. 264–271; April–June, 1960.) Recordings made at six stations have been analyzed. Results are produced in tabular form and photographic reproductions of typical records are given.

550.385.4 2572

The Steady State of the Chapman-Ferraro Problem in Two Dimensions—J. W. Dungey. (*J. Geophys. Res.*, vol. 66, pp. 1043–1047; April, 1961.) The form of the cavity in the plane of the dipole and uniform solar stream is derived using the method of complex potentials.

550.385.4:523.165 2573

Large-Scale Electron Bombardment of the Atmosphere at the Sudden Commencement of a Geomagnetic Storm—R. R. Brown, T. R. Hartz, B. Landmark, H. Leinbach, and J. Ortner. (*J. Geophys. Res.*, vol. 66, pp. 1035–1041; April, 1961.) X-ray bursts coincident in time with two sudden commencement peaks in magnetic records were observed with balloon-borne Geiger counters. Ionospheric absorption data are given. An estimate is made of the electron flux required to account for the X-ray intensities, and their origin is discussed.

550.385.4:551.594.5 2574

Solar-Stream Distortion of the Geomagnetic Field and Polar Electrojets—J. W. Kern. (*J. Geophys. Res.*, vol. 66, pp. 1290–1292; April, 1961.) The geomagnetic field distortion may introduce longitudinal field gradients which will lead to electrojet-current systems of the form observed.

550.386.37:550.37 2575

Radiation from a Current Filament above a Homogeneous Earth, with Application to Micropulsations—P. F. Law and B. M. Fannin. (*J. Geophys. Res.*, vol. 66, pp. 1049–1059; April, 1961.) Near-field considerations are used to steady the radiations at micropulsation frequencies from an ionospheric current.

550.386.6 2576

The Diurnal Variation of K Indices of Geomagnetic Activity on Quiet Days in 1940–1948—S. B. Nicholson and O. R. Wulf. (*J. Geophys. Res.*, vol. 66, pp. 1139–1144; April, 1961.) Local-time and universal-time components are derived from the K numbers from six observatories in moderately low latitudes.

551.507.362.1 2577

Measurement of the Temperature in the Upper Atmosphere to 150 km in a Rocket Experiment—J. E. Blamont, T. M. Donahue, and M. L. Lory. (*Phys. Rev. Lett.*, vol. 6, pp. 403–404; April, 1961.) Spectroscopic observation of sunlight resonantly scattered from a sodium cloud formed by ejection of sodium from a rocket, gave atmospheric temperatures between 100 and 150 km.

551.507.362.1 2578

The Motion of the Third Soviet Cosmic Rocket—V. T. Gontkovskaya and G. A. Chebotarev. (*Astron. Zhur.*, vol. 38, pp. 125–130; January/February, 1961.) An investigation of the motion of Lunik III from October 15, 1959, to March 30, 1960. Results are summarized in tabular form.

551.507.362.2 2579

Satellite Orbits about a Planet with Rotational Symmetry—C. M. Petty and J. V. Breakwell. (*J. Franklin Inst.*, vol. 270, pp. 259–282; October, 1960.) An approximate closed-form solution, of high accuracy and without restriction on the inclination angle or eccentricity, is obtained for the equations of motion of an earth satellite.

551.507.362.2 2580

Satellite Orbit Perturbations in Vector Form—R. R. Allan. (*Nature*, vol. 190, p. 615; May, 1961.)

551.507.362.2 2581

The Doppler Effect and Inertial Systems—K. Toman. (PROC. IRE, vol. 49, pt. 1, p. 971; May, 1961.) The minimum-range equation for the general case of curved orbits of satellite and observer is compared with the equation valid for inertial systems. See 2193 of July.

551.507.362.2 2582

Instrumentation for the First Anglo-American Scout Satellite—A. P. Willmore. (*J. Brit. Interplanetary Soc.*, vol. 18, pp. 11–16; January/February, 1961. Discussion.) The satellite is primarily designed for studies of the ionosphere. The techniques for measurement of electron density and temperature, ion mass, solar X rays and Lyman-α flux are described.

551.507.362.2:526.6 2583

Earth Satellites and Geodesy—I. D. Zhongolovich. (*Astron. Zhur.*, vol. 38, pp. 115–124; January/February, 1961.) Possible methods for determining geocentric coordinates of points on the earth's surface from observations of the moon and artificial earth satellites are examined. The determination of the difference between Ephemeris and Universal Time is considered.

551.507.362.2:526.6 2584

Determination of Position on the Earth from a Single Visual Observation of an Artificial Satellite—W. A. Scott. (*J. Inst. Nav.*, vol. 14, pp. 87–93; January, 1961.) If a reliable orbit is available and an observation of the satellite against a background of stars can be made to an accuracy within 0.1° and timed to 0.2 s, the position of the observer can be determined with sufficient accuracy for navigation purposes. A single visual observation of Echo 1 (1960*i*) provides the reference in a worked example.

551.507.362.2:621.396.722 2585

Ground Equipment for Radio Observations of Artificial Satellites—Pressey. (See 2777.)

551.507.362.2:778.53 2586

Design and Results of First Tests on a Camera with a Moving Film for the Photography of Faint Artificial Satellites—L. A. Panaiotov. (*Astron. Zhur.*, vol. 38, pp. 145–156; January/February, 1961.)

551.510.53:621.391.812.63 2587

Air Density Variations in the Mesophere, and the Winter Anomaly in Ionospheric Absorption—J. Mawdsley. (*J. Geophys. Res.*, vol. 66, pp. 1298–1299; April, 1961.) The air density variations observed in winter by Jones *et al.* (*J. Geophys. Res.*, vol. 64, pp. 2331–2340; December, 1959) may indicate air movements which could cause an enhancement of the NO content and give rise, in turn, to increased ionization and radio wave absorption.

551.510.535 2588

Ionization Loss Rates below 90 km—C. M. Crain. (*J. Geophys. Res.*, vol. 66, pp. 1117–1126; April, 1961.) Loss processes in the D region are discussed, with a review of data on the rate coefficients involved. Theoretical height distributions of electrons and of positive and negative ions are given.

551.510.535 2589

World Maps of F_2-Layer Critical Frequencies for the Solstice and Equinox Months of 1954 and 1957—P. Herrinck and J. Goris. (*Ann. Géophys.*, vol. 16, pp. 358–392; July–September, 1960.) Hourly world maps of f_0F_2 are analyzed as a function of solar activity. Results show 1) asymmetrical distribution over the two hemispheres, 2) discontinuous diurnal movement of the world, maximum ionization and 3) the existence of four "poles" in the distribution of the mean diurnal rate of increase of ionization due to solar activity, two of these poles corresponding to the magnetic poles and the other two being located in the equatorial belt where the geomagnetic equator is furthest from the geographic equator. It is concluded that these phenomena cannot be explained by existing theories and that the possibility of corpuscular discharge from a Van Allen belt should be investigated, particularly in relation to equatorial regions.

551.510.535 2590

On the Nature of Equatorial Spread-F—R. Cohen and K. L. Bowles. (*J. Geophys. Res.*, vol. 66, pp. 1081–1106; April, 1961.) Transequatorial propagation on 50 Mc via scattering from the F region above Huancayo was closely associated with equatorial-type (but not temperate-type) spread-F on Huancayo ionograms; *i.e.*, range spreading, not frequency spreading.

The irregularities take the form of thin sheets near the bottom of the F layer. They are elongated in the direction of the earth's field, being 1000 m or more in length, and of the order of 10 m in at least one dimension transverse to the field. It is suggested that equatorial spread-F can occur only when the contours of mean electron density are parallel to the lines of force of the earth's field.

551.510.535 2591

Critical Remarks on the Calculation of 'True Heights'—A. K. Paul. (*Geofis. pura e appl.*, vol. 47, pp. 69–78; September–December, 1960. In German.)

The conditions are given and discussed which permit an unambiguous solution of the integral equation of ionospheric virtual height. Practical procedures and possible sources of error are indicated with some proposals for improved methods of evaluation.

551.510.535 2592

The Anomalous Ionospheric Absorption on Winter Days—M. Bossolasco and A. Elena. (*Geofis. pura e appl.*, vol. 47, pp. 89–100; September–December, 1960. In English.) The mean diurnal variation is evaluated from ionospheric absorption measurements made at Genoa during 1959–1960. Abnormally high absorption observed in January and February, 1959, is discussed with reference to data obtained at other stations; the geographical distribution of the phenomenon and the influence of meteors are considered.

551.510.535:523.78 2593

The Ionosphere at the Garchy Station at the Time of the Eclipse of 2nd October 1959—A. Haubert. (*Ann. Géophys.*, vol. 16, pp. 426–427; July–September, 1960.) Ionization density for true heights ranging from 120 to 260 km is plotted as a function of time for the period 0900–1445 U.T. Results are briefly discussed.

551.510.535:551.507.362.1 2594

Some Results of Direct Probing in the Ionosphere—W. Pfister, J. C. Ulwick, and R. P. Vancour. (*J. Geophys. Res.*, vol. 66, pp. 1293–1297; April, 1961.) Results of electron density measurements at two frequencies using two different RF impedance probe techniques are given. See 1491 of May (Haycock and Baker).

551.510.535:551.507.362.2 2595

Ionospheric Electron Content and its Variations deduced from Satellite Observations—K. C. Yeh and G. W. Swenson, Jr. (*J. Geophys. Res.*, vol. 66, pp. 1061–1067; April, 1961.) Faraday fading observations of signals from satellite 1958 δ_2 on 20 and 40 Mc have been analyzed to show diurnal and seasonal variations of electron content from September, 1958, to December, 1959. In twelve instances a decrease in content was observed following a magnetic storm.

551.510.535:551.507.362.2 2596

A Local Reduction of F-Region Ionization due to Missile Transit—H. G. Booker. (*J. Geophys. Res.*, vol. 66, pp. 1073–1079; April, 1961.) An explanation of an unusual echo received on local ionospheric sounders following the firing of Vanguard II is given in terms of a reduction in the ionization density at the F-layer maximum. The interpretation is extended to explain spread-F and radio-star scintillation.

551.510.535:621.3.087.4 2597

Active High-Frequency Spectrometers for Ionospheric Sounding: Part 2—Selection of the Echo Signals from the Noise Background—K. Rawer. (*Arch. elekt. Übertragung*, vol. 14, pp. 373–379; September, 1960.) The prior knowledge of echo properties such as periodicity, signal shape, RF phase and direction of arrival may be used to improve ionospheric recording methods. [Part 1: 2209 of July (Bibl).]

551.510.535:621.391.812.63 2598

The Relationship of Low-Height Ionosonde Echoes to Auroral-Zone Absorption and V.H.F. D Scatter—J. K. Olesen and J. W. Wright. (*J. Geophys. Res.*, vol. 66, pp. 1127–1134; April, 1961.) Weak diffuse echoes are shown at heights between 75 and 95 km in the frequency range 2–8 Mc. The diurnal, seasonal and height characteristics of the layer indicate that it is related to auroral-zone absorption and is responsible for VHF forward scatter.

551.510.535:621.391.812.63 2599

Man-Made Heating and Ionization of the Upper Atmosphere—P. A. Clavier. (*J. Appl. Phys.*, vol. 32, pp. 570–577; April, 1961.) "Absorption of radio signals by cyclotron resonance is shown to be possible within a very narrow layer of the atmosphere (20 km thick just below 100 km). For a plane-polarized signal only 25 per cent of the power can be absorbed. Better results are obtained (50 per cent) with a circularly polarized radio wave. The absorbable power is limited by the effects obtained so that an electron density of 3000 cm^{-3} and an electron temperature of 1600°K cannot be exceeded. The reason for this is the weakness of the earth's magnetic field."

551.510.535:621.391.812.63:551.507.362.2 2600

New Principle of Measurement of Ionospheric Absorption—E. Vassy. (*C. R. Acad. Sci. (Paris)*, vol. 250, pp. 4189–4190; June, 1960.) The mean coefficient of absorption in the region of the ionosphere below an artificial satellite may be calculated from measurements of the signal strength of the satellite transmission, received on an omnidirectional antenna.

551.510.535(98):523.745 2601

The Arctic Ionosphere and Solar Activity—N. C. Gerson. (*Ann. Géophys.*, vol. 16, pp. 253–261; April–June, 1960.) Ionospheric conditions at several arctic stations have been correlated with solar activity using monthly median critical frequencies for the E, F_1 and F_2 layers and the 13-month mean Zürich sunspot numbers.

551.594.5 2602

A Neutral Line Discharge Theory of the Aurora Polaris—S. I. Akasofu and S. Chapman. (*Phil. Trans. Roy. Soc. London Ser. A.*, vol. 253, pp. 359–406; April, 1961.)

551.594.5 2603

Southernmost Extent of Auroras according to German Observations on Land and Sea during the International Geophysical Year—G. Lange-Hesse. (*Naturwiss.*, vol. 47, pp. 423–424; September, 1960.) Results of observations are interpreted with reference to data from U. S. satellite measurements.

551.594.5:523.75 2604

A Note on 106.1-Mc/s Auroral Echoes Detected at Stanford following the Solar Event of November 12, 1960—R. L. Leadabrand, W. E. Jaye, and R. B. Dyce. (*J. Geophys. Res.*, vol. 66, pp. 1069–1072; April 1961.) The time of transit of the auroral particles determined from radar observations was 20 hr 5 min. A change in range of echoes corresponding to a velocity of 100 km was also observed.

551.594.6 2605

On the Origin of VLF Noise in the Earth's Exosphere—T. Ondoh. (*J. Geomag. Geoelect.*, vol. 12, no. 2, pp. 77–83; 1961) The primary cause of VLF noise in the exosphere is Čerenkov radiation due to high-speed protons. The natural thermal noise and proton cyclotron radiation effects are considered to be secondary noise sources.

551.594.6 2606

Graphical Methods for the Determination of the Distance of Atmospherics from their Waveform—R. Schminder. (*Geofis. pura e appl.*, vol. 47, pp. 101–113; September–December, 1960. In German.) Extension of the graphical method outlined in 2222 of July. Delay-time diagrams are given for reflection heights of 70, 80 and 90 km; comparisons are made with tabulated meteorological data.

551.594.6 2607

Determination of the Direction of Arrival and the Polarization of Whistling Atmospherics—J. Delloue. (*J. Phys. Radium*, vol. 21, pp. 514–526 and 587–599, June and July, 1960.) Measurements have been made at 5.5 kc using two pairs of identical antennas located at the ends of perpendicular base lines. Received signals were passed to a central measuring station via microwave links. Results show that the direction of arrival of the signal makes an angle of between 5° and 25° with the magnetic field. Polarization is consistent with the direction of arrival observed and leads to electron densities about ten times smaller than those given by Storey (142 of 1954).

551.594.6:539.16 2608

Whistlers Excited by Sound Waves—K. Rawer and K. Suchy. (PROC. IRE, vol. 49, pt. 1, pp. 968–969; May, 1961.) Sound waves generated by a nuclear explosion could excite transverse waves in the ionosphere, capable of propagation in whistler modes.

LOCATION AND AIDS TO NAVIGATION

621.396.663:551.594.5 2609

The Ephi System for VLF Direction Finding—G. Hefley, R. F. Linfield, and T. L. Davis. (*J. Res. NBS*, vol. 65C, pp. 43–49; January–March, 1961.) In the system described, the bearing of the transient signal is determined from the relative phase ϕ of the vertical electric field E received at three spaced antennas which are separated by equal-length base lines of $\frac{1}{3}$–$\frac{1}{10}$ λ at 10 kc. Appropriate phase detectors, delay lines and coincidence circuits are used to obtain a directional code in preset sectors. Bearing errors are expected to be $<1°$.

621.396.932/.933 2610

Radio Navigation and Teleguidance at Long Range—É. Vassy. (*Ann. Télécommun.*, vol. 14, pp. 256–260; September/October, 1959.) Phase differences due to ionospheric effects are discussed in relation to the Rana system [3314 of 1953 (Honoré and Torcheux)]. For a given region and time, such a hyperbolic system can theoretically operate correctly at long range provided frequencies are chosen which correspond to plateaus on the relevant $h'(f)$ curves.

621.396.933 2611

Doppler in Practice—(*J. Inst. Nav.*, vol. 14, pp. 34–63; January, 1961.) The following papers, which concern intermediate results of evaluation trials of Doppler navigation equipment, were presented at a meeting of the Institute of Navigation on May 20, 1960.

1) Doppler Navigation in S.A.S.—E. S. Pedersen (pp. 34–42).

2) An Evaluation of the Marconi AD 2300—W. E. Brunt (pp. 42–55).

3) The Potential Application of Doppler to Air Navigation—J. E. D. Williams (pp. 55–58). Discussion (pp. 58–63).

621.396.96:629.13.052 2612

The Operation of Radio Altimeters over Snow-Covered Ground or Ice—W. R. Piggott.

(Proc. IRE, vol. 49, pt. 1, p. 965; May, 1961.) The reading of a HF altimeter above a snow- or ice-covered surface corresponds to the lower boundary of the frozen material and thus may be misleading. See 2346 of July (Piggott and Barclay).

621.396.962.25 2613
Analysis of a Frequency-Modulated Continuous-Wave Ranging System—L. Kay: A. J. Hymans, and J. Lait. (*Proc. IEE*, pt. B, vol. 108, pp. 238–239; March, 1961.) Discussion of 3523 of 1960.

621.396.963.3:621.396.677 2614
A Fast Electronically Scanned Radar Receiving System—D. E. N. Davies. (*J. Brit. IRE*, vol. 21, pp. 305–318; April, 1961. Discussion, pp. 319–321.) An experimental method of obtaining the dynamic antenna polar diagram for a 3-cm system with a scanning rate up to 1 Mc is described. Absolute limitations of the technique are considered and its application to a "within-pulse" scanning system is discussed. See 818 of 1959 and back reference.

621.396.963.325 2615
The Optimum Exploitation of the Radar P.P.I. Display by a Transmission System with Frequency-Band Compression—H. Gillmann. (*Frequenz.*, vol. 14, pp. 306–314; September, 1960.) A theoretical investigation is made to determine the optimum transmission system for exploiting fully the properties of the display screen, allowing for the influence of the antenna system on azimuthal resolution. Results are given in diagrammatic form.

MATERIALS AND SUBSIDIARY TECHNIQUES

535.215 2616
Peculiarities in the Temperature Dependence of the Photoemission of Multi-alkali Cathodes—G. Frischmuth-Hoffmann, P. Görlich and H. Hora. (*Z. Naturforsch.*, vol. 15a, pp. 1014–1016; November, 1960.) Results obtained during measurements of quantum yield at low temperatures using cathodes of the type $CsNa_xK_{3-x}Sb$ are discussed. See also 582 of February (Frischmuth-Hoffmann *et al.*).

535.215:546.47'221 2617
Electrical and Optical Properties of Zinc Sulphide Crystals in Polarized Light—J. A. Beun and G. J. Goldsmith. (*Helv. Phys. Acta*, vol. 33, pp. 508–513; October, 1960.) Optical transmission, photoconductivity and photovoltaic effect were measured on series of crystals.

535.215:546.47'48'231 2618
Spectral Distribution of the Internal Photoeffect in the ZnSe-CdSe System—B. T. Kolomiets and Lin' Tszyun'tin. (*Fiz. Tverdogo Tela*, vol. 2, pp. 168–170; January, 1960.)

535.215:546.48'221 2619
Enhancement of Photoconductivity upon Cadmium Sulphide Single Crystals—S. Kitamura, T. Kubo, and T. Yamashita. (*J. phys. Soc. Japan*, vol. 16, p. 351; February, 1961.) Experimental results on the quenching and enhancement of photoconductivity by infrared radiation, under various conditions of applied voltage, are given. They are not explicable by an existing theory of the effects.

535.215:546.48'221:539.23 2620
Effect of Heat Treatment upon Sintered Cadmium Sulphide Photoconductive Films—S. Kitamura. (*J. Phys. Soc. Japan*, vol. 15, p. 1697; September, 1960.) The relation between dark current and temperature was found to be reversible below, and irreversible above, 90°C.

535.215:546.48'231 2621
On the Mechanism of the Electrical Conduction in CdSe—H. Tubota, H. Suzuki, and K. Hirakawa. (*J. Phys. Soc. Japan*, vol. 15, p. 1701; September, 1960.) Experiment showed that the impurity centers contributing to the electrical conduction in CdSe are almost certainly Se vacancies.

535.215:546.48'231 2622
Nonequilibrium Carrier Lifetime in the Surface Layers of (CdSe+Ag) Single Crystals—U. B. Soltamov and I. G. Perestoronin. (*Fiz. Tverdogo Tela*, vol. 2, pp. 26–27; January, 1960.) Activation of the surface by electron bombardment produces a change of the recombination velocity in the surface layer; the non-equilibrium carrier lifetime rises with the amount of activation.

535.215:546.48'241 2623
Investigation of Surface Layers on CdTe Crystals—Yu. A. Vodakov, G. A. Lomakina, G. P. Naumov, and Yu. P. Maslakovets (*Fiz. Tverdogo Tela*, vol. 2, pp. 55–61; January, 1960.)

535.215:546.48'241 2624
Quantum Efficiency of CdTe *p-n* Junctions in the Ultraviolet Part of the Spectrum—G. B. Dubrovskiĭ. (*Fiz. Tverdogo Tela*, vol. 2, pp. 569–570; April, 1960.) A note of measurements was made of the spectral sensitivity of CdTe photocells of a type described earlier (2815 below), to determine if electron multiplication occurs when the cells are illuminated by short-wavelength light. The excess energy of the primary photocarriers is found to be about 2ev, *i.e.*, it exceeds the energy gap by about 0.5ev.

535.215:546.492'221 2625
Certain Features of the Photoconductivity of Mercuric Sulphide—N. I. Butsko. (*Fiz. Tverdogo Tela*, vol. 2, pp. 629–632; April, 1960.) The use and decay characteristics of photoconductivity in hexagonal MgS prepared artificially are similar to those of photoresistors of "hyperbolic" type such as Se or CdS at low temperatures.

535.215:546.817'231:548.5 2626
Growth from the Vapour of Large Single Crystals of Lead Selenide of Controlled Composition—A. C. Prior. (*J. Electrochem. Soc.*, vol. 108, pp. 82–87; January, 1961.)

535.215:546.863'231 2627
The Mechanism of Photoconductivity in Amorphous Chalcogenide Layers—B. T. Kolomiets and V. M. Lyubin. (*Fiz. Tverdogo Tela*, vol. 2, pp. 52–54; January, 1960.) Results are given of an investigation of amorphous layers of Sb_2S_3 relating to the dependence of photocurrent on illumination at comparatively high temperature and of the temperature dependence of photocurrent over a wide range of illumination intensities.

535.37:546.47'221 2628
Behaviour of Excited Electrons and Holes in Zinc Sulphide Phosphors—S. Shionoya, H. P. Kallmann, and B. Kramer. (*Phys. Rev.*, vol. 121, pp. 1607–1619; March, 1961.) Experimental data are used to correlate the various processes involved in fluorescence, phosphorescence, glow emission, stimulation and quenching. A theoretical discussion of possible transition mechanisms giving rise to these effects is given.

535.376 2629
Field Enhancement in ZnSCdS-Mn Phosphors—G. Wendel. (*Z. Naturforsch*, vol. 15a, pp. 1010–1011; November, 1960.) Report on luminescence measurements which suggests that the increase in enhancement ratio observed by Destriau (2753 of 1958) is not primarily due to sensitization by traces of Au.

535.376:546.47'221 2630
The Effects of Infrared Radiation on Trapped Electrons in Excited ZnS Phosphors—B. Kramer, and M. Schön. (*Z. Phys.*, vol. 160, pp. 145–148; October, 1960. In English.) Anomalies in light emission when infrared radiation is applied to ZnS phosphors under ultraviolet excitation are interpreted with reference to experimental results.

537.226:539.12.04 2631
Effect of Pile Irradiation on the Dielectric Properties of Triglycine Sulphate Single Crystals—E. Fatuzzo. (*Helv. Phys. Acta*, vol. 33, pp. 501–504; October, 1960.) Experimental investigation is made of hysteresis loops deformed as a consequence of neutron bombardment, and of changes in polarization, coercive field and intrinsic bias as a function of integrated neutron flux.

537.227 2632
Free Energy of 180° Walls and Surfaces in a Cubic Body-Centred Dipole Lattice—R. Sommerhalder. (*Helv. Phys. Acta*, vol. 33, pp. 617–626; October, 1960. In German.) The free energy of domain walls and of surfaces in ferroelectrics is estimated, assuming a simple model of dipole interaction in a body-centred cubic lattice.

535.227 2633
Antiferroelectric and Ferroelectric Properties of Certain Solid Solutions containing Pb_2MgWO_6—N. N. Kraĭnik and A. T. Agranovskaya. (*Fiz. Tverdogo Tela*, vol. 2, pp. 70–72; January, 1960.) An investigation is made of the permittivity of $PbMg_{0.5}W_{0.5}O_3 - PbTiO_3$ solid solutions in the range -200 to $+300$°C and the dependence of the Curie point on composition.

537.227 2634
Solid Solutions of Niobates and Tantalates based on $BaTiO_3$—E. V. Sinyakov and E. A. Stafiĭchuk. (*Fiz. Tverdogo Tela*, vol. 2, pp. 73–79; January, 1960.)

537.227 2635
Ferroelectric and Antiferroelectric Properties of $NaNbO_3$-$PbZrO_3$ Solid Solutions—N. N. Kraĭnik. (*Fiz. Tverdogo Tela*, vol. 2, pp. 685–690; April, 1960.)

537.227 2636
Order-Disorder Model Theory for the Ferroelectric Effect in the Dihydrogen Phosphates—M. E. Senko. (*Phys. Rev.*, vol. 121, pp. 1599–1604; March, 1961.)

537.227 2637
Ferroelectricity in the Potassium Ferrocyanide Group Ferroelectrics Substituted by Deuterium for Hydrogen—S. Waku, K. Masuno and T. Tanaka. (*J. Phys. Soc. Japan*, vol. 15, p. 1698; September, 1960.)

537.227:537.311.3 2638
The Nature of the Transitional Conduction Processes in Ferroelectric Materials—V. M. Gurevich, I. S. Zheludev and I. S. Rez. (*Fiz. Tverdogo Tela*, vol. 2, pp. 691–696; April, 1960.) Conductivity characteristics of $BaTiO_3$ (see 2639 below) and other ferroelectric crystals are analyzed.

537.227:546.431'824–31 2639
Transitional Direct-Current Conduction Processes in Ceramic $BaTiO_3$—V. M. Gurevich and I. S. Res. (*Fiz. Tverdogo Tela*, vol. 2, pp 673–678; April, 1960.) An experimental investigation is made of the gradual development of

current flow, which is attributed to ferroelectric polarization effects.

537.227:546.431'824–31 2640
Effect of Impurities on Electrical Solid-State Properties of Barium Titanate—C. F. Pulvari. (*J. Amer. Ceram. Soc.*, vol. 42, pp. 355–363; August, 1959.) An experimental investigation is made of the skin and bulk properties of $BaTiO_3$ single crystals with various impurity additions.

537.227:546.431'824–31 2641
Effect of Additives of Limited Solid Solubility on Ferroelectric Properties of Barium Titanate Ceramics—P. Baxter, N. J. Hellicar, and B. Lewis. (*J. Amer. Ceram. Soc.*, vol. 42, pp. 465–470; October, 1959.) Two classes of additives are considered: 1) those giving normal ferroelectric properties with particularly low electrical and mechanical losses and 2) those giving increased permittivity at room temperatures.

537.227:546.431'824–31 2642
Dielectric After-Effects in Ceramic Barium Titanates—G. Bullinger. (*Z. angew. Phys.*, vol. 12, pp. 410–423; September, 1960.) The polarization mechanism of polycrystalline $BaTiO_3$ is investigated experimentally with particular regard to the dependence of after-effects on temperature and voltage.

537.227:546.431'824–31 2643
Motion of 180° Domain Walls in $BaTiO_3$ under the Application of a Train of Voltage Pulses—R. C. Miller and A. Savage. (*J. Appl. Phys.*, vol. 32, pp. 714–721; April, 1961.) The lateral range of the opposing surface-layer field caused by an element of charge on the interface is of the order of 2000 Å. The observed phenomena are described in terms of the surface-layer model of Drougard and Landauer (923 of 1960).

537.228:546.431'824–31 2644
Piezoresistance and Piezocapacitance Effects in Barium Strontium Titanate Ceramics—H. A. Sauer, S. S. Flaschen, and D. C. Hoesterey. (*J. Amer. Ceram. Soc.*, vol. 42, pp. 363–366; August, 1959.) A large change of resistance with stress is reported for a series of ceramic compositions in the system (Ba, Sr, La)TiO_3, and positive piezocapacitive effect in these compositions in the absence of La.

537.228.1 2645
Approximate Method of Calculating Electromechanical Coupling Factor—M. Marutake. (PROC. IRE, vol. 49, pt. 1, p. 967; May, 1961.)

537.228.1 2646
Elastic Constants of Ammonium Dihydrogen Phosphate (ADP) and the Laval Theory of Crystal Elasticity—H. Jaffe and C. S. Smith. (*Phys. Rev.*, vol. 121, pp. 1604–1607; March, 1961.)

537.228.1 2647
Investigation of Temperature Dependence of the Electric and Elastic Parameters of Cancrinite—V. A. Koptsik and L. A. Ermakova. (*Fiz. Tverdogo Tela*, vol. 2, pp. 697–700; April, 1960.) A report of measurements is given of dielectric constant, piezoelectric modulus and coefficient of elasticity of cancrinite, a sodium calcium aluminosilicate, in the temperature range +20 to −140°C.

537.311.33 2648
Thermally Stimulated Conductivity in Semiconductors—I. I. Boĭko, É. I. Rashba, and A. P. Trofimenko. (*Fiz. Tverdogo Tela*, vol. 2, pp. 109–117; January, 1960.) A theory of stimulated conductivity based on a general semiconductor model is given. From an analysis of experimental data for various heating rates the depth of local levels can be determined.

537.311.33 2649
Absorption of Infrared Radiation by Semiconductors in an Electric Field—N. V. Fomin. (*Fiz. Tverdogo Tela*, vol. 2, pp. 605–607; April, 1960.) An expression is derived for the mean absorption probability as a function of the angle between the space vector of the radiation and the electric field direction.

537.311.33 2650
Determination of the Effective Mass of Free Charge Carriers in Semiconductors by Infrared Absorption—K. J. Palnker and E. Kauer. (*Z. angew. Phys.*, vol. 12, pp. 425–432; September, 1960.) The discrepancies in the determination of charge-carrier mass on the basis of various theories of infrared absorption are discussed. Experimental investigation on *n*-type CdTe gave an effective mass of 0.24 × free electron mass. Thirty-one references.

537.311.33 2651
Confirmation of Lifetimes by Noise and by Haynes-Shockley Method—S. Okazaki. (*J. Appl. Phys.*, vol. 32, pp. 712–713; April, 1961.) Values of minority-carrier lifetime in germanium filaments deduced from noise produced by photo-generation of carriers agree well with the values obtained by the Haynes-Shockley method.

537.311.33 2652
Nature of an Ohmic Metal/Semiconductor Contact—G. Diemer. (*Physica*, vol. 26, p. 889; November, 1960.) An apparent contradiction of the model suggested in 150 of 1957 (Kröger *et al.*) is explained.

537.311.33 2653
Determination of the Semiconductor Surface Potential under a Metal Contact—N. J. Harrick. (*J. Appl. Phys.*, vol. 32, pp. 568–570; April, 1961.) An adaptation of Johnson's method (3884 of 1958) is described in which the excess carrier density is measured by an infrared absorption technique.

537.311.33 2654
On the Electrical Conductivity of Polar Semi-conductors at High Frequencies—P. H. Fang. (*Ann. Phys., Lpz.*, vol. 6, pp. 115–119; September, 1960. In English.) The formula for the complex electrical conductivity of polar semiconductors as a function of applied frequency, derived by Stolz (3631 of 1959), is evaluated. A method of representing numerical values of conductivity on an Argand diagram is introduced, and the distribution of relaxation times is discussed.

537.311.33 2655
The Problem of Internal Breakdown in Nonpolar Semiconductors—G. V. Gordeev. (*Fiz. Tverdogo Tela*, vol. 2, pp. 611–619; April, 1960.) Equality of the energy obtained by electrons from the applied field and the energy transferred by the electrons to the lattice may occur at any electron temperature. A breakdown criterion is introduced which allows for ionization and recombination.

537.311.33 2656
Minerals as Prototypes for New Semiconductor Compounds—G. Busch and F. Hulliger (*Helv. Phys. Acta*, vol. 33, pp. 657–666; October, 1960. In German.) Numerous new semiconductors with low melting points and activation energies from 0.1 to 3 ev can be obtained by replacing certain elements in the series of minerals listed.

537.311.33 2657
Electrical Properties of Certain Semiconducting Oxide Glasses—V. A. Ioffe, I. B. Patrina, and I. S. Poberovskaya. (*Fiz. Tverdogo Tela*, vol. 2, pp. 656–662; April, 1960.) The conductivity, thermoelectric power, dielectric loss and permittivity of glasses in the systems $V_2O_5-P_2O_5$, $V_2O_5-P_2O_5-BaO$ and $WO_3-P_2O_5-K_2O$ have been investigated.

537.311.33 2658
Surface Structures and Properties of Diamond-Structure Semiconductors—D. Haneman. (*Phys. Rev.*, vol. 121, pp. 1093–1100; February, 1961.) Results of low-energy electron-diffraction and secondary-emission measurements on GaSb and InSb are discussed, and a general model (111) surfaces is proposed.

537.311.33 2659
Investigation of the Semiconducting Properties of Selenides and Tellurides of Germanium and Tin—J. W. Verstreepen. [*C.R. Acad. Sci., (Paris)*, vol. 251, pp. 1273–1274; September, 1960.]

537.311.33:538.63 2660
Magnetoelectric and Thermomagnetoelectric Effects in Semiconductors: Part 2—L. Godefroy and J. Tavernier. (*J. Phys. Radium*, vol. 21, pp. 544–550; June, 1960.) The results of a previous paper (3914 of 1960) are used to calculate the conductivity and thermoelectric power tensors in the general case of a crystal of cubic symmetry. Measurements of the magnetoelectric and thermomagnetoelectric effects are not sufficient to establish the band structure of a cubic crystal.

537.311.33:538.63 2661
Investigation of the Diffusion of Minority Current Carriers in a Magnetic Field—S. M. Ryvkin, A. A. Grinberg, Yu. L. Ivanov, S. R. Novikov, and N. D. Potekhina. (*Fiz. Tverdogo Tela*, vol. 2, pp. 575–590; April, 1960.) Theoretical discussion and report of measurements of the distribution of minority-carrier concentration in Ge are given. See 2792 of 1960.

537.311.33:539.23 2662
Interference Method for Measuring the Thickness of Epitaxially Grown Films—W. G. Spitzer and M. Tenenbaum. (*J. Appl. Phys.*, vol. 32, pp. 744–745; April, 1961.) In the case of a lightly doped epitaxial layer grown on a heavily doped substrate, incident infrared radiation is reflected at the surface and at the interface to produce interference fringes.

537.311.33:546.28 2663
Surface Properties of Silicon—V. G. Litovchenko and O. V. Snitko. (*Fiz. Tverdogo Tela*, vol. 2, pp. 591–604; April, 1960.) A report and discussion are given of measurements of the effect of an external electric field on the conductivity, the surface recombination and the capacitor photo-EMF in Si. Results show a complex system of surface levels, five fast and three slow.

537.311.33:546.28 2664
Surface Electrical Changes Caused by the Adsorption of Hydrogen and Oxygen on Silicon—J. T. Law. (*J. Appl. Phys.*, vol. 32, pp. 600–609; April, 1961.) Measurements of surface conductance, lifetime of injected carriers, change in contact potential with light and contact potential between the Si sample and a reference electrode were made on surfaces cleaned by ion bombardment and during the absorption of molecular oxygen and atomic hydrogen.

537.311.33:546.28 2665
The Surface Photovoltaic Effect in Silicon and its Application to the Measurement of Minority-Carrier Lifetimes—A. Quilliet and

P. Gosar. (*J. Phys. Radium*, vol. 21, pp. 575–578; July, 1960.) Measurements made by means of a modified form of the capacitive-contact method [e.g. 1173 of 1958 (Johnson)] have been used to determine minority-carrier lifetimes. Results are in good agreement with those obtained by the method of Valdes (741 of 1953).

537.311.33:546.28 2666
Investigation of the Accuracy of the Variational Method in the Problem of Impurity Absorption of Light in Silicon—V. M. Bulmistrov and V. N. Piskovoĭ. (*Fiz. Tverdogo Tela*, vol. 2, pp. 608–610; April, 1960.) The accuracy with which the transition frequency can be calculated is within 4 per cent.

537.311.33:546.28 2667
Heat-Treatment Centres in Silicon—Y. Matukura. (*J. Phys. Soc. Japan*, vol. 16, pp. 192–197; February, 1961.)

537.311.33:546.28 2668
α-Trapping Centres in n-Type Silicon—J. Okada and T. Suzuki. (*J. Phys. Soc. Japan*, vol. 15, p. 1709; September, 1960.) The α-trapping centers correspond to complexes which contain not only oxygen atoms [see 1926 of 1959 (Kaiser *et al.*)], but also vacancies, interstitials or dislocations.

537.311.33:546.28 2669
The Effect of Heat Treatment on the Electrical Properties of p-Type Silicon—I. D. Kirvaldze and V. F. Zhukov. (*Fiz. Tverdogo Tela*, vol. 2, pp. 571–574; April, 1960.) A report of measurements is given of the resistivity and carrier concentration of different single-crystal samples before and after heat treatment in air at temperatures up to 1200°C.

537.311.33:546.28 2670
Volume Recombination in p-Type Silicon Subjected to Heat Treatment at High Temperatures—G. N. Galkin. (*Fiz. Tverdogo Tela*, vol. 2, pp. 8–14; January, 1960.) Heat treatment above 1200°C produced a recombination level in the lower half of the forbidden band 0.13 ± 0.01 ev from the valence band. The temperature dependence of the capture cross sections for electrons and holes was determined.

537.311.33:546.28:539.12.04 2671
Defects in Irradiated Silicon: Part 1—Electron Spin Resonance of the Si-*A* Centre—G. D. Watkins and J. W. Corbett. (*Phys. Rev.*, vol. 121, pp. 1001–1014; February, 1961.)

537.311.33:546.28:539.12.04 2672
Defects in Irradiated Silicon: Part 2—Infrared Absorption of the Si-*A* Centre—J. W. Corbett, G. D. Watkins, R. M. Chrenko, and R. S. McDonald. (*Phys. Rev.*, vol. 121, pp. 1015–1022; February, 1961.) Part 1: 2671 above.

537.311.33:546.28:539.12.04 2673
Annealing of Radiation Damage on Lifetime in Silicon—K. Matsuura and Y. Inuishi. (*J. Phys. Soc. Japan*, vol. 16, p. 339; February, 1961.)

537.311.33:546.289 2674
Recombination Noise in Germanium in the Range of Defect Semiconductivity—G. Lautz and M. Pilkuln. (*Naturwiss.* vol. 47, pp. 394; September, 1960.) A report is made of noise measurements on n- and p-type single-crystal Ge with differing impurity content, in the temperature range 5–300°K.

537.311.33:546.289 2675
The Relation between Excess Noise and Surface Trapping in Germanium—L. S. Sochava and D. N. Mirlin. (*Fiz. Tverdogo Tela*, vol. 2, pp. 23–25; January, 1960.) Field-effect frequency characteristics are compared with the excess-noise spectrum for the same specimens to test the validity of the McWhorter model [see 173 of 1957 (Kingston and McWhorter)].

537.311.33:546.289 2676
Determination of the Impurity Concentration on Germanium—R. M. Vinetskiĭ and E. G. Miselyuk. (*Fiz. Tverdogo Tela*, vol. 2, pp. 67–69; January, 1960.) A method based on the effect of impurity scattering on resistivity is described. The impurity concentration is calculated from the measured values of resistivity at two temperatures, and the values are given for change in the resistivity due to lattice scattering on lowering the temperature from 290 to 100°K in p-type and n-type Ge.

537.311.33:546.289 2677
The Absorption of Light in Germanium—M. I. Kornfel'd. (*Fiz. Tverdogo Tela*, vol. 2, pp. 179–180; January, 1960.) An empirical expression for the absorption coefficient is given.

537.311.33:546.289 2678
Thermal Conductivity of p- and n-Type Germanium with Different Carrier Concentrations in the Temperature Range 80–440°K—E. D. Devyatkova I. A. Smirnov. (*Fiz. Tverdogo Tela*, vol. 2, pp. 561–565; April, 1960.) An earlier investigation is continued (1620 of 1959) using a different method of measurement.

537.311.33:546.289 2679
Anisotropy of the Surface Breakdown of Germanium in the Range of Strong Fields—A. I. Morozov. (*Fiz. Tverdogo Tela*, vol. 2, pp. 620–623; April, 1960.) Single current pulses of of 10–1000-μsec duration and maximum amplitude 30a were passed through a point contact on samples of n- and p-type Ge of resistivity 0.1–40Ω.cm. Discharges observed along the Ge surface were in the form of a straight band emitting reddish light. The experiment showed that the surface breakdown in Ge is anisotropic, which may be due to the anisotropy of "hot" electrons.

537.311.33:546.289 2680
Effect of a Constant Electrical Field on Germanium Fast Surface States—Y. Margoninski. (*Phys. Rev.*, vol. 121, pp. 1282–1285; March, 1961.) To resolve conflicting experimental evidence, careful measurements of surface recombination velocity and surface conductivity were performed before and after application of dc fields of about 2×10^6v/cm. Results confirm the assumption that the energy of the recombination centers is not affected by the field.

537.311.33:546.289 2681
Current Flow across Grain Boundaries in n-Type Germanium: Parts 1 and 2—R. K. Mueller. (*J. Appl. Phys.*, vol. 32, pp. 635–645; April, 1961.) A theory of current flow is given and confirmed by measurements. The measurements were made on specially grown bicrystals in the temperature range 200–350°K where carrier generation in the space-charge region could be neglected in the theoretical treatment.

537.311.33:546.289:535.215:538.639 2682
Theory of the Anisotropic Photomagnetic Effect in Germanium—A. A. Grinberg. (*Fiz. Tverdogo Tela*, vol. 2, pp. 153–156; January, 1960.) A mechanism is proposed accounting for the effects observed by Kikoin and Bykovskiĭ (2460 of 1958).

537.311.33:546.289:538.632 2683
Sign Reversal of Hall Coefficients at Low Temperatures in Heavily Compensated p-type Germanium—H. Yonemitsu, H. Maeda, and H. Miyazawa. (*J. Phys. Soc. Japan*, vol. 15, pp. 1717–1718; September, 1960.) Sign reversal occurred at about 5°K.

537.311.33:546.289:539.12.04 2684
Mobility of Radiation-Induced Defects in Germanium—P. Baruch. (*J. Appl. Phys.*, vol. 32, pp. 653–659; April, 1961.) The high electric field in the space-charge region of a reverse-biased Ge $p \pm n$ junction is used to study the motion of defects induced in the structure by 1-Mev electrons or γ rays. Evidence is obtained of the nature of these defects and they are correlated with thermal annealing studies.

537.311.33:546.289:548.0 2685
Crystal Dislocation and Growth of Etch Pits—W. Riessler. (*Z. angew. Phys.*, vol. 12, pp. 433–442; October, 1960.) Experimental investigations are made on Ge to determine the effects of various etchants and to interpret the course of etch-pit formation from an examination of their shape.

537.311.33:546.57'72'241 2686
Semiconducting "Compound" $AgFeTe_2$—J. H. Wernick and R. Wolfe. (*J. Appl. Phys.*, vol. 32, p. 749; April, 1961.) $AgFeTe_2$ is shown to contain at least two phases, one of which is Ag_2Te. The ternary phase, ideally $AgFeTe_2$, has not been identified.

537.311.33:546.571'241 2687
Degeneracy in Ag_2Te—C. Wood, V. Harrap, and W. M. Kane. (*Phys. Rev.*, vol. 121, pp. 978–982; February, 1961.)

537.311.33:546.571'241:539.23 2688
Electrical Conduction in Thin Films of Silver Telluride—W. M. Kane and C. Wood. (*J. Electrochem. Soc.*, vol. 108, pp. 101–102; January, 1961.)

537.311.33:546.681'86 2689
Electrical Properties of n-Type GaSb—A. J. Strauss. (*Phys. Rev.*, vol. 121, pp. 1087–1090; February, 1961.) Certain experimental data are not explained by the two-band model of Sagan (2448 of 1960). Systematic differences between the properties of Se-doped and Te-doped samples are probably associated with impurity conduction of the metallic type.

537.311.33:[546.628'18+546.681'19 2690
Diffusion in Compound Semiconductors—B. Goldstein. (*Phys. Rev.*, vol. 121, pp. 1305–1311; March, 1961.) Self-diffusion in single-crystal InP and GaAs has been measured, together with the diffusion of Cd, Zn, S and Se in GaAs; the object was primarily to find the diffusion constants and activation energies and then to determine the specific mechanism of diffusion.

537.311.33:546.682'86 2691
Observations of Electron-Hole Current Pinching in Indium Antimonide—M. Glicksman and R. A. Powlus. (*Phys. Rev.*, vol. 121, pp. 1659–1661; March, 1961.) Observations of the current and voltage as a function of time provide substantial corroboration for the occurrence of pinching suggested earlier [3388 of 1959 (Glicksman and Steele)].

537.311.33:546.73'28 2692
An Investigation of the Semiconducting Properties in the Silicon-Cobalt System—E. N. Nikitin. (*Fiz. Tverdogo Tela*, vol. 2, pp. 633–636; April, 1960.)

537.311.33:546.814–31 2693
Semiconducting Tin Dioxide—A. Ya. Kuznetsov. (*Fiz. Tverdogo Tela*, vol. 2, pp. 35–42; January, 1960.) Methods of preparation

and properties of SnO_2 films for heating applications are described.

537.311.33:546.817'241:538.63 2694
Oscillatory Magnetoresistance in *n*-Type PbTe—Y. Kanai, R. Nii, and N. Watanabe. (*J. Phys. Soc. Japan*, vol. 15, p. 1717; September, 1960.) Oscillatory galvanomagnetic effects were observed in *n*-type PbTe at 4.2° K in a strong pulsed magnetic field.

537.311.33:548.5 2695
Method of Growing Uniform Single Crystals of Alloyed Semiconductor Materials, Solid Solutions and Intermetallic Compounds of Given Composition Determined by the Composition of the Melt—S. V. Airapetyants and G. I. Shmelev. (*Fiz. Tverdogo Tela*, vol. 2, pp. 747–755; April, 1960.) Details are given of a floating-crucible technique different from that described by Leverton (3896 of 1958), in which the melt composition in the socket of the floating crucible from which the crystal is pulled is that of the melt entering from the outer crucible.

537.311.33:621.317.3 2696
Electrodeless Measurement of Semiconductor Resistivity at Microwave Frequencies—Jacobs, Brand, Meindl, Benant, and Benjamin. (See 2730.)

537.311.33:621.362 2697
Semiconducting Materials for Thermoelectric Power Generation—F. D. Rosi, E. F. Hockings, and N. E. Lindenblad. (*RCA Rev.*, vol. 22, pp. 82–121; March, 1961.)

537.311.33:621.391.822 2698
Fluctuation Noise in Semiconductor Space-Charge Regions—L. J. Giacoletto. (PROC. IRE, vol. 49, pt. 1, pp. 921–927; May, 1961.) In addition to circuit noise, basic noise arises from fluctuations in the ionization state of the impurity atoms. Experimental verification of this noise would provide a new method for evaluating some of the properties of semiconductors.

537.311.33:621.391.822 2699
$1/f$ Noise and Channel in Ge *p-n* Junction—K. Komatsubara, Y. Inuishi, H. Edagawa, and T. Shibaike. (*J. Phys. Soc. Japan*, vol. 15, pp. 1713–1714; September, 1960.) Direct evidence is given that the inversion-layer channel formation is a predominant source of $1/f$ noise in reverse-biased *p-n* junctions.

537.311.35 2700
Electrokinetic Effects in Liquid Semiconductors—V. B. Fiks and G. E. Pikus. (*Fiz. Tverdogo Tela*, vol. 2, pp. 65–66; January, 1960.) The application of an electric field to a liquid semiconductor filling a capillary is considered. By measuring the electrokinetic effects, the potential difference between the semiconductor surface and bulk can be determined.

537.323 2701
Effects of Doping Additions on the Thermoelectric Properties of the Intrinsic Semiconductor $Bi_2Te_{2.1}Se_{0.9}$—L. C. Bennett and J. R. Wiese. (*J. Appl. Phys.*, vol. 32, pp. 562–564; April, 1961.)

537.323 2702
Effect of Freezing Conditions on the Thermoelectric Properties of $BiSbTe_3$ Crystals—G. J. Cosgrove, J. P. McHugh, and W. A. Tiller. (*J. Appl. Phys.*, vol. 32, pp. 621–623; April, 1961.)

537.533.8 2703
Fine Structure of Secondary Emission vs Angle of Incidence of the Primary Beam on Titanium Single Crystals—R. W. Soshea and A. J. Dekker. (*Phys. Rev.*, vol. 121, pp. 1362–1369; March, 1961.)

538.221 2704
Magnetic Viscosity due to Solute Atom Pairs: Part 2—Experimental Results—G. Biorci, A. Ferro, and G. Montalenti. (*J. Appl. Phys.*, vol. 32, pp. 630–635; April, 1961.) The results confirm the theory given in Part 1 (1250 of April).

538.221 2705
Domain Configurations about Nonmagnetic Particles in Iron—W. D. Nix and R. A. Huggins. (*Phys. Rev.*, vol. 121, pp. 1038–1042; February, 1961.)

538.221 2706
Small-Angle Grain Boundaries as Obstacles to the Movement of Bloch Walls in Silicon Iron—W. Stephan. (*Z. angew. Phys.*, vol. 12, pp. 398–400; September, 1960.)

538.221:537.311.31 2707
The Influence of Aging Treatment on the Temperature Dependence of the Electric Resistance in Alnico 5 Magnet—T. Fujiwara and T. Kato. (*J. Phys. Soc. Japan*, vol. 15, p. 1705; September, 1960.)

538.221:539.23 2708
Direct Measurement of the Uniaxial Magnetic Anisotropy of Vapour-Deposited Thin Films of Iron, Nickel, Permalloy and Cobalt—Z. Málek and W. Schüppel. [*Ann. Phys. (Lpz.)*, vol. 6, pp. 252–261; September, 1960.] See also 267 of January (Málek *et al.*).

538.221:539.23 2709
Spin-Wave Resonance in Ni Films—H. Nosé. (*J. Phys. Soc. Japan*, vol. 15, pp. 1714–1715; September, 1960.)

538.221:539.23 2710
Magnetization-Reversal Processes in Thin Ferromagnetic Ni-Fe Films—S. Middlehoek. (*Helv. Phys. Acta*, vol. 33, pp. 519–524; October, 1960. In German.) A study is made of hysteresis loops in directions parallel and perpendicular to the applied magnetic field, to determine the remanence characteristics.

538.221:539.23 2711
Ni-Fe Single-Crystal Films and their Magnetic Characteristics—R. R. Verderber and B. M. Kostyk. (*J. Appl. Phys.*, vol. 32, pp. 696–699; April, 1961.)

538.221:539.23 2712
Free and Forced Oscillations of the Magnetization in Thin Permalloy Films—P. Wolf. (*Z. Phys.*, vol. 160, pp. 310–319; October, 1960.) Free oscillations in the range 500–1100 Mc have been excited in films of thickness 1000–3000 Å. Comparisons are made with the characteristics of forced oscillations observed in ferromagnetic resonance experiments. Results show reasonable agreement with theoretical results based on the Landau-Lifshitz equation. See also 3591 of 1960 (Dietrich *et al.*).

538.221:539.23 2713
Magnetoresistance Effect in the Magnetization Reversal of Permalloy Films—E. Tatsumoto, K. Kuwahara, and M. Goto. (*J. Phys. Soc. Japan*, vol. 15, p. 1703; September, 1960.) Confirmation was obtained that the magnetization reversal in low frequency fields takes place by domain wall motion and rotation respectively parallel and perpendicular to the easy direction.

538.221:539.23:621.385.833 2714
Display of Weiss Domains in Thin Ferromagnetic Films by means of an Electromagnetic Electron Microscope—E. Fuchs. (*Naturwiss.*, vol. 47, p. 392; September, 1960.) A method is described for using electromagnetic lenses without affecting the magnetic structure of the film, and without having recourse to shadow and schlieren methods.

538.221:539.234:538.61 2715
The Application of the Magnified Magneto-optical Kerr Effect to Render Visible the Magnetic Domains of Polycrystalline Cobalt and Nickel—J. Kranz and A. Schauer. (*Naturwiss.*, vol. 47, pp. 392–393; September, 1960. Further application of the method used in 1281 of 1959 (Kranz and Drechsel).

538.221:621.318.134 2716
Effects of a Magnetic Field on Heat Conduction in some Ferrimagnetic Crystals—D. Douthett and S. A. Freidberg. (*Phys. Rev.*, vol. 121, pp. 1662–1667; March, 1961.

538.221:621.318.134 2717
The Measurement of Galvanomagnetic Properties of Ferrites—K. Zaveta. (*Fiz. Tverdogo Tela*, vol. 2, pp. 106–108; January, 1960.) The anomalous temperature dependence of the change of resistance with magnetic field measured near Curie point [3912 of 1958 (Belov and Talalaeva)] can be considered as a magnetothermal effect.

538.221:621.318.134 2718
Experimental Determination of the Components of the Permeability Tensor and the Spectroscopic Splitting Factor of Mg-Mn Ferrites in the Microwave Region: Part 1—K. H. Gothe. [*Ann. Phys., (Lpz)*, vol. 6, pp. 298–306; September, 1960.)] An HF method was used for measurement at 3.2 cmλ with the apparatus described. Additional measurements to determine the frequency dependence of the splitting factor were made at 1.25 cmλ.

538.221:621.318.134 2719
Time Decrease of Magnetic Permeability in some Mixed Ferrites—K. Ohta. (*J. Phys. Soc. Japan*, vol. 16, pp. 250–258; February, 1961.) Disaccommodation measurements for a number of ceramic ferrites and also for a single crystal of Ni-Zn ferrite, are described. The displacement of either vacancies or interstitial ions may be the main origin of the phenomenon.

538.221:621.318.134 2720
Ferromagnetic Alignment by Antiferromagnetic Exchange Interaction. Note on the Magnetic Behaviour of Neodymium Garnet—W. P. Wolf. (*J. Appl. Phys.*, vol. 32, pp. 742–743; April, 1961.)

538.221:621.318.134:537.311.33 2721
Electric Conduction of Ferrites containing Fe^{2+} Ions—N. Miyata. (*J. Phys. Soc. Japan*, vol. 16, pp. 206–208; February, 1961.) A measurement and interpretation are given of dc conductivities from 100–300°K, for the ferrite solid solution $(MFe_2O_4)_{1-y}(Fe_3O_4)_y$, where M = Mn, Ni, Mn-Ni, or Zn.

538.221:621.318.134:538.569.4 2722
Subsidiary Absorption above Ferrimagnetic Resonance—P. C. Fletcher and N. Silence. (*J. Appl. Phys.*, vol. 32, pp. 706–711; April, 1961.) Theory is developed and confirmed by experiment showing that subsidiary absorption can be observed above Kittel resonance. This verifies Suhl's theory of high-power phenomena in ferrites. The absorption occurs at many unsuspected field strengths and is controlled to a certain extent by sample shape and material.

538.221:621.318.134:538.569.4 2723
Measurement of Saturation Magnetization of Ferrites by means of Ferromagnetic Resonance—F. Schneider. (*Z. angew. Phys.*, vol. 12, pp. 447–450; October, 1960.) The saturation

magnetization of three polycrystalline ferrites is calculated from the line spacing of the absorption spectrum. Good agreement with values measured by magnetic balance is obtained.

538.221:621.318.134:538.569.4 2724
Temperature Dependence of the Line Width of Ferrimagnetic Resonance in Polycrystalline Nickel-Cadmium Ferrite—S. Takemoto. (*J. Phys. Soc. Japan*, vol. 16, p. 344; February, 1961.)

538.221:621.318.134:548.5 2725
Voluntary and Forced Growth Orientation in the Growing of Ferrite Single Crystals—U. Rösler and G. Elbinger. [*Ann. Phys.*, (*Lpz.*), vol. 6, pp. 236–240; September, 1960.]

538.222:538.569.4 2726
Paramagnetic Relaxation Rates Determined by Pulsed Double Resonance Experiments—B. Bölger and B. J. Robinson. (*Physica*, vol. 26, pp. 133–141; February, 1960.) Results of experiments on synthetic ruby and $K_3Cr(CN)_6/K_3Co(CN)_6$ indicate that the Cr concentration in these salts can be increased to give maser action at higher temperatures.

538.222:538.569.4:621.375.9 2727
Cross-Relaxation and Concentration Effects in Ruby—R. W. Roberts, J. H. Burgess, and H. D. Tenney. (*Phys. Rev.*, vol. 121, pp. 997–1000; February, 1961.) Cross-relaxation can improve maser performance even in the absence of doping. Its effect in ruby maser crystals is treated by the introduction of a cross-relaxation probability in the rate equations.

MATHEMATICS

517.432.1 2728
New Substantiation of Heaviside's Operational Calculus: Contribution to the Theory of the Solution of Linear Differential Equations—G. Wunsch. (*Hochfrequenz. und Elektroak.*, vol. 69, pp. 133–139; August, 1960.) An alternative method is proposed which is not based on the Laplace transformation; it is simpler mathematically and more adaptable to the solution of practical electrical engineering problems.

MEASUREMENTS AND TEST GEAR

621.3.087.4 2729
An Automatic Check-Out and Recording Network—R. Mansey. (*Electronic Eng.*, vol. 33, pp. 284–291; May, 1961.) A description is given of British equipment, designed for the automatic checking of a missile system, which has proved suitable for any aircraft or similar system where the parameters are predominantly electrical.

621.317.3:537.311.33 2730
Electrodeless Measurement of Semiconductor Resistivity at Microwave Frequencies—H. Jacobs, F. A. Brand, J. D. Meindl, M. Benant, and R. Benjamin. (Proc. IRE, vol. 49, pt. 1, pp. 928–932; May, 1961.) The new method depends on the absorption of microwave power in the semiconductor medium. It gives results which depend on bulk properties of the medium and is less subject to errors arising from surface leakage and crystal imperfections.

621.317.3:538.632 2731
The Voltage Sensitivity of Hall-E.M.F. Probes—V. V. Galavanov. (*Fiz. Tverdogo Tela*, vol. 2, pp. 62–64; January, 1960.) Ge probes have a sensitivity almost 3.7 times that of InSb under no-load conditions. With an external load InAs and InSb probes have a higher figure of merit than Ge. Below 120°K the sensitivity of a probe of high-purity InSb is 20,000 μv/oersted, 400 times higher than at room temperature.

621.317.3:621.374.32 2732
Digital Measurements—P. R. Darrington. (*Wireless World*, vol. 67, pp. 313–318; June, 1961.) Counter techniques and display methods for frequency, time and voltage measurements are reviewed.

621.317.3:621.391.822 2733
Measurement of Noise Power Spectra by Fourier Analysis—A. Z. Akcasu. (*J. Appl. Phys.*, vol. 32, pp. 565–568; April, 1961.) The theory of the calculation of the power spectrum by direct Fourier analysis is developed and shown to be comparable with autocorrelation analysis in resolution, accuracy and computer requirements.

621.317.335:537.311.33 2734
Measurement of the Electrical Conductivity and Dielectric Constant without Contacting Electrodes—T. Ogawa. (*J. Appl. Phys.*, vol. 32, pp. 583–592; April, 1961.) The torque exerted on a specimen of semiconducting or dielectric material suspended in a circularly or linearly polarized electric field gives the imaginary and real parts of the dielectric constant respectively. The theory of the method is given together with some experimental results obtained on CdS crystals and powders in the frequency range 25 cps–2kc.

621.317.7:621.373.421 2735
A Transistorized Frequency Synthesizer—G. Husson and B. N. Sherman. (*J. Brit. IRE*, vol. 21, pp. 347–350; April, 1961.) A brief description is given of a light-weight unit providing discrete frequencies in the range 2–32 Mc in 1-kc steps from a 1-Mc frequency standard. Spurious responses are reduced to levels impracticable with conventional filter techniques by using an automatic phase-control circuit.

621.317.7:621.391.82 2736
A Portable Instrument for the Measurement of Radio Interference in the Frequency Range 0.15–3 Mc/s—H. Albsmeier. (*Elektrotech. Z., Edn B.*, vol. 12, pp. 483–486; October, 1960.) The battery-operated instrument described conforms to the German VDE specifications for interference-measurement equipment.

621.317.7.029.63/.64 2737
A Coaxial Connector System for Precision R. F. Measuring Instruments and Standards—D. Woods. (*Proc. IEE*,, pt. B, vol. 108, pp. 205–213; March, 1961.) The connector system does not introduce uncertainties greater than about 3 parts in 10^4 in the admittance parameter, for frequencies up to 4 Gc.

621.317.725:621.374.32 2738
Digital Voltmeter Employs Voltage-to-Time Converter—B. Barker and M. McMahan. (*Electronics*, vol. 34, pp. 67–69; May, 1961.) An inexpensive instrument using no stepping switches is described, in which clock pulses are gated into a counter in proportion to the amplitude of the input voltage.

621.317.733 2739
Transformer-Ratio-Arm Bridges—J. F. Golding. (*Wireless World*, vol. 67, pp. 329–335; June, 1961.) The principle of the three-terminal impedance-measuring facility and various circuit arrangements are described. An assessment of accuracy and a comparison with conventional bridges are made.

621.317.733.029.4 2740
An Ultra-Low-Frequency Bridge for Dielectric Measurements—D. J. Scheiber. (*J. Res. NBS*, vol. 65C, pp. 23–42; January–March, 1961.) The bridge described is capable of measuring the parallel capacitance and resistance of dielectric specimens in the frequency range 0.008–200 cps.

621.317.738 2741
Highly Stabilized and Sensitive Reactance Meter—B. Ichijo and T. Arai. (*Rev. Sci. Instr.*, vol. 32, pp. 122–130; February, 1961.) The instrument has a range of 10^{-3}–10^6 pf with a sensitivity of 0.001 pf when measured with an ammeter of 100μ f.s.d. Possible applications are mentioned.

621.317.742 2742
Reflectometers—D. E. Watt-Carter. (*P.O. Elec. Engrg. J.*, vol. 54, pt. 1, pp. 37–39; April, 1961.) The principles of directional-coupler and of wattmeter types of reflectometer suitable for inclusion in coaxial feeders from HF transmitters are described.

621.317.755:621.374 2743
Distortion of Steep Pulse Edges due to Finite Electron Transit Time between Parallel Deflection Plates—H. Lotsch. (*Frequenz*, vol. 14, pp. 264–268; August, 1960.) Investigations of the CRO distortion of step functions with vertical or sloping fronts in relation to electron transit time. A formula is given for calculating true rise time from the measured value.

OTHER APPLICATIONS OF RADIO AND ELECTRONICS

621–52:621.387.3 2744
Cold-Cathode Tube Circuits for Automation—R. S. Sidorowicz. (*Electronic Eng.*, vol. 33, pp. 138–143, 232–237, and 296–302; March–May, 1961.)

621.362+621.56 2745
The Influence of the Temperature Dependence of Parameters of the Materials on the Efficiency of Thermoelectric Generators and Refrigerators—B. Ya. Moĭzhes. (*Fiz. Tverdogo Tela*, vol. 2, pp. 728–737; April, 1960.)

621.362:537.227 2746
Application of Ferroelectricity to Energy Conversion Processes—W. H. Clingman and R. G. Moore, Jr. (*J. Appl. Phys.*, vol. 32, pp. 675–681; April, 1961.) Simplified and more general expressions are derived for the energy conversion efficiency of a ferroelectric device converting heat energy to electrical energy. Numerical values are obtained for $BaTiO_3$ which has an efficiency in the range 0.5–1.0 per cent. Future applications are discussed.

621.362:537.311.33 2747
Semiconducting Materials for Thermoelectric Power Generation—F. D. Rosi, E. F. Hockings, and N. E. Lindenblad. (*RCA Rev.*, vol. 22, pp. 82–121; March, 1961.)

621.362:621.387 2748
Plasma Synthesis and its Application to Thermionic Power Conversion—K. G. Hernqvist. (*RCA Rev.*, vol. 22, pp. 7–20; March, 1961.) Thermionic energy converters are discussed in which the electron space charge is neutralized by positive ion injection.

621.362:621.387 2749
Direct Conversion of Heat to Electromagnetic Energy—F. M. Johnson. (*RCA Rev.*, vol. 22, pp. 21–28; March, 1961.) "The conversion of heat into electromagnetic energy is achieved by utilizing the intrinsically unstable space-charge properties of a thermionic cesium plasma diode. Experimental studies of this phenomenon are described. A physical model for the observed relaxation oscillations is proposed which is in qualitative agreement with experiments."

621.362.012.8 2750
Equivalent Circuits for a Thermoelectric

Converter—E. L. R. Webb. (PROC. IRE, vol. 49, pt. 1, pp. 963–964; May, 1961.)

621.375.9:621.372.44:621.313.13 2751
Parametric Variable-Capacitor Motor—H. E. Stockman. (PROC. IRE, vol. 49, pt. 1, p. 970; May, 1961.) A note on the operation of an experimental electric motor analogous to the variable-inductance devices considered earlier (3232 of 1960).

621.384.621 2752
Ion Optics in Long, Multistage Accelerator Tubes—M. Sonoda, A. Katase, M. Seki, and Y. Wakuta. (*J. Phys. Soc. Japan*, vol. 15, pp. 1680–1684; September, 1960.)

621.387.422:537.311.33 2753
P-N Junctions as Solid-State Ionization Chambers—E. Baldinger, W. Czaja, and A. Z. Faroogi. (*Helv. Phys. Acta*, vol. 33, pp. 551–557; October, 1960. In German.) The characteristics of *p-n* junction diodes used for counting α-particles and protons are discussed with reference to experimental results.

621.398:621.3.087.4 2754
An Equipment for Processing Time-Multiplexed Telemetry Data—D. J. McLauchlan and T. T. Walters. (*J. Brit. Interplanetary Soc.*, vol. 18, pp. 33–38; January/February, 1961. Discussion, pp. 38–39.) A description of the TIMTAPE equipment. It has a magnetic-tape input and, after analogue processing, produces outputs in the form of film and punched cards.

PROPAGATION OF WAVES

621.371:621.396.945 2755
Propagation of Electromagnetic Pulses in a Homogeneous Conducting Earth—J. R. Wait. (*Appl. Sci. Res.*, vol. B8, No. 3, pp. 213–253; 1960.) The theory of EM propagation in both infinite and semi-infinite conducting media is derived, using Laplace transform theory, for various forms of pulse excitation.

621.391.812 2756
The Phase Variation of Very-Low-Frequency Waves Propagated over Long Distances—B. G. Pressey, G. E. Ashwell, and J. Hargreaves. (*Proc. IEE*, pt. B, vol. 108, pp. 214–226; March, 1961.) A description and analysis are given of long-term phase variations between two receivers spaced up to 280 km apart and oriented both transverse to and along the direction of the transmitter, at 17.2 kc over a 1000 km path and 15.5 kc over 6000 km.

621.391.812.63 2757
Propagation in a Plasma—P. A. Clavier. (*J. Appl. Phys.*, vol. 32, pp. 578–582; April, 1961.) "The boundary conditions for a radio signal incident normally on a layer of plasma are discussed. It is shown that 10 different modes must in general propagate in the layer, instead of the usually assumed six. The 10 modes are obtained when the Langevin form of the force is used in Boltzmann's equation."

621.391.812.63:550.389.2 2758
Radio Propagation Conditions in the International Geophysical Year—B. Beckmann and A. Ochs. (*Nachrtech. Z.*, vol. 13, pp. 414–418; September, 1960.) The work during the IGY of the radio propagation service of the German Federal Post Office is reviewed.

621.391.812.63:551.507.362 2759
Doppler Shifts and Faraday Rotation of Radio Signals in a Time-Varying, Inhomogeneous Ionosphere: Part 2—Two-Signal Case—J. M. Kelso. (*J. Geophys. Res.*, vol. 66, pp. 1107–1115; April, 1961.) The work described in Part 1 (1294 of April) is extended to the calculation of frequency shift in a two-frequency Doppler experiment and to the determination of rate of Faraday rotation. The formulas contain parameters which require a knowledge of the ray paths.

621.391.812.63:551.507.362.2 2760
Calculation of the Faraday Effect relative to the Ionosphere—É. Argence, E. Harnischmacher, H. A. Hess, and K. Rawer. (*Ann. Géophys.*, vol. 16, pp. 272–275; April–June, 1960.) Some relations concerning the Faraday effect are established in order to study transmissions from 1958 δ_2 at Breisach, Germany. The effect is also examined for frequencies greater than 100 Mc.

RECEPTION

621.391.8:538.312 2761
On the Reception of Electromagnetic Waves—H. Bondi. [*Proc. Roy. Soc.* (*London*) *A*, vol. 261, pp. 1–9; April, 1961.] The energy that can be obtained by a receiver from a wave is calculated, assuming that the receiver has full knowledge of the structure of the incident radiation.

621.391.812.6:551.507.362.2 2762
VHF Satellite Signals Received at Extra-Optical Distances—L. J. Anderson. (PROC. IRE, vol. 49, pt. 1, pp. 959–960; May, 1961.) Data is given on the reception of VHF signals from distances up to 1900 miles beyond the radio horizon.

621.391.822 2763
A Method of Measurement of the Probability Density of a Noise Voltage and Experimental Verification of the Tendency towards a Gaussian Law by Selective Filtering—B. Picinbono. [*C. R. Acad. Sci., (Paris)*, vol. 250, pp. 4123–4125; June, 1960.] An experimental method of determining the probability law of background noise by sampling and analyzing the sample with an amplitude selector is described.

621.391.822.1 2764
The High-Frequency Minimum Protection Ratio between Two Transmission Channels Amplitude-Modulated with the Same Program—W. Freutel and F. von Rautenfeld. (*Rundfunktech. Mitt.*, vol. 4, pp. 181–193; October, 1960.) The protection ratios required for various test conditions are determined on the basis of subjective assessments by a group of listeners. See also 3464 of 1959 (Belger and von Rautenfeld). For English version see *E. B. U. Rev.*, no. 63A, pp. 197–208; October, 1961.

621.396.62:621.396.677:538.632 2765
Pick-Up Devices for Very-Low-Frequency Reception—G. J. Monser. (*Electronics*, vol. 34, pp. 68–69; April, 1961.) The sensitivities of loop and whip antennas vary by as much as 60 db over the frequency range 10 cps-10kc. The advantages of using a Hall device as a receiving element are discussed.

621.396.62.001.4:621.391.82 2766
Evaluating Radio Receiver Susceptibility to Interference—B. T. Newman, H. Cahn, and R. Keyes. (*Electronics*, vol. 34, pp. 70–74; April, 1961.) A method is described for comparing the various receiver characteristics which affect intelligibility with those of an idealized standard receiver.

621.396.62.029.63/.64:523.164.32 2767
Microwave Swept Receiver uses Zero Intermediate Frequency—D. W. Casey, H. (*Electronics*, vol. 34, pp. 59–63; April, 1961.) A frequency sweep from 2 to 4 Gc is achieved every 10 sec in synchronism with a cr tube sweep using a backward-wave local oscillator. The signal band of the IF amplifier extends from zero to 5 Mc, giving a 3-db improvement in noise figure and eliminating image rejection problems.

STATIONS AND COMMUNICATION SYSTEMS

621.39:621.372.8 2768
Long-Distance Waveguide Transmission—Hamer. (See 2458.)

621.396.1 2769
Radio Supervision—V. Vincentz. (*Elektrotech. Z., Edn B*, vol. 12, pp. 581–583; November, 1960.) International arrangements for supervising the occupation of allocated frequency bands and for eliminating sources of interference to radio services are reviewed. Specially designed receiving equipment for use at monitoring stations is mentioned.

621.396.65 2770
Bases for Planning a Telecommunication Network in North-West Spain—A. Arbones Mariño. [*Rev. Telecommun.* (*Madrid*), vol. 16, pp. 26–34; December, 1960.] Considerations underlying the planning of a radio-link network for local broadcast and television services in difficult terrain are detailed with reference to a projected system.

621.396.65 2771
A Radio-Link System for the Transmission of Five High-Quality Broadcast Channels from 30 c/s to 15 kc/s—H. Oberbeck. (*Telefunken Ztg.*, vol. 33, pp. 216–222; September, 1960. English summary, p. 246.) Application is given, with slight modifications, of the PPM system described in 597 of 1958 and back references.

621.396.65 2772
The Determination of Harmonic Distortion Coefficients of Radio Links starting from the Linearity Characteristics—R. Codelupi. (*Note Recensioni Notiz.*, vol. 9, pp. 823–834; September/October, 1960.) A general method is given for deriving the coefficients of harmonic distortion of the output voltage from a quadripole with nonlinear response characteristic.

621.396.65:621.372.55 2773
The Use of Echo Equalizers at Carrier Frequencies in Wide-Band Transmission Systems—H. Gutsche. (*Frequenz*, vol. 14, pp. 295–299; September, 1960.) The function and adjustment procedure of echo equalizers for use, *e.g.*, in television cable links, are discussed.

621.396.65:621.376.55 2774
PPM60—a Transistorized Pulse-Phase-Modulation Equipment for 60 Channels—H. M. Christiansen and M. Schlichte. (*Nachrtech. Z.*, vol. 13, pp. 392–399; August, 1960.) The design is partly based on that of 24-channel equipment described in 2166 of 1960 (Christiansen and Senft).

621.396.65.029.63 2775
The Standardization of International Microwave Radio-Relay Systems—W. J. Bray. (*Proc. IEE*, pt. B, vol. 108, pp. 180–200; March, 1961.) The reasons for defining the particular characteristics adopted by CCIR and CCITT for line-of-sight paths are discussed.

621.396.721:621.396.932 2776
Problems in the Design of a Marine V.H.F. F.M. Radio Telephone—D. W. Ford and G. Eyre. (*Marconi Rev.*, vol. 24, no. 140, pp. 1–25; 1961.) Features in the design of low-cost 50-channel equipment using a simple synthesized drive source are discussed.

621.396.722:551.507.362.2 2777
Ground Equipment for Radio Observations of Artificial Satellites—B. G. Pressey. (*J. Brit.*

Interplanetary Soc., vol. 18, pp. 20–27; January/February, 1961. Discussion.) Interferometers for directional measurements, equipment for the precise measurement of Doppler frequency shift and methods of recording and analyzing telemetry signals from both Russian and American satellites are described.

621.396.74:621.395.97 2778
The Swiss Program Transmission Network—R. Ziegler. (*Tech. Mitt. PTT*, vol. 38, pp. 406–419; December, 1960. In German and French.) Description of the development, present extent and operation of the Swiss system of broadcast transmission over telephone lines.

621.396.93 2779
The Problem of the Reduction of Channel Width for Mobile Radio Services—A. Essmann. (*Elektrotech. Z., Edn. B*, vol. 12, pp. 584–588; November, 1960.) The reduction of frequency excursion in FM systems and its effect on receiver sensitivity and range are discussed. In comparison, the use of SSB systems would increase the number of channels available but would introduce other difficulties. A reduction of channel width combined with a reduction of service area may be the answer.

SUBSIDIARY APPARATUS

621.311.69:551.507.362.2 2780
Power Supply for the Tiros I Meteorological Satellite—S. H. Winkler, I. Stein, and P. Wiener. (*RCA Rev.*, vol. 22, pp. 131–146; March, 1961.)

621.311.69:621.382.23 2781
Low-Impedance Thermoelectric Device powers Tunnel Diodes—E. L. R. Webb and J. K. Pulfer. (*Canad. Electronics Engrg.*, vol. 5, pp. 40–43; February, 1961.) The power supply described consists of several Bi_2Te_3 couples in series, heated by ac- or dc-driven resistance elements and having an output impedance of 0.02 Ω. Results obtained with tunnel-diode microwave oscillators are briefly discussed.

621.311.69:621.383.5 2782
The Effect of Series Resistance on Photovoltaic Solar Energy Conversion—J. J. Wysocki. (*RCA Rev.*, vol. 22, pp. 57–70; March, 1961.) "The series resistance in a photovoltaic cell is divided into two components: contact and sheet resistance. Each of the components is examined theoretically and experimetally, and qualitative agreement between theory and experiment is shown. It is concluded that contact resistance reduces the conversion efficiency more than sheet resistance."

621.311.69:621.383.5 2783
Considerations of Photoemissive Energy Converters—W. E. Spicer. (*RCA Rev.*, vol. 22, pp. 71–81; March, 1961.) "The efficiency of a solar-energy converter consisting of a [Cs]Na_2KSb emitter and an Ag-O-Cs collector is calculated, taking into account the initial velocities of the photoelectrons but ignoring space charge. Efficiencies between 2 and 2.1% are obtained for output voltages between 0.8 and 1.6 v. The efficiency increases as the percentage of blue and ultraviolet radiation in the source is increased. To minimize space-charge effects, the emitter-collector spacing must be of the order of 0.01 cm or less."

621.311.69:629.19 2784
Optimum Capacitor Charging Efficiency for Space Systems—P. M. Mostor, J. L. Newinger, and D. S. Rigney. (PROC. IRE, vol. 49, pt. 1, pp. 941–948; May, 1961.) Several theorems for the "perfect" time-shaped source voltages which optimize the efficiency of energy transfer from source to load are derived. The practical application of the theorems is discussed.

621.314.58:629.19 2785
Three-Phase Static Inverters power Space-Vehicle Equipment—R. J. Kearns and J. J. Rolfe. (*Electronics*, vol. 34, pp. 70–73; May, 1961.) A 115-v three-phase output at 400 cps is obtained from a dc input of 22–29 v by means of Si controlled rectifiers.

TELEVISION AND PHOTOTELEGRAPHY

621.397:[535.7+159.931 2786
Physiology and Psychology of Television—E. Otto. (*Tech. Mitt. BRF, Berlin*, vol. 4, pp. 94–100; September, 1960.) Various factors controlling the process of vision and the formation of visual impressions are discussed in relation to television.

621.397.132:621.317.755 2787
Test Instrument for Colour Television—H Görling and J. Lindner. (*Nachrtech. Z.*, vol. 12, pp. 428 431; September, 1960.) The mode of operation, the construction and the application of a vectorscope are described.

621.397.331.222 2788
Origin and Possible Methods for Compensation of Retrace Noise in Vidicon Camera Equipment—H. D. Schneider. (*Elektron. Rundschau*, vol. 14, pp. 367–368,371; September, 1960.) The flyback in the horizontal scan circuit produces noise in vidicon cameras, which may result in errors in the output signal. Causes of the noise are analyzed and methods for its elimination are quoted.

621.397.331.24 2789
Development of a High-Slope Television Picture Tube—E. Gundert and H. Lotsch. (*Telefunken Ztg.*, vol. 33, pp. 223–230; September, 1960. English summary, pp. 246–247.) An experimental tube for use with low modulation voltages is described (see also 1042 of March). The electron beam is controlled by a very fine frame grid at 30 μ from the cathode.

621.397.61.029.6 2790
Problems of U.H.F. Television: Transmission—T. M. J. Jaskolski. (*J. Telev. Soc.*, vol. 9, pp. 351–366; January–March, 1961.) Factors affecting the effective radiated power at UHF are briefly surveyed under the following headings, 1) transmitting tubes for the power amplifier, 2) techniques in RF amplifier design, 3) antennas and transmission lines, 4) combining filters.

621.397.61.029.63 2791
Operational Experience with a 10-kW Television Transmitter for Band IV with Klystron Output Stage—A. Kolarz and A. Schweisthal. (*Rundfunktech. Mitt.*, vol. 4, pp. 194–200; October, 1960.) Report on the experience gained with the high-power band-IV transmitter described in 682 of 1960.

621.397.62:621.314.222 2792
Third-Harmonic Tuning of E.H.T. Transformers—E. M. Cherry. (*Proc. IEE*, pt. B, vol. 108, pp. 227–236; March, 1961.) Tuning the leakage inductance of a television receiver line output transformer to the "2.8th harmonic" of the flyback pulse prevents ringing and maximizes the h.v. pulse. A detailed analysis is given.

621.397.712.3 2793
Technical Equipment and Facilities of the B.B.C. Television Centre, London—H. Bishop. (*E. B. U. Rev.*, no. 63A, pp. 190–196; October, 1960.)

621.397.74 2794
Television Standards Conversion—(*Wireless World*, vol. 67, pp. 290–292; June, 1961.) A method of removing the 10-cps flicker produced when converting from 50- to 60-cps field frequency, is described.

621.397.74 2795
A Standards Converter for Television Exchanges between Europe and North America—A. V. Lord. (*E. B. U. Rev.*, no. 63A, pp. 209–213; October, 1960.) Converter equipment incorporating a storage-type camera tube is described which is suitable for use between television standards having 50- and 60-cps field frequencies. For German version see *Rundfunktech. Mitt.*, vol. 4, pp. 201–204; October, 1960.

621.397.74:621.396.65 2796
U.K. Television Links—W. L. Newman. (*Wireless World*, vol. 67, pp. 323–326; June, 1961.) The distribution network of the British Post Office is described.

TUBES AND THERMIONICS

621.38:621.375.029.64/.65 2797
Low-Noise Amplifiers for Centimetre and Shorter Wavelengths—Wade. (See 2515.)

621.382 2798
Operation of Tunnel-Emission Devices—C. A. Mead. (*J. Appl. Phys.*, vol. 32, pp. 646–652; April, 1961.) The operation of tunnel emission devices using thin layers of metals and insulators is discussed. Diode and triode devices are described, with their frequency, current-density and transfer-ratio limitations. Experimental results are presented for both types using various materials. See 2180 of 1960.

621.382.22 2799
Surface Currents in Inversion Layers on Semiconductors—E. Groschwitz, E. Hofmeister, and R. Ebhardt. (*Arch. elekt. Übertragung*, vol. 14, pp. 380–396; September, 1960.) Theoretical and experimental results are given relating to the structure of inversion layers and to physical phenomena causing structural changes. Investigations are carried out on point-contact Ge diodes and cover low direct-voltage conditions. See also 3670 of 1960 (Groschwitz and Ebhardt).

621.382.22:621.376.23 2800
Measurements on Power-Conversion Gain and Noise Ratio of the 1N26 Crystal Rectifiers—A. Dymanus and A. Bouwknegt. (*Physica*, vol. 26, pp. 115–126; February, 1960.)

621.382.23 2801
Tunnelling Current in Esaki Diodes—C. W. Bates, Jr. (*Phys. Rev.*, vol. 121, pp. 1070–1071; February, 1961.) The integral giving the net current in a tunnel diode is evaluated. Curves calculated for 200, 300 and 350°K compare favorably with those given by Esaki (1784 of 1958).

621.382.23 2802
Impurity-Band Conduction and the Problem of Excess Current in Tunnel Diodes—T. P. Brody. (*J. Appl. Phys.*, vol. 32, pp. 746–747; April, 1961.) Tunnel currents calculated on the basis of different impurity-band theories are compared. A number of observations support an impurity-band model which postulates a Fermi level close to the conduction band edge.

621.382.23:621.317.61 2803
Tunnel-Diode Curve Tracer is Stable in Negative-Resistance Region—J. A. Narud and T. A. Fyfe. (*Electronics*, vol. 34, pp. 74–75; May, 1961.) The unit described can trace the characteristics of tunnel diodes having G_d^2/C_d ratios as high as 10^9 mhos²/pF.

621.382.23:621.372.44 2804
R.F.-Induced Negative Resistance in Junction Diodes—J. C. McDade. (PROC. IRE, vol.

49, pt. 1, pp. 957–958; May, 1961.) While the fundamental RF power is driving a junction diode used as a harmonic amplifier, a negative-resistance effect is present near zero bias whether the frequency power is dissipated or not.

621.382.3–71 2805
Cooling Transistors with Beryllia Heat Sinks—K. H. McPhee. (*Electronics*, vol. 34, pp. 76–78; May, 1961.) Particular advantages of the ceramic material are high thermal conductivity and low dielectric loss.

621.382.3.012.8 2806
Transistor Parameters—G. de Visme. (*Wireless World*, vol. 67, pp. 293–299; June, 1961.) Transistor characteristics are defined and the interrelation of the different sets of parameters is discussed.

621.382.3.012.8 2807
A Valve Analogue Circuit for Representing Transistor Properties in the Low-Frequency Region—K. H. Franke. (*Elektronik*, vol. 9, pp. 330–332; November, 1960.) For proof of the analogy on which the circuit given is based see 1343 of April (Tigler).

621.382.333 2808
The Frequency Characteristics of Alloy Transistors—R. Paul. (*Nachrtech.*, vol. 10, pp. 340–347; August, 1960.) An equivalent circuit of a *p-n-p* alloy junction transistor is derived on which investigation of the frequency dependence of circuit parameters is based.

621.382.333 2809
The Mutual Conductance of H.F. Alloy-Junction and Drift Transistors as a Function of Frequency and Working Point and its Derivation—W. Minner. (*Arch. elekt. Übertragung*, vol. 14, pp. 411–420; September, 1960.) Equations are derived and their validity is confirmed by reference to measured values.

621.382.333.33:621.318.57 2810
Designing Avalanche Switching Circuits—R. P. Rufer. (*Electronics*, vol. 34, pp. 81–87; April, 1961.) Avalanche operation of Si mesa transistors is discussed and a criterion for the selection of suitable transistors is given. Typical circuits and operating conditions are described.

621.383.032.217.2 2811
Photoelectric and Optical Properties of Sb-Cs and Sb(Mg)-Cs Films—M. Wada, T. Takahashi, and M. Hagino. (*Sci. Repts. Res. Insts. Tohoku Univ., Ser. B*, vol. 11 no. 2, pp. 75–96; 1959.) A method proposed by Schaetti (1611 of 1954) for reducing the dark current of photomultipliers by the addition of Mg to the Sb-Cs cathode material is investigated.

621.383.292 2812
Photomultiplier with Sb-Na-K Cathode—W. Baumgartner and J. Linder. (*Helv. Phys. Acta*, vol. 33, pp. 608–611; October, 1960. In German.) A preliminary report is given on the preparation of Sb-Na-K films and on results obtained with photomultipliers incorporating such cathodes.

621.383.5:621.311.69 2813
Spectral Response of Photovoltaic Cells—J. J. Loferski and J. J. Wysocki. (*RCA Rev.*, vol. 22, pp. 38–56; March, 1961.) A theoretical and experimental investigation is made of the response of *p-n*-junction photocells.

621.383.5:621.311.69 2814
Large-Area Thin-Film Photovoltaic Cells—H. I. Moss. (*RCA Rev.*, vol. 22, pp. 29–37; March, 1961.) Progress has been made with vacuum deposition of CdS on to heated transparent conducting surfaces. Solar conversion efficiencies of 1 per cent are reported.

621.383.5:621.311.69 2815
A p-n Junction Photocell of Cadmium Telluride—Yu. A. Vodakov, G. A. Lomakina, G. P. Naumov, and Yu P. Maslakovets. (*Fiz. Tverdogo Tela*, vol. 2, pp. 3–7; January, 1960.) CdTe photocells have been produced with *I/V* characteristics similar to those of Si. Their efficiency as solar-energy converters is 4 per cent.

621.383.5:621.311.69 2816
Properties of *p-n* Junctions in Cadmium Telluride Photocells—Yu. A. Vodakov, G. A. Lomakina, G. P. Naumov, and Yu. P. Maslakovets. (*Fiz. Tverdogo Tela*, vol. 2, pp. 15–22; January, 1960.) The *I/V* characteristics of CdTe photocells are discussed. With an appropriate technique of preparation *p-n* junctions can be produced near the surface which give good efficiency at high and low illumination intensities.

621.385.032.213.23 2817
Thermionic Emission of Barium Tungstate—A. I. Mel'nikov, A. V. Morozov, R. B. Sobolevskaya, and A. R. Shul'man. (*Fiz. Tverdogo Tela*, vol. 2, pp. 704–708; April, 1960.)

621.385.032.26 2818
On the Problem of Magnetic Focusing of a Beam of Electrons Emitted with Thermal Velocities—J. Vejvodova. (*J. Brit. IRE*, vol 21, pp. 337–344; April, 1961.) An analysis is made to determine the distribution of the current density in a beam of circular or rectangular cross section focused by a homogeneous longitudinal magnetic field and simultaneously accelerated by a longitudinal electrostatic field. The dependence of the total current passing through the anode aperture on the intensity of the focusing magnetic field is calculated, the source of electrons being located in the magnetic field.

621.385.032.269.1 2819
Effect of Filament Magnetic Field on the Electron Beam from a Pierce Gun—A. S. Gilmour, Jr. (PROC. IRE, vol. 49, pt. 1, p. 976; May, 1961.) Graphs show the measured current density distributions across the beam for different instantaneous filament currents.

621.385.1:534.29 2820
Microphony in Electron Tubes—S. S. Dagpunar, E. G. Meerburg and A. Stecker. (*Philips Tech. Rev.*, vol. 22, pp. 71–88; January, 1961.)

621.385.13:621.391.822.33 2821
Experimental Investigation of the Amplitude Distribution of Scintillation Noise—H. Rogenhagen and K. H. Simon. (*Z. angew. Phys.*, vol. 12, pp. 395–397; September, 1960.) Statistical analysis of LF noise in the region of 12.5 cps produced by a narrow-band filter amplifier with an oxide-cathode thermionic valve in the first stage. Results are compared with those based on theoretical distribution.

621.385.15:621.391.822.33 2822
Secondary-Emission Flicker Noise—R. C. Schwantes and A. Van der Ziel. (*Physica*, vol. 26, pp. 1162–1166; December, 1960.) The method used to study flicker noise in pentodes (2824 below) has been extended to secondary-emission valves. Results confirm that the secondary-emission flicker effect is real.

621.385.3:621.391.822.33 2823
Flicker Noise in Triodes with Positive Grid—R. C. Schwantes and A. Van der Ziel. (*Physica*, vol. 26, pp. 1143–1156; December, 1960.) Results were obtained for the magnitude of flicker noise and its correlation at grid and anode for low and high frequencies.

621.385.5:621.391 822.33 2824
Flicker Noise in Pentodes: Flicker Partition Noise—R. C. Schwantes and A. Van der Ziel. (*Physica*, vol. 26, pp. 1157–1161; December, 1960.) The approach used to study flicker noise in positive-grid triodes (2823 above) is modified for pentodes. The existence of a partition component [see 898 of 1955 (Tomlinson)] is confirmed, which is represented by a noise current generator connected between screen grid and anode.

621.387:621.362 2825
Plasma Synthesis and its Application to Thermionic Power Conversion—Hernqvist. (See 2748.)

621.387:621.362 2826
Direct Conversion of Heat to Electromagnetic Energy—Johnson. (See 2749.)